GEOLOGIJA

2017 | št.: **60/2**

GeoZS
Geološki zavod Slovenije

ISSN
Tiskana izdaja / Print edition: 0016-7789
Spletna izdaja / Online edition: 1854-620X

GEOLOGIJA

60/2 – 2017

GeoZS
Geološki zavod Slovenije

GEOLOGIJA	2017	60/2	169-344	Ljubljana

GEOLOGIJA
ISSN 0016-7789

Izdajatelj: Geološki zavod Slovenije, zanj direktor Miloš Bavec
Publisher: Geological Survey of Slovenia, represented by Director Miloš Bavec
Financirata Javna agencija za raziskovalno dejavnost Republike Slovenije in Geološki zavod Slovenije
Financed by the Slovenian Research Agency and the Geological Survey of Slovenia

Vsebina številke 60/2 je bila sprejeta na seji Uredniškega odbora, dne 8. 12. 2017.
Manuscripts of the Volume 60/2 accepted by Editorial and Scientific Advisory Board on December 8, 2017.

Naslov uredništva / Editorial Office: GEOLOGIJA Geološki zavod Slovenije / Geological Survey of Slovenia
Dimičeva ulica 14, SI-1000 Ljubljana, Slovenija
Tel.: +386 (01) 2809-700, Fax: +386 (01) 2809-753, e-mail: urednik@geologija-revija.si
URL: http://www.geologija-revija.si/

GEOLOGIJA izhaja dvakrat letno. / GEOLOGIJA is published two times a year.
GEOLOGIJA je na voljo tudi preko medknjižnične izmenjave publikacij. /
GEOLOGIJA is available also on exchange basis.

Izjava o etičnosti
Izdajatelji revije Geologija se zavedamo dejstva, da so se z naglim naraščanjem števila objav v svetovni znanstveni literaturi razmahnili tudi poskusi plagiatorstva, zlorab in prevar. Menimo, da je naša naloga, da se po svojih močeh borimo proti tem pojavom, zato v celoti sledimo etičnim smernicam in standardom, ki jih je razvil odbor COPE (Committee for Publication Ethics).

Publication Ethics Statement
As the publisher of Geologija, we are aware of the fact that with growing number of published titles also the problem of plagiarism, fraud and misconduct is becoming more severe in scientific publishing. We have, therefore, committed to support ethical publication and have fully endorsed the guidelines and standards developed by COPE (Committee on Publication Ethics).

Baze, v katerih je Geologija indeksirana / Indexation bases of Geologija: Scopus, Directory of Open Access Journals, GeoRef, Zoological Record, Geoscience e- Journals, EBSCOhost

Cena / Price

Posamezni izvod / Single Issue	Letna naročnina / Annual Subscription
Posameznik / Individual: 15 €	Posameznik / Individual: 25 €
Institucija / Institutional: 25 €	Institucija / Institutional: 40 €

Tisk / Printed by: Tiskarna Formatisk d.o.o.

Slika na naslovni strani: Panoramski pogled s Svetega Socerba (Vipavska brda) na Zgornjo Vipavsko dolino, pobočje Rebrnic in Nanoško planoto. (Popit, članek v tej številki, foto: T. Popit)

Cover page: A panoramic view from Sveti Socerb to the Upper Vipava Valley, Rebrnice area and Nanos plateau. (Popit, paper in this issue, photo: T. Popit)

VSEBINA – CONTENTS

Poročila

Nekrolog

GEOLOGIJA *60/2*, 173-180, Ljubljana 2017

https://doi.org/10.5474/geologija.2017.012

High arsenic (As) content in coals from Neogene deposits of the Pannonian Basin in Slovenia

Visoka vsebnost arzena (As) v premogih iz neogenskih plasti Panonskega bazena na območju Slovenije

Miloš MARKIČ

Geološki zavod Slovenije, Dimičeva ulica 14, SI–1000 Ljubljana, Slovenija;
e-mail: milos.markic@geo-zs.si

Prejeto / Received 17. 1. 2017; Sprejeto / Accepted 18. 9. 2017; Objavljeno na spletu / Published online 22. 12. 2017

Dedicated to Professor Jože Pezdič on the occasion of his 70th birthday

Key words: Coal, arsenic (As), Pannonian Basin, Neogene, Slovenia
Ključne besede: premog, arzen (As), Panonski bazen, neogen, Slovenija

Abstract

High contents of arsenic (As) in coal samples from four localities within Neogene deposits of the Pannonian Basin in Slovenia are presented and discussed in this paper. Data from three localities represent interval samples of coal cuttings from wells TER-1 (Terbegovci), Sob-3g (Murska Sobota), and MD-1 (Mislinjska Dobrava). The fourth locality is Globoko, where the main lignite seam was analysed already in 1989. The oldest are coal samples from the MD-1 well which are supposed to be of the Lower Miocene age (except for the shallowest one, which is of the Plio-Quaternary age). Coal samples from the TER-1 and Sob-3g wells are of the Upper Miocene age (Mura Formation). The lignite sample from Globoko is of the Upper Miocene age too (Pontian; Globoko Formation). Most samples were prepared for the ICP-MS method analysis as "whole coal", dry, pulverized lab-samples, weighting ca. 10 g. The results show for all "whole coals" samples considerably increased contents of As: 22.7, 111.4, 222.1, and 131.4 µg/g for the Lower Miocene (?), and 84.5 µg/g for the Plio-Quaternary coals from MD-1 well, 392 µg/g for coals from the Sob-3g well, and 116 µg/g for a coal from the TER-1 well (both Upper Miocene – Mura Formation). In the case of Globoko, not "whole coal" but its high temperature ash was analysed and showed As content as high as 170 µg/g applying AAS method of analysis, and even 260 µg/g applying the ICP-MS. Origin of As could be pre-Neogene rocks of the hinterland and/or Neogene calc-alkaline volcanites. Mineral-gas exhalations from the under-continental upper mantle, containing As, could also be a source of this highly volatile element.

Izvleček

V članku predstavljamo in razlagamo rezultate o visoki vsebnosti arzena (As) v vzorcih premoga iz štirih lokalnosti znotraj neogenskih plasti na območju Panonskega bazena v Sloveniji. Podatki iz treh lokalnosti predstavljajo intervalne vzorce drobcev premoga iz vrtin TER-1 (Terbegovci), Sob-3g (Murska Sobota) in MD-1 (Mislinjska Dobrava). Četrta lokalnost je Globoko, kjer je bil glavni lignitni sloj analiziran že leta 1989. Najstarejši premog je iz vrtine MD-1 in je spodnjemiocenske starosti, razen najzgornejšega vzorca, ki je pliokvartarne starosti. Premogi iz vrtin TER-1 in Sob-3g so zgornjemiocenske starosti (Murska formacija). Lignit iz Globokega je tudi zgornjemiocenske starosti, določneje, pontijske (Globoška formacja). Večina vzorcev je bila pripravljena za analizno metodo ICP-MS kot vzorcev »celotnega premoga«. Laboratorijski vzorci so bili suhi, uprašeni in so tehtali okoli 10 g. Rezultati so pokazali za celotne premoge naslednje vsebnosti As: 22,7; 111,4; 222,1 in 131,4 µg/g za spodnjemiocenske premoge in 84,5 µg/g za plio-kvartarni premog iz vrtine MD-1 ter 392 µg/g za premoge iz vrtine Sob-3g in 116 µg/g za premog iz vrtine TER-1. Lignit iz Globokega je bil analiziran kot visokotemperaturni pepel z metodama AAS in ICP. Prva je pokazala vsebnost As 170 µg/g, druga pa 260 µg/g. Izvore As in njegove vezave na organsko/mineralno premoško snov je iskati v pred-neogenskih kamninah zaledja, v alkalnih neogenskih vulkanitih in morda tudi kot posledico plinsko-mineralnih razplinjevanj iz zgornjih delov plašča pod kontinentalno skorjo.

Introduction

This paper presents a continuation of the paper by Markič & Brenčič (2014), which described a finding of high arsenic (As) content in coal cuttings from the TER-1 well. In this well they found the As content in the Miocene coal matter as high as 116 μg/g. Contents of As in coal samples from three additional localities, i.e. from the Sob-3g and MD-1 wells, and from the mine workings at Globoko are presented in this paper. All four localities are situated in the Slovenian part of the Pannonian Basin System (PBS). They are shown in Fig. 1 and cited in Table 1 (upper part in grey). TER-1 was a water-supply well drilled in 2003 at Terbegovci ca. 12 km SW of Murska Sobota (NE Slovenia). Sob-3g was a geothermal well drilled in 2012 at Murska Sobota (NE Slovenia). MD-1 was a geothermal well drilled in 2005 on Mislinjska Dobrava S of Slovenj Gradec (N Slovenia). The fourth locality, Globoko, was a lignite exploration area in the northern part of the Krško Polje basin (E Slovenia), where dozens of boreholes were drilled and the lignite seams were explored with underground mine workings between 1981 and 1988 (Markič & Rokavec, 2002).

Occurrence of As in coals of Slovenia attracted a significant attention for the first time with the study of the Velenje lignite. Geochemical study of this intermontane (out of PBS) Pliocene lignite (Markič, 2006) revealed that it is a Ca-characteristic ortho-lignite depleted in almost all trace elements in comparison to the Clarke values. The only exceptions were uranium (U) and molybdenum (Mo) contents, which are about 3 (U) and 6 (Mo) times higher in the Velenje lignite than are the Clarke values for coals of the world as cited in Ketris & Yudovich (2009). Another anomaly was detected for arsenic (As) – not so much in the content but in bonding. Namely, Šlejkovec & Kanduč (2005) pointed out on the basis of special extraction procedures that As in the Velenje lignite is both organically and inorganically bound. “At least partial” organic bonding of As (together with even higher organic bonding affinity of U and Mo) was first mentioned in the author’s yearly report for the Velenje Lignite Mine for 2002/2003 (Markič et al, 2004) based on the fact that As was not considerably depleted in lignite versus inorganic sediments in the roof and the floor deposits. This indication – and a general statement that As is an environmentally hazardous element – focused us to investigate this element more in detail in other coals outside the Pannonian Basin as well. Besides Velenje, few data existed for brown coals of Trbovlje, Senovo, and Kanižarica, published by Pirc & Žuža (1989), and Šlejkovec & Kanduč (2005). These data are gathered in lower part of Table 1.

Methods

Coal samples from Neogene deposits of the Pannonian Basin interpreted in this study were collected from four localities shown in Fig. 1 and cited in Table 1 (upper part in grey). All samples, except for the Globoko one, were coal cuttings from not-cored wells. Coal cuttings of mm–cm dimensions were collected from several cm–dm thick coal interlayers not precisely defined by thickness and depth. Coal cuttings were therefore joined from several intervals (because not weigh enough separately) into composite coal cuttings samples. Coal cuttings from the TER-1 well were collected and analysed as one composite sample from a 14.5 m long interval in a depth of 141.0–155.5 m (Markič & Brenčič, 2014). Coal cuttings from the Sob-3g well were collected from a 35 m long interval in a depth of 460–495 m. Five coal cuttings samples were analysed from the MD-1 well, one from a depth of 25 m and other four from four 2–4 m thick intervals in a depth of 742–1030 m. In Globoko, the main lignite seam (2.2 m thick) from exploration mine workings was analysed on trace elements already in 1989, and results were published by Pirc & Žuža (1989).

Samples from the wells TER-1, Sob-3g, and MD-1 were prepared for the Inductively Coupled Plasma – Mass Spectroscopy (ICP-MS) method for the main and trace elements analysis as “whole coal”, dry, pulverized lab-samples, weighting ca. 10 g. In the case of Globoko (Pirc & Žuža, 1989), not “whole coal” but its high temperature (750–950 °C) ash was analysed using both Atomic Absorbtion Spetroscopy (AAS) and ICP-MS method. Therefore, results between Globoko and the three well localities are not directly comparable. Even recalculation to a unique basis would not be relevant because As is a highly volatile element.

Coal from the TER-1 well (Markič & Brenčič, 2014) was extensively analysed comprising proximate, ultimate and calorific value analysis, loss on ignition, and analyses of total sulphur, total organic carbon, and of minor and trace element contents. In the mentioned paper, also methods of preparation and laboratory analyses have been described in detail, together with comments on accuracy and precision of trace element analytics, which are also valid for this study. Coals from the Sob-3g and MD-1 wells were not analysed for their calorific value and ash content.

In presenting results of a coal analysis (proximate, ultimate, geochemical etc.), the basis of analysis must be cited to which the data are reported on. It should be precisely cited, whether the analysis is on the "whole coal basis" or on the "ash basis" etc. (e.g. Thomas, 1992; ISO Standards). In the case of expression of results from different bases to a unique basis, recalculations are needed (e.g. Thomas, 1992; ISO Standards). Concerning analyses of ash, which is obtained with ashing at high temperatures (750–950 °C), it is important to consider volatility of certain elements. Arsenic (As) is very sensible in this sense. Some other highly volatile elements are Hg, I, Se, B, Br, Ge, Mo (e.g. Huggins, 2002; Ketris & Yudovich, 2009). Therefore, these elements are better to be analysed on the "whole coal" basis. Previous analyses of coals in Slovenia, in last 25 years, also showed, that a great majority of elements in "whole coals" is above detection limits at ca. 10 g weigh samples.

Geological coal samples from Slovenia, collected by researchers of the Geological survey of Slovenia, are routinely analysed from the late 1980-ies onwards with the ICP method, mostly in the ACME Laboratory in Vancouver (Canada), after the 1st of January 2015 renamed to Bureau Veritas. Their own re-run testing, as well as our testing with duplicate samples and geo-standards exhibit a relevant reliability of the analysed values that we can use for further geological interpretations.

Results and Discussion

Ketris & Yudovich (2009) published average contents (the Clarke values or Clarkes) for trace elements for "whole coals" of the world, and for their ashes. Their Clarkes are medians. The Clarke value for As for all coals is 8.3 µg/g. The As Clarke value for brown coals is somewhat lower, 7.6 µg/g, and for hard coals somewhat higher, 9.0 µg/g. Coal ashes of brown coals have the As Clarke value of 48 µg/g and of hard coals of 46 µg/g.

In the book of Valković (1983) we find that the average content of As in coals of the world is 5 µg/g. Bowen (1979) and Swaine (1990) (both cited in Taylor et al., 1998, p.272) gave a range of As for "most" coals of the world to be 0.5–80 µg/g. In this paper, values by Ketris & Yudovich (2009) are taken into account.

Data for all coals in Slovenia analysed for As contents are presented in Table 1. It is evident that quite few data exist about As contents in coals of Slovenia, which are mainly Tertiary in age, humic by type and brown coals in rank, ranging from ortho- to meta-lignites and hard brown coals (Markič et al. 2007 and references there-in). In this paper, Clarkes after Ketris & Yudovich's (2009) are taken into account. For some coals, the age is not well defined, partly due to lack of age indicative fossils, partly due to lack of paleontological investigations. In these cases of Kanižarica and MD-1 well, geological descriptions from Basic Geologic Map of SFRJ 1:100.000 and analogies are considered. For some coals (MD-1 well, Sob-3 well) also rank is not precisely defined.

Coals cited in Table 1 are divided into Neogene paralic coals of the Pannonian Basin (MD-1, Globoko, TER-1 and Sob-3), coals within Mio-Pliocene and Pliocene deposits of intermontane basins (Velenje and Kanižarica), and Oligocene coals formed from biomass accumulation in gulfs of than existing periphery of the Paratethys (Senovo, Trbovlje). Only samples from MD-1 and Sob-3 wells were newly analysed for As contents for this study, while others have been already analysed in the past (Pirc & Žuža, 1989; Šlejkovec & Kanduč, 2005; Markič, 2006, and Markič & Brenčič, 2014).

According to the Basic Geological Map of Yugoslavia - Sheets Goričko (Pleničar, 1968), Slovenj Gradec (Mioč & Žnidarčič, 1977), Zagreb (Šikić et al., 1978), and Čakovec (Mioč & Marković, 1997), among coals of the Pannonian basin the oldest are coal cuttings samples from the MD-1 well, which are supposed to be of the Lower Miocene age (except for the shallowest one, which is of the Plio-Quaternary age) (Table 1). Coal cuttings samples from TER-1 and Sob-3g wells are of the Upper Miocene age (Mura Formation). The lignite sample from Globoko is of the Upper Miocene age too – lignite-bearing strata having been defined as the Pontian strata (Globoko Formation) (Markič & Rokavec, 2002 - after numerous reports of Ž. Škerlj in the 1980s on the Ostracoda fauna).

Table 1. Coals of Slovenia analysed for As content – for locations of the Neogene Pannonian Basin coals see Fig. 1. Coal rank is signed with oL – ortho-lignite; mL – meta-lignite, hbC – hard brown coal. All coals are humic. Number of samples is signed with "n". References are: (a): Pirc & Žuža, 1989; (b): Markič & Brenčič, 2014; (c): Šlejkovec & Kanduč, 2005; (d): Markič (2006). Types of basins and geological ages refer to coal/lignite-bearing sediments. As contents for Neogene coals from the Pannonian Basin are also written in Fig. 1. Reporting on different bases is signed with WC ("whole coal" analysis) and with HTA (high temperature ash analysis). Clarkes are medians for brown coals (for WC and HTA, respectively), ± values mean $\pm 1\sigma Me$ ($\sigma Me=(Q3-Q1)/2n^{1/2}$) Q1 and Q3 being quartiles, n= 66 (Ketris & Yudovich, 2009). Enrichment factor, rounded to a whole number, is ratio between As content in a coal of Slovenia versus the Clarke.

Coals of Slovenia analysed for As contents	Basin type	Age	Basis of analysis	As contents of coals in Slovenia (in µg/g)	Clarkes for As (in µg/g) for brown coals (for WC and HTA) (Ketris, & yudovich, 2009)	Enrichment factor (rounded)
MD-1 well: oL? cuttings (n=1) **THIS STUDY**	Pannonian Basin – Neogene – paralic coals	Plio-Quaternary	WC	**84.5**	7.6 ± 1.3	**11**
Globoko: oL seam (n=1) (a)		Pontian	HTA	**170^{AAS}, 260**	48 ± 7	**4-5**
TER-1 well: mL. cuttings (1 composite sample) (b)		Upper Miocene (Mura Fm.)	WC	**116.1**	7.6 ± 1.3	**15**
Sob-3 well: mL ? cuttings (1 comp. sample) **THIS STUDY**			WC	**392.1**	7.6 ± 1.3	**52**
MD-1 well: mL? cuttings (n=4) **THIS STUDY**		Lower Miocene?	WC	**131.4** **222.1;** **111.4;** **22.7;**	7.6 ± 1.3	**17** **29** **15** **3**
Velenje: oL seam (n=2) (a) Velenje: oL seam (n=5) (c) Velenje: oL seam (n=29) (d)	Intermontane basins	Pliocene	HTA WC WC	25^{AAS}, 30 1.59-14.3 2.5-23.9	48 ± 7 7.6 ± 1.3 7.6 ± 1.3	<1 <1-2 <1-3
Kanižarica: mL seam (n=4) (a)		Mio-Pliocene?	HTA	20-50	48 ± 7	<1
Senovo: hbC seam (n=1) (a)	Gulfs of Paratethys	Oligocene	HTA	50	48 ± 7	1
Trbovlje: hbC seam (n=5) (a) Trbovlje: hbC seam) (n=1) (c)			HTA WC	27-42^{AAS}, 40-50, 8.03	48 ± 7 7.6 ± 1.3	<1 1

ICP-MS analyses of "whole coal" samples for all coals from the Pannonian Basin showed considerably increased contents of As (Table 1) (Fig. 1): 22.7, 111.4, 222.1, and 131.4 µg/g for the Lower Miocene (?), and 84.5 µg/g for the Plio-Quaternary coals from the MD-1 well, 392 µg/g for coal from the Sob-3g well, and 116 µg/g for coal from the TER-1 well. In the case of Globoko, not "whole coal" but its (high temperature!) ash was analysed and showed as high as 170 µg/g (AAS analysis) and even 260 µg/g (ICP-MS analysis) As contents. In comparison to the Clarkes for brown coals (Table 1) the cited contents mean enrichment factors mostly above 10, extremely 29 (one coal in the MD-1 well), and even 52 in the coal from the Sob-3 well. Only two coals are not so much enriched in As – ortho-lignite from Globoko (analysed was ash) and the deepest coal sample from the MD-1 well (maybe even older than the Lower Miocene?). Their content of As is only 3–5 times greater than the Clarke.

Coals outside the Pannonian Basin (Tab. 1 – lower part) are characterized by "normal" As contents, with enrichment factors mostly below 1. Enrichment factor 3 was only detected for ash-rich lignite of the lower part of the Velenje lignite seam (Markič, 2006).

The question of As bonding of the high As containing coals of the Pannonian Basin, either organic or inorganic, rests unanswered in this paper. Sink and float analyses were not carried out. For some elements in the Trbovlje coal these were made only by Uhan (1993), but not for As. Arsenic compounds in low-rank coals (two from Slovenia – Velenje and Trbovlje – and one from the Sokolov Basin in the Czech Republic) were investigated by Šlejkovec & Kanduč (2005). They found a high As content in one coal from the Sokolov Basin – 142 µg/g in the Oligocene Josef coal seam - whereas other samples were low in As contents. They interpreted high As content in the Josef coal seam to be inorganically bound. Inorganic bonding was also ascertained

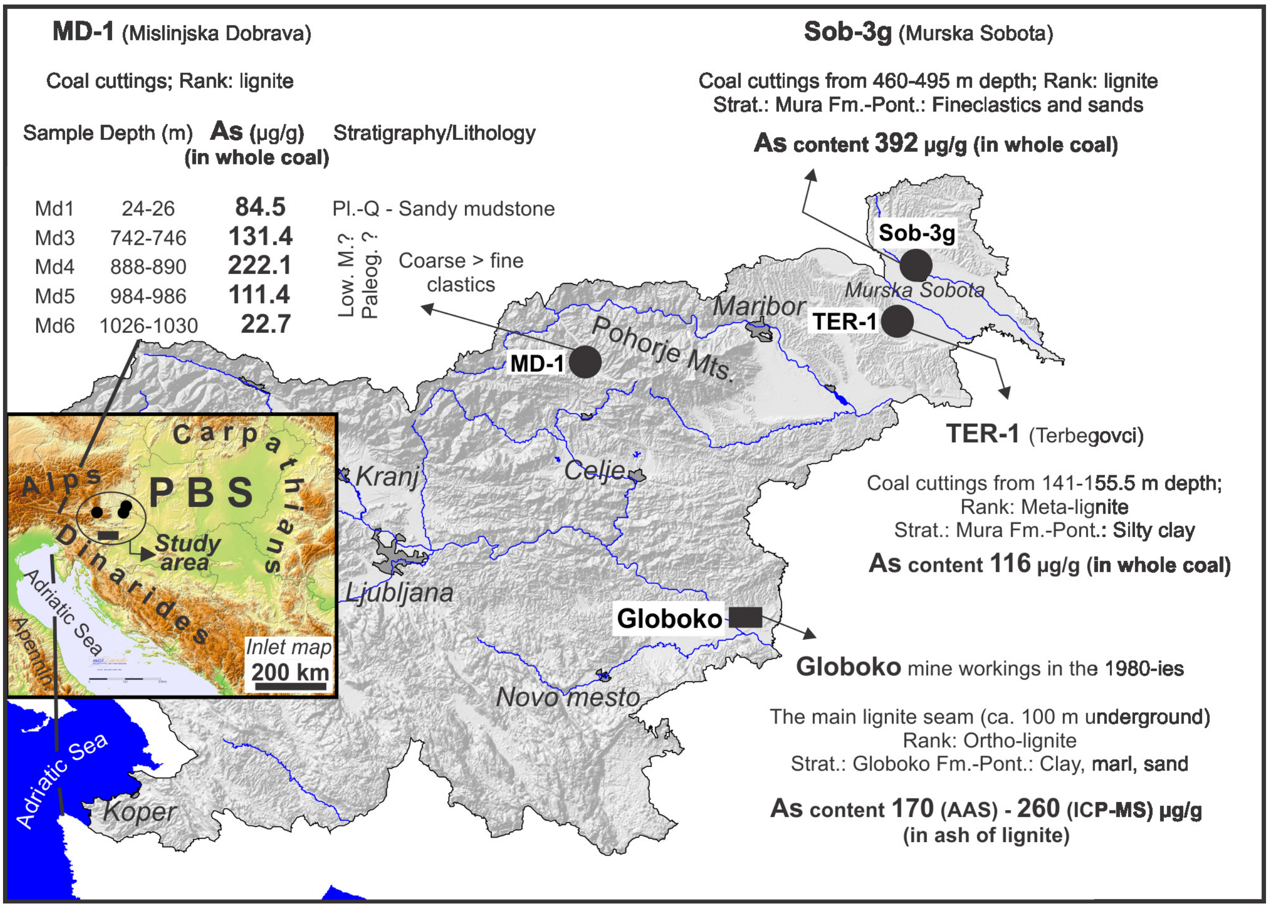

Fig. 1. Locations (TER-1, Sob-3g, MD-1 wells, and Globoko coal mining workings) with cited As contents in the Neogene coals of the Pannonian Basin (based on data from Table 1).

for the Trbovlje coal, with As content of only 8.03 μg/g. Low contents were determined by Šlejkovec & Kanduč (2005) in the Velenje lignite as well (between 1.59 and 14.3 μg/g), but a considerable organic bonding of As was interpreted for this lignite (Markič, 2004; Šlejkovec & Kanduč, 2005).

Ash content analyses for the Neogene coals have been only made for the Globoko lignite and for the TER-1 well. Both showed ash contents (HTA) <10 mass %. Coal from the Sob-3 and MD-1 wells was not analysed, but was macropetrographically clean with estimated <10 vol. % of mineral matter. If a low ash coal (of a low specific gravity) has a high As content this may indicate that As is organically bound, at least partly (Diessel, 1992, p.238, 239 - fig. 5.37 and table 5.10 after Warbrooke & Doolan, 1986).

Regardless of different bases of analyses and different constraints (lack of complete coal analyses), it is evident that the Pannonian Basin Neogene coals in Slovenia are considerably enriched in As contents. A question arises, what is the situation with coals in other parts/countries of the Pannonian Basin. High As content in the Neogene coals in Slovenia is not so much a question of these thin coals themselves, which do not have a high economic value (at present) - it is more a question of geochemical influence that As content could have on e.g. geothermal waters in water-bearing deposits with As-rich coals stratified within.

Concerning the origin of As in coals, main aspects have been presented in the paper of Markič & Brenčič (2014), taking into account published data by Zupančič (1994), Kralj (1996, 2000, 2003), and Trajanova (2013). To these authors, the Smrekovec andesite and its tuff, Grad basaltic tuff, magmatic and metamorphic rocks that form the hinterland of the Pannonian Basin and its basement do not contain more than 10 μg of As per gram of rock. The only known exceptions are A and B soil horizons above serpentinite in the Pohorje Mountains with As contents between 30 and 60 μg/g, and granodiorite with As contents up to 21 μg/g (Zupančič, pers. comm.; Zupančič & Plaskan, pers. comm.). Volcanism (calc-alkaline) during the Neogene could also contribute significantly to the geochemistry of the synchronous deposits including organic matter, which later developed to coals. For a wide discussion on As in world coals, the reader is referred to Yudovich & Ketris (2005).

As a contribution in the explanation of the As content - in fact As capture – in the organic matter in the Pannonian Basin may serve a very interesting work of Bräuer et al. (2016). Reading their explanation it becomes reasonable to suppose that As was maybe the result of degassing of the Earth's mantle and later "catching" to organic matter and/or its admixtured inorganic matter (see the concept of CAI – Coal Affinity Index, Ketris & Yudovich, 2009). Similar "mantle degassing" enrichments of economically highly interesting elements are known from the geological history: among the best known in Slovenia is Hg mineralization in Paleozoic and Triassic strata of Idrija caused by Middle Triassic volcanic activity initiated by degassing of the upper part of the Earth's mantle (Pirc & Herlec, 2009, p.533 - after cited authors there-in).

A similar story about "very deep gasses" was debated with respect to the origin of gasses in the Pliocene Velenje Lignite Mine (Kanduč & Pezdič, 2005) connected to very deep faults in the realm of the Periadriatic Fault System and the Šoštanj Fault, respectively (e.g. Vrabec & Fodor, 2006, and references there-in).

Conclusion

All available data for the Neogene coals of the Pannonian Basin in Slovenia show moderate to high enrichment in arsenic (As) content. However, results are based on samples from only four localities (Fig. 1). Number of samples is statistically low. Further investigations would be welcome but coal samples from wells are quite rarely available.

In the investigated "whole coal" samples from three localities (wells TER-1, Sob-3 and MD-1), As contents vary mostly in a range of 23–392 µg/g (slightly rounded), being the highest in the Sob-3 well from a depth interval of 460–495 m (Upper Miocene), and the lowest in the lowermost sample in the MD-1 well in a depth of 1026–1030 m (Lower Miocene) (Fig. 1, and Table 1). Other As contents are 116 µg/g in TER-1 well for a composite coal sample from a depth of 141.0–155.5 m (Upper Miocene), and 111, 131, and 222 µg/g in the MD-1 well in three depth intervals of 742–986 m (Lower Miocene).

In Globoko, the fourth locality (Fig. 1), the main lignite seam (2.2 m thick) was sampled. Its "high temperature ash" was analysed. Results showed as high as 170 µg/g (AAS analysis) and even 260 µg/g (ICP-MS analysis) As contents.

The Clarke value for As contents for brown coals is 7.6 µg/g, whereas for ashes of brown coals it is 48 µg/g. Ratio between As content in an individual coal in Table 1 and the Clarke value is termed as an enrichment factor. For the Pannonian Basin coals (Table 1 – upper part in grey), this factor is mostly above 10, extremely 29 (one coal in the MD-1 well), and even 52 in a coal from the Sob-3 well. Only two coals are not so much enriched in As – ortho-lignite from Globoko (analysed was ash) and the deepest coal sample from the MD-1 well. Their contents of As are only 3–5 times greater than the brown coal and ash Clarke values, respectively.

Coals outside the Pannonian Basin (Velenje, Kanižarica, Senovo, and Trbovlje) (Table 1 – lower part) do not exhibit any spectacular differences in As contents in comparison to the "world coals". Based on few available data, enrichment factors are mostly around or below 1. The only exception is the Velenje lignite. It was analysed for minor and trace elements with 29 samples. In the lower part of the lignite seam, which is ash--rich, As contents vary in a range of 10–25 µg/g, whereas in the upper part, which is ash poor, in a range of 3–10 µg/g.

We do not know As contents in coals of other areas of the Pannonian Basin. This fact may represent a challenge for international cooperation on As contents in coals of the Pannonian Basin, maybe as well as of As contents in Neogene deposits, including waters.

Acknowledgements

Colleagues who provided coal cuttings samples are sincerely appreciated for their highly responsible sense that coal material from "their" wells could be petrologically interesting – even-though originating from only thin coal inter-layers. My further thanks go to the reviewers and editors of the journal. This study was carried out in the frame of the Slovenian national scientific programme Mineral Resources P1-0025.

This paper was written at the occasion of the 70th anniversary of Prof. Dr. Jože Pezdič who was one of the excellent mentors of the author's PhD work about the Veleje lignite in 2009 and from whom the author got many positive initiatives and ideas for his further work.

References

Bowen, H.J.M. 1979: Environmental Chemistry of Elements. Academic Press, London: 333 p.

Bräuer, K., Geissler, W.H., Kämpf, K., Niedermann, S. & Rman, N. 2016: Helium and carbon isotope signatures of gas exhalations in the westernmost part of the Pannonian Basin (SE Austria/NE Slovenia): Evidence for active lithospheric mantle degassing. Chemical Geology, 422: 60-70, doi:10.1016/j.chemgeo.2015.12.016.

Diessel, C.F.K. 1992: Coal-Bearing Depositional Systems. Springer-Verlag: 721 p.

Huggins, F.E. 2002: Overview of analytical methods for inorganic constituents in coal. International Journal of Coal Geology, 50/1–4: 169–214, doi:10.1016/S0166-5162(02)00118-0.

Kanduč, T. & Pezdič, J. 2005: Origin and distribution of coalbed gasses from the Velenje basin, Slovenia. Geochemical Journal, 39/5: 397-409, doi:10.2343/geochemj.39.397.

Ketris, M.P. & Yudovich,Ya., E. 2009: Estimations of Clarkes for Carbonaceous biolithes: World averages for trace element contents in black shales and coals. International Journal of Coal Geology, 78/2: 135–148, doi:10.1016/j.coal.2009.01.002.

Kralj, P. 1996: Lithofacies characteristics of the Smrekovec volcaniclastics, northern Slovenia. Geologija, 39: 159–191, doi:10.5474/geologija.1996.007.

Kralj, P. 2000: Upper Pliocene alkali basalt at Grad, northeastern Slovenia. Geologija, 43/2: 213–218, doi:10.5474/geologija.2000.015.

Kralj, P. 2003: Geochemistry of Upper Pliocene silty and sandy deposits from the well Mt-7, Moravci Spa, North-Eastern Slovenia. Geologija 46/1: 117–122, doi:10.5474/geologija.2003.011.

Markič, M., Zavšek, S., Vrenčur, L. & Papež, D. 2004: Petrologija velenjskega lignita in prostorska litofacielna interpretacija = Petrology of the Velnje lignite and its lithofacies interpretation (in Slovene). Poročilo v arhivu Geološkega zavoda Slovenije (Report in the archive of the Geological Survey of Slovenia): 32 p.

Markič, M. 2006: Anorgansko-geokemična opredelitev velenjskega lignita v reprezentativnem profilu vrtine P-9k/92 = Inorganic geochemical characterisation of the Velenje lignite in the representative P-9k/92 borehole profile (in Slovene). Geologija, 49/2: 311–338, doi:10.5474/geologija.2006.023.

Markič, M., Kalan, Z., Pezdič, J. & Faganeli, J: 2007: H/C versus O/C atomic ratio characterization of selected coals in Slovenia = Opredelitev nekaterih premogov na ozemlju Slovenije s H/C proti O/C atomskimi razmerji. Geologija, 50/2, 403–426, doi:10.5474/geologija.2007.028.

Markič, M. & Brenčič, M. 2014: High arsenic (As) content in the Upper Miocene coal matter from TER-1/03 borehole (Terbegovci – Sveti Jurij ob Ščavnici). Geologija, 57/1: 015-026, doi:10.5474/geologija.2014.002.

Markič, M. & Rokavec, D. 2002: Geološka zgradba, nekovinske mineralne surovine in lignit okolice Globokega (Krška kotlina) = Geological setting, non-metallic raw materials and lignite in the area of Globoko (Krško basin, E Slovenia) (in Slovene). RMZ - Materials and geoenvironment, 49/2: 229–266.

Mioč, P. & Marković, S. 1997: Basic Geological Map of Slovenia and Croatia 1:100,000, Sheet Čakovec. Inštitut za geologijo, geotehniko in geofiziko, Ljubljana and Inštitut za geološka istraživanja, Zagreb.

Mioč, P. & Žnidarčič, M. 1977: Basic Geological Map of Yugoslavia 1:100,000 – Sheet Slovenj Gradec. Zvezni geološki zavod Beograd.

Pirc, S. & Herlec, U. 2009: Mineral and energy raw materials. In: Pleničar, M., Ogorelec, B. & Novak, M. (eds.): The Geology of Slovenia. Geological Survey of Slovenia: 517–540.

Pirc, S. & Žuža, T. 1989: Sledne prvine v premogih v SR Sloveniji = Trace elements in coals in Socialist republic Slovenia (Yugoslavia) (in Slovene). Rudarsko-metalurški zbornik, 36/2: 161–172.

Pleničar, M. 1968: Basic Geological Map of Yugoslavia 1:100,000 – Sheet Goričko. Zvezni geološki zavod Beograd.

Swaine, D.J. 1990: Trace Elements in Coal. Butterworths, London: 278 p.

Šikić, K., Basch, O. & Šimunić, A. 1978: Basic Geological Map of Yugoslavia 1:100,000 – Sheet Zagreb. Zvezni geološki zavod Beograd.

Šlejkovec, Z. & Kanduč, T. 2005: Unexpected arsenic compounds in low-rank coals. Environmental Science &Technology, 39: 3450–3454.

Taylor, G.H., Teichmüller, M., Davis, A., Diessel, C.F.K., Littke, R. & Robert, P. 1998: Organic Petrology. Gebrüder Borntraeger, Berlin:704 p.

Thomas, L. 1992: Handbook of Practical Coal Geology. John Wiley & Sons, Chichester: 338 p.

Trajanova, M. 2013: Starost pohorskega magmatizma; nov pogled na nastanek Pohorskega tektonskega bloka = Age of the Pohorje Magmatism – New Insight on the Origin of the Pohorje Tectonic Block (in Slovene). Doktorska disertacija = PhD thesis. Univerza v Ljubljani: 183 p.

Uhan, J. 1993: Geokemična tipomorfnost zasavskega premoga = Geochemical typomorphism of the Zasavje coal (in Slovene). Rudarsko-metalurški zbornik, 40/1-2: 45-58.

Valković, V. 1983: Trace elements in coal, Vol. 1. CRC Press, Boca Raton, Florida: 210 p.

Vrabec, M. & Fodor, L. 2006: Late Cenozoic tectonics of Slovenia: structural styles at the northeastern corner of the Adriatic microplate. In: Pinter, N., Grenerczy, G., Weber, J., Stein, S. & Medak, D. (eds.): The Adria microplate: GPS geodesy, tectonics and hazards. NATO Science Series, IV, Earth and Environmental Sciences. Dordrecht–Springer, 61: 151-168.

Warbrooke, P.r. & Doolan, K.j. 1986: The distribution of elements in some Sydney Basin coals. Aust. Inst. Energy, Austin Coal Sci. Conf. 2 Proc., 1: 404-409.

Yudovich, Ya. E. & Ketris, M.P. 2005: Arsenic in coal: a review. International Journal of Coal Geology, 61/3-4: 141–196, doi:10.1016/j.coal.2004.09.003.

Zupančič, N. 1994: Geokemične značilnosti in nastanek pohorskih magmatskih kamnin = Geochemical characteristics of the Pohorje magmatic rocks (in Slovene). Rudarsko-metalurški zbornik, 41/1-2: 113–128.

GEOLOGIJA *60/2*, 181-198, Ljubljana 2017

https://doi.org/10.5474/geologija.2017.013

Geochemical baseline for chemical elements in top- and subsoil of Idrija

Geokemično ozadje kemičnih prvin v zgornjem in spodnjem sloju tal na območju Idrije

Špela BAVEC

Geološki zavod Slovenije, Dimičeva ulica 14, SI–1000 Ljubljana, Slovenija;
e-mail: spela.bavec@geo-zs.si

Prejeto / Received 20. 9. 2017; Sprejeto / Accepted 6. 10. 2017; Objavljeno na spletu / Published online 22. 12. 2017

Key words: multi-elemental analyses, geochemistry, urban area, correlation matrix, spatial distribution, Idrija
Ključne besede: multi-elementna analiza, geokemija, urbano območje, korelacijska matrika, prostorska porazdelitev, Idrija

Abstract

This study is a continuation of our previous study (Bavec et al., 2015), where the geochemical baseline levels of potentially harmful elements (As, Cd, Co, Cr, Cu, Hg, Mo, Ni, Pb and Zn) in Idrija top- and subsoil (0-10 cm and 10-20 cm) at 45 locations were reported. Here we summarise our previous work and present baseline levels of additional 33 elements (Ag, Al, Ba, Be, Bi, Ca, Ce, Cs, Fe, Ga, Hf, In, K, La, Li, Mg, Mn, Nb, P, Rb, S, Sb, Sc, Se, Sn, Sr, Th, Ti, Tl, U, V, Y and Zr) in order to round off the first systematic geochemical survey of soil in Idrija town and establish a data set of soil elements, which will serve as a baseline for monitoring future changes in the soil chemical composition of the studied area.

The baseline levels were determined after aqua regia digestion, their statistical distribution was examined and the medians were compared to the recently established European grazing land and Maribor urban soil medians. To investigate relationships between elements, a correlation-matrix-based hierarchical clustering method was performed and the spatial distribution of their highest levels was examined. The results showed that in general, the median levels of elements in Idrija soil are mostly similar or slightly higher than in European and Maribor soil, with exception of Hg. Elements Al, Bi, Ca, Ce, Co, Cr, Cs, Fe, Ga, Hf, La, Li, Mg, Mn, Nb, Ni, Rb, S, Sc, Th, Ti, Tl, V, Y and Zr are enriched in the rural surroundings, while elements Ag, Ba, Cu, Hg, P, Pb, Se, Sb, Sn and Zn are enriched only partly in the rural surroundings, but mostly in the urban part of the study area. It is assumed that elements, which are enriched only in the rural surroundings, are of natural origin, while elements, which are enriched also in the urban area, are to a certain extent influenced by anthropogenic activities.

Izvleček

Predstavljena študija je nadaljevanje preteklih raziskav (Bavec et al., 2015), kjer smo obravnavali vrednosti geokemičnega ozadja potencialno škodljivih elementov (As, Cd, Co, Cr, Cu, Hg, Mo, Ni, Pb in Zn) v zgornjem in spodnjem (0-10 cm in 10-20 cm) sloju tal Idrije na 45. lokacijah. V članku povzemamo prejšnje preiskave in obravnavamo geokemična ozadja dodatnih 33 elementov (Ag, Al, Ba, Be, Bi, Ca, Ce, Cs, Fe, Ga, Hf, In, K, La, Li, Mg, Mn, Nb, P, Rb, S, Sb, Sc, Se, Sn, Sr, Th, Ti, Tl, U, V, Y in Zr) z namenom, da bi zaokrožili prve sistematične geokemične raziskave tal v mestu Idrija, ter da bi vzpostavili nabor podatkov o elementih v tleh, ki bodo služili kot osnova za spremljanje prihodnjih sprememb v kemijski sestavi tal na preiskovanem območju.

Vrednosti ozadja smo določili po razklopu z zlatotopko, preiskali njihovo statistično porazdelitev in primerjali ugotovljene mediane z medianami elementov v evropskih pašniških in mariborskih mestnih tleh, ki so bile vzpostavljene nedavno. Z namenom, da bi prepoznali povezave med elementi, smo uporabili metodo hierarhičnega razvrščanja na podlagi korelacijske matrike in ugotavljali prostorsko porazdelitev najvišjih vrednosti elementov. Rezultati so pokazali, da so na splošno mediane elementov v idrijskih tleh večinoma podobne ali nekoliko višje kot v evropskih in mariborskih tleh, z izjemo Hg. Elementi Al, Bi, Ca, Ce, Co, Cr, Cs, Fe, Ga, Hf, La, Li, Mg, Mn, Nb, Ni, Rb, S, Sc, Ti, Tl, V, Y in Zr so obogateni na ruralnem obrobju, medtem ko so elementi Ag, Ba, Cu, Hg, P, Pb, Se, Sb, Sn in Zn obogateni deloma na ruralnem obrobju ter v urbanem predelu preiskovanega območja. Predpostavljamo, da so elementi, ki so obogateni le na ruralnem obrobju, naravnega izvora, medtem ko so elementi, ki so obogateni tudi v urbanem predelu, v določeni meri antropogenega izvora.

Introduction

With regard to our previous study (Bavec et al., 2015), the geochemical baseline levels of 10 potentially harmful elements (As, Cd, Co, Cr, Cu, Hg, Mo, Ni, Pb and Zn) in Idrija top- and subsoil (0-10 cm and 10-20 cm) at 45 locations were reported with intention to evaluate them according to the metal concentrations reported in other areas around the world and to the national guidelines. Current Slovenian legislation (Official Gazette RS, 1996) sets their limit, warning and critical soil levels. These levels are based on aqua regia digestion. However, the levels of 33 additional elements, which are not nationally considered as potentially harmful, were also established, which will be presented in this paper.

With regard to the European Thematic strategy on soil protection (COM(2006)231final)), anthropogenic activities (inadequate agricultural and forestry practices, industrial activities, tourism, urban and industrial sprawl and construction works) affect the soil negatively and prevent it from performing its broad range of functions and services to humans and ecosystems. As a consequence soil degradation problems (erosion, organic matter decline, compaction, salinization, landslides, contamination, sealing and biodiversity decline (SEC(2006)1165) arise. The problem of soil contamination reflects the use and presence of dangerous elements and substances in many production processes with respect to more than two hundred years of industrialisation.

In order to trace the anthropogenic contribution to soil element distribution, it is necessary to determine the baseline levels of elements in soils and monitor them through time. With the latter in mind, international, national and regional datasets on the 'actual' concentration and distribution of dozens of chemical elements in soils (Table 1) were established by many authors with the performance of multi-element geochemical baseline surveys. However, it is emphasized, that two different extraction methods (4-acid and aqua regia digestion) (Table 1) were used to determine the baseline levels, therefore the levels in Table 1 are not directly comparable between each other, except those determined after the same extraction.

For Europe (EU) the first geochemical baseline for topsoil (0-25 cm) was established by Salminen et al. (2005), when the levels of 64 elements were determined at up to 845 locations from 26 EU countries. Almost a decade later geochemical baselines (the levels of 52 elements) were established for grazing soil (0-10 cm) at 2023 locations and for agricultural soil (0-20 cm) at 2108 locations from 33 EU Countries (Reimann et al., 2014).

For Slovenia soil geochemical baselines were provided by the following authors. Šajn (2003) determined the levels of 42 elements in topsoil (0-5 cm) at 82 locations, which were situated in the rural area settlements without known industry and in six largest towns. With intention to monitor soil pollution on a national scale long-term, Zupan et al. (2008) determined the levels of 15 elements and 55 organic substances in Slovenian top- and subsoil (0-5 cm and 5-20 cm) at 376 locations covering the whole territory of Slovenia. Andjelov (2012) determined the levels of 24 elements in topsoil (0-10 cm) at 819 locations covering the whole territory of Slovenia. The mentioned studies provide fundamental background reference levels for distribution of elements in national soils.

Moreover regional geochemical baselines were established with intention to (1) provide reference element levels in soil at specific time and space that will be useful for monitoring future changes and (2) to detect pollution problems and pinpoint target areas, where adversities for its inhabitants threaten to become most pronounced. Šajn et al. (1998, 2011) determined the levels of 35 elements in Ljubljana topsoil (0-5 cm) at 477 locations. Žibret & Šajn (2008) determined the levels of 41 elements in the topsoil (0-5 cm) from Celje and near surroundings at 38 locations, Bavec et al. (2015) determined the levels of 10 elements in Idrija top- (0-10 cm) and subsoil (10-20 cm) at 45 locations. Gosar et al. (2016) determined the Hg levels in Slovenian topsoil (0-10 cm) at 817 locations. Gaberšek and Gosar (2017) determined the levels of 65 elements in Maribor topsoil (0-10 cm) at 118 locations.

The main objective of this paper is to summarise geochemical distribution of 10 elements (As, Cd, Co, Cr, Cu, Hg, Mo, Ni, Pb and Zn) in Idrija soil from our previous study (Bavec et al., 2015) and to present geochemical distribution of 33 additional chemical elements (Ag, Al, Ba, Be, Bi, Ca, Ce, Cs, Fe, Ga, Hf, In, K, La, Li, Mg, Mn, Nb, P, Rb, S, Sb, Sc, Se, Sn, Sr, Th, Ti, Tl, U, V, Y and Zr) in Idrija soil. Furthermore statistical analyses (descriptive statistics and correlation-matrix-based hierarchical clustering

Table 1. Overview of some international, national and regional geochemical baselines of chemical elements, which are considered in this study (all levels are in mg/kg, except where otherwise stated).

	Salminen et al. (2005)	**Reimann et al. (2014)**	**Šajn (2003)**	**Šajn (2003)**	**Zupan et al. (2008)**	**Zupan et al. (2008)**	**Andjelov (2012)**	**Šajn et al. (1998, 2011)**	**Gaberšek & Gosar (2018)**	**Žibret & Šajn (2008)**
Area	Europe	Europe	Slovenia rural areas	Slovenia urban areas	Slovenia	Slovenia	Slovenia	Ljubljana	Maribor	Celje
Depth	0-25 cm	0-10 cm	0-5 cm	0-5 cm	0-5 cm	5-20 cm	0-10 cm	0-5 cm	0-10 cm	0-5 cm
N	845	2026	59	23	135-288	124-253	819	477	118	37
Value	median	median	average	average	median	median	median	median	median	median
Extraction method	aqua regia	aqua regia	4-acid	4-acid	aqua regia	aqua regia	4-acid	4-acid	aqua regia	4-acid
Ag	0.27	0.04	/	/	/	/	/	/	0.093	0.1
Al (%)	11	1.07	6.8	4.7	/	/	6.92	5.55	1.64	5.7
As	6	5.6	15	12	10.2	12.5	/	/	10.1	15
Ba	65	63	355	459	/	/	360	333	96.5	408
Be	<2	0.51	/	/	/	/	/	/	0.7	/
Bi	<0.5	0.18	/	/	/	/	/	/	0.28	/
Ca (%)	0.922	0.31	/	/	/	/	0.78	3.88	1.1	3.5
Cd	0.145	0.2	0.52	1.3	0.62	0.48	/	0.6	0.32	2.2
Ce	48.2	27	/	/	/	/	/	/	28.1	51
Co	7	7.2	16	7.2	13.9	14.3	26	/	10.2	11
Cr	22	20	85	75	51	61	88	85	31	67
Cs	3.71	1.06	/	/	/	/	/	/	1.56	/
Cu	12	14.5	35	70	26.3	27	23	32	40.1	42
Fe (%)	1.96	1.7	3.5	2.6	/	/	3.8	2.94	2.58	3.1
Ga	13.5	3.4	/	/	/	/	/	/	4.45	/
Hf	5.55	0.0458	/	/	/	/	/	/	/	/
Hg	0.037	0.035	0.66	0.311	0.17	0.13	/	0.244	0.095	/
In	0.05	0.0177	/	/	/	/	/	/	/	/
K (%)	1.92	0.113	/	/	/	/	1.4	1.2	0.125	1.5
La	23.5	13.6	32	23	/	/	30	22	13.5	28
Li	/	11.3	/	/	/	/	/	/	18.95	37
Mg (%)	0.77	0.282	/	/	/	/	10.87	1.56	0.79	1.3
Mn	382	435	1090	802	862	871	902	753	612.5	714
Mo	0.62	0.42	1	2.4	1	1	/	/	0.85	1.2
Nb	9.68	0.52	8.4	5.3	/	/	/	/	0.685	7.1
Ni	14	14.4	47	36	29.2	32.5	47	29	27.5	32
P (%)	0.128	0.065	/	/	/	/	0.063	0.09	0.09	0.1
Pb	15	17.7	42	217	42	37	34	56	43.95	74
Rb	80	13.9	/	/	/	/	/	/	19.15	93
S (%)	227	0.03	/	/	/	/	/	/	0.04	0.1
Sb	0.6	0.28	1.1	3.9	/	/	/	/	0.86	1.1
Sc	8.21	2	12	9.4	/	/	13	9.5	3.1	10
Se	/	0.4	/	/	1.23	1.27	/	/	0.4	/
Sn	3	0.81	3.2	7.9	/	/	/	/	2.3	3.4
Sr	89	17.8	76	116	/	/	82	81	20.05	106
Th	7.24	2.5	11	7.8	/	/	11	6	2	9
Ti (%)	0.572	0.007	0.31	0.23	/	/	0.36	0.19	0.026	0.3
Tl	0.66	0.115	/	/	0.68	0.66	/	/	0.17	/
U	2	0.74	/	/	/	/	3.4	/	1.1	2.9
V	33	26	101	70	71	79	113	82	32	81
Y	21	6.5	16	16	/	/	15	16	8.9	14.1
Zn	48	46	124	465	99	95	104	25	130.5	314
Zr	231	1.6	39	23	/	/	46	40	0.3	36

method) were performed using the data of all 43 elements in order to investigate relationships between elements. The presented data will also serve as a baseline for monitoring future changes in the soil chemical composition.

Study site

The small town Idrija (Fig. 1) with 5,905 inhabitants reported in 2016 (STAT, 2017) is situated approximately 50 km west of Ljubljana, the capital of Slovenia. Along the Nikova and Idrijca rivers a small densely populated centre is developed, where residential apartment buildings as well as individual houses are located. The highly urbanized town centre quickly passes into steep, sparsely populated rural area, where mostly individual houses are situated. In the most urbanized parts, there are still several urban green spaces, such as parks and playgrounds. Two main roads follow the Idrijca and Nikova rivers, where traffic is heavy during rush hours, while on other streets and roads, traffic is light. Mercury mining and ore-processing presented the main reasons for urban and economic growth in the studied area. Mercury was discovered in 1490 and exploited for almost 500 years. The mine was closed in 1995. Idrija, one of the world's largest mercury mining site, was enlisted recently in the UNESCO World heritage list. After the mine closure, Kolektor, a commutator production company, that had started in the year 1963 as a small factory, developed into a successful global company (Kolektor, 2014). Its manufacturing facilities are located on both banks of the river Idrijca in the northern part of Idrija, where Hg ore roasting facilities were formerly located. The dominant wastes in the Kolektor's manufacturing process are plastic and nonferrous metals, primarily copper (Benčina, 2007).

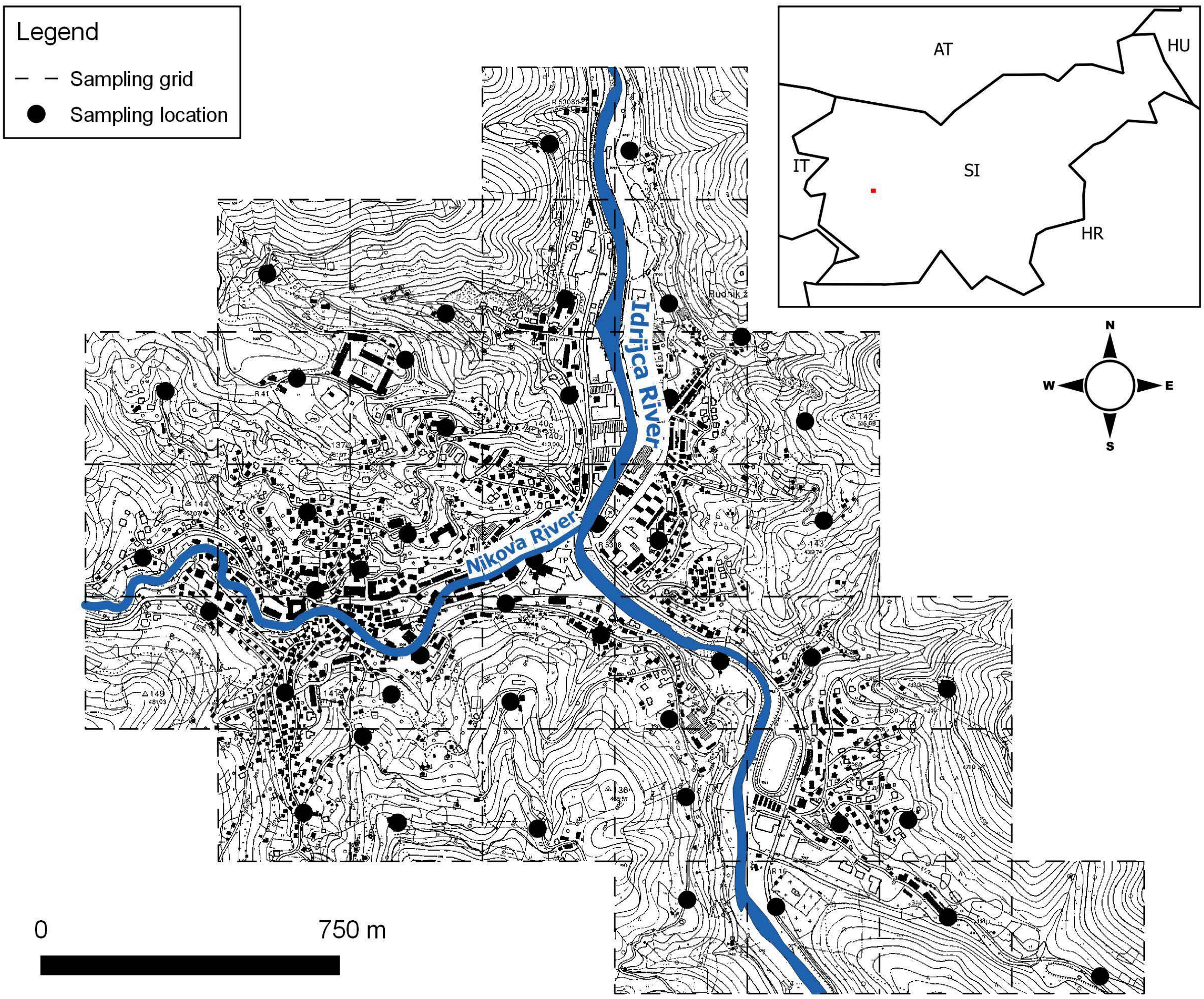

Fig. 1. Study area with sampling locations.

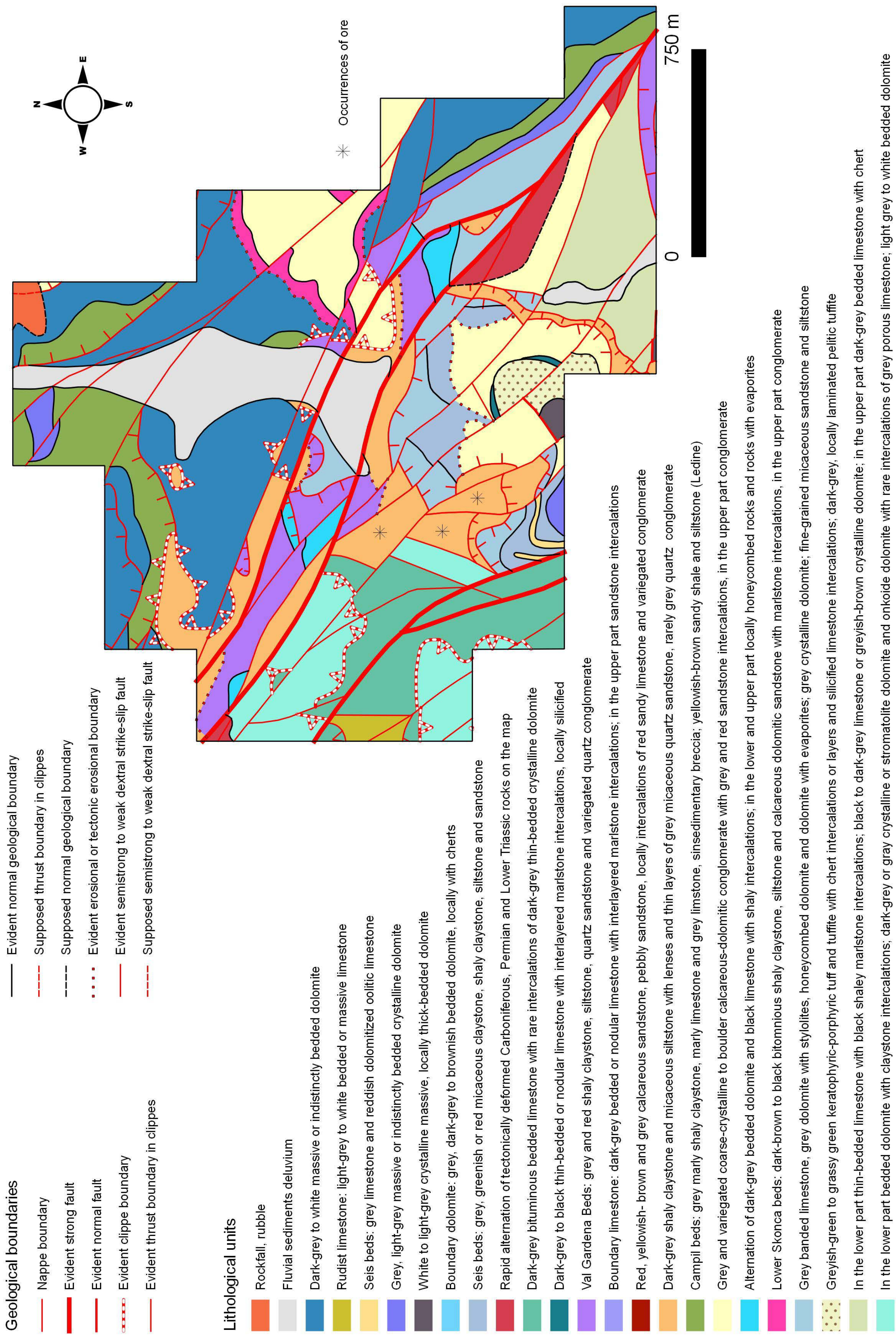

Fig. 2. Geological structure and lithological composition of the study area based on the data by Mlakar & Čar (2009, 2010)

A special characteristic of the town is that it is situated directly over the Idrija ore deposit. Ore deposit is monometallic, because mercury is the only mineral found in economically important quantities, while other ore elements occur only in traces or insignificant quantities (Čar, 1998). Several Hg sources were identified in the urbanised area, such as outcrops of rocks containing Hg ore, former ore roasting sites, ore residue dumps and mine ventilation shafts, which are discussed in detail by Bavec et al. (2014).

Geological properties

The detailed geological properties of the study area are presented in Fig. 2. The data were extracted out of the Geological map of the Idrija - Cerkljansko hills between Stopnik and Rovte 1:25000 and the associated explanatory book (Mlakar & Čar, 2009, 2010). In general about 70 % of the investigated territory consists of chemical sedimentary rocks (mainly different types of carbonate rocks - limestones and dolomites, rarely cherts), while about 30 % consists of detrital sedimentary rocks (breccias, conglomerates, sandstones, mudstones, claystones and shales). On the banks, along the Idrijca River, fluvial sediments deluvium occurs on the surface (Mlakar & Čar, 2009, 2010).

Pedological properties

With regard to the soil map of Slovenia (MKGP, 2017) (Fig. 3), the investigated territory in the urbanized area, along the Nikova and Idrijca rivers, consists of 100 % urban, water and non-fertile

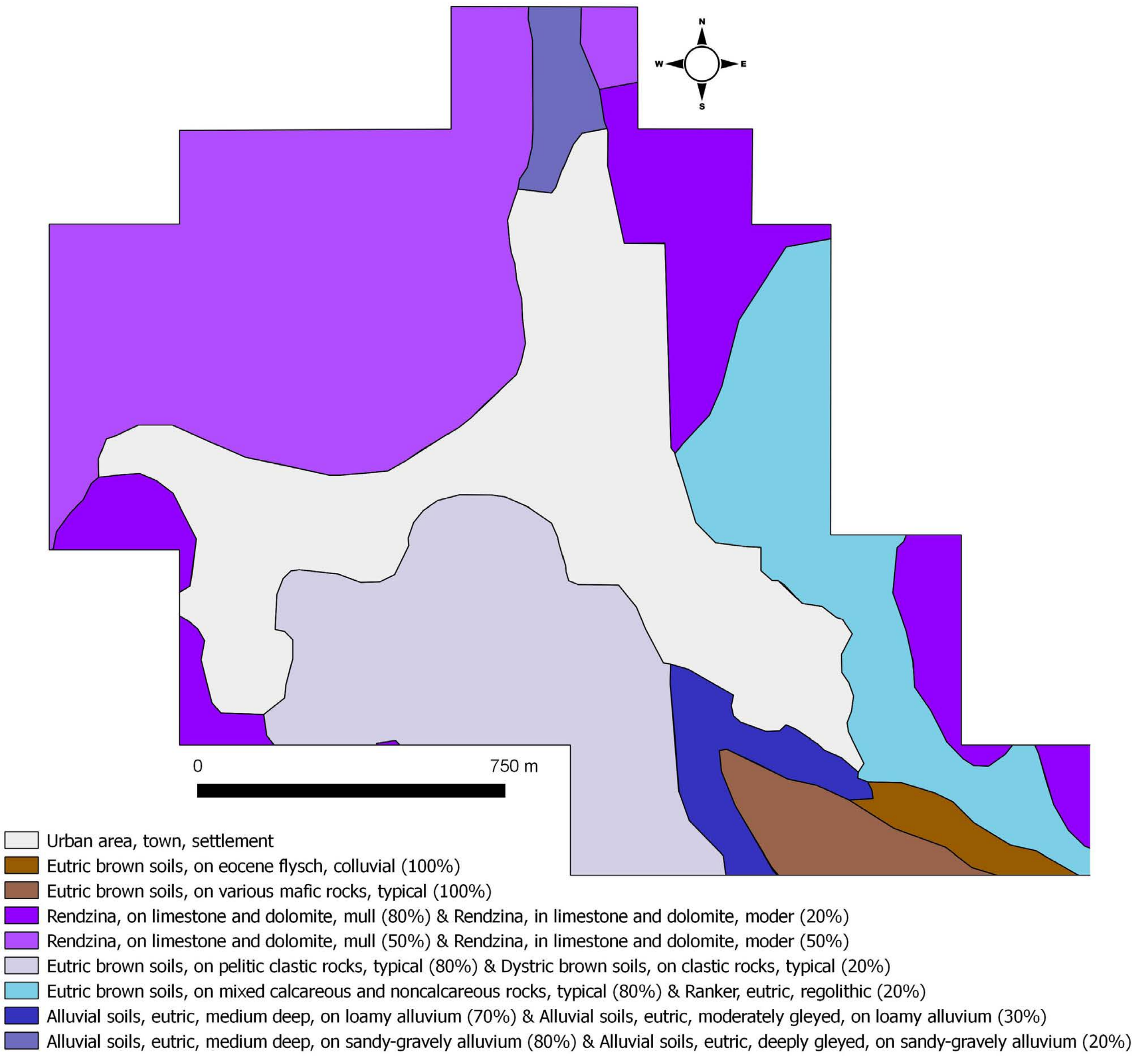

Fig. 3. Pedological composition of the study area based on the data by MKGP (2017).

surfaces. In the SW, NW and NE part rendzinas on limestone and dolomite with mull or moder humus are developed. In the SE eutric brown soils, on mixed carbonate rocks and regolithic eutric ranker with inclusions of eutric non-gleyic colluvial and deluvial soils are developed. In the S eutric brown soils on pelitic clastic rocks and dystric brown soils on clastic rocks are developed. In the E eutric brown soils on mixed calcareous and noncalcareous rocks and regolithic eutric ranker are developed. Along the Idrijca River at the SE part of the area eutric, medium deep or deeply gleeyed alluvial soils on sandy-gravely alluvium are developed. In the most SE part eutric brown soils on Eocene flysch or various mafic rocks are developed (MKGP, 2017).

Materials and Methods

The details of sampling, sample preparation, chemical analyses and quality control are described in Bavec et al. (2015) and are summarised below as follows:

Sampling and sample preparation

A total of 45 sampling locations were established following the sampling grid (Fig. 1). On each location, grassland topsoil (0–10 cm) and subsoil (10–20) samples were collected at urban area and nearby rural surroundings. Approximately 1 kg of each sample was collected and treated in the laboratory to determine aqua regia extractable concentrations of investigated elements. Samples were oven dried at below 30°C. Dry samples were gently crushed in a ceramic mortar, sieved through a 2 mm mesh sieve and homogenised in agate ball mill to the analytical fineness of <0.063 mm.

Chemical analyses and quality control

After aqua regia (1:1:1 $HCl:HNO_3:H_2O$) digestion, the levels of elements (N = 53; Ag, Al, As, Au, B, Ba, Be, Bi, Ca, Cd, Ce, Co, Cr, Cs, Cu, Fe, Ga, Ge, Hf, Hg, In, K, La, Li, Mg, Mn, Mo, Na, Nb, Ni, P, Pb, Rb, Re, S, Sb, Sc, Se, Sn, Sr, Ta, Te, Th, Ti, Tl, U, V, W, Y, Zn, Zr, Pd and Pt) were determined at Bureau Veritas Minerals, Canada-Vancouver (accredited under ISO 9001:2008) with inductively coupled plasma (ICP) mass spectrometry (MS). The samples that contained Hg levels above the upper detection limit for ICP-MS (50 mg/kg) were analysed with ICP emission spectrometry (ES). To ensure quality control of the analysis (AOAC INTERNATIONAL, 2016) standard reference materials (SRMs) provided by Bureau Veritas Minerals (DS8 and OREAS45CA for ICP-MS run and GC-7 for ICP-ES run), blank spikes and sample replicates were used. Quality control is an integral part of any project in environmental geochemistry, because it enables the quantification of analytical recovery (accuracy) and relative standard deviation (precision), which clearly show whether the results of the multi-elemental analysis are trustworthy (Reimann et al., 2008). During the ICP-MS run additional SRMs, OREAS44P and NGU, which was provided by the urban geochemistry project (EGS, 2011, 2013, 2014, 2015, 2016), were used in order to independently check the quality control of analysis. SRM DS8 and OREAS45CA included referenced values for all investigated elements, except B and Ta, which were immediately excluded from the further analyses. SRM OREAS45PP included referenced values for As, Ba, Cu, Au, Pb, Mo, Ni, W and Zn and NGU for As, Pb, Cd, Cu, Cr, Hg, Ni and Zn. Elements (Au, Na, W, Te, Ge, Re, Pd and Pt), which had more than 20 % of measured values below the lower limit of detection (LDL), were also excluded from geochemical analyses with regard to Miesch (1976). With regard to AOAC INTERNATIONAL (2016) guidelines, analytical recoveries (RE) and relative standard deviations (RSD) were acceptable (80 % ≤ RE ≤ 120 %; 0 % ≤ RSD ≤ 20 %;) for studied elements (Table 2) with only few exceptions (Hg in SRM STD8 and OREAS45CA and Mo, Nb, Sb and Se in SRM OREAS45CA). However, analytical recoveries and relative standard deviations were good or acceptable at least in one SRMs tested for each investigated element, therefore the reliability of the chemical analysis was considered satisfactory for the purposes of this study and the results were used for further statistical and spatial analyses.

Statistical analyses

Analyses of statistical distribution (descriptive statistics) were performed using Excel 2010 software. Distribution of the data was examined with the use of box-plot diagrams, histograms and calculation of skewness and kurtosis. The majority of the elements is non-normally distributed, thus nonparametric Spearman correlations (r_s) were calculated and a correlation-matrix-based hierarchical clustering method was performed with the use of R 3.4.0. and R studio software in order to extract correlation patterns between elements in topsoil and display them

Table 2. Data set of quality control

			STD8				OREAS45CA				OREAS44P				NGU			
EL	**Unit**	**LDL**	**ME (N=4)**	**RV**	**RE (%)**	**RSD (%)**	**ME (N=7)**	**RV**	**RE (%)**	**RSD (%)**	**ME (N=4)**	**RV**	**RE (%)**	**RSD (%)**	**ME (N=4)**	**RV**	**RE (%)**	**RSD (%)**
Ag	**µg/kg**	**2**	1691.7	1690	100	5.8	259.6	275	94	6.6	610.5	/	/	0.9	47.8	47.5	101	2.7
Al	**%**	**0.01**	0.9	0.93	97	4.9	3.6	3.592	101	6.5	1.0	/	/	0.9	0.8	/	/	3.4
****As***	**mg/kg**	**0.1**	25.9	26	100	5.2	3.7	3.8	97	10.0	97.5	95	103	1.1	2.4	1.14	206	7.1
Ba	**mg/kg**	**0.5**	281.1	279	101	3.8	157.7	164	96	5.2	169.8	167	102	1.8	31.8	/	/	3.0
Be	**mg/kg**	**0.1**	5.5	5.2	105	6.2	0.6	/	/	20.3	1.7	/	/	12.4	0.1	/	/	34.6
Bi	**mg/kg**	**0.02**	6.3	6.67	94	5.7	0.2	0.19	91	13.7	8.2	/	/	3.6	0.1	/	/	6.9
Ca	**%**	**0.01**	0.7	0.7	100	4.1	0.4	0.427	93	3.1	0.3	/	/	2.6	0.3	/	/	2.0
****Cd***	**mg/kg**	**0.01**	2.4	2.38	101	5.0	0.1	0.1	104	8.7	0.4	/	/	6.4	0.1	0.103	97	12.2
Ce	**mg/kg**	**0.1**	26.0	29.8	87	9.7	34.2	35	98	5.2	37.1	/	/	2.4	27.4	/	/	4.8
****Co***	**mg/kg**	**0.1**	7.3	7.5	97	4.5	85.4	92	93	2.8	57.8	/	/	1.9	7.9	/	/	4.7
****Cr***	**mg/kg**	**0.5**	115.0	115	100	2.2	681.3	709	96	6.3	437.9	/	/	4.1	38.6	58.4	66	6.2
Cs	**mg/kg**	**0.02**	2.4	2.48	95	4.7	1.1	1.03	105	8.9	1.3	/	/	4.6	0.8	/	/	4.2
****Cu***	**mg/kg**	**0.01**	106.4	110	97	4.3	489.3	494	99	3.8	404.9	410	99	0.6	19.2	17	113	5.0
Fe	**%**	**0.01**	2.4	2.46	99	3.8	15.2	15.69	97	4.3	24.0	/	/	2.5	1.4	/	/	3.4
Ga	**mg/kg**	**0.1**	4.7	4.7	99	4.8	18.1	18.4	99	6.8	2.6	/	/	2.8	2.6	/	/	3.8
Hf	**mg/kg**	**0.02**	0.1	0.08	79	7.4	0.5	0.5	103	9.4	0.1	/	/	17.9	0.1	/	/	16.1
****Hg***	**µg/kg**	**5**	216.8	192	113	25.7	42.9	30	143	35.5	97.5	/	/	21.4	63.8	66	96.59	7.6
In	**mg/kg**	**0.02**	2.2	2.19	99	7.5	0.1	0.09	102	7.0	0.1	/	/	18.6	/	/	/	/
K	**%**	**0.01**	0.4	0.41	100	4.0	0.1	0.072	98	7.6	0.2	/	/	2.6	0.1	/	/	0.0
La	**mg/kg**	**0.5**	15.1	14.6	103	12.0	16.5	15.9	104	8.4	18.1	/	/	2.2	13.6	/	/	5.5
Li	**mg/kg**	**0.1**	26.9	26.34	102	5.8	7.7	6.2	124	11.1	7.1	/	/	1.9	9.2	/	/	6.1
Mg	**%**	**0.01**	0.6	0.605	100	3.9	0.2	0.139	111	9.7	0.3	/	/	1.2	0.6	/	/	2.9
Mn	**mg/kg**	**1**	605.2	615	98	2.9	902.7	943	96	3.8	714.8	/	/	2.2	269.0	/	/	4.4
****Mo***	**mg/kg**	**0.01**	12.6	13.44	94	5.7	0.7	1	71	19.9	354.0	407	87	0.5	0.3	/	/	6.9
Nb	**mg/kg**	**0.02**	0.7	1.1	63	13.5	0.1	0.22	68	23.7	0.03	/	/	14.1	0.5	/	/	6.0
****Ni***	**mg/kg**	**0.1**	36.3	38.1	95	4.3	243.2	240	101	4.3	460.8	401	115	0.2	25.4	27.8	91	4.7
P	**%**	**0**	0.1	0.08	100	6.9	0.04	0.039	101	2.5	0.03	/	/	2.3	0.05	/	/	5.0
****Pb***	**mg/kg**	**0.01**	121.8	123	99	6.4	20.1	20	101	8.8	182.5	183	100	1.2	8.4	8.29	101	3.9
Rb	**mg/kg**	**0.1**	37.1	39	95	6.7	8.9	8.2	108	10.4	11.5	/	/	3.2	12.3	/	/	2.9
S	**%**	**0.02**	0.2	0.168	95	3.6	0.0	0.021	107	19.2	/	/	/	/	/	/	/	/
Sb	**mg/kg**	**0.02**	3.8	4.8	78	11.6	0.1	0.13	56	36.5	2.4	/	/	19.0	0.1	/	/	20.0
Sc	**mg/kg**	**0.1**	2.1	2.3	93	6.4	38.5	39.7	97	6.0	4.1	/	/	2.9	2.0	/	/	5.4
Se	**mg/kg**	**0.1**	5.2	5.23	99	4.3	0.6	0.5	123	20.3	0.3	/	/	21.1	0.3	/	/	30.2
Sn	**mg/kg**	**0.1**	6.7	6.7	100	4.1	1.9	1.8	106	4.4	1.1	/	/	0.0	0.5	/	/	8.2
Sr	**mg/kg**	**0.5**	66.6	67.7	98	6.2	15.8	15	105	5.6	17.8	/	/	1.6	12.0	/	/	3.4
Th	**mg/kg**	**0.1**	6.3	6.89	91	10.7	6.8	7	97	10.8	6.0	/	/	0.6	2.8	/	/	3.9
Ti	**%**	**0**	0.1	0.113	94	3.9	0.1	0.128	97	6.3	0.0	/	/	14.9	0.1	/	/	1.5
Tl	**mg/kg**	**0.02**	5.3	5.4	97	4.9	0.1	0.07	108	23.3	0.3	/	/	2.4	0.1	/	/	4.4
U	**mg/kg**	**0.1**	2.6	2.8	93	12.9	1.1	1.2	94	11.3	2.6	/	/	1.8	0.6	/	/	0.0
V	**mg/kg**	**2**	39.8	41.1	97	4.9	200.6	215	93	2.8	25.8	/	/	1.5	22.8	/	/	1.9
Y	**mg/kg**	**0.01**	5.6	6.1	91	7.9	8.1	7.84	104	6.2	6.9	/	/	0.7	6.5	/	/	1.4
****Zn***	**mg/kg**	**0.1**	314.3	312	101	3.8	60.3	60	101	5.3	585.0	579	101	1.4	40.1	/	/	4.2
Zr	**mg/kg**	**0.1**	1.7	2.1	80	10.5	20.7	21.6	96	7.3	4.1	/	/	20.9	2.9	/	/	6.5

LDL = lower detection limit, ME = median, RV = referenced value, RE = Analytical recovery, RSD = relative standard deviation,

*after Bavec et al. (2015)

graphically (Wei & Simko, 2016). It was qualitatively assumed that correlations at statistically high significance ($p < 0.001$) reveal a strong association between elements. Correlation network model (Epskamp, 2014) was produced to visualize correlation patterns between elements in topsoil. With the use of Surfer 13 software, the universal kriging with linear variogram interpolation method (Davis, 1986) was applied for the construction of surface grid models showing the spatial distribution of elements in topsoil. For a graphical display of spatial distribution the maps with percentile distribution, where different colours represent different concentration arrangements, were produced with the use of QGIS 2.18.7 software. The seven classes of following percentile values were applied: 0–10, 10–25, 25–40, 40–60, 60–75, 75–90 and 90–100. The rest of the maps in this study were produced with the use of QGIS 2.18.7 software.

Results and discussion

Descriptive statistics of analysed elements (n = 43) in the Idrija top- and subsoil are given in Table 3 together with limit/ warning/ critical soil levels from current Slovenian legislation (Official Gazette RS, 1996), indicative/ intervention levels for severe contamination from the International guidelines (Soil Remediation Circular, 2013) and correlation coefficients of elements between top- and subsoil. The statistical distribution of elements in top- and subsoil is presented with boxplots (Fig. 4, 5, 6, 7 and 8) together with European grazing land soil medians (Reimann et al., 2014; European medians in further text) and Maribor urban soil medians (Gaberšek & Gosar, 2017; Maribor medians in further text), which were also determined after aqua regia digestion.

Potentially harmful elements (PHE; Ag, As, Ba, Be, Cd, Co, Cr, Cu, Hg, Mo, Ni, Sb, Se, Sn, Pb, Th, V and Zn)

First, attention is drawn to the 10 elements (As, Cd, Co, Cr, Cu, Hg, Mo, Ni, Pb and Zn), which are recognized as the most hazardous for ecosystems and human health in the national legislative regulations (Official Gazette RS, 1996). The comparison of the 10 elements to legislative levels was already established by Bavec et al. (2015), where it was found that 82 out of the 90 investigated soil samples exceeded the value for Hg of 10 mg/kg (Official Gazette RS, 1996), while other elements were below the national guidelines, with few exceptions; critical level for Cu (300 mg/kg) was exceeded in a single topsoil sample and critical level for As (55 mg/kg) in 2 topsoil and its subsoil pair samples. The 10 dangerous element median levels were also compared to median levels in soil of different urban areas around the world and the comparison showed only Hg is significantly enriched (several hundred or even thousand times) in Idrija top- and subsoil, while other elements were below, within or slightly above the reported metal concentrations in worldwide studies (Bavec et al., 2015). High Hg values, that were already discussed by Bavec et al. (2015), are in good agreement with other studies (Gosar et al., 2006; Teršič et al. 2011a, 2011b; Bavec et al. 2016; Baptista-Salazar et al., 2017), which showed mercury enrichment in Idrija soil due to the 500 years of mining and processing of mercury ore.

In addition to the above 10 elements, the international guidelines (Soil Remediation Circular, 2013) include intervention values for 2 elements, Ba and Sb, and indicative levels for severe contamination for six elements (Ag, Be, Se, Sn, Th,

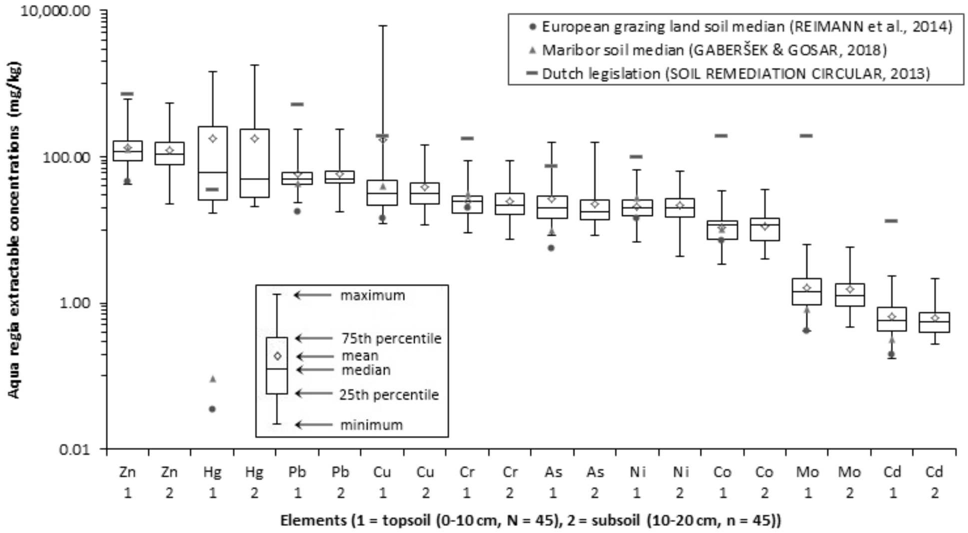

Fig. 4. Statistical distribution of PHE in Idrija topsoil and subsoil (the figure was modified after Bavec et al., 2015) together with European grazing land soil medians (Reimann et al., 2014), Maribor urban soil medians (Gaberšek & Gosar, 2018) and Dutch legislation values (Soil Remediation Circular, 2013).

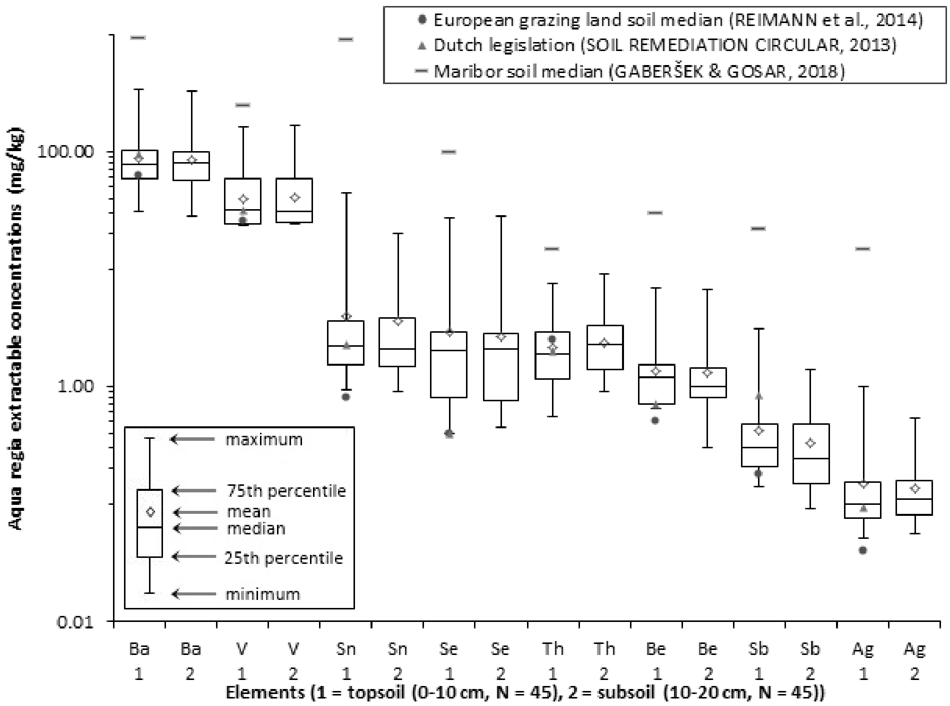

Fig. 5. Statistical distribution of PHE in Idrija topsoil and subsoil together with European grazing land soil medians (Reimann et al., 2014), Maribor urban soil medians (Gaberšek & Gosar, 2018) and Dutch legislation values (Soil Remediation Circular, 2013).

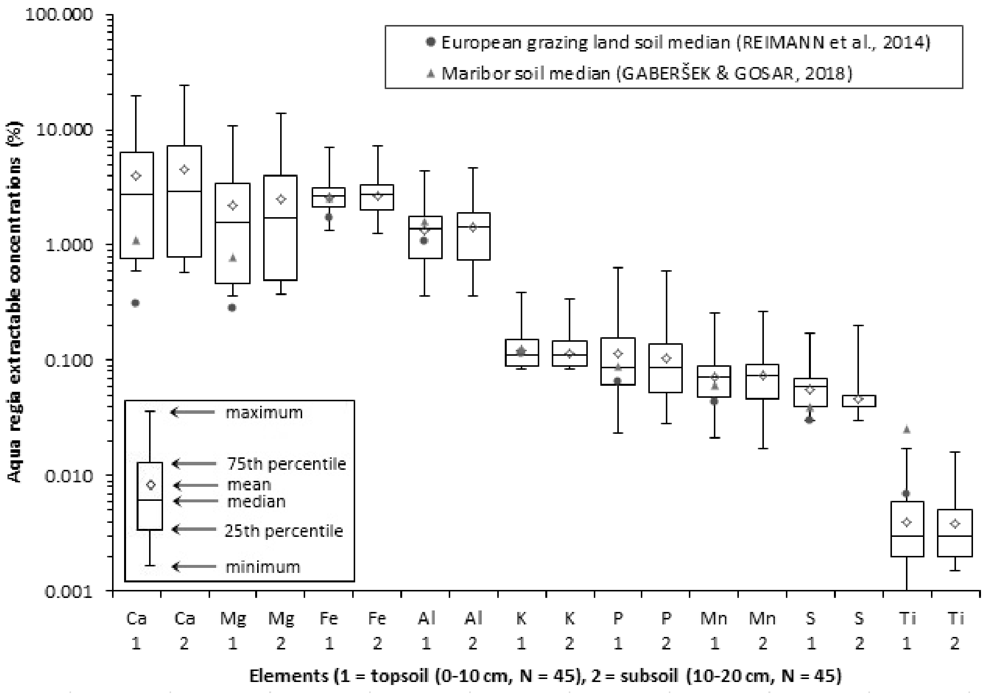

Fig. 6. Statistical distribution of major elements in Idrija topsoil and subsoil together with European grazing land soil medians (Reimann et al., 2014) and Maribor urban soil medians (Gaberšek & Gosar, 2018).

V). In Fig. 4 and 5 it is shown that PHE are not exceeded in Idrija soils with regard to the international guidelines, except Hg, as expected. It is also shown that top- and subsoil samples have similar statistical distribution of PHE, and that Idrija top- and subsoil medians are similar to Maribor soil medians and slightly higher than European soil medians, with exception of Hg and Se median. Mercury and Se median are much higher in comparison with both, Maribor and European median, especially Hg.

Major elements (Al, Ca, Fe, K, Mg, Mn, P, S and Ti)

Top- and subsoil samples have similar statistical distribution of major elements (Fig. 6). Calcium and Mg median levels in Idrija soil are slightly higher than in Maribor and European soil. Iron, Al, K, P, Mn and S median levels are similar to European and Maribor medians, while median level of Ti is lower.

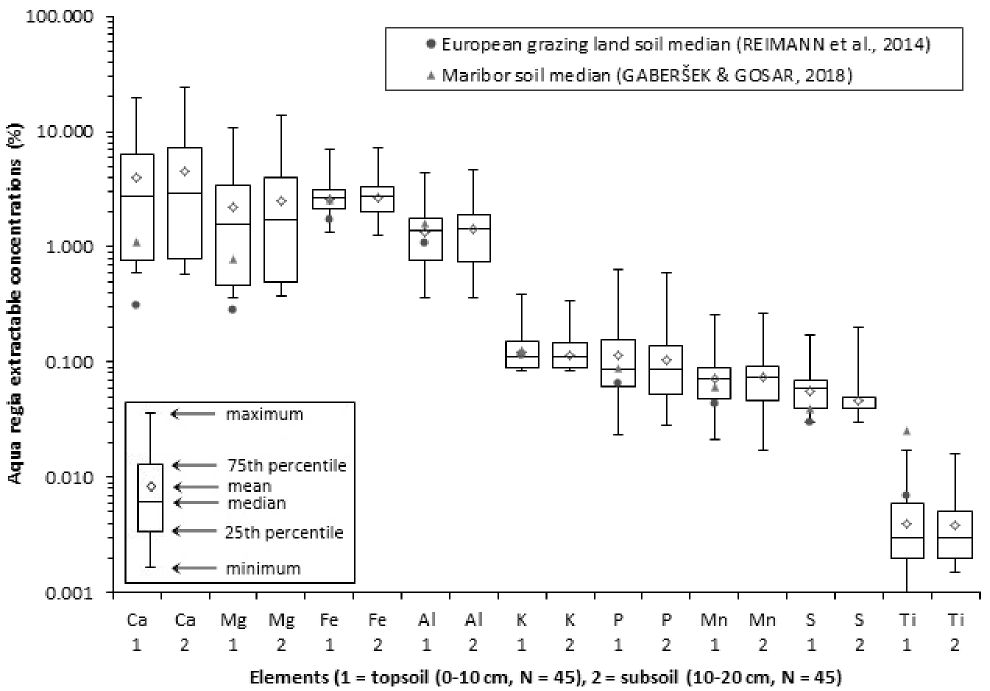

Fig. 7. Statistical distribution of REE in Idrija topsoil and subsoil together with European grazing land soil medians (Reimann et al., 2014) and Maribor urban soil medians (Gaberšek & Gosar, 2018).

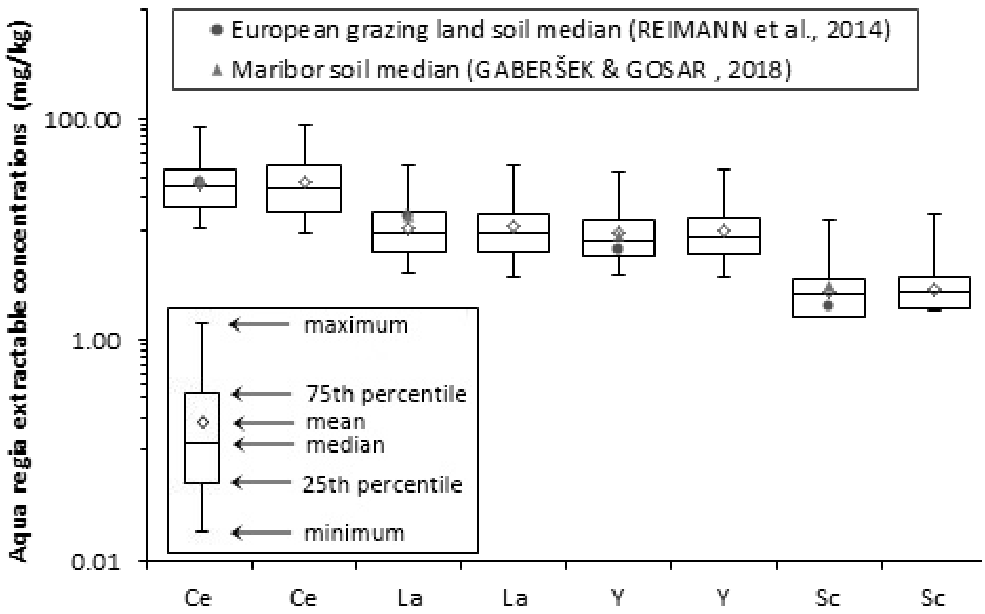

Fig. 8. Statistical distribution of other elements in Idrija topsoil and subsoil together with European grazing land soil medians (Reimann et al., 2014) and Maribor urban soil medians (Gaberšek & Gosar, 2018).

Rare earth elements (REE; Ce, La, Y and Sc) and other elements (Sr, Rb, Li, Ga, Zr, U, Cs, Nb, Bi, Tl, Hf and In)

Top- and subsoil samples have similar statistical distribution of REE (Fig. 7) and other elements (Fig. 8). Median levels of REE and other elements are similar to European and Maribor medians, with exception of Hf and In. Hafnium median in Idrija soil is lower in comparison with European and Maribor soil. Indium median in Idrija soil is higher in comparison with European soil.

Correlations and spatial distribution

Spearman rank correlation test for 10 PHE between top- and subsoil was already performed by Bavec et al. (2015) who found out strong positive correlation of element concentrations between topsoil and subsoil. The rest of the elements presented in this study (Table 3) also show strong positive correlation between topsoil and subsoil, except Be. It was shown that element distribution in topsoil and subsoil is not statistically different.

Table 3. Mean, median, minimum and maximum levels of 43 elements in Idrijan top- (0-10 cm) and subsoil (10-20 cm) (all levels are in mg/kg, except where otherwise stated); Slovenian and Dutch legislation data (in mg/kg); correlation coefficients (r_s) of elements between top- and subsoil.

Element	mean	median	min	max	mean	median	min	max	r_s	Slovenian legislation[1]	Dutch legislation[2]
Depth (cm)	0-10	0-10	0-10	0-10	10-20	10-20	10-20	10-20			
Ag	0.147	0.1	0.026	0.832	0.137	0.109	0.026	0.389	0.81	-	15**
Al (%)	1.3	1.4	0.4	2.7	1.4	1.4	0.4	2.8	0.96	-	-
As3	26.3	20.3	6.3	128.9	22.7	18.0	5.1	131.2	0.783	20/30/55	76*
Ba	86.6	77.0	27.7	241.0	84.9	80.5	29.7	230.3	0.93	-	920***
Be	1.3	1.2	0.1	5.3	1.3	1.0	0.5	5.3	0.37	-	30**
Bi	0.4	0.4	0.1	1.2	0.4	0.4	0.1	0.8	0.89	-	-
Ca (%)	4.0	2.7	0.2	13.5	4.6	3.0	0.2	17.3	0.98	-	-
Cd3	0.8	0.7	0.3	1.6	0.6	0.6	0.1	1.4	0.833	1.02.2012	13*
Ce	25.8	25.1	5.3	50.6	26.9	24.1	5.2	51.8	0.97	-	-
Co3	11.0	11.7	4.2	20.5	11.4	11.8	3.1	21.2	0.923	20/50/240	190*
Cr3	24.5	24.5	8.0	598.0	24.8	22.2	9.1	55.9	0.933	100/150/380	180/78*
Cs	0.7	0.6	0.1	2.1	0.9	0.7	0.2	2.2	0.97	-	-
Cu3	170.6	31.6	10.0	6067.8	38.0	31.1	10.7	98.1	0.863	60/100/300	190*
Fe (%)	2.6	2.7	0.8	3.8	2.7	2.7	0.7	4.0	0.92	-	-
Ga	3.8	3.9	1.3	7.2	3.8	4.0	1.1	7.4	0.96	-	-
Hf	0.08	0.07	0.01	0.22	0.08	0.08	0.01	0.20	0.53		
Hg3	1768.0	608	8.5	1210	178.8	50	6.9	1550.0	0.973	0.8/2/10	36/4*
In	0.06	0.04	0.01	0.40	0.05	0.04	0.01	0.21	0.53		
K (%)	0.12	0.11	0.01	0.23	0.11	0.11	0.01	0.20	0.88	-	-
La	10.4	9.3	2.4	24.0	10.6	9.5	2.7	23.9	0.96	-	-
Li	13.4	11.0	3.2	29.6	14.3	12.1	4.3	35.0	0.93	-	-
Mg (%)	2.2	1.6	0.1	7.4	2.5	1.7	0.1	9.9	0.98	-	-
Mn	722.8	725.0	264.0	1687.0	735.9	747.0	297.0	1715.0	0.95	-	-
Mo3	1.7	1.5	0.6	4.2	1.6	1.3	0.4	4.1	0.913	10/40/200	190*
Nb	0.5	0.5	0.0	1.5	0.5	0.4	0.1	1.3	0.92	-	-
Ni3	21.0	19.7	8.7	40.2	21.6	20.3	10.3	37.6	0.93	50/70/210	100*
P (%)	0.1	0.1	0.0	0.5	0.1	0.1	0.0	0.5	0.94	-	-
Pb3	59.5	49.5	19.2	174.5	59.1	50.1	25.5	170.4	0.923	85/100/530	530*
Rb	13.1	12.4	4.4	30.0	13.6	13.4	3.9	29.0	0.98	-	-
S (%)	0.06	0.06	0.01	0.10	0.05	0.05	0.01	0.15	0.67	-	-
Sb	0.42	0.30	0.07	2.66	0.33	0.24	0.06	0.93	0.89	-	22*
Sc	2.7	2.6	0.1	8.6	2.9	2.7	0.1	10.2	0.91	-	-
Se	2.9	2.0	0.4	24.7	2.7	2.1	0.3	25.2	0.76	-	100**
Sn	3.9	2.2	0.6	40.7	3.6	2.1	0.6	16.4	0.93	-	900**
Sr	29.0	25.9	5.2	71.7	32.5	29.3	4.8	98.4	0.97	-	-
Th	2.1	1.9	0.6	4.7	2.3	2.3	0.5	5.8	0.97	-	15**
Ti (%)	0.004	0.003	0.001	0.011	0.004	0.003	0.001	0.011	0.9	-	-
Tl	0.32	0.30	0.09	0.63	0.33	0.33	0.08	0.63	0.87	-	-
U	1.6	1.5	0.6	3.3	1.6	1.6	0.7	3.6	0.94	-	-
V	40.0	31.5	1.0	103.0	40.5	31.0	1.0	111.0	0.93	-	250**
Y	9.4	7.9	2.0	20.8	9.7	8.5	2.4	23.1	0.96	-	-
Zn3	133.4	119.6	45.7	464.3	123.9	109.3	54.7	391.1	0.943	200/300/720	720*
Zr	1.7	1.8	0.1	4.7	1.9	1.8	0.1	5.1	0.91	-	-

min = minimum; max = maximum, r_s = Spearman correlation coefficients of elements between top- and subsoil; [1]Official Gazette RS, 1996 (limit/warning/critical values), [2]Soil Remediation Circular, 2013 (*intervention value, **indicative level for severe contamination, *** intervention value for Ba has been temporarily repealed, that is former value), [3]Bavec et al. 2015 (aqua regia, n=45); r_s = correlation coefficient

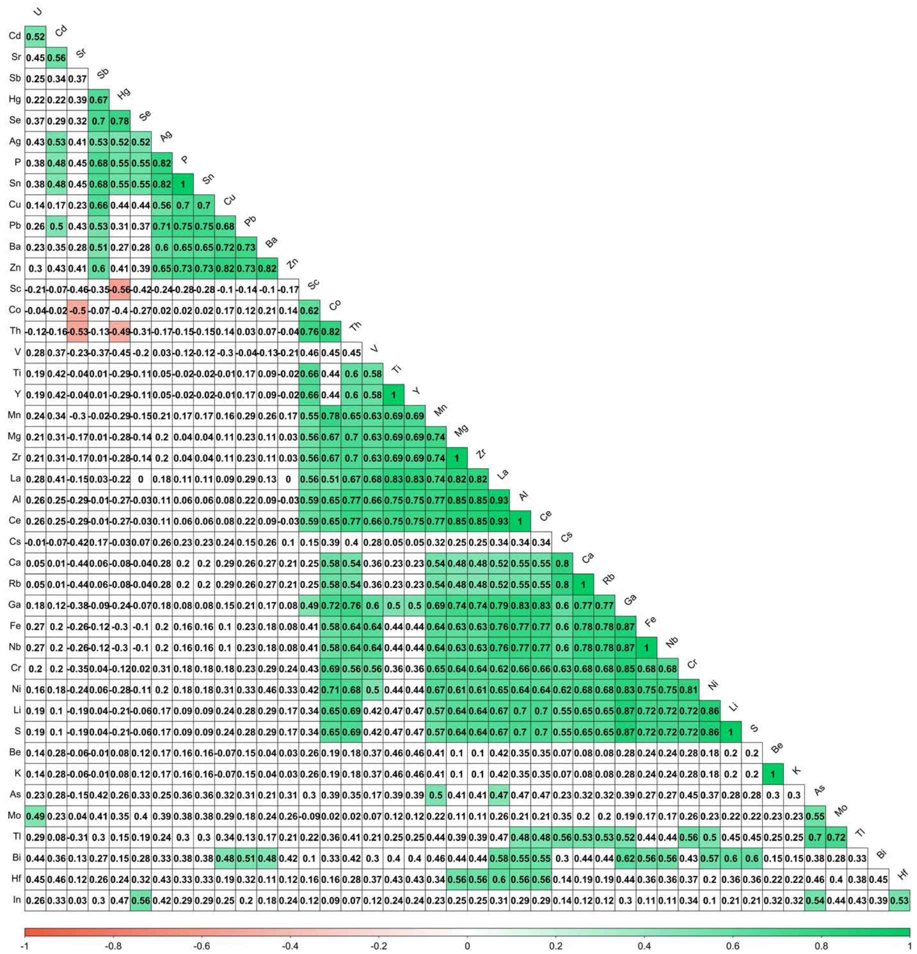

Fig. 9. Correlogram with correlation patterns between elements in topsoil; statisticaly significant positive (green) and negative (red) correlations at $p < 0.001$.

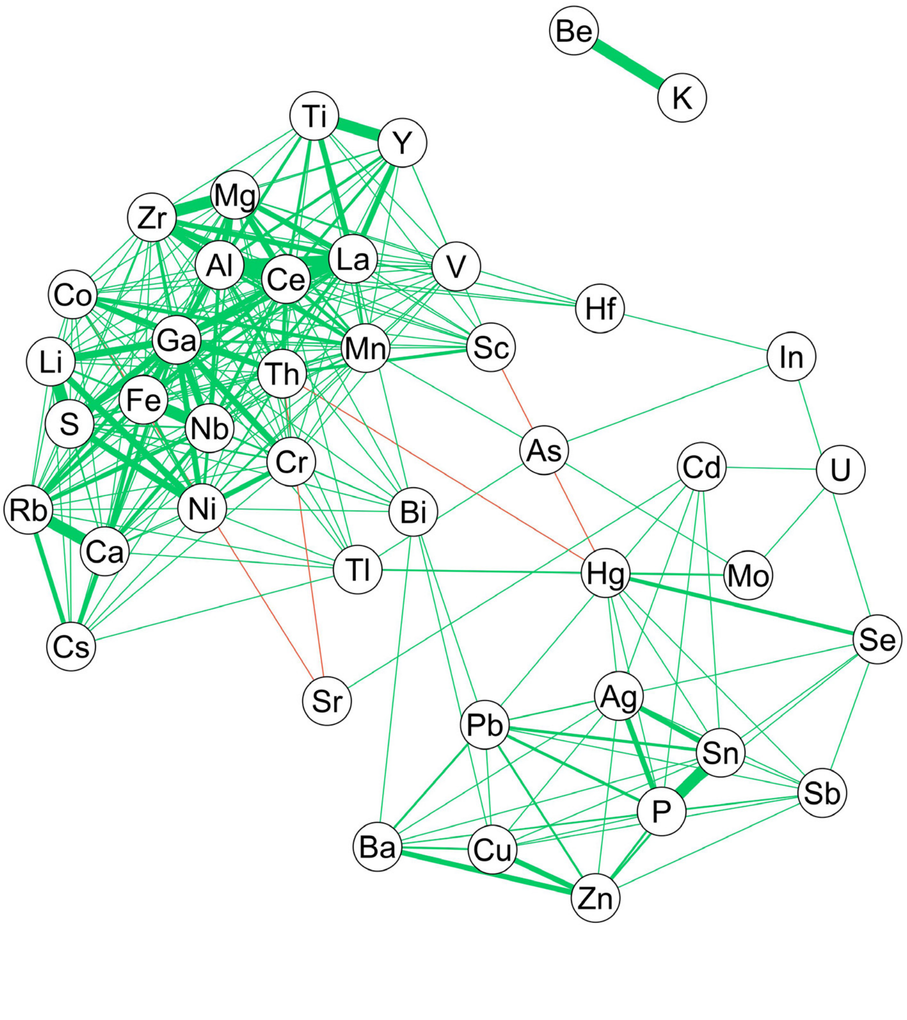

Fig. 10. Correlation network model between elements in topsoil; strong positive (green) and negative (red) coefficients ($p < 0.001$) are presented with proportional nodes.

Hierarchically ordered Spearman rank correlation coefficients between elements in topsoil (Fig. 9) and their network model (Fig. 10) indicated the following associations of elements, with regard to their significant positive correlations. A so called rural association of elements consisting of Al, Bi, Ca, Ce, Co, Cr, Cs, Fe, Ga, Hf, La, Li, Mg, Mn, Nb, Ni, Rb, S, Sc, Th, Ti, Tl, V, Y and Zr and rural-urban association of elements consisting of Ag, Ba, Cd, Cu, Hg, P, Pb, Se, Sb, Sn and Zn. In addition to rural and rural-urban associations, strong association was observed between Be-K. The associations of elements As, In, Mo, Sr and U are very limited compared to the above mentioned elements and these elements present an indirect links between rural and urban associations of elements. The association of elements with regard to their significant negative correlations (Co-Sr-Th and Sc-Hg-Th) (Fig. 9 and 10), are very limited as well.

The rural association of elements is closely related to their spatial distribution of higher concentrations. The higher concentrations of all the elements from the rural association, except Ca and Mg, are mostly found in the N, NE, NW, S and SW rural surroundings (see spatial distribution model of Mn as representative in Fig. 11), where limestone and dolomite bedrock predominate (Fig. 2). Therefore it is assumed that these elements reflect natural geological background levels that have been released during weathering processes of bedrock. Ca and Mg show very similar distribution (see spatial distribution model of Ca as representative in Fig. 11) and their higher concentrations occur, where dolomite bedrock (Fig. 2) prevails; that is in the central (urban) part of the studied area and in the SE surroundings (Fig. 2). However, higher concentrations of Ca and Mg could also originate from the material, which is underlying investigated soils in the urban area. During sampling it was observed that at urban green spaces, soil contained anthropogenic particles, such as plastic and brick particles, which indicated that the soil underlying material is embankment material. In the latter, Ca is found in residues of mortar, cement, gypsum and other components of building material. In addition, higher values can be due to the erosion of buildings and roads within the urban area.

With regard to the rural-urban association of elements, higher concentrations (see spatial distribution models of Cu, Pb and Zn as representative distributions in Fig. 11) were found in (1) N and SW rural surroundings, where limestone and dolomite bedrock prevail, (2) in the urban area at SW part, where ore containing clastic bedrock prevail and (3) along the Idrijca river, where fluvial sediments deluvium (Fig. 2) mixed with ore residue dumps (ČAR, 1998) prevail. DROVENIK et al. (1980) reported that BERCE (1958) analysed 4 samples of mercury ore and 2 samples of cinnabar and determined Cu in all samples. Later analyses (DROVENIK et al., 1980) also showed that Cu was detected in all samples in addition to Pb in 4 cinnabar samples and Zn in 2 samples (Table 4). Two samples of steel ore from Skonca beds contained organic substances and were especially enriched with Pb (Sample 6 and 7 in Table 4). Zn was especially high in metacinnabar sample (sample 10 in Table 4), which was explained as understandable, because Hg is often replaced by Zn in metacinnabar (DROVENIK et al., 1980). The authors also em-

Table 4. Geochemical contents of elements (in mg/kg; - means undeterminable and blank not measured) in mercury ore from Idrija by DROVENIK et al. (1980)

	5	6	7	8	9	10
Ag	-	4	-	/	/	/
Cu	1	200	16	100	11	5
Ga	-	13	10	3	-	-
Ge		3	10	7	-	-
Mn	5	5				
Ni	2.5	2.5				
Pb	32	1000	150	5	-	30
Tl		10	-	-	-	-
Zn	-	200	-	-	-	>1000

5 = Idrija (GRAFENAUER, 1969), 6-8 = Idrija, steel ore from Skonca beds, 7 = Idrija, steel ore from Upper Permian dolomite, 9 = Idrija, Cinnabar crystals from dolomite sheet, 10 = Idrija, metacinnabar aggregate from a fracture in Upper Sythian dolomite)

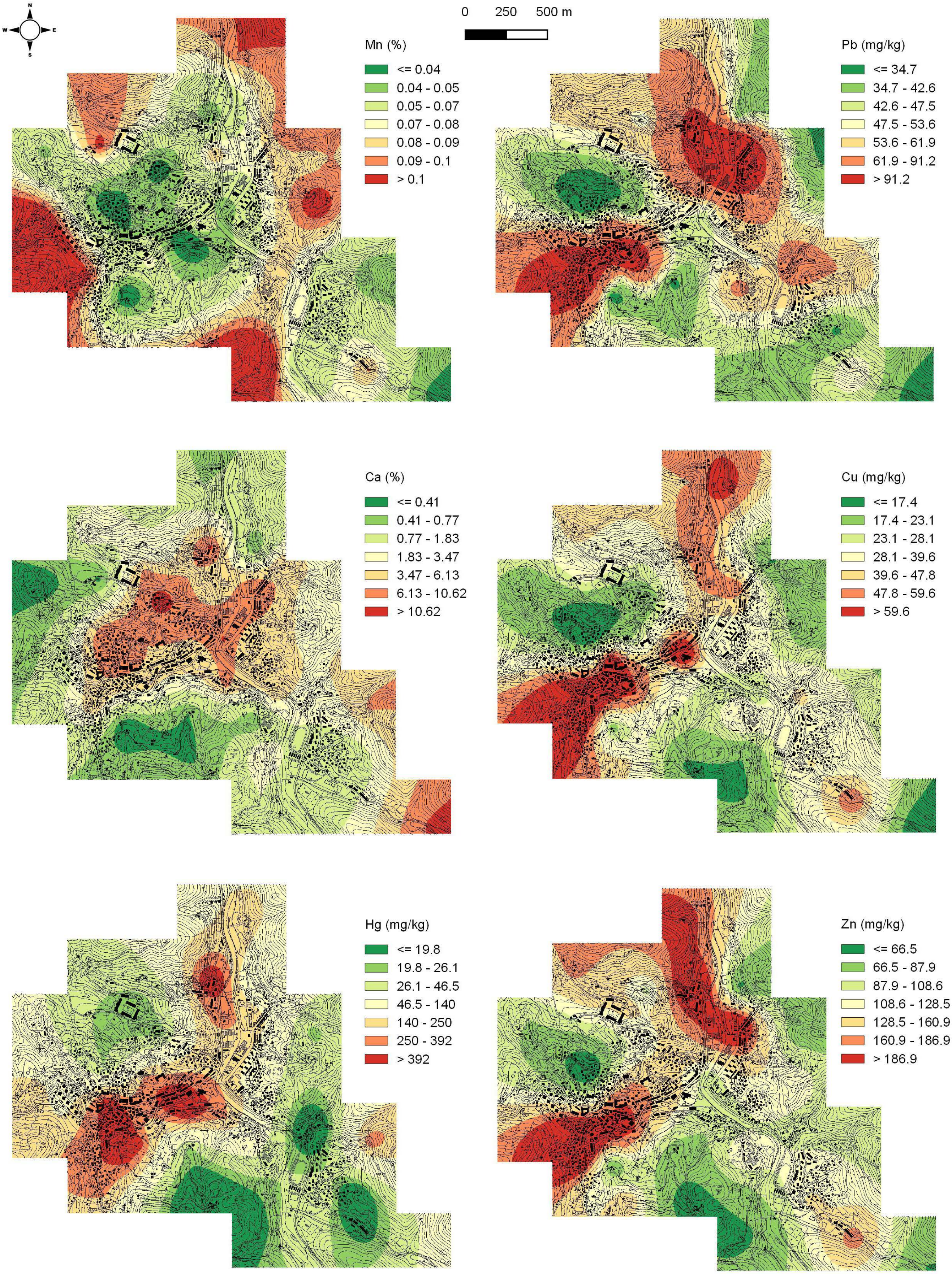

Fig. 11. Models of spatial distribution of selected elements in topsoil.

phasized that As and Sn were below the limit of detection in analysed samples. It is assumed that elements from rural-urban association reflect natural geological background levels, but are to a certain extent influenced by anthropogenic activities, such as traffic, industry (Kolektor's manufacturing process wastes are plastic and nonferrous metals, primarily Cu), households, but also past mining activities; especially deposits of mercury ore residues along the Nikova and Idrijca river. If we compare Hg distribution with Cu, Pb and Zn (Fig. 11), it is shown that higher concentrations occur in general from the SW along the Nikova River, toward the N along the Idrijca River after the confluence with Nikova. Spatial distribution of high Hg concentrations (Fig. 11) was already discussed by Bavec et al (2015). They found out that high Hg concentrations occur in the urban area and form a certain pattern of contamination in the SW-NE direction. The authors showed that contamination was only to a small extent a consequence of natural origin; in the SW part of the area, where soils overlie rocks containing mercury ore. However the contamination is predominantly of anthropogenic origin, such as ore residue dumps, roasting sites and related emissions and ventilation shafts that are/ were situated in the urban area.

Conclusion

The Idrija town urban area along the Nikova and Idrijca River, where anthropogenic influence is high, quickly passes into steep, sparsely populated rural surroundings with individual houses and farms, where anthropogenic is influence low. In this study geochemical baseline data set of 43 elements in soil of Idrija town was established to enable monitoring of future changes in the soil chemical composition. The results of soil levels of 43 elements, their hierarchically ordered Spearman rank correlation coefficients and their spatial distribution of highest levels are presented. The determined Idrija soil element medians were also compared to European grazing land and Maribor urban soil element medians. The results indicated that elements Al, Bi, Ca, Ce, Co, Cr, Cs, Fe, Ga, Hf, La, Li, Mg, Mn, Nb, Ni, Rb, S, Sc, Th, Ti, Tl, V, Y and Zr are enriched in the rural surroundings, while elements Ag, Ba, Cd, Cu, Hg, P, Pb, Se, Sb, Sn and Zn are enriched partly in the rural surroundings, but mostly in the urban area. It is assumed that elements, which are enriched in the rural surroundings, are of natural origin, while elements, which are enriched also in the urban area, are to a certain extent influenced by anthropogenic sources (ore residue dumps, households, traffic and industry). The statistical distribution of elements in top- and subsoil and strong positive correlation of elements between top- and subsoil showed that soil element distribution in the two investigated layers is not statistically different. In general, the median levels of elements in Idrija soil are mostly similar or slightly higher than in European grazing land soil and Maribor urban soil, with exception of Hg.

Acknowledgement

The presented study was financially supported by the Slovenian Research Agency (ARRS) in the frame of research programme Groundwater and Geochemistry (P1-0020), which is carried out by the Geological Survey of Slovenia. The author would like to thank the Mayor, Mr. Bojan Sever, and the Deputy Mayor, Mr. Bojan Režun, of the Idrija Municipality and the former staff, especially Ms. Tatjana Dizdarevič, of the now closed Idrija Mercury mine in liquidation, for their support during sampling of the soil in Idrija town. Special thanks go to dr. Mateja Gosar for help during fieldwork and for the very constructive comments and suggestions for improvement of the manuscript.

Literature

Andjelov, M. 2012: Regionalna porazdelitev geokemičnih prvin v tleh Slovenije = Regional distribution of geochemical elements in Slovenian soils. RMZ – Materials and Geoenvironment, 59/2: 125–140.

AOAC 2016: AOAC official methods of analysis. Guidelines for standard method performance requirements. Appendix F. Internet: http://www.eoma.aoac.org/app_f.pdf (29.1.2017).

Baptista-salazar, C., Richard, J.H., Horf, M., Rejc, M., Gosar, M. & Biester, H. 2017: Grain-size dependence of mercury speciation in river suspended matter, sediments and soils in a mercury mining area at varying hydrological conditions. Appl. Geochem., 81: 132-142, doi:10.1016/j.apgeochem.2017.04.006.

Bavec, Š. & Gosar, M. 2016: Speciation, mobility and bioaccessibility of Hg in the polluted urban soil of Idrija (Slovenia). Geoderma, 273: 115-130. doi:10.1016/j.geoderma.2016.03.015.

Bavec, Š., Biester, H. & Gosar, M. 2014: Urban sediment contamination in a former Hg mining district, Idrija, Slovenia. Environ. Geochem. and Health, 4/3: 427-439, doi:10.1007/s10653-013-9571-6.

Bavec., Š., Gosar, M., Biester, H. & Grčman, H. 2015: Geochemical investigation of mercury and other elements in urban soil of Idrija (Slovenia). J. Geochem. Explor., 154, 213-223, doi:10.1016/j.gexplo.2014.10.011.

Benčina, T. 2007: The development of environmental design in municipality of Idrija. Graduation thesis. University of Ljubljana. http://repozitorij.uni-lj.si/IzpisGradiva.php?id=38377&lang=eng. Accessed 30 January 2014.

Berce, B. 1958: Geologija živosrebrovega rudišča Idrija. Geologija, 4: 5-62. (In Slovene).

COM(2006)231 final. Communication from the Commission to the Council, the European Parliament, the European Economic and Social Committee and the Committee of the Regions - Thematic Strategy for Soil Protection [SEC(2006)620] [SEC(2006)1165].

Čar, J. 1998: Mineralized rocks and ore residues in the Idrija region. In: Miklavčič, V. (ed.):, Proceedings of the meeting of researchers entitled: Idrija as a natural and anthropogenic laboratory, Mercury as a major pollutant, (pp. 10-15). Idrija, Mercury mine Idrija.

Davis, J.C. 1986: Statistic and Data Analysis in Geology. Wiley in Sons, New York: 651 p.

Drovenik, M., Pleničar, M. & Drovenik, F. 1980: The origin of Slovenian ore deposits. Geologija, 23/1: 1-175.

EGS 2011: Urban Geochemistry. EuroGeoSurveys 2010 annual report. EuroGeoSurveys, Brussels, 45-46. Internet: http://www.eurogeosurveys.org/wp-content/uploads/2013/01/EuroGeoSurveys-Annual-Report-2011.pdf (4. 10. 2017).

EGS 2013: Urban Geochemistry Project (URGE). EuroGeoSurveys 2012 annual report. EuroGeoSurveys, Brussels, 30-31. Internet: http://www.eurogeosurveys.org/wp-content/uploads/2014/04/Annual-Report-2013_med.pdf (4. 10. 2017).

EGS 2014: Urban Geochemistry Project (URGE). EuroGeoSurveys 2013 annual report. EuroGeoSurveys, Brussels, 33. Internet: http://www.eurogeosurveys.org/wp-content/uploads/2014/12/Annual-Report-2013_2.pdf (4. 10. 2017).

EGS 2015: Urban Geochemistry Project (URGE). EuroGeoSurveys 2014 annual report. EuroGeoSurveys, Brussels, 51. Internet: http://www.eurogeosurveys.org/wp-content/uploads/2014/12/Annual-Report-2013_2.pdf (4. 10. 2017).

EGS 2016: Urban Geochemistry Project (URGE). EuroGeoSurveys 2015 annual report. EuroGeoSurveys, Brussels, 17-18. Internet: http://www.eurogeosurveys.org/wp-content/uploads/2017/01/Annual-Report-2015_5.pdf (4. 10. 2017).

Epskamp, S. 2014: Network Model Selection Using qgraph 1.3. Internet: http://psychosystems.org/network-model-selection-using--qgraph-1-3-10/ (18. 09. 2017).

Gaberšek, M. & Gosar, M. 2018: Geochemistry of urban soil in the industrial town of Maribor, Slovenia. J. Geochem. Explor., online first, doi:10.1016/j.gexplo.2017.06.001.

Gosar, M., Šajn, R. & Biester, H. 2006: Binding of mercury in soils and attic dust in the Idrija mercury mine area (Slovenia). Sci. Total. Environ., 369: 150-162, doi:10.1016/j.scitotenv.2006.05.006.

Gosar, M., Šajn, R. & Teršič, T. 2016: Distribution pattern of mercury in the Slovenian soil: Geochemical mapping based on multiple geochemical datasets. J. Geochem. Explor., 167: 38-48, doi:10.1016/j.gexplo.2016.05.005.

Grafenauer, S. 1969: O triadni metalogeni dobi v Jugoslaviji. Rudarsko-metalurški zbornik, 3-4: 353-364.

Kolektor 2014: Offical website of the company. Internet: http://www.kolektor.com/. 31. 1. 2014.

Miesch, A. T. 1976: Geochemical Survey of Missouri-Methods of Sampling, Laboratory Analysis and Statistical Reduction of Data. Geological Survey Professional Paper 954-A. US Geological Survey, Washington: 39 p.

MKGP 2017: Republic of Slovenia, Ministriy of Agriculture, Forestry and Food. Internet: http://rkg.gov.si/GERK/. 18. 8. 2017.

Mlakar, I. & Čar, J. 2009: Geological map of the Idrija - Cerkljansko hills between Stopnik and Rovte 1:25.000. Geološki zavod Slovenije, Ljubljana.

Mlakar, I. & Čar, J. 2010: Geological structure of the Idrija – Cerkljansko hills: Explanatory Book to the Geological map of the Idrija – Cerkljansko hills between Stopnik and Rovte 1:25.000. Ljubljana, Geološki zavod Slovenije.

Official Gazette RS, 1996: Uredba o mejnih, opozorilnih in kritičnih imisijskih vrednostih nevarnih snovi v tleh (in Slovene). Uradni list Republike Slovenije, 68/1996: 5773-5774.

Reimann, C., Filmozer, P., Garrett, R. G. & Dutter, R. 2008: Statistical data analysis explained. Applied environmental statistics with R. John Wiley & Sons, Ltd. 343 p.

Reimann, C., Birke, M., Demetriades, A., Filzmoser, P., O'connor, P. (eds.) 2014: Chemistry of Europe's Agricultural Soils. Part A: Methodology and Interpretation of the GEMAS Data Set. Geol. Jb., Hannover: 523 p.

Salminen, R. (Chief-ed.) 2005: Geochemical Atlas of Europe. Part 1 – Background Information, Methodology and Maps. Geological Survey of Finland, Espoo: 96 p.

SEC(2006)1165: Commission staff working document - Accompanying document to the Communication from the Commission to the Council, the European Parliament, the European Economic and Social Committee and the Committee of the Regions - Thematic Strategy for Soil Protection - Summary of the impact assessment {COM(2006)231 final} {SEC(2006)620}.

Soil Remediation Circular 2013: Rijkswaterstaat, Ministry of Infrastructure and the Environment, Netherlands. Internet: http://rwsenvironment.eu/subjects/soil/legislation-and/soil-remediation/ (7. 9. 2016).

STAT 2017: Statistical office of the republic of Slovenia. Internet: http://pxweb.stat.si/pxweb/Dialog/Saveshow.asp. 19. 9. 2017.

Šajn, R. 2003: Distribution of chemical elements in attic dust and soil as reflection of lithology and anthropogenic influence in Slovenia. Journal de Physique IV, 107: 1173-1176, doi:10.1051/jp4:20030509.

Šajn, R., Bidovec, M., Andjelov, M., Pirc, S. & Gosar, M. 1998. Geokemični atlas Ljubljane in okolice = Geochemical atlas of Ljubljana and environs. Inštitut za geologijo, geotehniko in geofiziko, Ljubljana: 34 p

Šajn, R., Gosar, M., Bidovec, M., Pirc, S. & Alijagić, J. 2011: Geochemical Mapping of Ljubljana Urban and Suburban Area, Slovenia. In: Johnson, C. C., Demetriades, A., Locutura, J. & Ottesen, R. T. (eds.): Mapping the Chemical Environment of Urban Areas. Wiley-Blackwell: 375-392.

Teršič, T., Gosar, M. & Biester, H. 2011a: Environmental impact of ancient small-scale mercury ore processing at Pšenk on soil (Idrija area, Slovenia). Appl. Geochem., 26/11: 1867–1876, doi:10.1016/j.apgeochem.2011.06.010.

Teršič T., Gosar, M. & Biester, H. 2011b: Distribution and speciation of mercury in soil in the area of an ancient mercury ore roasting site, Frbejžene trate (Idrija area, Slovenia). J. Geochem. Explor., 110/2: 136–145, doi:10.1016/j.gexplo.2011.05.002.

Wie, T. & Simko, V. 2016: Visualisation of a Correlation Matrix. Internet: https://cran.r-project.org/web/packages/corrplot/corrplot.pdf (18. 9. 2017).

Zupan, M., Grčman, H. & Lobnik, F. 2008: Raziskave onesnaženosti tal Slovenije. (in Slovene). Agencija RS za okolje, Ljubljana: 63 p.

Žibret, G. & Šajn, R. 2008: Modelling of atmospheric dispersion of heavy metals in the Celje area, Slovenia. J. Geochem. Explor., 97/1: 29-41, doi:10.1016/j.gexplo.2007.08.001.

GEOLOGIJA *60/2*, 199-210, Ljubljana 2017

https://doi.org/10.5474/geologija.2017.014

Analysis of systematic fracturing in Eocene flysch of the Slovenian coastal region

Analiza sistematične razpokanosti eocenskih flišnih kamnin Slovenske obale

Marko VRABEC & Galena JORDANOVA

Univerza v Ljubljani, Naravoslovnotehniška fakulteta, Oddelek za geologijo, Privoz 11, SI –1000 Ljubljana, Slovenija; e-mail: marko.vrabec@geo.ntf.uni-lj.si

Prejeto / Received 1. 3. 2017; Sprejeto / Accepted 10. 10. 2017; Objavljeno na spletu / Published online 22. 12. 2017

Dedicated to Professor France Šušteršič on the occasion of his 70th birthday

Key words: Eocene flysch, systematic fractures, paleostress, joints, fracture spacing index, Istria, Slovenia
Ključne besede: Eocenski fliš, sistematične razpoke, paleonapetosti, natezne razpoke, indeks oddaljenosti razpok, Istra, Slovenija

Abstract

We analyse systematic fractures occurring in sandstone beds in Eocene flysch of the Slovenian coastal area. Two nearly perpendicular fracture sets were identified: fractures F1 are generally NW-SE oriented, well-expressed and predominately planar, whereas fractures F2 are NE-SW-striking, shorter, more irregular in shape, and terminate against the F1 set. The average orientation of both sets does not change significantly in a coastal transect crossing all principal structural domains of the area. We analysed fracture spacing with respect to layer thickness and determined fracture spacing index for both fracture sets. We interpret both fracture sets as tensional (Mode I) joints originating in two distinct extensional episodes. Set F1 is older and formed in NE-SW directed tension which we correlate with the well-documented regional post-Dinaric orogen-perpendicular extension of presumably mid-Miocene age. Set F2 formed in NW-SE oriented tension, which is compatible with previously documented NE-SW-striking normal faults occurring in the area, but was so far not documented elsewhere. We interpret that F1 fractures predate folding and thrusting in the coastal belt. Earlier, Eocene-Oligocene Dinaric thrusting therefore did not significantly affect the coastal area, whereas post-F1 shortening, associated with northward indentation and underthrusting of the Adria microplate, did not commence before late Miocene.

Izvleček

Raziskali smo sistematične razpoke, ki se pojavljajo v plasteh peščenjaka v eocenskem flišu Slovenske obale. Pojavljata se dve, medsebojno skoraj pravokotni družini razpok: razpoke družine F1 so generalno usmerjene v SZ-JV smeri in so dobro izražene in pretežno planarne, razpoke družine F2 pa imajo smer SV-JZ in so krajše, bolj nepravilno oblikovane in se zaključujejo na ploskvah razpok F1. Povprečna orientacija razpok obeh družin se bistveno ne spreminja vzdolž raziskanega profila, ki preči vse glavne strukturne domene ob Obali. Analizirali smo medsebojno oddaljenost razpok glede na debelino plasti in obema družinama določili indeks oddaljenosti razpok (fracture spacing index). Obe družini interpretiramo kot natezne razpoke tipa I, ki so nastale v dveh ločenih fazah natezne tektonike. Družina F1 je starejša in je nastala v SV-JZ usmerjeni tenziji in jo povezujemo z dobro poznano regionalno fazo post-Dinarske ekstenzije, ki je domnevno srednje miocenske starosti. Družina F2 je nastala v SZ-JV usmerjeni tenziji in je skladna z SV-JZ usmerjenimi normalnimi prelomi, ki so bili že prej dokumentirani v območju Obale, ni pa še bila odkrita v ostalih delih Slovenije. Po naši interpretaciji so razpoke družine F1 starejše od narivanja in gubanja v območju Obale. Zato sklepamo, da predhodno Dinarsko narivanje eocensko-oligocenske starosti ni bistveno prizadelo obalnega območja. Krčenje ozemlja po nastanku razpok F1, ki ga povezujemo s podrivanjem Jadranske mikroplošče proti severu, pa se ni začelo pred mlajšim miocenom.

Introduction

The territory of Slovenia was affected by polyphase tectonic deformation (e.g. Vrabec et al. 2009 and references therein), which not only produced a complex regional assemblage of tectonic units (Placer, 2008), but is also reflected in outcrop-scale structural geometry. It is therefore rarely possible to observe structurally homogeneous systematic sets of structures. One such exception occurs in the coastal region of Slovenia, which structurally represents the most external part of the Dinaric fold-and-thrust belt. Here, the generally flat-lying to gently-dipping beds of Eocene flysch nearly everywhere have pervasive systematic fractures. We present a first structural analysis of these fracture sets with the aim to examine their geometry, to interpret their origin and tectonic significance, and to investigate whether meaningful statistical properties, specifically the fracture spacing index (FSI), can be derived to characterize the fracture sets. These data are useful not only for understanding the tectonic evolution of the area, but may also be relevant for various applications such as in hydrogeology, engineering geology, and in geothermal resources development.

Geological setting

The coastal region of Slovenia, geographically situated in northwestern part of the Istria penninsula (Fig. 1), sits in the Adriatic – Apulian foreland of the fold-and-thrust belt of the northwestern External Dinarides (Placer, 2008; Placer et al., 2010). The coastal area was affected by two major Tertiary shortening episodes: the Eocene-Oligocene SW-directed thrusting of the External Dinarides, and the subsequent underthrusting of the Adriatic microplate below the Dinarides and the Southern Alps, which is at present time NNW-directed (e.g. Weber et al, 2010).

Major stratigraphic units of the area comprise Mesozoic – Palaeocene carbonates of the Adriatic carbonate platform, which are uncomfortably overlain by Eocene turbidites (flysch) deposited in SW-ward migrating foreland basin in front of the advancing Dinaric orogen (Otoničar, 2007). Flysch in the Slovenian coastal area is of distal facies where well-bedded predominately cm-dm thick siliciclastic sandstones are interbedded with marls in approximately equal proportion (Pavšič & Peckmann, 1996). This monotonous sequence is interrupted by a number of distinct 1 – 5 m thick calciturbiditic horizons, derived from the carbonate platform which persisted in front of the foreland basin throughout Eocene (Pavšič & Peckmann, 1996; Placer et al. 2004, Vrabec & Rožič, 2014). In the offshore in the Gulf of Trieste, a several hundred m thick succession of Pliocene to Quaternary continental and marine sediments is covering the flysch sequence, with the topmost sedimentary cover represented by up to ten m of Holocene marine clay (Busetti et al., 2010).

The transition from the inland karstic plateau of Kras where Mesozoic carbonate rocks prevail to the coastal lowland area dominated by Eocene flysch siliciclastics is structurally and morphologically defined by the NW-SE-striking Palmanova Thrust System (Fig. 1), comprising several sub-parallel thrust faults with various local names, spanning from Palmanova in Italy to Mt. Učka in Croatia (Placer, 2008, Carulli, 2011). A vertical displacement component of approx. 1000 m is inferred on this thrust system, hence the name Dinaric Frontal Ramp was also proposed (e.g. Busetti et al., 2010). External to this thrust boundary, between the Bay of Milje (Muggia) and Bay of Koper, careful structural mapping has revealed a series of low-angle thrust faults with km-scale displacements, cutting the Eocene flysch and locally producing vertical or even inverted

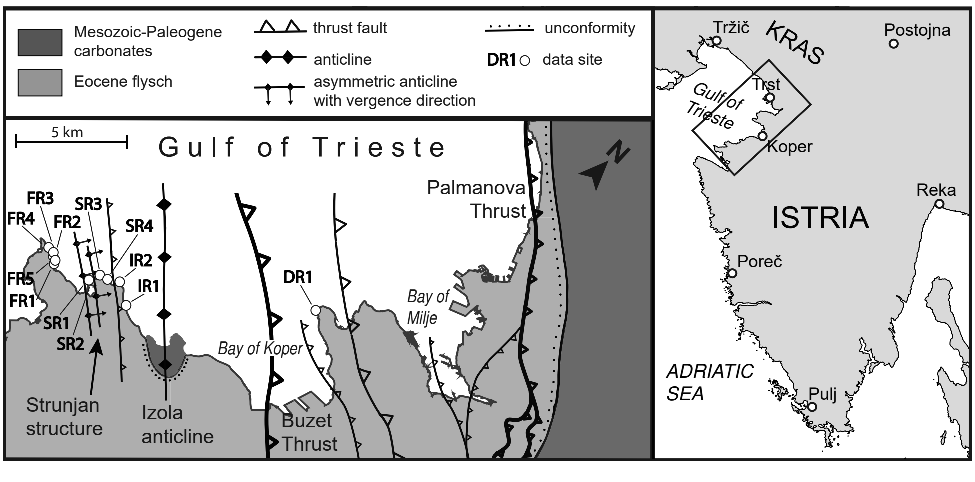

Fig. 1. Structural map of the investigated area with locations of measurement sites (simplified from Placer, 2007, Vrabec et al., 2014 & Placer, 2015).

bedding (Placer, 2007). Of those, the prominent Buzet Thrust, reaching the coastline at Koper, was inferred to have a displacement in excess of 10 km (Placer et al. 2004; Placer, 2007) and can be traced on marine seismic reflection profiles towards the middle of the Gulf of Trieste (Vrabec et al., 2014). The considerable amount of shortening deformation and the generally low-angle geometry of these structures led Placer (2007) to interpret them as reflecting a younger phase of convergence related to Adria underthrusting and not as the frontal imbricate structures of the Dinaric thrust system, as previously believed.

Further southwest of the Buzet Thrust, the degree of deformation is much lower. Here, the strata are gently folded forming the Izola Anticline with Paleocene carbonates outcropping in the fold core near the town of Izola (Fig.1). The most external deformation observed along the Slovenian coastline occurs at Strunjan, where several NE-verging reverse faults and asymmetric folds disrupt the flysch sequence (Strunjan structure of Placer, 2005). Still further southwest, from Fiesa to Piran, the beds are essentially undeformed and nearly flat-lying.

At least two extensional episodes were also documented in the region. First is a NE-SW oriented extension postdating the Dinaric thrusting and occurring everywhere along the Dinarides. This extension is probably concurrent with mid-Miocene extension and basin subsidence in the Pannonian domain (Vrabec & Fodor, 2006; Žibret & Vrabec, 2016). A second episode, documented so far only in the coastal area, exhibits NW-SE-oriented tension, which is manifested in normal faults with NE-SW strike, occurring both in map-scale (Placer, 2005) and in outcrop-scale (Vrabec & Rožič, 2014).

The youngest tectonic phase documented in the region is the ongoing NNW-SSE directed compression, which probably started in Pliocene (Vrabec & Fodor, 2006; Weber et al., 2010; see also Moulin et al., 2016). This phase is mainly manifested by dextral slip on NW-SE-striking faults (Žibret & Vrabec, 2016), which however are not common in the Slovenian coastal area.

Methods

We collected fracture data at 12 sites spanning all principal structural domains of the coastal region (Fig. 1): the low-angle thrust system between the Palmanova Thrust and Buzet Thrust (site DR1), the southern limb of the Izola Anticline (sites IR1 and IR2), the Strunjan structure (sites SR1 to SR4), and the undeformed foreland (sites FR1 to FR5). A list of sites with their coordinates is presented in Table 1. At each site, we measured fractures in several sandstone beds of different thickness to provide representative bed thickness / fracture density data. We were primarily choosing beds with good 3D exposure to maximize measurement quality.

Orientations of bedding planes and fractures were measured with digital geological compass GeoClino Digital Clinometer, which provides fast and reliable measuring procedure, and conveniently facilitates data storage into internal memory. To ensure measurement precision, digital compass was carefully calibrated according to manufacturer instructions at each measurement site. For additional control, digital readouts were checked several times against measurements with classical Freiberg-style geological compass.

Fracture spacing and bed thickness was measured with ordinary measuring tape. Fracture spacing was measured perpendicular to fracture strike. Sections of the outcrops with well-developed straight and parallel fracture traces were exclusively considered for measuring.

Orientation data were processed and analysed with Orient software, version 2.1.2.2 (Vollmer, 2015). Software utility GeoCalculator version 4.9.8 written by Rob Holcombe was used to calculate intersecting angles between fracture sets. Fractures were separately analysed on a per-bed, per-site and per-domain basis.

Structural analysis

Strata at investigated sites predominately dip gently to the SSW (Table 1; Fig. 4a). Dip angles mostly range between 10° and 15°, except in the most external part of the study area (sites FR), where bedding is nearly flat-lying. At all investigated sites, systematic fractures predominately occur in thick (decimetre-scale) sandstone beds as planar to moderately curviplanar planes (Fig. 2). Only occasionally fractures exhibit more irregular configurations resembling polygonal structure, but such configurations appear to be limited to certain beds, whereas adjacent beds above and below in the stratigraphic succession normally have more regular fracture geometry.

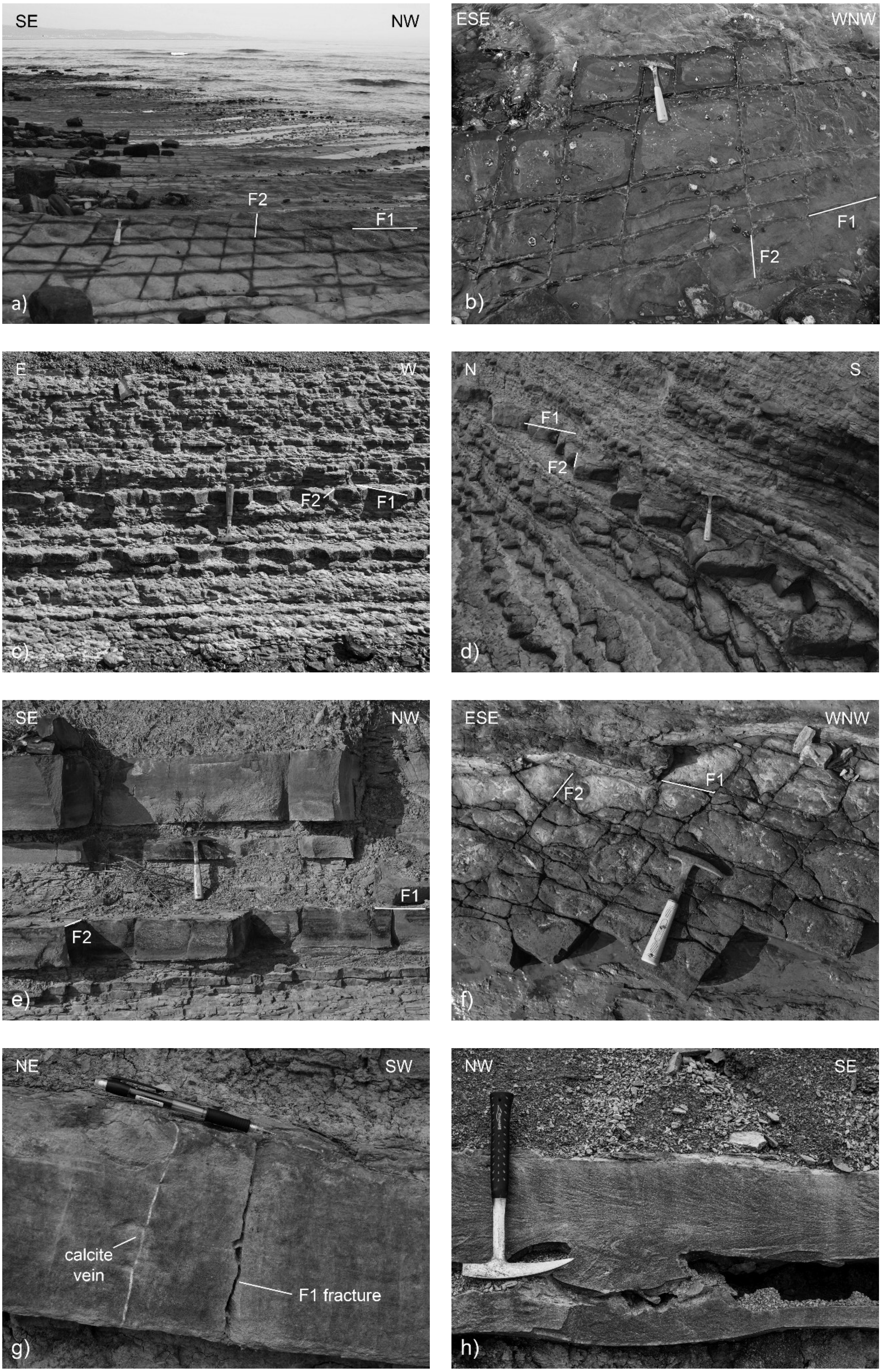

Fig. 2. Typical outcrop examples of investigated systematic fractures in Eocene flysch. a) and b) Debeli rtič (site DR1). c) Bele skale (site IR1). d) Rtič Strunjan (site SR3). e) Fiesa (site FR1). f) Fiesa (site FR2). g) Calcite-filled tension gash parallel to F1 fracture planes, Strunjan (close to Site SR1). h) Plumose ornamentations on F1 fracture plane, indicating horizontal (Mode I) propagation directed from right to left, Rt Ronek (between sites SR4 and IR2).

Systematic fractures appear in two well-defined sets, which we name F1 and F2 (Table 1; Figs. 2, 3, 4). The NW-SE-striking F1 fractures are normally longer with more straight traces. The generally NE-SW-trending F2 fractures are shorter and mainly appear to terminate against F1 set, although this relationship between the two sets is not everywhere clear. F2 fractures are also more curviplanar and irregular in orientation. This is reflected in orientation distributions (Fig. 3), where F2 fractures show considerably greater spread of orientations compared to F1 fractures. The angle of intersection between the two sets is quite constant at around 80° on the average, but ranges from 65° to nearly perpendicular (Table 1).

The NW-SE orientation of F1 fractures is relatively stationary between the sites and in all structural domains investigated in the study, with the exception of Strunjan structure (Figs. 3, 4b, 4d). There, a pronounced deviation to WNW-ESE or even E-W orientation is observed. Additionally, a large variation in fracture sets orientation from bed to bed in the same section can be seen (see data for sites SR1 and SR2 in Fig. 2), reflecting perhaps the mechanical influence of intervening soft layers and the varying thickness of the sandstone beds and their interlayers. This was not noted at other sites. Within the Strunjan structure also F2 fracture orientations deviate from their general NE-SW trend towards a more N-S orientation, which is particularly clear at site SR2 (Fig. 2).

Fig. 3. Measured fracture orientations in spherical projection (equal-area projection, lower hemisphere). First column: present-day orientation. Bedding orientation is displayed with thick dark-grey traces. Second column: data backtilted to original (bedding-horizontal) position. Thick black traces indicate the average orientation (medium vector) of each fracture set. Third and fourth column: circular histogram of fracture strike directions (in backtilted orientation) for each fracture set. Bin size is 5°.

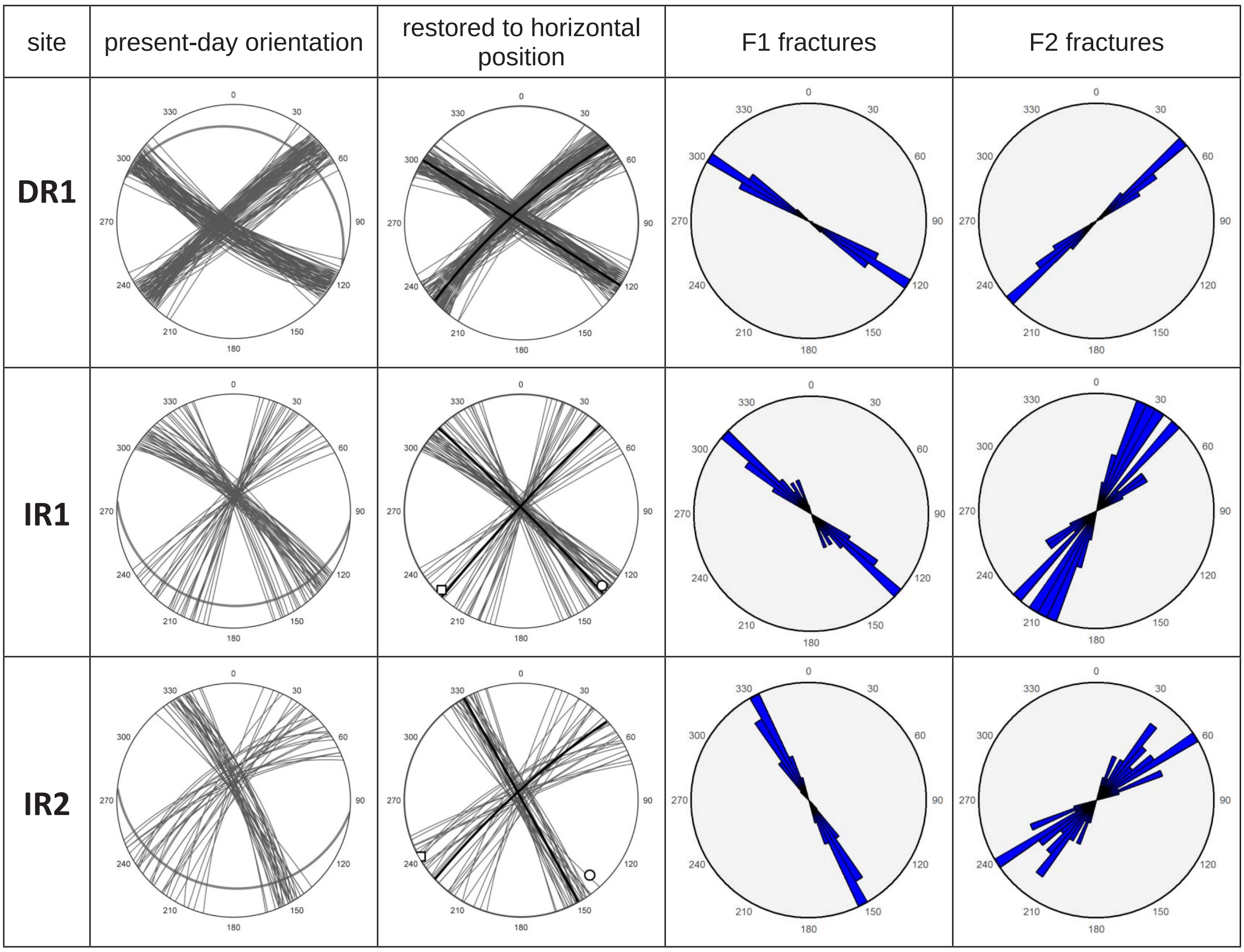

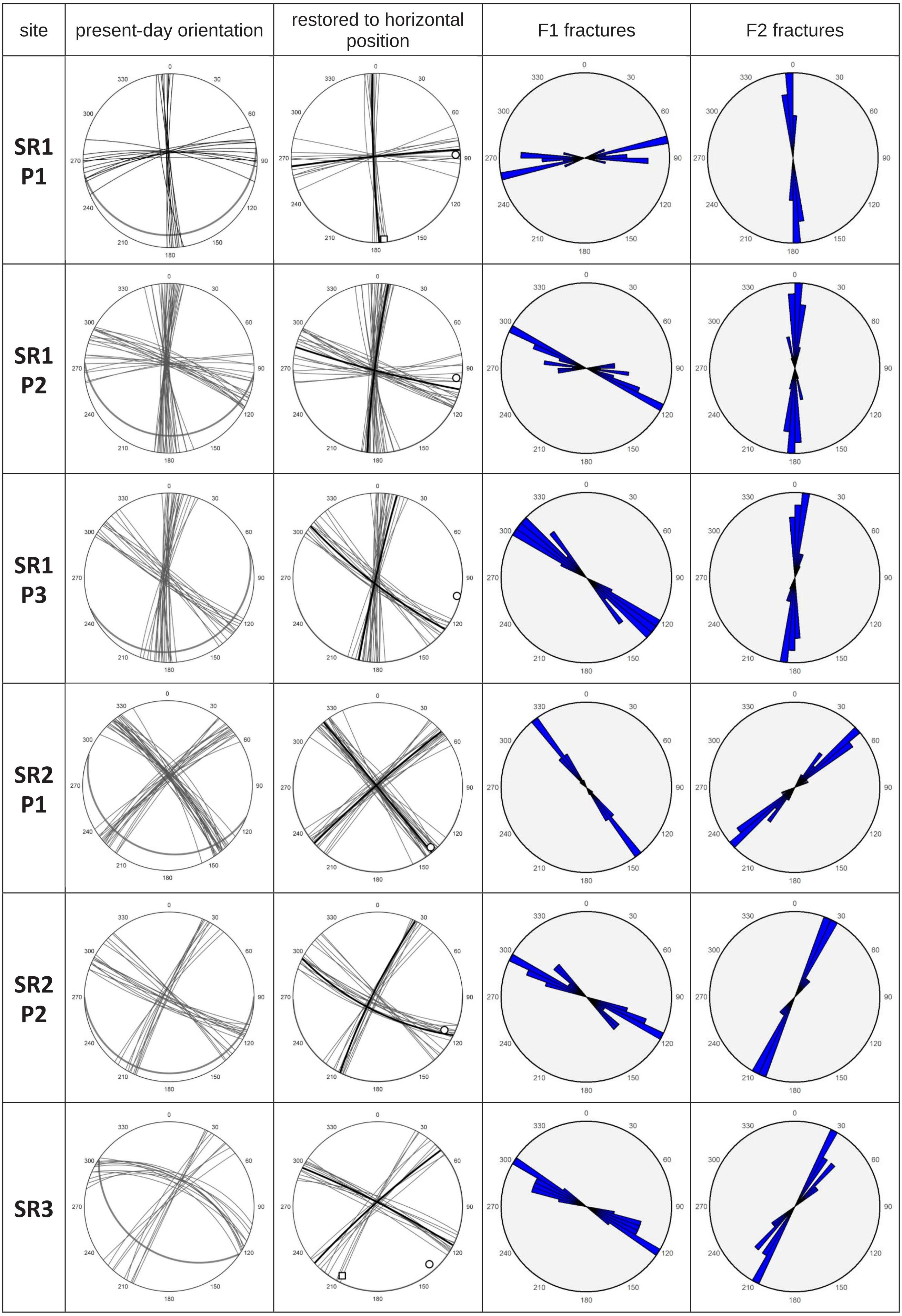
site
present-day orientation
restored to horizontal position
F1 fractures
F2 fractures
SR1 P1
SR1 P2
SR1 P3
SR2 P1
SR2 P2
SR3

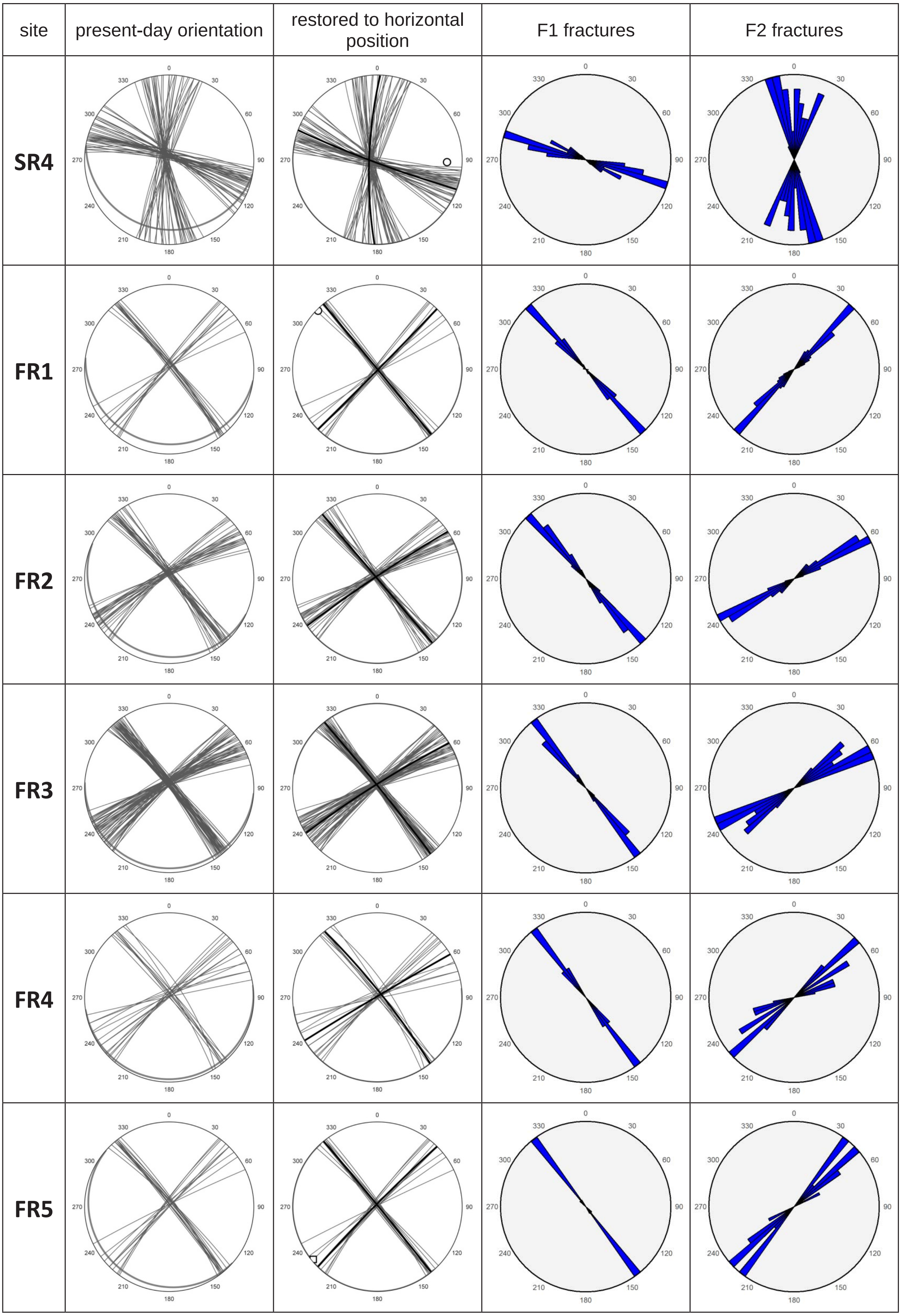
site
present-day orientation
restored to horizontal position
F1 fractures
F2 fractures
SR4
FR1
FR2
FR3
FR4
FR5

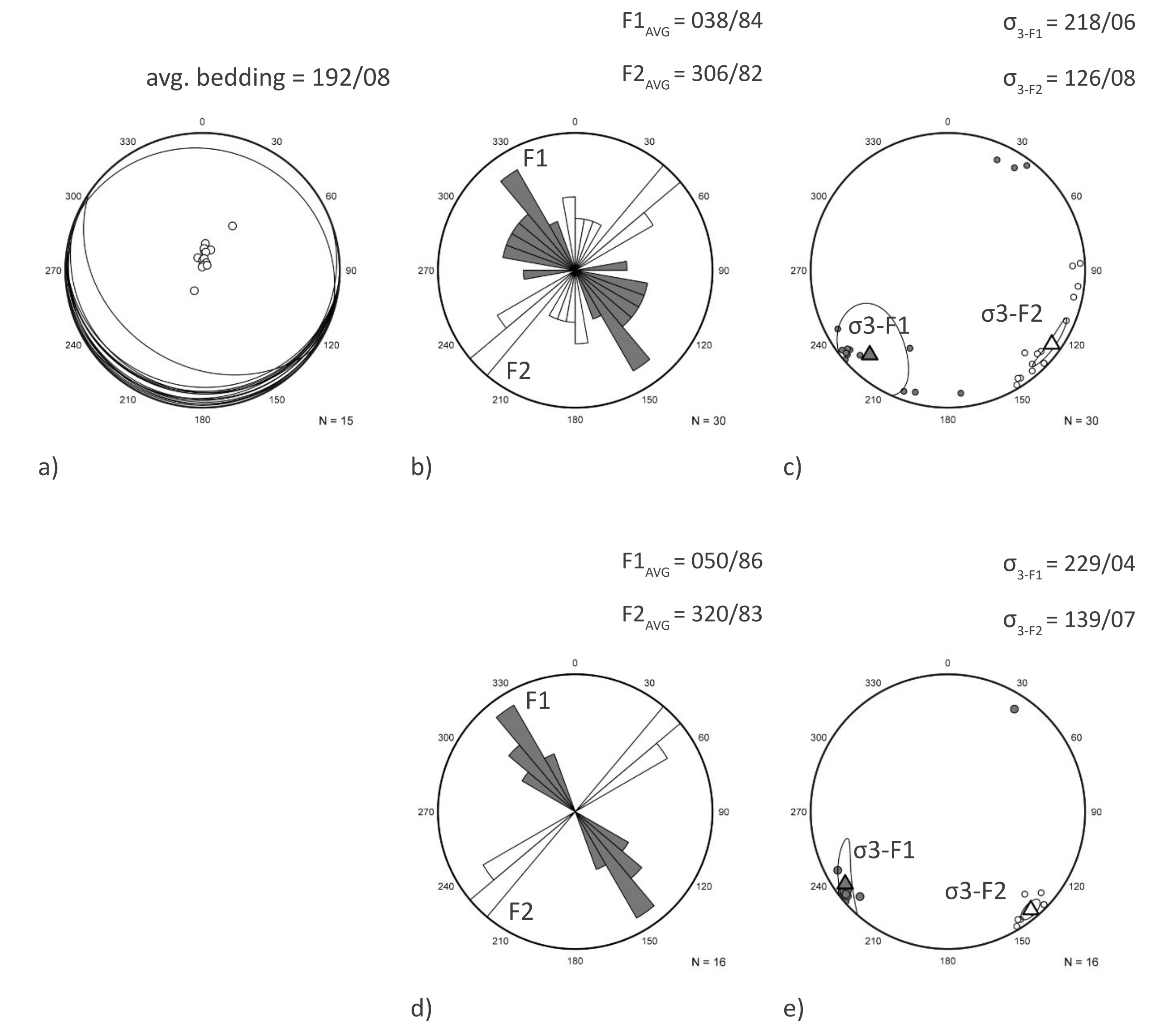

Fig. 4. Summary plots of orientations of investigated structures, averaged for each measurement site. a) Bedding. b) Circular histogram of fracture sets orientations. Bin size is 10°. c) Inferred directions of tensional stress axes from fracture sets F1 in and F2, assuming tension is perpendicular to the plane of average fracture orientation. d) and e): same as in b) and c), but excluding sites SR from the Strunjan structure. See text for discussion.

In few places, weak plumose ornamentations were found on F1 and F2 fracture faces (Fig. 2h), suggesting Mode I opening with horizontal propagation direction. Additionally, up to several mm thick calcite-filled tensional gashes paralleling F1 fractures are occasionally found in sandstone beds (Fig. 2g). We therefore interpret F1 and F2 fractures as tensional joints which originated perpendicular to the axis of minimal stress σ_3.

According to this interpretation, we infer the σ_3 direction at the time of F1 formation to match the normal to average fracture orientation, which implies that F1 joints formed in NE-SW-directed tension (Table 1; Figs. 4c, 4e). This matches well with the known regional extensional episode of probable mid-Miocene age (Vrabec & Fodor, 2006), which was documented in External Dinarides of central Slovenia by fault-slip data inversion (Žibret & Vrabec, 2016).

From the observed field relationships we interpret that F2 fractures postdate the F1 fractures. Inferred σ_3 orientations (Table 1; Figs. 4c, 4e) suggest their origin in NW-SE-oriented tension. We therefore presume that F2 fractures formed in an independent extensional phase concurrently with the NE-SW-striking normal faults that were previously documented both in outcrop scale in the coastal cliff (Vrabec & Rožič, 2014) and in map scale in the interior (Rokava Fault of Placer, 2005).

Table 1. Site coordinates and average orientation of fracture sets for each investigated site.

site	site coordinates		bedding orientation	fracture set F1				fracture set F2				angle between D1 and D2
	φ	λ		N	average orientation	dispersion (°)	average pole orientation	N	average orientation	dispersion (°)	average pole orientation	
DR1	45°35'23.8"N	13°42'12.1"E	022/13	73	213/78	2	033/12	88	320/85	2	140/05	70
IR1	45°32'07.4"N	13°37'29.2"E	185/12	47	046/78	3	226/12	26	311/79	11	131/11	87
IR2	45°32'23.0"N	13°37'02.1"E	186/16	30	062/80	4	242/10	29	317/71	7	137/19	79
SR1-1	45°31'59.8"N	13°36'03.7"E	187/11	9	354/79	5	174/11	12	267/86	5	087/04	86
SR1-2	45°31'59.8"N	13°36'03.7"E	184/13	29	015/81	11	195/09	20	277/85	6	097/05	83
SR1-3	45°31'59.8"N	13°36'03.7"E	159/08	13	217/85	19	037/05	23	282/83	39	102/07	65
SR2-1	45°31'59.8"N	13°36'03.7"E	202/13	24	051/79	3	231/09	20	318/81	5	138/09	89
SR2-2	45°31'59.8"N	13°36'03.7"E	180/06	10	204/77	126	024/13	16	293/83	142	113/07	87
SR3	45°32'13.0"N	13°36'07.2"E	214/32	11	026/53	4	206/37	9	313/78	44	133/12	69
SR4	45°32'15.3"N	13°36'15.8"E	190/11	40	020/83	3	200/07	42	268/80	11	088/10	70
FR1	45°31'42.2"N	13°34'27.4"E	188/07	81	049/89	32	229/01	69	314/87	5	134/03	85
FR2	45°31'43.0"N	13°34'25.8"E	205/05	22	050/85	11	230/05	29	326/84	164	146/06	87
FR3	45°31'45.3"N	13°34'15.7"E	184/03	49	053/86	2	233/04	58	327/83	3	147/07	86
FR4	45°31'43.8"N	13°34'22.8"E	172/02	9	052/82	6	232/08	14	329/87	8	149/03	83
FR5	45°31'35.6"N	13°34'40.1"E	222/04	14	051/85	2	231/05	10	314/87	8	134/03	83

Fracture Spacing Index

It is commonly observed that the density, or spacing, of systematic fractures in layered rocks is roughly proportional to layer thickness, but may also be dependent on rock type (e.g. Davis & Reynolds, 1996). In our study area, clearly expressed fractures only occur in sandstone beds, therefore the effect of lithology on their spacing should be negligible. For analysing fracture spacing – layer thickness relationship it is common to use the median of fracture spacing for each measured bed since the frequency distribution of interfracture distances is usually skewed from normal distribution (Narr & Suppe, 1991). A summary of our fracture spacing measurements is presented in Table 2. For each joint set, we then plotted median joint spacing against the respective layer thickness (Fig. 5) to derive fracture spacing index (FSI), which is the slope of the regression line in this plot (Narr & Suppe, 1991). Thus defined, larger FSI values indicate higher joint density.

We find that spacing of joint sets F1 and F2 in Eocene flysch sandstone of the Slovenian coastal area is reasonably-well correlated to bed thickness (Fig. 5). Whereas the recorded range of joint spacing is quite high, the median values tend to stay at the lower end of the range, reflecting that modest joint spacings dominate the frequency distribution. For both joint sets, the dispersion in median joint spacings values appears to be lower for smaller layer thicknesses under 20 cm than for layers between 20 and 35 cm thick. For joint set F1 the derived FSI value is 0.483 with correlation coefficient R^2 of 0.6331. For joint set F2 the FSI value is 0.616 with correlation coefficient R^2 of 0.5035.

We conclude that joint spacing in sets F1 and F2 is reasonably predictable. The joint density may additionally depend on the degree of deformation. We could not conclusively determine this since the total number of measurements was relatively low, therefore FSI determinations for individual structural domains did not yield satisfactory high correlations. Moreover, the structural domains used in this study were defined with respect to the style and amount of shortening deformation, whereas the joints have originated in independent tensional episodes. Joint density is therefore not likely to spatially correlate with shortening domains.

Table 2. Summary statistical data for fracture spacing measurements.

site	bed	bed thickness (cm)	fracture set F1 spacing (cm)					fracture set F2 spacing (cm)				
			median	average	standard deviation	minimum	maximum	median	average	standard deviation	minimum	maximum
SR1	P1	17,0	26,3	28,5	15,4	6,9	64,8	34,3	42,2	30,8	16,1	76,1
SR1	P2	8,5	18,5	19,4	8,6	3,1	35,1	7,1	11,0	8,1	3,8	27,3
SR1	P3	11,1	21,3	23,0	11,4	8,1	52,3	15,9	17,5	8,1	4,2	33,0
SR2	P1	16,2	19,6	21,1	11,9	3,1	47,2	18,2	19,3	8,7	5,2	38,0
SR2	P2	13,0	19,2	25,3	16,5	6,9	62,9	26,0	26,3	15,7	2,5	50,9
SR3	P1	13,0	26,2	21,0	11,2	6,8	32,5	16,0	19,3	9,0	9,5	34,1
SR4	P1	10,0	16,1	11,7	7,7	2,6	21,6	11,2	16,3	4,6	3,9	28,6
SR4	P2	10,2	9,0	8,3	2,3	4,1	12,4	8,4	9,8	3,5	4,9	17,9
IR1	P1	5,0	7,6	7,6	2,5	3,1	12,5	10,2	11,0	5,2	2,9	21,0
IR1	P2	4,6	6,3	7,1	2,6	3,1	12,6	13,2	12,7	3,6	4,9	17,6
IR2	P1	24,0	54,9	58,7	13,6	41,7	81,3	33,2	31,0	6,1	24,0	36,8
IR2	P2	26,4	39,3	33,8	17,5	5,0	60,1	19,8	18,5	7,1	2,7	30,2
FR1	P1	32,0	33,4	36,6	21,1	7,9	89,0	33,6	35,4	10,9	23,4	57,3
FR1	P2	16,0	28,2	29,5	11,4	8,3	59,1	19,3	20,5	8,0	8,6	35,1
FR2	P1	9,0	25,5	25,2	7,4	12,4	39,3	15,0	16,2	6,1	8,2	31,4
FR3	P1	12,0	23,6	22,5	11,2	2,2	47,2	13,4	15,2	6,9	4,5	26,2
FR3	P2	10,5	16,0	17,7	7,7	2,2	47,2	11,2	11,3	5,5	1,8	30,0
FR4	P1	17,7	26,1	25,6	10,5	12,6	47,9	25,9	26,1	4,9	19,7	33,7
FR5	P1	23,2	47,7	47,4	20,5	14,8	81,8	13,3	14,5	6,4	8,8	21,5
DR1	P1	11,5	26,9	27,1	10,0	5,8	55,4	16,7	17,1	7,1	6,1	34,5
DR1	P2	24,8	31,9	36,8	17,7	12,3	74,4	29,0	27,2	8,6	9,6	39,1
DR1	P3	12,2	25,4	23,3	7,0	9,0	34,1	20,0	20,0	8,1	7,6	34,3

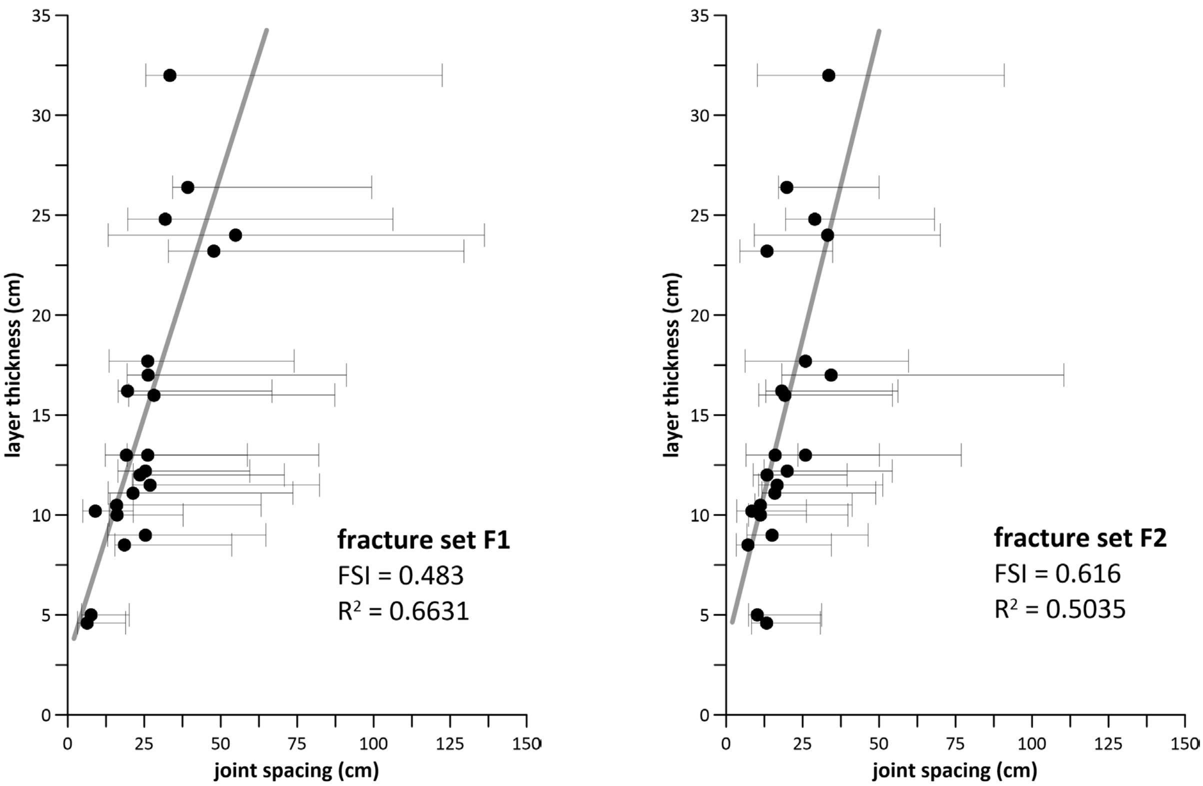

Fig. 5. Fracture spacing index (FSI) determination in Eocene flysch sandstone layers according to Narr & Suppe (1991). Plotted are median fracture spacing distances (black dots) with indicated range of measured spacing values against respective layer thicknesses. FSI value corresponds to the slope of the regression line. a) Fracture set F1; b) fracture set F2.

Discussion and conclusions

The first structural study of systematic fractures in Eocene flysch sandstones in the foreland of the External Dinarides fold-and-thrust belt of the Slovenian coastal area has revealed that the fractures occur in two major sets. The first set F1 comprises NW-SE oriented tensional (Mode I) joints which originated in NE-SW directed tension. This direction is roughly parallel to the shortening direction implied from the orientation of thrusts and folds in the coastal area, therefore we assume that extension is independent of thrusting (i.e., it does not represent shortening-perpendicular extension which is relatively common in thrustbelts). We correlate the origin of F1 joints to the well-documented regional extensional episode, which postdates Dinaric thrusting (see Žibret & Vrabec, 2016 for outcrop-scale and map-scale evidence). In the Slovenian coastal area however, the F1 joints and associated tensional gashes clearly formed when bedding was still in horizontal orientation. This implies that Dinaric shortenting did not significantly (if at all) affect the Slovenian coastal area. The thrusting and folding which tilted the beds must therefore be both post-Dinaric and younger than NE-SW extension which is presumably of mid-Miocene age (Vrabec & Fodor, 2006). This conclusion corroborates well with the early interpretation of Placer (2007) that the coastal shortening deformation reflects young underthrusting of the Adria microplate which is independent of and subsequent to Dinaric thrusting. Our tentative chronology constrains the start of underthrusting to Late Miocene, as already presumed by Placer (2007), or even to Miocene – Pliocene transition.

Fractures of the second set F2 are NE-SW-oriented and intersect F1 joints in a nearly perpendicular orientation, with the average intersection angle of 80°. In our interpretation F2 fractures are younger and probably originated as tensional joints in a distinct extensional episode with NW-SE oriented tension, which was so far not documented in other parts of Slovenia. The relative timing of this second extension is not clear as the available data is contradictory. The orientation of F2 joints and of mesoscopic normal faults originating in the same extensional regime (Vrabec & Rožič, 2014) with respect to bedding implies that this extension also predates the tilting of the beds and is therefore probably older than shortening. On the other hand, the map-scale Rokava Fault, also implying NW-SE extension, is interpreted by Placer (2005) to cut and postdate the Buzet Thrust, a major thrust structure of the post-Dinaric coastal belt, but it apparently does not cut other thrusts in the hinterland of Buzet Thrust. Finally, geodetic data from GNSS campaigns convincingly demonstrate ongoing NNW-SSE-directed shortening in the area with no indications for contemporaneous NW-SE extension (Weber et al., 2010).

Our study shows that the orientations of F1 and F2 fractures remain reasonably constant along the entire transect crossing all major structural domains of the coastal belt. This implies that the fracture orientations probably reflect regional-scale paleostress fields and are largely independent of local influences. The only significant deviations occur in the Strunjan structure, which is a frontal deformed area with reverse faults and asymmetric folds verging in the opposite direction to the overall SW-ward vergence of the coastal area structures.

We also investigated the fracture spacing with respect to layer thickness to determine the fracture spacing index (FSI), and found that the correlation is reasonably good. The systematic relationships of fracture orientations and their spacing with respect to bedding thickness established in this study may be utilized in future engineering and resource utilization projects.

References

Busetti, M., Volpi, V., Nicolich, R., Barison, E., Romeo, R., Baradello, L., Brancatelli, G., Giustiniani, M., Marchi, M., Zanolla, C., Wardell, N., Nieto, D. & Ramella, R. 2010: Dinaric tectonic features in the Gulf of Trieste (Northern Adriatic Sea). Bolletino di Geofisica Teorica e Applicata, 51: 117–128.

Carulli, G.B. 2011: Structural model of the Trieste Gulf: A proposal. Journal of Geodynamics, 51/2-3: 156–165, doi:10.1016/j.jog.2010.05.004.

Davis, G.H. & Reynolds, S.J. 1996: Structural Geology of Rocks and Regions. John Wiley & Sons, New York: 776 p.

Moulin, A., Benedetti, L., Rizza, M., Jamšek Rupnik, P., Gosar, A., Bourlès, D., Keddadouche, K., Aumaître, G., Arnold, M., Guillou, V. & Ritz, J-F. 2016: The Dinaric fault system: Large-scale structure, rates of slip, and Plio-Pleistocene evolution of the transpressive northeastern boundary of the

Adria microplate. Tectonics, 35: 2258–2292, doi:10.1002/2016TC004188.

Narr, W. & Suppe, J. 1991: Joint spacing in sedimentary rocks. Journal of Structural Geology, 13/9: 1017-1048, doi:10.1016/0191-8141(91)90055-N.

Otoničar, B. 2007: Upper Cretaceous to Paleogene forbulge unconformity associated with foreland basin evolution (Kras, Matarsko podolje and Istria; SW Slovenia and NW Croatia). Acta Carsologica, 30: 101-120, doi:10.3986/ac.v36i1.213

Pavšič, J. & Peckmann, J. 1996: Stratigraphy and sedimentology of the Piran flysch area (Slovenia). Annales: Seria Historia Naturalis, 9: 123–138.

Placer, L. 2005: Strukturne posebnosti severne Istre. Geologija, 48/2: 245-251, doi:10.5474/geologija.2005.020.

Placer, L. 2007: Kraški rob - Geološki prerez vzdolž AC Kozina – Koper. Geologija, 50/1: 29-44, doi:10.5474/geologija.2007.003.

Placer, L. 2008: Osnove tektonske razčlenitve Slovenije. Geologija, 51/2: 205-217, doi:10.5474/geologija.2008.021.

Placer, L. 2015: Simplified structural map of Kras Kras (Slovene), Carso (Italian) = Geographical unit. Geologija, 58/1: 89-93, doi:10.5474/geologija.2015.008.

Placer, L., Košir, A., Popit, T., Šmuc, A. & Juvan, G., 2004: Buzetski narivni prelom v Istri in inverzne karbonatne megaplasti v eocenskem flišu v dolini Dragonje. Geologija, 47/2: 193-198, doi:10.5474/geologija.2004.015.

Placer, L., Celarc, B. & Vrabec, M. 2010: Osnove razumevanja tektonske zgradbe NW Dinaridov in polotoka Istre. Geologija, 53/1: 55-86, doi:10.5474/geologija.2010.005.

Vollmer, F.W. 2015: Orient 3: A new integrated software program for orientation data analysis, kinematic analysis, spherical projections, and Schmidt plots. Geological Society of America Abstracts with Programs, 47: 49.

Vrabec, M. & Fodor, L. 2006: Late Cenozoic Tectonics of Slovenia: Structural Styles at the Northeastern Corner of the Adriatic Microplate. In: Pinter, N., Grenerczy, G., Weber, J., Stein, S. & Medak, D. (eds.): The Adria Microplate: GPS Geodesy, Tectonics and Hazards, NATO Science Series, IV, Earth and Environmental Sciences, 61, 151–168, doi:10.1007/1-4020-4235-3_10.

Vrabec, M., Šmuc, A., Pleničar, M. & Buser, S. 2009: Geološki razvoj Slovenije – povzetek. In: Pleničar, M., Ogorelec, B. & Novak, M. (eds.): Geologija Slovenije, Geološki zavod Slovenije, Ljubljana: 29-33.

Vrabec, M. & Rožič, B. 2014: Strukturne in sedimentološke posebnosti obalnih klifov. In: Rožič, B., Verbovšek, T. & Vrabec, M. (eds.): 4. slovenski geološki kongres, Ankaran, 8.-10. oktober 2014. Povzetki in ekskurzije, Naravoslovnotehniška fakulteta, Ljubljana: 84-91.

Vrabec, M., Busetti, M., Zgur, F., Facchin, L., Pelos, C., Romeo, R., Sormani, L., Slavec, P., Tomini, I., Visnovic, G. & Žerjal, A. 2014: Refleksijske seizmične raziskave v slovenskem morju SLOMARTEC 2013. In: Kuhar, M., Čop, R., Gosar, A., Kobold, M., Kralj, P., Malačič, V., Rakovec, J., Skok, G., Stopar, B. & Vreča, P. (eds.): Raziskave s področja geodezije in geofizike 2013. University of Ljubljana, Faculty of Civil and Geodetic Engineering, Ljubljana: 97-101.

Weber, J., Vrabec, M., Pavlovčič-Prešeren, P., Dixon, T., Jiang, Y. & Stopar, B. 2010: GPS-derived motion of the Adriatic microplate from Istria Peninsula and Po Plain sites, and geodynamic implications. Tectonophysics, 483: 214-222, doi:10.1016/j.tecto.2009.09.001.

Žibret, L. & Vrabec, M. 2016: Palaeostress and kinematic evolution of the orogen-parallel NW-SE striking faults in the NW External Dinarides of Slovenia unraveled by mesoscale fault-slip data analysis. Geologia Croatica, 69/3: 295-305, doi:10.4154/gc.2016.30.

GEOLOGIJA 60/2, 211-221, Ljubljana 2017
https://doi.org/10.5474/geologija.2017.015

Flow dynamics in a karst aquifer studied by means of natural and artificial tracers: a case study of the Malenščica and Unica karst springs

Študij dinamike toka vode v kraškem vodonosniku z metodami sledenj z naravnimi in umetnimi sledili: primer kraških izvirov Malenščica in Unica

Metka PETRIČ

Karst Research Institute ZRC SAZU, Titov trg 2, SI-6230 Postojna, Slovenia and UNESCO Chair on Karst Education, University of Nova Gorica, Glavni trg 8, SI-5271 Vipava, Slovenia; e-mail: petric@zrc-sazu.si

Prejeto / Received 1. 3. 2017; Sprejeto / Accepted 18. 10. 2017; Objavljeno na spletu / Published online 22. 12. 2017

Dedicated to Professor Miran Veselič on the occasion of his 70th birthday

Key words: karst aquifer, natural and artificial tracers, Malenščica, Unica, Slovenia
Ključne besede: kraški vodonosnik, naravna in umetna sledila, Malenščica, Unica, Slovenija

Abstract

The Malenščica and Unica karst springs on the southern edge of Planinsko Polje are recharged from a complex karst system that is characterised by interchange between surface and subsurface flow. For periods of two hydrological years from 2007 to 2009 and one hydrological year from 2013 to 2014, selected physical properties of water (precipitation, water level and discharge, temperature, electrical conductivity - EC) were measured at various sites of the system. Time series data were elaborated using various methods. First, the characteristic values of measured parameters were compared, then an alternative method was employed to evaluate the measurement results using the frequency distribution diagram of long-term EC data sets. The temporal variations of EC in various hydrological conditions were analysed and apparent groundwater flow velocities were assessed on the basis of the time lags between the peaks (maximums) or troughs (minimums) of the EC curves of the sinking streams and springs. The aim of the study was to understand the relationships between different parts of the recharge area and their changing contributions to the springs in various hydrological conditions. The results, which were validated by the findings of previous tracer tests using artificial tracers, indicate that the use of selected natural tracers provides a comprehensive understanding of the functioning of karst aquifers.

Izvleček

Kraška izvira Malenščica in Unica, na južnem robu Planinskega polja v jugozahodni Sloveniji, se napajata iz obsežnega kraškega vodonosnika, za katerega je značilno prepletanje površinskih in podzemnih tokov. V obdobju dveh hidroloških let od 2007 do 2009 in v obdobju enega hidrološkega leta od 2013 do 2014 smo na različnih mestih znotraj kraškega sistema merjeni izbrani fizikalni parametri (padavine, nivo vode in pretok, temperatura, specifična električna prevodnost - SEP). Časovne serije podatkov smo analizirali z uporabo različnih metod. Najprej smo primerjali karakteristične vrednosti merjenih parametrov, potem smo privzeli alternativni način obdelave rezultatov merjenja z uporabo diagramov frekvenčne porazdelitve dolgotrajnih časovnih serij vrednosti SEP. Analizirali smo časovno spremenljivost vrednosti SEP v različnih hidroloških razmerah in na osnovi določitve časovnih zamikov med vrhovi in doli krivulj SEP za ponikalnice in izvire ocenili navidezne hitrosti toka podzemne vode. Cilj raziskave je bil razumevanje odnosov med različnimi deli zaledja in spreminjanja njihovih deležev pri napajanju izvirov ob različnih hidroloških razmerah. Rezultati, ki so bili primerjani z izsledki predhodno izvedenih sledenj z umetnimi sledili, potrjujejo primernost uporabe izbranih naravnih sledil za izboljšanje razumevanja delovanja kraških vodonosnikov.

Introduction

Karst aquifers are very complex systems with heterogeneous structure and various types of porosity. They are characterised by concentrated recharge with sinking streams or diffuse infiltration through karstified terrain. Underground, water flows through karst conduits, fissures and pores of different sizes towards karst springs, where it again flows out onto the surface. Together with the water, pollutants – the consequence of various human activities in the sensitive karst environment – can also spread quickly and represent an increasing threat to the quality of karst springs. Karst aquifers as important sources of water supply are therefore highly vulnerable to pollution. For the efficient planning of protection measures it is essential to understand their functioning and to consider the characteristics of groundwater flow and solute transport within karst systems.

Various research methods are used to study karst aquifers. Artificial tracers have proven to be very useful in research of groundwater flow, its directions and characteristics, and identification of recharge areas (e.g. Käss, 1998; Benischke et al., 2007; Kogovšek & Petrič, 2014). Another very important tool for the study of functioning of karst springs is the use of natural tracers (e.g. Ryan & Meiman, 1996; Grasso & Jeannin, 2002; Birk et al., 2004; Hunkeler & Mudry, 2007; Ravbar et al., 2011). This method involves detailed monitoring of natural properties, such as discharge, temperature, electrical conductivity, and chemical composition of water at different sites within a karst system. Based on the comparison of the data obtained, it is possible to make inferences about the characteristics of groundwater flow, the influence of different types of recharge, exchange between

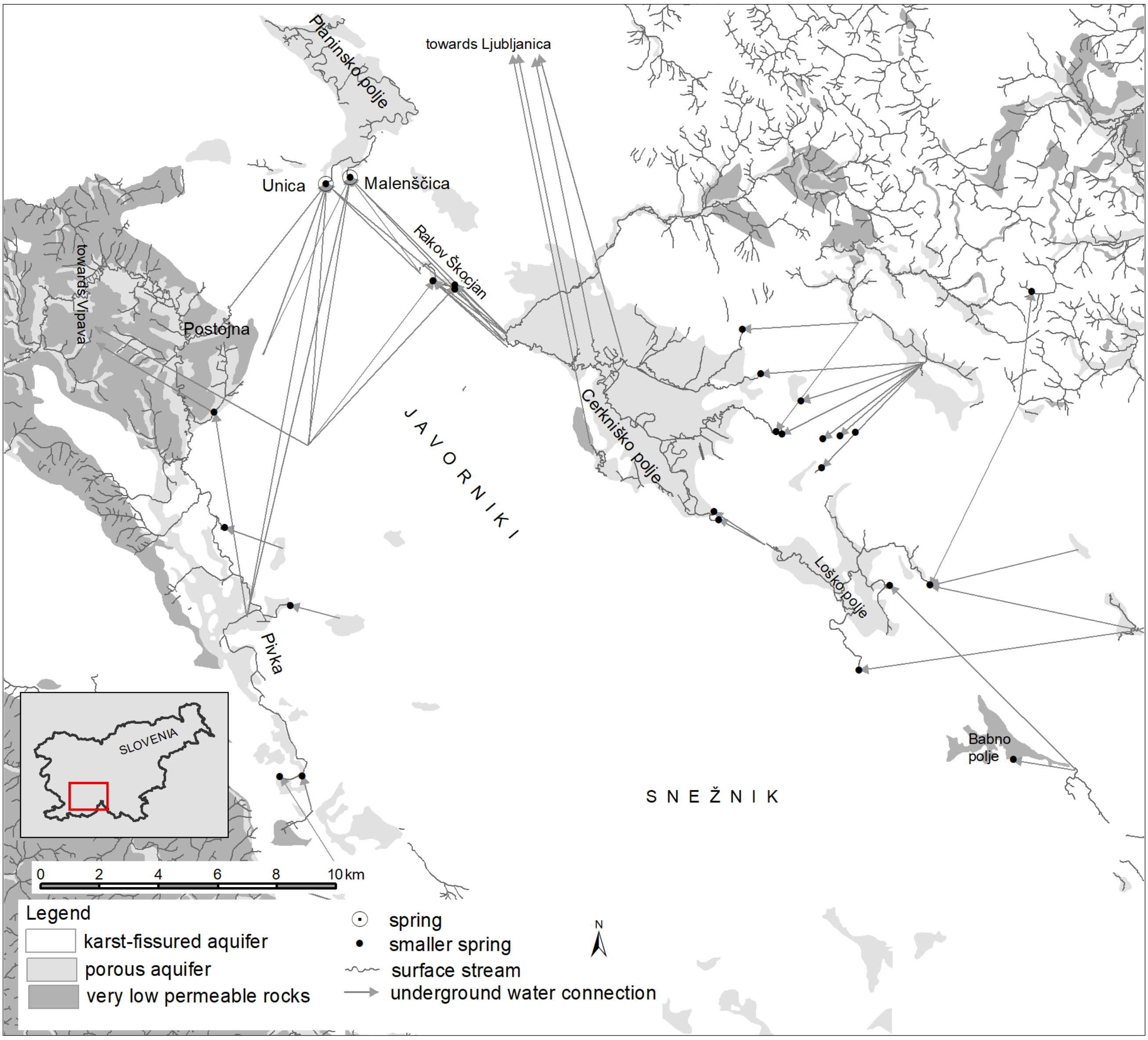

Fig. 1. Hydrogeological context of the study area with proven groundwater flow connections.

surface water and groundwater, and the relationship between inflows from various parts of the catchment and their contributions to the springs. In some cases, natural and artificial tracers were applied in conjunction in order to investigate the hydrogeological functioning of karst aquifers (Kogovšek, 2001; Einsiedl, 2005; Ravbar et al., 2012; Mudarra, et al., 2014; Lauber & Goldscheider, 2014).

In the research presented here, natural tracers were used for an investigation of recharge dynamics in the catchment area of the Malenščica and Unica springs in south-western Slovenia. The former is a regional source of water supply. The relatively high discharge of the spring when water levels are low is an important advantage, but due to the large size and complex structure of the recharge area it is difficult to plan and implement the protection and control of water quality. To understand the relationships between different parts of the recharge area and the changes in their contributions, the physical parameters of water at different locations within the recharge area and at the springs were monitored and analysed. The emphasis was on a detailed analysis and comparison of spatial and temporal variations of natural tracers in various hydrological conditions. The information obtained about the characteristics of groundwater flow and solute transport was compared with the results of tracer tests with artificial tracers previously carried out in the study area.

Study area

Hydrogeological characteristics

Several karst springs are located on the southern margin of Planinsko Polje in south-western Slovenia. The biggest among them are the Unica and Malenščica springs (Fig. 1). The latter is an important source of water supply for approximately 21,000 inhabitants in the Postojna and Pivka municipalities. The overall daily discharge of the Malenščica spring is regularly measured by the Environmental Agency of the Republic of Slovenia. According to data for the 1961–1990 period, the lowest discharge was 1.1 m^3/s, the mean discharge 6.7 m^3/s, and the maximum discharge 9.9 m^3/s (Kolbezen & Pristov, 1998). Higher discharges were measured in 2002, with a maximum daily value of 11.2 m^3/s on 24 October 2002. Long-term data on discharges of the Unica spring before its confluence with the Malenščica spring are only available for the period from 1954 to 1975 (Internet 1). In this period the lowest discharge was 0.04 m^3/s, the mean discharge 16.6 m^3/s, and the highest discharge 75.6 m^3/s. The obvious difference in discharges at high water levels indicates that the maximum flow rates of the Malenščica spring are limited by the structure of the outflow zone. At low water levels this spring is the main outflow of the karst system (more than 90 %), but when water levels are high only one tenth of the overall discharge on Planinsko Polje comes through it. At medium water levels the discharge of the Malenščica spring exceeds 8 m^3/s, but only at very high water levels does it increase above 9 m^3/s.

The recharge area of the Malenščica and Unica springs, which is estimated to extend over about 746 km^2, is a complex karst system that can be divided into three separate but hydrologically connected parts (Petrič, 2010). The central part is the Javorniki–Snežnik karst massif, which is composed of Cretaceous carbonate rocks, mostly limestone. It is bordered on the western side by the valley of the river Pivka, which has a karst catchment in its upstream section and is additionally recharged by surface water through less permeable Quaternary alluvial sediments and Eocene flysch in its downstream section. At the contact with carbonate rocks, the Pivka sinks underground in the cave Postojnska Jama and provides allogenic recharge to the studied karst system (Fig. 2).

On the eastern and northern sides, the karst massif is bordered by a string of karst poljes, which are distributed along a SE–NW trend (Fig. 1). The area between the Planinsko and Cerkniško poljes is composed of Upper Triassic dolomite, which is bordered on the north-eastern side by Jurassic limestone and, locally, dolomite. Quaternary alluvial sediments are deposited on the karst poljes. At high water levels these are flooded and intermittent lakes form. From the ponors on the north-western margin of Cerkniško Polje, water flows underground towards the springs of the Rak river and continues for a distance of 2 km on the surface in the valley of Rakov Škocjan. This area is composed of Cretaceous limestones, which are covered along the stream reach by Holocene sediments. The Rak sinks again in the cave known as Tkalca Jama and flows underground toward the springs on Planinsko Polje (Fig. 2). The Unica spring emerges from the cave Planinska Jama,

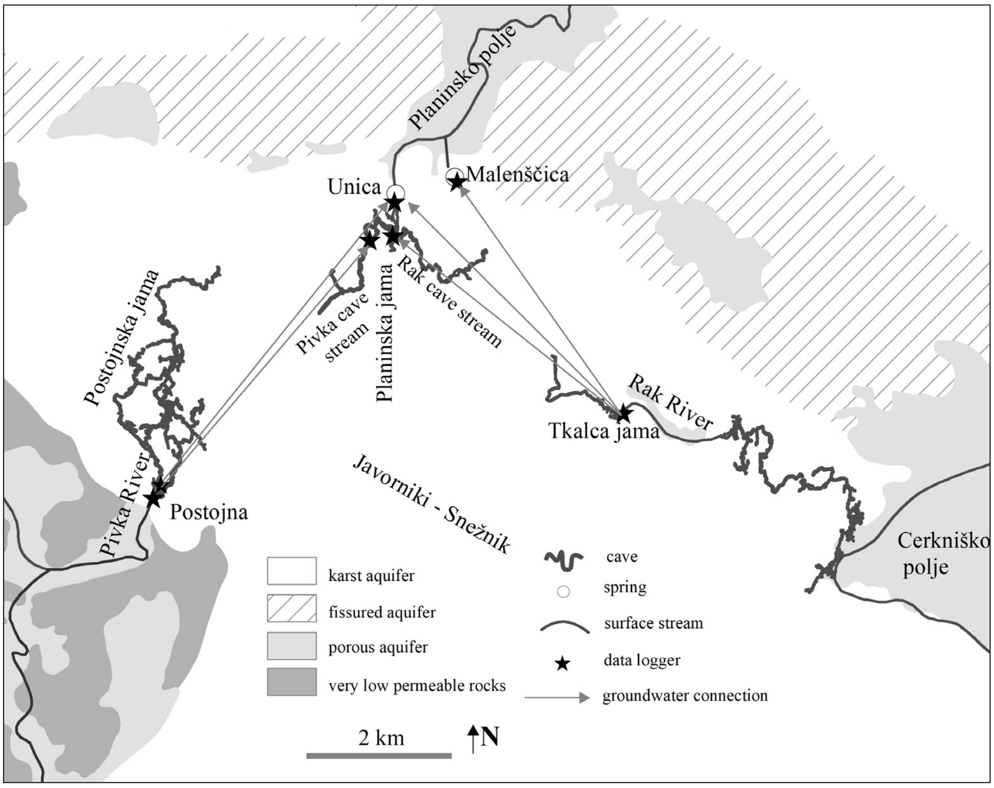

Fig. 2. Detailed hydrogeological map of the study area with marked monitoring sites.

in which the subsurface waters from the Pivka area (along the Pivka cave stream) and from the area of Rakov Škocjan (along the Rak cave stream) flow together and form a unique subsurface confluence.

The three areas contributing to the Malenščica and Unica springs are referred to as the Javorniki, Pivka and Cerknica parts of the recharge area. In the Javorniki part, subsurface flow dominates, while in the other two parts surface streams also are present. As a result, surface water and groundwater constitute a single hydrodynamic system.

Groundwater flow velocities defined by tracer tests with artificial tracers

The groundwater connections within the system have been demonstrated by several past tracer tests using artificial tracers. Apparent dominant flow velocities were calculated taking into account the time from injection of tracer to the maximum achieved concentration and the distances between the ponors and springs. The Pivka was traced at the ponor into the cave Postojnska Jama in 1928, 1974, 1977, 2008 and 2009 (Šerko, 1946; Habič, 1987; Gabrovšek et al., 2010; Ravbar et al., 2010). Groundwater flow toward the Pivka cave stream and the Unica spring was proved, whereas no connection with the Malenščica spring was detected. None of these tracer tests was carried out at high water levels. The highest apparent dominant flow velocity 145 m/h was determined in May 2008 when the discharge of the Unica spring was less than 12 m^3/s (Gabrovšek et al., 2010).

The groundwater connections between the ponors of the Rak in Rakov Škocjan and between the Rak cave stream and the Unica and Malenščica springs were proved by tracer tests in 1928, 1939, 1964, 1967, 2008 and 2009 (Šerko, 1946; Gams, 1970; Habič, 1987; Gabrovšek et al., 2010; Ravbar et al., 2010). In various hydrological conditions apparent dominant flow velocities of between 7 and 196 m/h were determined. The highest velocity of 196 m/h was defined by a tracer test in November 1967, when the discharge of the Malenščica spring was around 9 m^3/s. Other tracer tests were carried out at lower water levels.

In the Javorniki part of the catchment, tracer tests were carried out in 1955, 1988, 1997, 2008 and 2009 (Habič, 1987; Kogovšek, 1999; Kogovšek & Petrič, 2004; Gabrovšek et al., 2010; Ravbar et al., 2010). From various injection sites, groundwater flow towards the Rak and Pivka cave streams and the Unica and Malenščica springs with apparent dominant flow velocities of between 4 and 25 m/h was proved.

Methods

Data for two hydrological years from 4 September 2007 to 15 September 2009 were first gathered by field measurements. Precipitation was measured near Postojna by an Onset RG-M rain gauge. At the Malenščica and Unica springs, the water level, temperature (T) and electrical conductivity (EC) were measured using an ISCO 6700 with a 750 area-velocity flow module and YSI 600 probe, and a Logotronic Gealog S data logger. At the Rak cave stream, water levels, T and EC were measured using an Eikelkamp CTD diver. The second measuring campaign started in 2012, with data for the hydrological year from 9 September 2013 to 29 June 2014 used for comparison. The same type of equipment as in the first period was used for precipitation measurements and at the Malenščica spring. At the Unica karst spring, in the Rak and Pivka cave streams and in the Rak and Pivka rivers, water levels, T and EC were measured using Onset HOBO water level and conductivity data loggers. For both measuring periods all data were collected at 30-minute intervals and the discharges for the Malenščica and Unica springs were calculated on the basis of stage-discharge curves prepared by the Slovenian Environmental Agency.

The minimum, average and maximum values of discharges, T and EC for the two selected periods were calculated and compared.

Additionally, an alternative method was employed to evaluate the measurement results using the frequency distribution diagram of long-term EC data sets (Massei et al., 2007; Mudarra & Andreo, 2011; Caetano Bicalho et al., 2012). The data from the second measuring campaign were used and the range of the classes of EC was 10 µS/cm. For each measurement site the percentage of measured values within each class was defined and EC frequency distribution (ECFD) curves were formed. They reflect the variability of the mineralisation and of the chemical composition of the water. Based on a comparison of the curves, it was possible to identify the existence of different types of water recharging the Malenščica and Unica springs.

In the next step, the temporal variations of EC in various hydrological conditions were analysed. For the selected time interval from 18 December 2013 to 16 February 2014, the change of hydrological conditions from low to high water levels is characteristic. Comparison of the EC curves of the sinking rivers, cave streams and springs with precipitation and discharges within this period enables the assessment of the influence of hydrological conditions on the shares of recharge of the springs from different parts of the catchment.

Based on the assumption that the velocity of the transfer of the EC signal along the groundwater flow is equal to the velocity of water flow, the positions of the peaks (maximums) or troughs (minimums) of the EC curves at ponors and springs are compared and the time lags between them assessed. Considering these time lags and the distance as the crow flies between the ponors and springs, the apparent velocities of flow between them were calculated. The values obtained were compared with the apparent flow velocities defined by the tracer tests with artificial tracers carried out in the study area in the context of previous research.

Results and discussion

Comparison of characteristic values

Table 1 compares the characteristic values of discharges, T and EC for the two hydrological years 2007–2009 and one hydrological year 2013–2014. Data for three measurement sites are available for the first period, along with data for six measurement sites for the second period. Similar maximum discharges were measured in the two periods, while significantly higher values of mean discharges and the absence of very low discharges in the second period characterise it as a wet year.

The largest range of values is characteristic for the river Pivka. It is recharged by karst springs with higher EC values, which after precipitation events are significantly lowered by surface streams from flysch areas. The highest values at low water levels are probably also a result of pollution (untreated waste waters, agriculture). The high range of T values is due to the long distance of surface flow and adaptations to changes in air temperature. The Rak also has the characteristics of surface flow but the fluctuations are smaller because it is mostly recharged by karst springs, there is no significant influence of surface tributaries, and the distance of surface flow from karst springs to the measurement site is shorter.

Table 1. Characteristic values of measured parameters in the two hydrological years 2007–2009 and in the hydrological year 2013–2014.

	2007-2009				2013-2014			
Location/parameter	Min	Mean	Max	Max-Min	Min	Mean	Max	Max-Min
Malenščica spring								
Discharge (m³/s)	1.09	5.93	9.91		2.56	7.06	9.89	
Temperature (°C)	1.7	8.9	17.7	16.0	2.5	9.0	14.3	11.8
Conductivity (µS/cm)	278	369	440	162	312	359	402	90
Unica spring								
Discharge (m³/s)	0.04	11.20	69.34		0.68	25.8	69.3	
Temperature (°C)	3.0	9.2	14.6	11.6	2.7	8.6	12.3	9.6
Conductivity (µS/cm)	221	377	479	258	274	364	480	186
Rak cave stream								
Temperature (°C)	2.6	9.4	15.0	12.4	3.6	8.6	12.7	9.1
Conductivity (µS/cm)	267	362	451	184	314	358	429	115
Pivka cave stream								
Temperature (°C)					2.1	9.1	12.3	10.2
Conductivity (µS/cm)					229	371	519	290
Rak River								
Temperature (°C)					2.3	9.9	18.0	15.7
Conductivity (µS/cm)					294	378	477	183
Pivka River								
Temperature (°C)					0.9	10.7	26.9	26.0
Conductivity (µS/cm)					192	371	536	344

Both described rivers are sinking streams which flow underground through highly permeable channels toward cave streams in Planinska Jama and the Unica and Malenščica springs. High fluctuations of measured values in the Pivka river are mostly reflected in the Pivka cave stream. This shows that this stream is mainly recharged by the Pivka river and that the share of recharge from other parts is very low. Noticeable but far less marked is the influence of the river Pivka on the Unica spring, which additionally receives an important share of recharge from the Rak cave stream.

EC Frequency Distribution (ECFD)

Various ranges of EC values in the hydrologically connected system indicate the existence and mixing of different types of water, which contribute in various shares to the recharge of the Unica and Malenščica springs. EC Frequency Distribution (ECFD) was used to identify the existence of and relationships between these groundwater types. In Figure 3A the ECFD for the Malenščica and Unica springs is first compared. The curves for the two springs differ significantly, which indicates the existence of different types of water in the recharge area.

In the next step, the curves for both springs were compared with the curves for the monitoring sites in their recharge area. First the curve for Unica spring was compared with the curves for the Rak and Pivka cave streams, which flow together in Planinska Jama and form the Unica spring. The two cave streams differ significantly in terms of ECFD, and the Unica spring is a mixture of them (Fig. 3B).

The ECFD curves for the Pivka river and the Pivka cave stream are practically identical (Fig.3C), which confirms the direct connection between the sinking stream and the cave stream and fast water flow through well-developed karst channels.

The connection between the Rak river, Rak cave stream and Malenščica spring is more complex and some additional source of recharge with lower EC values exists (Fig. 3D). Based on the known characteristics of the area, it can be concluded that this source is autogenic recharge from the Javorniki–Snežnik karst aquifer. Differences in the shape of the ECFD curves for the Rak cave stream and Malenščica spring point to some differences in the characteristics of distribution and shares of this autogenic recharge.

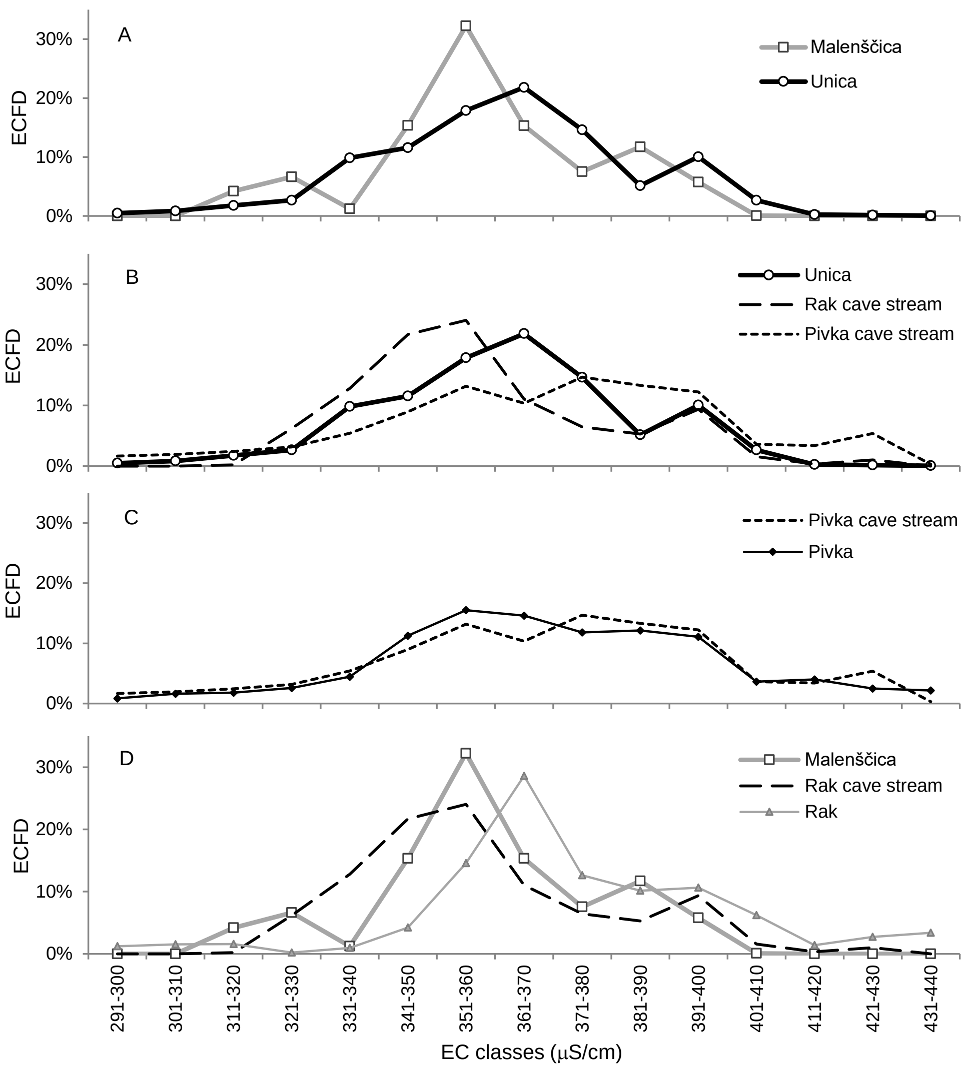

Fig. 3. Comparison of electrical conductivity frequency distribution (ECFD) curves. EC data measured in the period from 9 September 2013 to 29 June 2014 at 30-minute intervals were used.

Temporal evolution of EC values

The analysis described above enables a general characterisation of different types of recharge waters based on the whole set of measured parameters in the period of a hydrological year. A more detailed review of data shows that the shares of recharge from different contribution areas change with hydrological conditions. The data presented in Figure 4 enable an assessment of the temporal evolution of measured EC values. The selected interval begins in December 2013 with low water conditions. In the subsequent period the discharges react to each precipitation event with a typical peak, gradually increasing to high water conditions in February 2014.

As in the case of ECFD, the two main springs, the Unica and the Malenščica, were compared first. Significant differences indicate different sources of recharge. The EC curves of the Unica spring show an important influence of the recharge from the sinking Pivka river that is not characteristic for the Malenščica spring. Comparison of the EC values of the Unica with the EC values of the two cave streams shows that the Unica is a mixture of both cave streams. These two differ significantly in EC values, and the EC value of the Unica is somewhere in between, depending on the share of water from the individual streams. The highest EC values in the Unica were measured at low water levels, when the spring was mainly recharged from the Rak cave stream. After each precipitation event, inflow from the Pivka cave stream, with characteristic lowering of EC values, prevails for the first few hours, after which the share of inflow from the Rak cave stream gradually increases.

Comparison of the EC curves for the Pivka river and Pivka cave stream confirms a direct connection between the two water flows. The shapes of the curves are very similar, only the one of the Pivka cave stream is slightly attenuated and has a certain time delay.

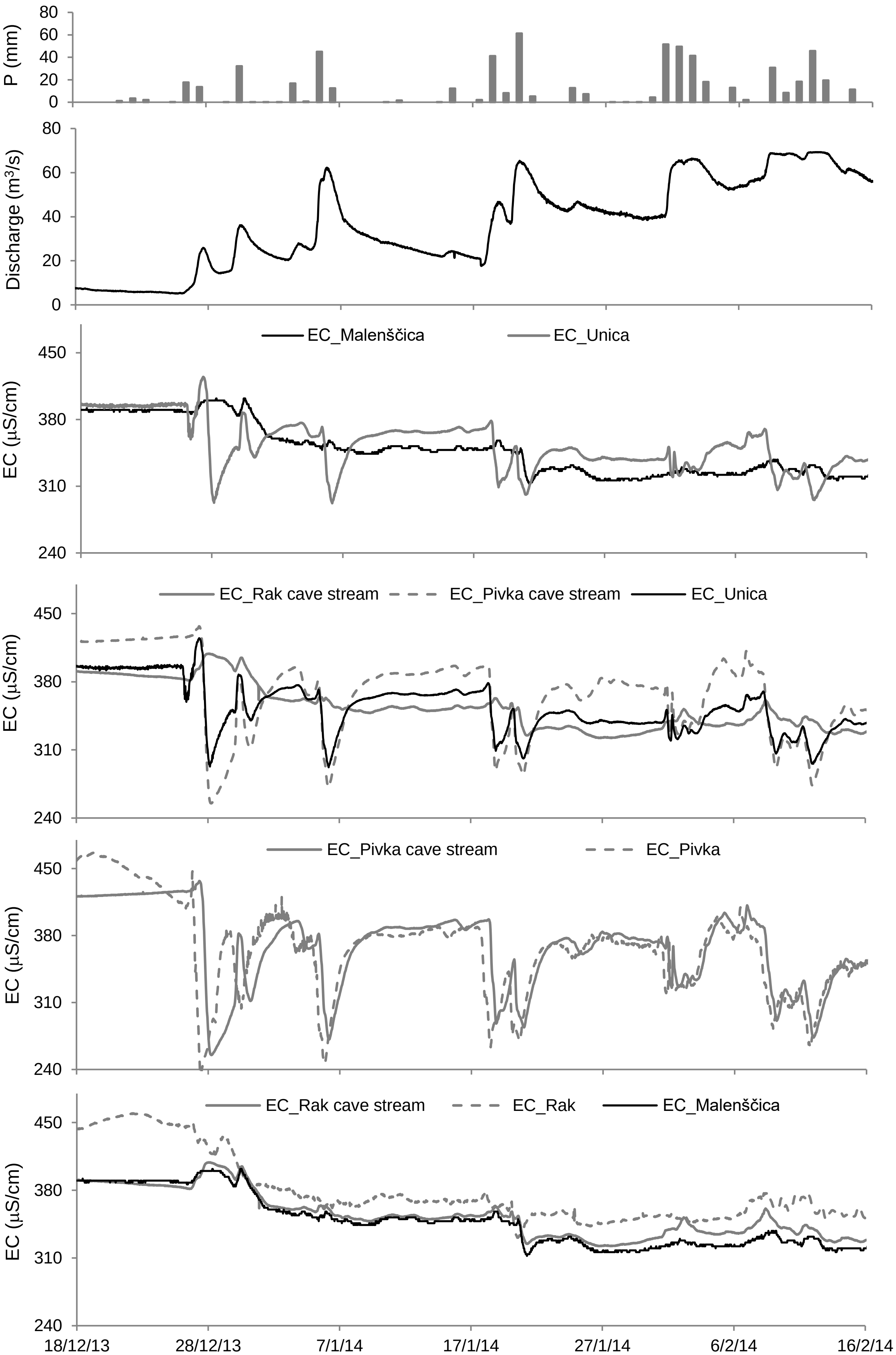

Fig. 4. Temporal evolution of precipitation in Postojna, discharge of the Unica spring and electrical conductivity (EC) of water at various locations within the studied karst system in the selected time interval from 18 December 2013 to 16 February 2014.

The EC curves for the Rak cave stream and the Malenščica spring are significantly different from the EC curves of the Pivka and very similar to those of the Rak river. This excludes their connection with the Pivka river and confirms their recharge from the Rak river. Significantly lower EC values in the cave stream and spring (by 20 to 30 μS/cm) are due to an important share of autogenic recharge from the Javorniki–Snežnik karst aquifer. The EC values of the Rak cave stream and Malenščica spring are practically the same, only differing significantly when water levels are high. The shift of the EC values of the Rak cave stream toward the EC values of the Rak river could be explained by limited maximum discharges of the Malenščica spring at high water levels and an increased share of recharge of the Rak cave stream from the Rak river.

Finally, for the assessment of the flow velocities between the ponors and the springs, the positions of the peaks (maximums) or troughs (minimums) of the EC curves at these monitoring sites were compared. Using the graphs, the time lags of peaks and troughs were defined for groundwater flow between the Pivka river, Pivka cave stream and Unica spring, and between the Rak river, Rak cave stream and Malenščica spring in various hydrological conditions. On the basis of these time lags and the distance as the crow flies between the monitoring sites, the apparent flow velocities were calculated. The circles and squares in Figure 5 represent the relationships between assessed flow velocities and the discharges of the springs. For the Unica spring (left graph in Fig. 5) it is evident that the velocities increase with increasing discharges, while for the Malenščica spring (right graph in Fig. 5) such a relationship does not exist. The apparent flow velocities in the Pivka river–Unica spring system range from 263 to 769 m/h for discharges of the Unica spring between 18 and 69 m^3/s. For the Rak river–Malenščica spring system, apparent flow velocities from 129 to 258 m/h were defined for discharges of the Malenščica spring ranging from 8 to 8.5 m^3/s. A further increase of discharge is not followed by an increase of velocity, and for the discharge of 9.5 m^3/s the apparent flow velocity was only 166 m/h. This indicates that when water levels in the Rak river–Malenščica spring system are very high, water flow is retained and slower due to the limited outflow from the Malenščica spring. On the other hand, the karst channels in the Pivka river–Unica spring system are large and permeable enough to allow the unimpeded transfer of water.

The calculated apparent flow velocities were compared with the apparent flow velocities defined by the tracer tests using artificial tracers. For these values, the ratios to discharges are presented as triangles in Figure 5. The established good correlation between the two sets of defined apparent flow velocities supports the applicability of the method of apparent flow velocity assessment based on a comparison of EC curves.

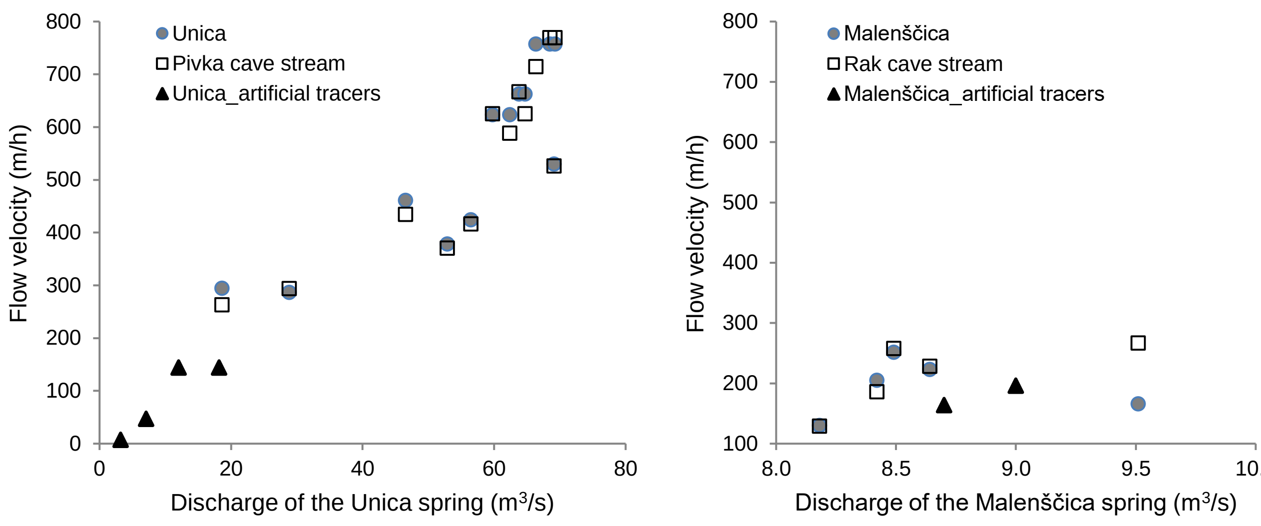

Fig. 5. Dependence between hydrological conditions and estimated flow velocities (based on the comparison of electrical conductivity (EC) curves and tracer tests with artificial tracers).

Conclusions

The Malenščica and Unica springs on the southern edge of Planinsko Polje are recharged from a large and complex karst aquifer in which different sources of allogenic and autogenic recharge are combined. Several tracer tests using artificial tracers have been carried out in this area in past years, so the directions and characteristics of subsurface flow are relatively well defined. This study, however, tested the potential of the use of natural tracers for the investigation of recharge dynamics and understanding of hydrological relations between different parts of the recharge area. Some general properties of the groundwater connections and relations between various recharge sources and the springs were already indicated on the basis of a comparison of the characteristic values of the measured parameters, while a more detailed analysis was enabled by the use of ECFD curves. In the next step, a temporal evolution of the EC values for different monitoring sites was compared and the influence of changes in hydrological conditions on the relationships between different types of recharge and the springs were evaluated. The important influence of hydrological conditions was confirmed. However, a more detailed analysis of the EC curves and the use of adequate statistical tools would be needed for a better understanding of these relationships.

The defined connections and the similar shapes of the EC curves also enabled an estimate of flow velocities between the ponors and the springs based on the comparison of the positions of the peaks (maximum) or troughs (minimums) of the EC curves at these monitoring sites. The estimated values of apparent flow velocities are in good agreement with the velocities defined by the tracer tests using artificial tracers. This supports the applicability of the method tested, particularly for periods of high water levels, where data from the tracer tests using artificial tracers are lacking. Information about the velocity of flow and solute transport in high water conditions is essential for testing various scenarios of pollution spread and the planning of protection of drinking water sources. The method described for processing the EC time series is straightforward, while the equipment for field measurements of EC is relatively cheap and simple to use.

The results presented in the paper were obtained through some basic, mostly qualitative analysis of data. However, the research project continues with new activities, including a more detailed, quantitatively based analysis of the time series data. The monitoring net has been expanded with new measuring sites, most notably the data loggers installed in caves within the Javorniki–Snežnik karst aquifer, which will provide some additional information about the characteristics of autogenic recharge.

Acknowledgement

The author acknowledges the financial support from the Slovenian Research Agency (research core funding No P6-0119) and from the Slovenian National Commission for UNESCO (intergovernmental programme IHP). Special thanks are due to Franjo Drole for his help with installation of measuring instruments.

References

Benischke, R., Goldscheider, N. & Smart, C. 2007: Tracer techniques. In: Goldscheider, N. & Drew, D. (eds.): Methods in karst hydrogeology. Taylor & Francis, London: 147–170.

Birk, S., Liedl, R. & Sauter, M. 2004: Identification of localised recharge and conduit flow by combined analysis of hydraulic and physico-chemical spring responses (Urenbrunnen, SW-Germany). Journal of Hydrology, 286/1: 179–193, doi:10.1016/j.jhydrol.2003.09.007.

Caetano Bicalho, C., Batiot-Guilhe, C., Seidel, J. L., Van Exter, S. & Jourde, H. 2012: Geochemical evidence of water source characterization and hydrodynamic responses in a karst aquifer. Journal of Hydrology, 450–451: 206–218, doi:10.1016/j.jhydrol.2012.04.059.

Einsiedl, F. 2005: Flow system dynamics and water storage of a fissured-porous karst aquifer characterized by artificial and environmental tracers. Journal of Hydrology, 312:312–321, doi:10.1016/j.jhydrol.2005.03.031.

Gabrovšek, F., Kogovšek, J., Kovačič, G., Petrič, M., Ravbar, N. & Turk, J. 2010: Recent results of tracer tests in the catchment of the Unica River (SW Slovenia). Acta Carsologica, 39/1: 27–38.

Gams, I. 1970: Maksimiranost kraških podzemeljskih pretokov na primeru ozemlja med Cerkniškim in Planinskim poljem. Acta Carsologica, 5: 171–187.

Grasso, D. A. & Jeannin, P.-Y. 2002: A global experimental system approach of karst springs, hydrographs and chemographs. Ground Water, 40: 608–618, doi:10.1111/j.1745-6584.2002.tb02547.x.

Habič, P. 1987: Raziskave kraških izvirov v Malnih pri Planini in zaledja vodnih virov v občini Postojna. Inštitut za raziskovanje krasa ZRC SAZU, Postojna: 58 p.

Hunkeler, D. & Mudry, N. 2007: Hydrochemical methods. In: Goldscheider, N. & Drew, D. (eds.): Methods in karst hydrogeology. Taylor & Francis, London: 93–121.

Käss, W. 1998: Tracing technique in geohydrology. A. A. Balkema, Rotterdam: 581 p.

Kogovšek, J. 1999: Nova spoznanja o podzemnem pretakanju vode v severnem delu Javornikov (Visoki kras). Acta Carsologica, 28/1: 161–200.

Kogovšek, J. 2001: Monitoring the Malenščica water pulse by several parameters in November 1997. Acta Carsologica, 30/1: 39–53.

Kogovšek, J. & Petrič, M. 2004: Advantages of longer-term tracing three case studies from Slovenia. Environmental Geology, 47/1: 76–83, doi:10.1007/s00254-004-1135-8.

Kogovšek, J. & Petrič, M. 2014: Solute transport processes in a karst vadose zone characterized by long-term tracer tests (the cave system of Postojnska Jama, Slovenia). Journal of Hydrology, 519: 1205–1213, doi:10.1016/j.jhydrol.2014.08.047.

Kolbezen, M. & Pristov, J. 1998: Surface streams and water balance of Slovenia. Hidrometeorološki zavod Republike Slovenije, Ljubljana: 98 p.

Lauber, U. & Goldscheider, N. 2014: Use of artificial and natural tracers to assess groundwater transit-time distribution and flow systems in a high-alpine karst system (Wetterstein Mountains, Germany). Hydrogeology Journal, 22/8: 1807–1824, doi:10.1007/s10040-014-1173-6.

Massei, N., Mahler, B. J., Bakalowicz, M., Fournier, M. & Dupont, J. P. 2007: Quantitative interpretation of specific conductance frequency distribution in karst. Groundwater, 45/3: 288–293, doi:10.1111/j.1745-6584.2006.00291.x.

Mudarra, M. & Andreo, B. 2011: Relative importance of the saturated and the unsaturated zones in the hydrogeological functioning of karst aquifers: the case of Alta Cadena (Southern Spain). Journal of Hydrology, 397/3–4, 263–280, doi:10.1016/j.jhydrol.2010.12.005.

Mudarra, M., Andreo, B., Marín, A. I., Vadillo, I. & Barberá, J. A. 2014: Combined use of natural and artificial tracers to determine the hydrogeological functioning of a karst aquifer: the Villanueva del Rosario system (Andalusia, southern Spain). Hydrogeology Journal, 22/5: 1027–1039, doi:10.1007/s10040-014-1117-1.

Petrič, M. 2010: Characterization, exploitation, and protection of the Malenščica karst spring, Slovenia. In: Kresic, N. & Stevanovic, Z. (eds.): Groundwater hydrology of springs. Elsevier, Butterworth-Heinemann, Oxford: 428–441.

Ravbar, N., Barberá, J. A., Petrič, M., Kogovšek, J. & Andreo, B. 2012: The study of hydrodynamic behaviour of a complex karst system under low-flow conditions using natural and artificial tracers (the catchment of the Unica River, SW Slovenia). Environmental Earth Sciences, 65/8: 2259–2272, doi:10.1007/s12665-012-1523-4.

Ravbar, N., Engelhardt, I. & Goldscheider, N. 2011: Anomalous behaviour of specific electrical conductivity at a karst spring induced by variable catchment boundaries: the case of the Podstenjšek spring, Slovenia. Hydrological Processes, 25/13: 2130–2140, doi:10.1002/hyp.7966

Ravbar, N., Petrič, M. & Kogovšek, J. 2010: The characteristics of groundwater flow in karst aquifers during long lasting low flow conditions, example from SW Slovenia. In: Carrasco, F., Durán Valsero, J. J. & LaMoreaux, J.W. (eds.): Advances in research in karst media. Springer, Berlin, Heidelberg: 131–136.

Ryan, M. & Meiman, J. 1996: An examination of short-term variations in water quality at a karst spring in Kentucky. Groundwater, 34: 23–30, doi:10.1111/j.1745-6584.1996.tb01861.x.

Šerko, A. 1946: Barvanje ponikalnic v Sloveniji. Geografski vestnik, 18: 125–139.

Internet resource:

Internet 1: http://vode.arso.gov.si/hidarhiv/ (3.10.2016).

GEOLOGIJA 60/2, 223-234, Ljubljana 2017

https://doi.org/10.5474/geologija.2017.016

Mineralogical and geochemical characteristics of mudstones in the Jersovec chert deposit

Mineraloške in geokemične značilnosti muljevcev iz nahajališča roženca Jersovec

Simona JARC[1], Simon JERINA[2], Miloš MILER[3] & Nina ZUPANČIČ[1,4]

[1]University of Ljubljana, Faculty of Natural Sciences and Engineering, Department of Geology, Aškerčeva 12, SI-1000 Ljubljana, Slovenia, e-mails: simona.jarc@ntf.uni-lj.si; nina.zupancic@ntf.uni-lj.si
[2]Aškerčeva ul. 8, SI-8000 Novo mesto, Slovenia, e-mail: simon.jerina@gmail.com
[3]Geological Survey of Slovenia, Dimičeva ulica 14, SI-1000 Ljubljana, Slovenia, e-mail: milos.miler@geo-zs.si
[4]Ivan Rakovec Institute of Paleontology, ZRC SAZU, Novi trg 2, SI-1000 Ljubljana, Slovenia

Prejeto / Received 11. 9. 2017; Sprejeto / Accepted 26. 10. 2017; Objavljeno na spletu / Published online 22. 12. 2017

Key words: mudstone, chert, geochemistry, SEM/EDS, Jersovec
Ključne besede: muljevec, roženec, geokemija, SEM/EDS, Jersovec

Abstract

Jersovec chert deposit is a part of the transitional zone between the internal and the external Dinarides. Tethyan cherts are often interlaid with fine-grained material, as is also the case in Jersovec, where chert beds interchange with several thin, up to 10 cm thick layers of fine-grained sedimentary rocks. The source of this material is often questionable and interpreted to be terrigenous, volcanogenic or even combination of both. In order to determine origin and depositional environment of fine-grained material, detailed mineralogical and geochemical analyses were performed.

Fine-grained sedimentary rocks were characterised by X-ray diffraction (XRD), scanning electron microscopy/energy dispersive X-ray spectroscopy (SEM/EDS) and inductively coupled plasma emission spectroscopy (ICP-ES) and mass spectroscopy (ICP-MS). All samples are mineralogically very similar but differ in mineral ratios. They contain quartz and clay minerals, predominantly illite/muscovite and chlorite group minerals. SEM/EDS analysis additionally revealed zircon, monazite, Ti-oxide (probably rutile) and iron oxides/hydroxides in all samples, whereas chromite, ilmenite, xenotime, apatite and baryte were found only in some of them. The average sizes of accessory minerals range from 3–20 µm. Two samples differ from the others by their brown colour and higher Fe_2O_3 and lower SiO_2 contents. All other samples are green. Chemical analysis showed that they consist mostly of SiO_2 (46.3–69.3 %), Al_2O_3 (15–24.1 %) and minor contents of K_2O (2.8–3.4 %), Fe_2O_3 (2.1–8.4 %), MgO (1.6–2.3 %), TiO_2 (0.5–0.7 %), CaO (0.3–1.4 %), Na_2O (0.1 %) and P_2O_5 (up to 0.5 %).

Position of all samples in the Zr/TiO_2 vs. $(V+Ni+Cr)/Al_2O_3$ diagram points to terrigenous origin and sedimentation on the continental margin. According to the chemical weathering indices (CIA and CIW) material has been subjected to the intense and long weathering, supported also by the index of compositional variability (ICV), which corresponds to the compositionally mature material, and by rounded zircon and ilmenite grains.

Izvleček

Nahajališče roženca Jersovec se nahaja v prehodni coni med Zunanjimi in Notranjimi Dinaridi. V nahajališču so med roženci tanke, do 10 cm debele plasti drobnozrnatih sedimentnih kamnin. Takšne sedimentne kamnine z roženci so zelo značilne na območju Tetide. Izvor medplastovnega materiala je pogosto vprašljiv in ga razlagajo kot terigen ali vulkanski ali kombinacijo obeh. Je pomemben indikator sedimentacijskega okolja. Z geokemičnimi in mineraloškimi analizami smo skušali določiti izvor teh sedimentov.

Mineralno sestavo smo določili z metodo rentgenske difrakcije (XRD) in z vrstično elektronsko mikroskopijo v kombinaciji z energijsko disperzijsko spektroskopijo rentgenskih žarkov (SEM/EDS), geokemično sestavo z metodo induktivno vezane plazme z emisijsko spektrometrijo (ICP-ES) in masno spektrometrijo (ICP-MS). Vsi vzorci imajo podobno mineralno sestavo. Prevladujejo kremen in glineni minerali, med njimi največ illita/muskovita in mineralov kloritove skupine. SEM/EDS analiza je poleg omenjenih mineralov v vseh vzorcih pokazala še prisotnost cirkona, monacita, Ti-oksida (najverjetneje gre za rutil) in železovih oksidov/hidroksidov, medtem ko smo kromit, ilmenit, ksenotim, apatit in barit našli le v posameznih vzorcih. Povprečne velikosti akcesornih mineralov so med 3 in 20 µm. Dva vzorca se od preostalih razlikujeta po rjavi barvi in večji vsebnosti Fe_2O_3 in manjši vsebnosti SiO_2. Ostali vzorci so zelene barve. Kemijska analiza je pokazala, da v vseh vzorcih prevladujeta SiO_2 (46,3–69,3 %) in Al_2O_3 (15–24,1 %), sledijo K_2O (2,8–3,4 %), Fe_2O_3 (2,1–8,4 %), MgO (1,6–2,3 %), TiO_2 (0,5–0,7 %), CaO (0,3–1,4 %), Na_2O (0,1 %) in P_2O_5 (do 0,5 %).

Položaj vseh vzorcev na diagramu Zr/TiO2 vs. $(V+Ni+Cr)/Al_2O_3$ kaže na terigen izvor materiala in sedimentacijo na kontinentalnem robu. Indeksa kemičnega preperevanja (CIA in CIW) kažeta na intenzivno in dolgo preperevanje, kar potrjuje tudi indeks spremenljivosti sestave (ICV), ki skupaj z zaobljenostjo zrn cirkona in ilmenita kaže na zrelost sestave materiala.

Introduction

Sedimentary rocks with cherts are very common Mesozoic pelagic sediments of the entire Tethys (Baumgartner, 2013). In Slovenia, they are found in the transitional zone between the internal and the external Dinarides. The stratigraphy of several Tethyan chert outcrops has been extensively studied, whereas the studies on the fine-grained clastics, interbedded with cherts, are not very common (Barrett, 1981; Baltuck, 1982, Amodeo, 1999; Di Leo et al.,2002a, b; Halamić et al., 2005; Peh & Halamić, 2010, Skobe et al., 2013). The origin of the fine-grained material could be either terrigenous and/or volcanogenic; it reflects the depositional environment, ranging from a shelf to a mid-ocean ridge or continental margin (Boström, 1973; Murray, 1994; Girty et al., 1996; Andreozzi et al., 1997; Di Leo et al., 2002a). Therefore, it helps to interpret the palaeoenvironmental and palaeogeographic position of the area in Tethys realm.

In Jersovec deposit in Dolenjska region, chert is still being quarried. Here, chert beds interchange with thin, up to 10 cm thick layers of fine-grained sediments. The origin of this fine-grained material has not been determined yet. In the vicinity, very similar clastic material of Jurassic age has been found and studied in the abandoned quarry near Izvir village in Krško depression (Skobe et al., 2013), in Italy, where the interbedded material is also of Jurassic age (Barrett, 1981), and in Croatia, where the clastics are of Triassic and Jurassic age (Peh & Halamić, 2010).

The aim of the paper is to characterise the fine-grained material from Jersovec deposit, to establish its provenance and depositional environment, and to compare it with similar rocks from neighbouring deposit near Izvir in Krško depression.

Geological setting

The investigated area is located in the south-eastern Slovenia, in the vicinity of Mirna and Trebnje, Dolenjska region. The area is a part of the transitional zone between the internal and the external Dinarides (Fig. 1). In the area several outcrops of cherts are reported, the closest one to Jersovec is Izvir (Fig 1).

The rocks from Jersovec deposit are of upper Triassic age, the so called »transitional« beds (the expression is used for rock of indefinable age, laying between upper Triassic and lower Cretaceous beds), lower Cretaceous and Quaternary age (Šolar, 1991). Upper Triassic beds are characterised by light grey »Bača dolomite« with chert nodules and beds, and crisscrossed with calcite veins. Upper parts of the dolomite are strongly weathered (Šolar, 1991). The transitional beds are represented by dolomite-chert breccia, bedded and laminated cherts and beds of muddy sandy to sandy muddy chert gravel. Cretaceous beds consist of quartz sandstones, shales and micritic limestones transiting to calcarenites and containing chert nodules and beds. The youngest is Quaternary alluvium (Šolar, 1991).

Jersovec quarry is intersected by the NW-SE (Dinaric) fault and therefore the rocks have been tectonically deformed. Also, the older faults with W-E direction had caused some minor deformations (Šolar, 1991).

Between the chert beds there are very thin, at most up to 10 cm thick layers and lenses of fine-grained green to brown sediments. The colour is interpreted as a result of different degree of oxidation of some iron mineral(s) (Šolar, 1991). No mineralogical and geochemical studies of these fine-grained materials have been performed yet.

Materials and methods

Altogether, 7 samples were taken at two sites, located about 50 m from each other (Figs. 2 and 3). All samples were dried at 50 °C for two weeks and afterwards pulverised by hand in agate mortar to a grain size of <0.063 mm for geochemical and XRD analysis. Fragments of original rock samples were also prepared for SEM/EDS analysis. Heavy mineral fraction was prepared from one sample (Je-01) using bromoform (density 2.89 g/cm^3) and then inspected by SEM/EDS.

Mineral composition of all samples was determined by powder X-ray diffraction (XRD) at the Faculty of Natural Sciences and Engineering, Department of Geology, University of Ljubljana. XRD measurements were conducted using a Philips PW3710 diffractometer (PANalytical B.V.) equipped with CuKα radiation and a graphite monochromator. The X-Ray radiation was generated at a voltage of 10 kV and a current of 10 mA. Data were recorded in the range $2° \leq 2\Theta \leq 70°$. Mineral compositions of the samples were determined by X'pert Highscore Plus database.

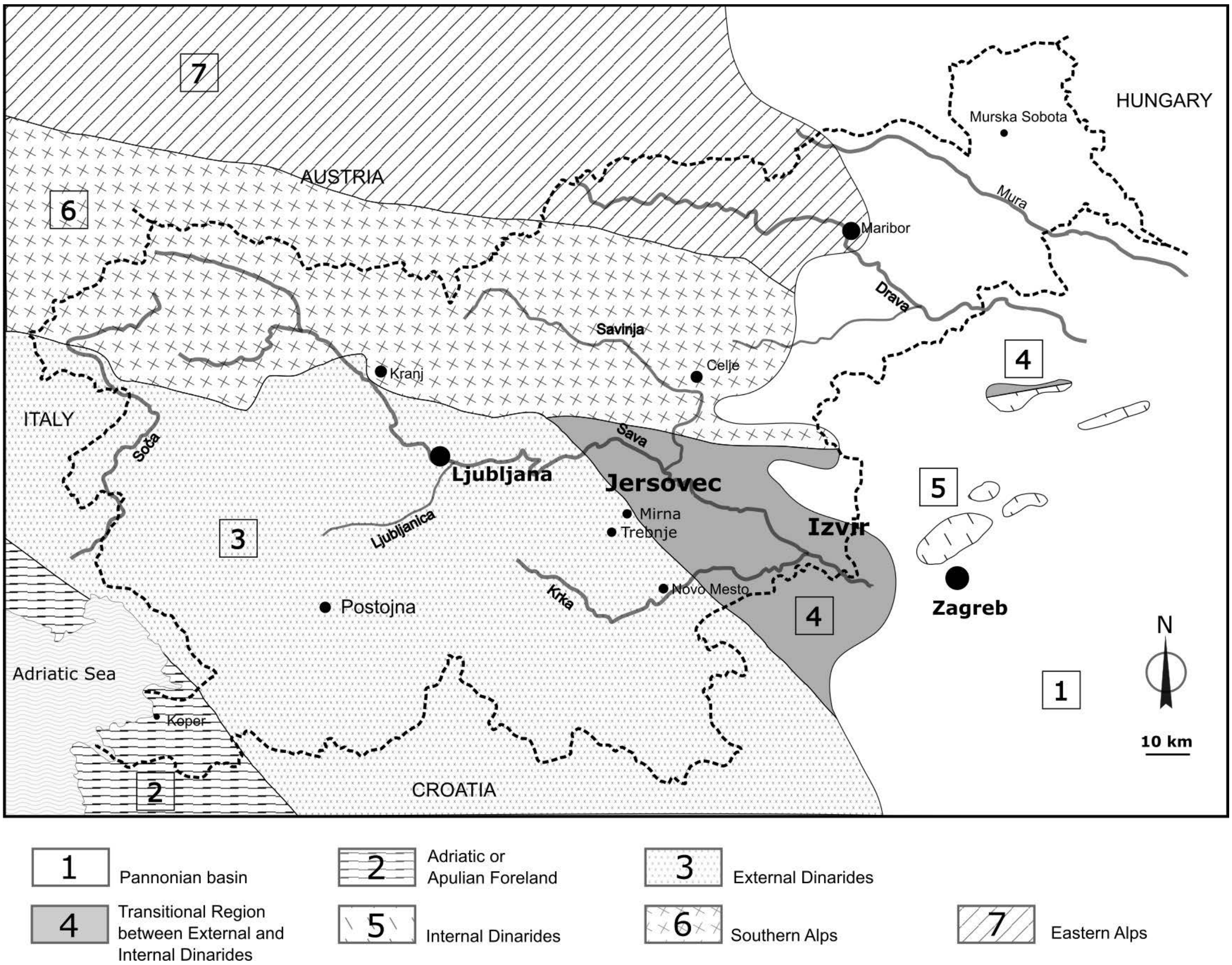

Fig. 1. Location map of the Jersovec deposit within main geotectonic units (after Placer, 1999; Skobe et al., 2013).

Fig. 2. Position of first sample Je-01; measuring rod equals 1.8 m; photo: S. Jerina.

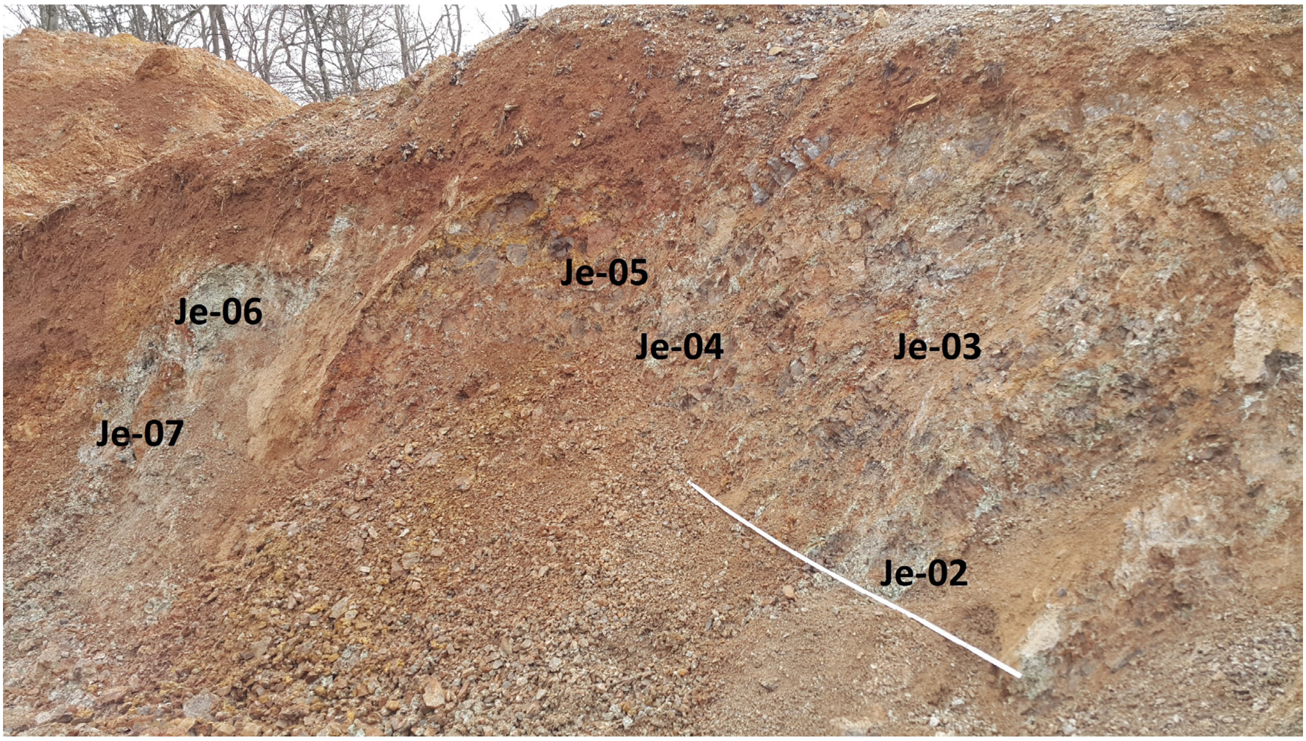

Fig. 3. Position of samples Je-02, Je-03, Je-04, Je-05, Je-06 in Je-07; measuring rod equals 1.8 m; photo: S. Jerina.

A whole rock geochemical analysis of major oxides and several trace elements, including rare earths was carried out by inductively coupled plasma emission spectroscopy (ICP-ES) and mass spectroscopy (ICP-MS) at Bureau Veritas Commodities Canada. The analytical quality based on international standards and one replicate sample (Je-06-1) is satisfactory, with the precision and accuracy error below 10 %. Precision error >10 % was established for CaO, Cu, Hg, Pb, Sn, Ta, U, W and Zn, due to their low content. These elements, and additionally Sb and total sulphur (TOT/S), whose contents were below detection limit (0.1 and 0.02 %), were omitted from further study. Also contents of MnO were below detection limit in some samples. As MnO is necessary for one of the used discriminant diagrams, half of the detection limit value was used for the calculation.

Scanning electron microscopy with energy dispersive X-ray spectroscopy (SEM/EDS) of original rock fragments and one sample of heavy mineral fraction was carried out at Geological Survey of Slovenia. The samples were coated with carbon and then observed in high vacuum, in backscattered electron (BSE) mode by JEOL JSM 6490LV SEM, coupled with an Oxford INCA EDS at an accelerating voltage of 20 kV, working distance 10 mm and acquisition time of 60 s. Minerals were determined using known mineral databases (Anthony et al., 2009; Barthelmy, 2010).

Results and discussion

Macroscopically, the colour of the samples varies from green and greenish grey (5GY 7/2, 5GY8/1) to brown (5YR 5/6, 5YR 3/4). The mineral compositions of all samples are very similar (Fig. 4) with prevailing quartz and illite/muscovite (illite and muscovite cannot be distinguished), and possible minor presence of chlorite group minerals. Samples differ only in mineral ratios. The sample Je-05 contains less quartz than others and also seems to be of lower crystallinity, whereas samples Je-02 and Je-06 contain the maximum content of quartz.

SEM/EDS analysis supports the results of XRD analysis and additionally reveals the presence of some accessory minerals (Table 1). Quartz grains are the most abundant in all samples, followed by clay minerals. The average grain size of quartz is approximately 15 μm. Also, clay minerals are abundant in all samples. Micas, most probably muscovite, and minerals of chlorite group, are around 10 μm in size with frequently pseudohexagonal shapes. In all samples, zircon, iron oxides/hydroxides, monazite and Ti-oxide mineral, most probably rutile, have been detected. Rutile grains are euhedral, sometimes elongated, prismatic and around 7 μm in size (Fig. 5a). They are more abundant in samples Je-01, Je-02, Je-03 and Je-07 (Table 1). Iron oxides/hydroxides are around 5 μm in size and more

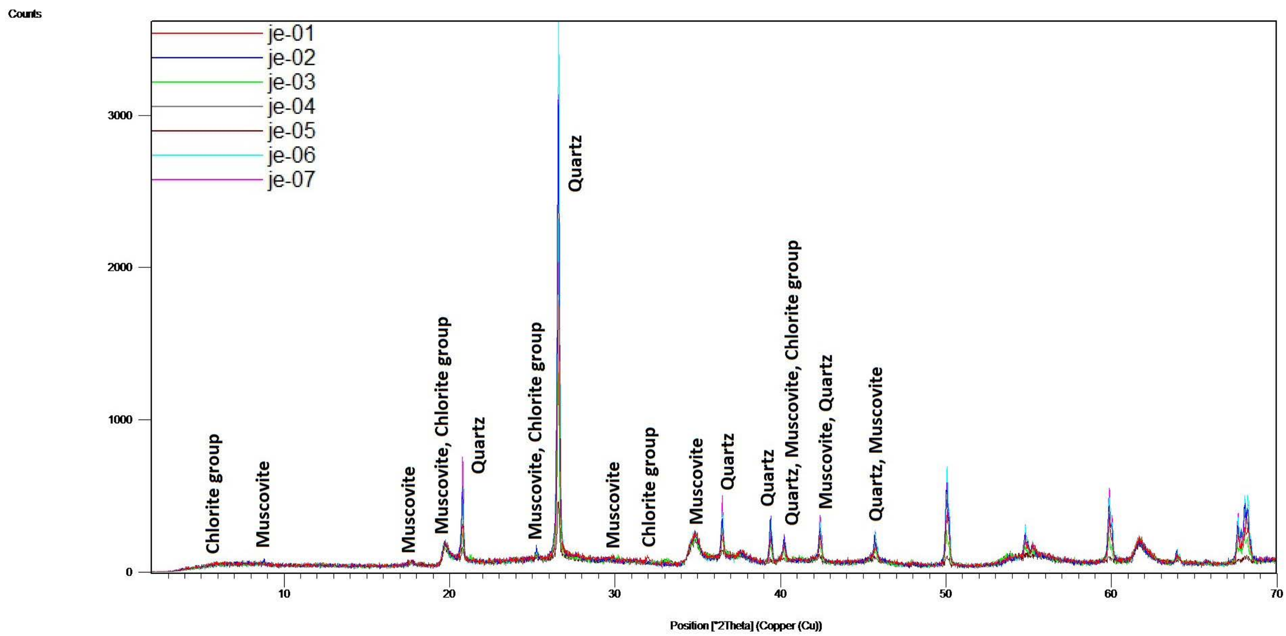

Fig. 4. XRD patterns of the investigated mudstone samples from Jersovec chert deposit.

Table 1. Minerals detected by SEM/EDS and their relative abundances;
Legend: *** – very frequent; ** – frequent; * – rare.

Mineral	Sample						
	Je-01	Je-02	Je-03	Je-04	Je-05	Je-06	Je-07
Quartz	***	***	***	***	***	***	***
Clay minerals	***	***	***	***	***	***	***
Mica	***	***	***	***	***	***	***
Iron oxides/hydroxides	**	**	***	**	***	**	**
Rutile (TiO_2)	**	**	**	*	*	*	**
Zircon	*	*	*	**	**	**	*
Monazite	*	*	*	*	*	*	*
Chromite	*			*		*	*
Ilmenite	*			*		*	
Xenotime						*	*
Apatite	**						
Baryte				*			

abundant in samples Je-03 and Je-05. The majority of zircon grains are around 20 µm in size, but sometimes larger grains are also present (>150 µm) – some rounded grains point to long transportation (Fig. 5b). Zircon grains are more abundant in samples Je-04, Je-05 and Je-07 (Table 1). Monazite is frequently found in clusters of 5 µm (Fig. 5c). Chromite is detected in some samples (Je-01, Je-04, Je-06 and Je-07) – it is angular and about 5 µm in size (Fig. 5d). Ilmenite was detected only in samples Je-01 and Je-04. It has an average grain size of 10 µm, with the exception of one rounded grain (sample Je-01) larger than 150 µm, which could indicate a long transportation (Fig. 6a). About 3 µm large xenotime grains were found in samples Je-06 and Je-07 (Fig. 6b). Apatite, most probably fluorapatite of 70 µm in size, has been found only in one sample (Je-01; (Fig. 6c), and one very small baryte grain (~ 2 µm) in sample Je-04. The heavy minerals in sample Je-01 represent approximately 0.95 % of the total sample weight. According to mineral compositions and grain sizes all investigated samples are mudstones.

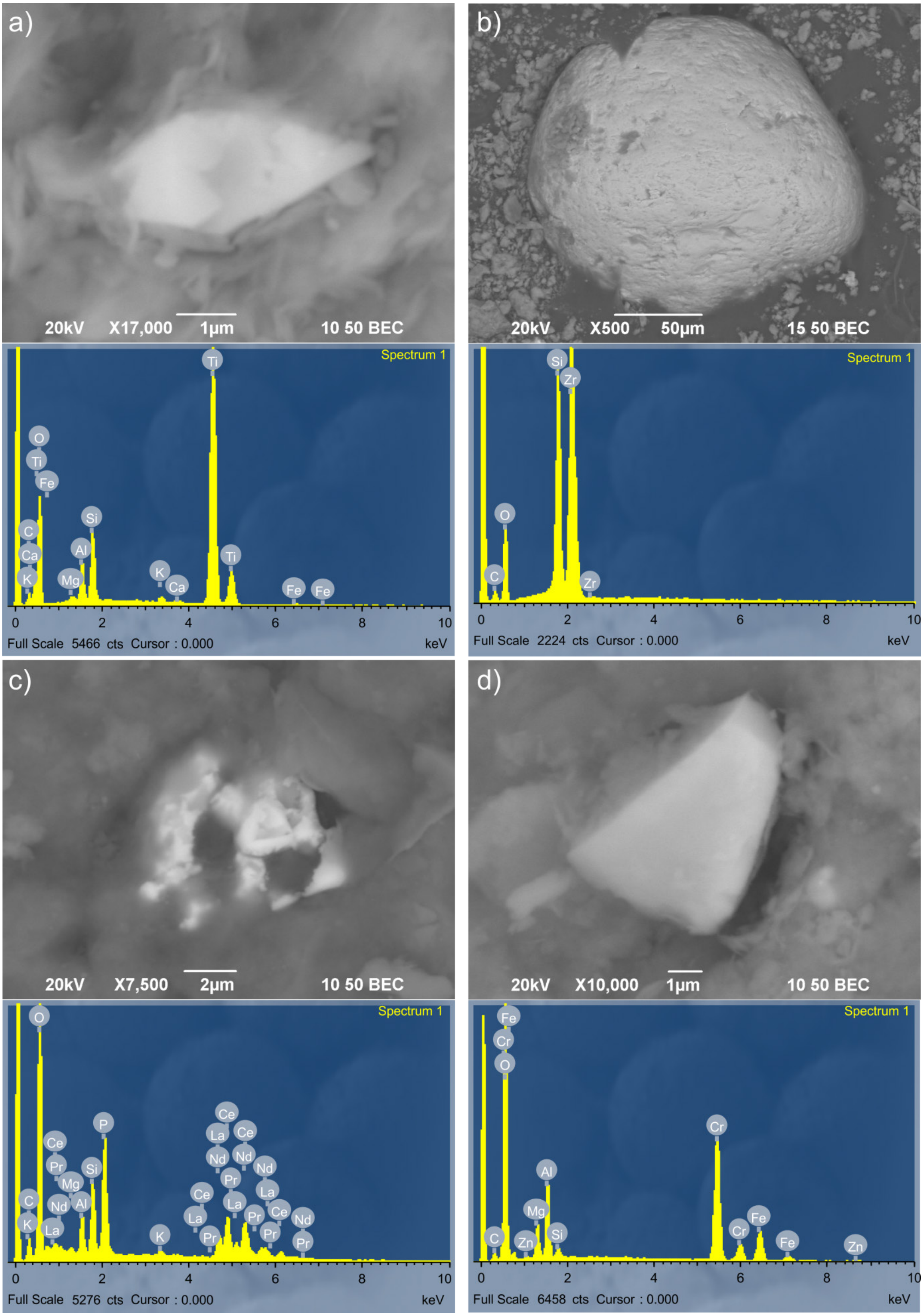

Fig. 5. SEM (BSE) images and EDS spectra of: a) rutile (sample Je-01); b) rounded zircon grain in heavy mineral fraction (sample Je-01); c) monazite (sample Je-04) and d) chromite (sample Je-04).

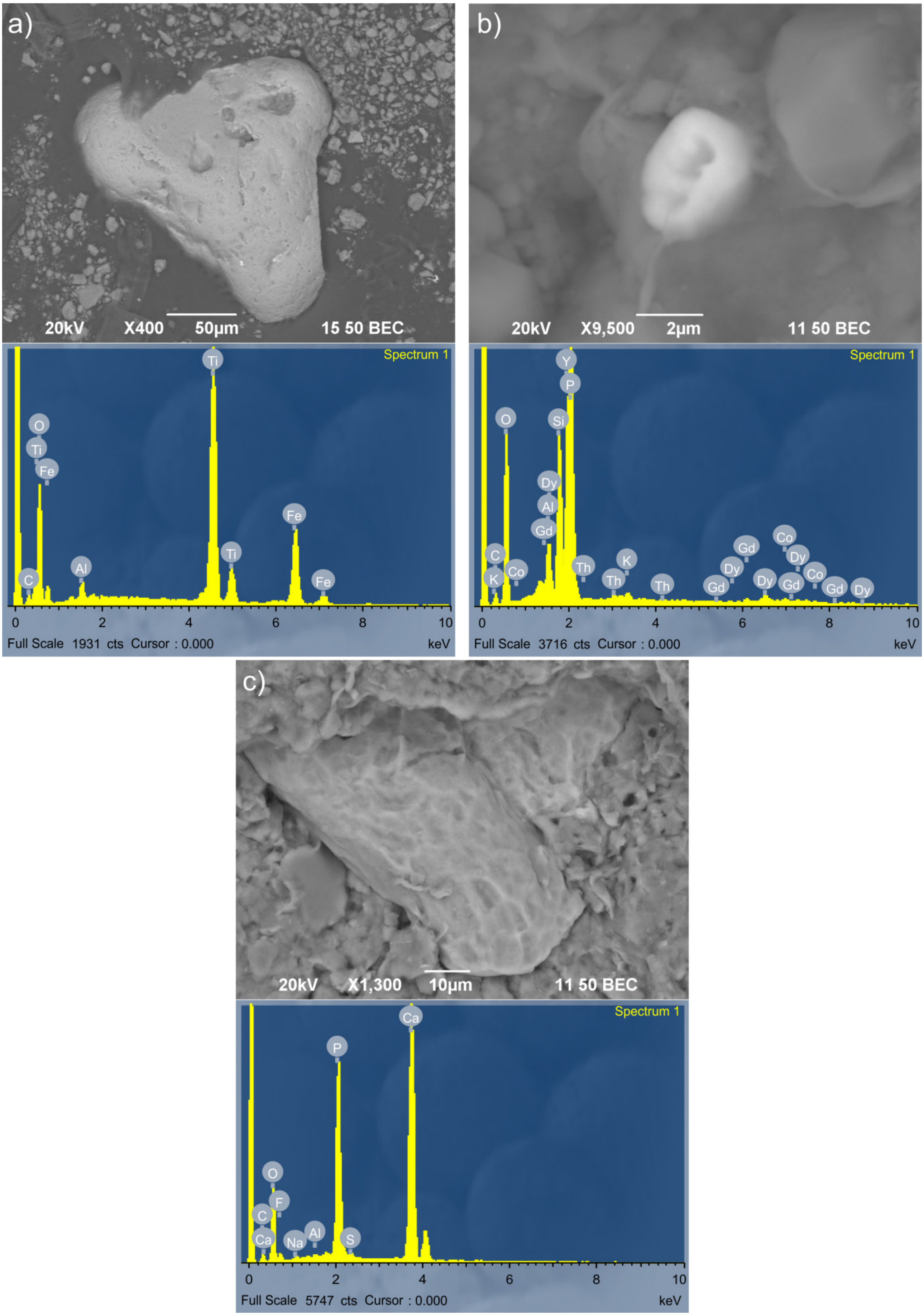

Fig. 6. SEM (BSE) images and EDS spectra of: a) rounded ilmenite grain in heavy mineral fraction (sample Je-01); b) xenotime (sample Je-06) and c) apatite (sample Je-01).

The layers and lenses of fine-grained sedimentary rocks from Jersovec are macroscopically quite similar to up to 2 cm thick shale intercalations from the closest chert outcrop at Izvir. However those from Jersovec do not have fissile structure. Mineralogically, fine-grained materials from both Jersovec and Izvir consist of quartz, clay minerals (illite and minor chlorite); however K-feldspar was found additionally in some samples from Izvir (Skobe et al., 2013).

The geochemical composition of all the samples is generally similar (Table 2). In all samples SiO_2 prevails, with the contents ranging from 46.3 % (Je-05) to 69.3 % (Je-06), followed by Al_2O_3 (15 % in Je-06-1 to 24.1 % in Je-05) and K_2O (2.8 % in Je-02 to 3.4 % in Je-05). The content of Fe_2O_3 is very variable, from 2.1 % in Je-06-1 to 8.4 % in Je-05. The content of MgO is from 1.6 % (Je-02) to 2.3 % (Je-05). The content of CaO is <1 %, except in sample Je-01 (1.4 %). The values of Na_2O, TiO_2, P_2O_5 and MnO are all <1%.

Table 2. Chemical compositions of the mudstone from the Jersovec chert deposit.

wt %	SiO_2	Al_2O_3	Fe_2O_3	MgO	CaO	Na_2O	K_2O	TiO_2	P_2O_5	MnO	LOI	TOT/C
Je-01	59.06	19.20	2.80	2.23	1.40	0.13	3.32	0.63	0.34	<0.01	10.70	0.04
Je-02	66.93	16.38	2.40	1.63	0.43	0.11	2.76	0.47	0.04	<0.01	8.70	0.02
Je-03	53.61	20.13	6.68	1.91	0.47	0.12	3.18	0.67	0.48	0.04	12.20	0.23
Je-04	64.25	17.49	2.67	1.79	0.49	0.11	3.02	0.52	0.06	<0.01	9.40	<0.02
Je-05	46.32	24.12	8.42	2.29	0.57	0.11	3.36	0.53	0.26	0.12	13.60	0.14
Je-06	69.25	15.16	2.19	1.62	0.39	0.10	2.94	0.57	0.07	<0.01	7.50	0.03
Je-07	66.16	16.77	2.60	1.66	0.34	0.11	3.03	0.57	0.04	0.07	8.50	0.02
Je-06-1	69.00	15.04	2.13	1.63	0.84	0.10	3.00	0.57	0.07	<0.01	7.40	0.11

mg/kg	As	Cr	Ba	Co	Cs	Hf	Nb	Ni	Pb	Sc	Sr	Ta
Je-01	0.8	212	240	7.4	37.3	3.7	11.6	125.8	6.3	17	61.2	1.0
Je-02	<0.5	137	216	5.4	31.7	2.9	8.4	104.2	2.9	16	52.0	0.7
Je-03	15.5	171	959	8.3	34.6	3.5	13.1	132.3	45.4	31	324.4	1.0
Je-04	<0.5	164	280	6.5	36.2	3.2	9.8	122.8	3.6	15	70.9	0.7
Je-05	21.3	178	361	9.7	45.0	3.2	10.2	152.0	11.4	30	89.7	1.2
Je-06	<0.5	129	251	4.7	25.2	2.9	10.1	79.9	6.3	14	61.2	1.4
Je-07	1.2	123	240	13.0	28.2	3.3	10.0	68.5	4.7	16	54.3	0.8
Je-06-1	<0.5	137	251	4.9	25.2	3.1	10.2	73.1	5.3	14	64.8	1.1

mg/kg	Th	U	V	W	Y	Zn	Zr	Bi	Hg	Sn	Rb	Cu
Je-01	12.6	5.3	198	2.2	35.3	120	137.0	0.3	0.08	3	186.1	41.2
Je-02	10.6	3.9	140	1.8	69.2	129	106.4	0.2	0.06	3	160.9	43.9
Je-03	15.6	17.9	231	1.7	136.0	149	135.9	0.6	0.36	4	172.2	103.7
Je-04	11.9	4.6	157	2.1	82.0	147	124.9	0.2	0.06	3	171.0	52.4
Je-05	15.0	9.2	219	1.3	114.7	154	108.4	0.6	0.43	4	187.5	101.1
Je-06	10.8	6.4	133	2.1	58.8	114	115.1	0.2	0.05	2	144.8	44.5
Je-07	10.5	3.8	133	1.9	54.1	91	115.1	0.2	0.06	3	154.2	37.3
Je-06-1	10.2	4.3	133	1.8	57.8	98	116.5	0.2	0.04	3	147.0	40.2

mg/kg	La	Ce	Pr	Nd	Sm	Eu	Gd	Tb	Dy	Ho	Er	Tm	Yb	Lu
Je-01	53.1	65.9	10.0	36.7	6.8	1.4	5.9	0.8	4.8	1.0	2.9	0.4	2.8	0.4
Je-02	51.0	51.5	9.4	35.0	6.4	1.5	7.3	1.1	6.9	1.6	4.8	0.7	4.2	0.7
Je-03	290.9	213.0	70.1	305.6	52.8	10.7	41.5	4.7	23.1	3.8	9.4	1.2	7.2	1.0
Je-04	75.6	73.4	16.8	67.7	12.0	2.7	11.5	1.6	9.5	1.9	5.6	0.8	4.9	0.8
Je-05	131.4	88.1	25.9	105.5	20.4	4.6	20.6	2.6	15.1	2.9	8.4	1.1	7.3	1.1
Je-06	72.3	66.6	14.3	54.8	9.5	2.0	8.7	1.2	7.3	1.5	4.4	0.6	3.9	0.6
Je-07	56.9	63.5	11.7	44.3	7.8	1.8	7.8	1.1	6.9	1.5	4.4	0.6	4.0	0.6
Je-06-1	70.6	64.2	14.0	53.8	8.8	1.9	8.7	1.2	7.0	1.5	4.3	0.6	4.0	0.6

With regard to SiO_2 and Al_2O_3, samples Je-01, Je-03 and Je-05 differ from others, as they are poorer in SiO_2 and enriched in Al_2O_3. However, with respect to Fe_2O_3 content and content of majority of other elements, sample Je-01 differs from Je-03 and Je-05 and is more similar to the other samples. On the contrary, Je-03 and Je-05 have more Fe_2O_3 and also elevated contents of some trace elements, i.e. As, Ba, Ni, Pb, Sr, U, V and REE, and higher values of loss on ignition (LOI). Both samples macroscopically differ from others by their brown colour. Colour and geochemical characteristics could indicate more intense weathering. Further, the results of SEM/EDS analysis have shown the highest abundance of iron oxides/hydroxides in mentioned samples.

In a discrimination diagram of ANDREOZZI et al. (1997) and DI LEO et al. (2002a, b), Jersovec samples plot in the field of terrigenous sediments (Fig. 7).

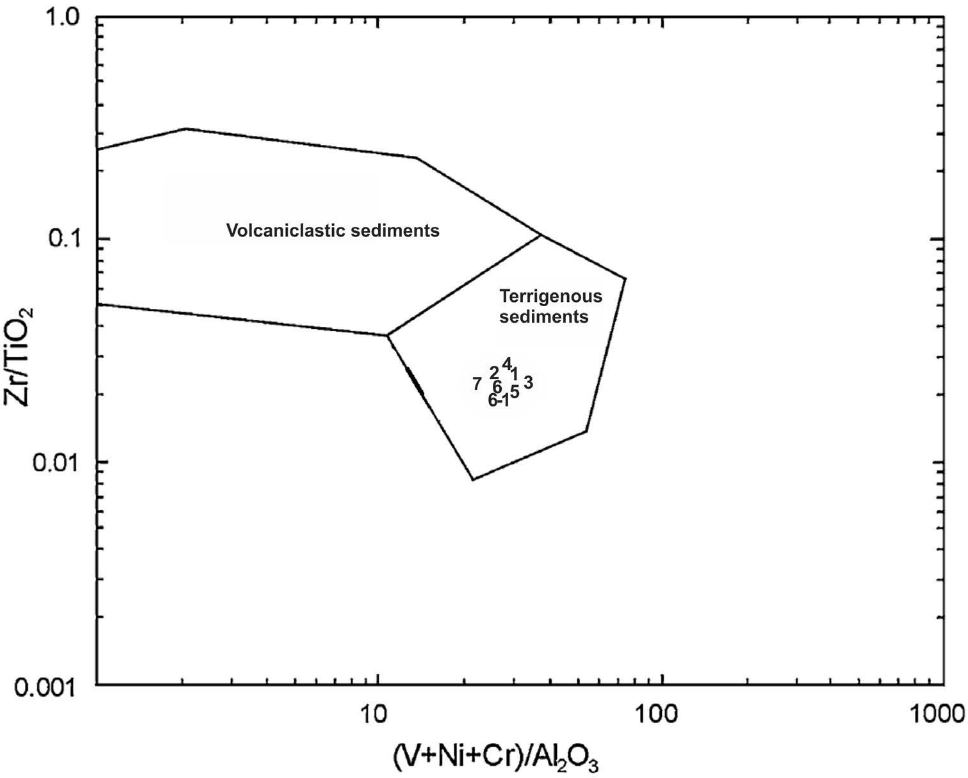

Fig. 7. Plot of the Jersovec mudstone samples in the discrimination diagram for the volcanogenic *vs.* terrigenous origin of the material (according to ANDREOZZI et al., 1997; DI LEO et al., 2002a, b).

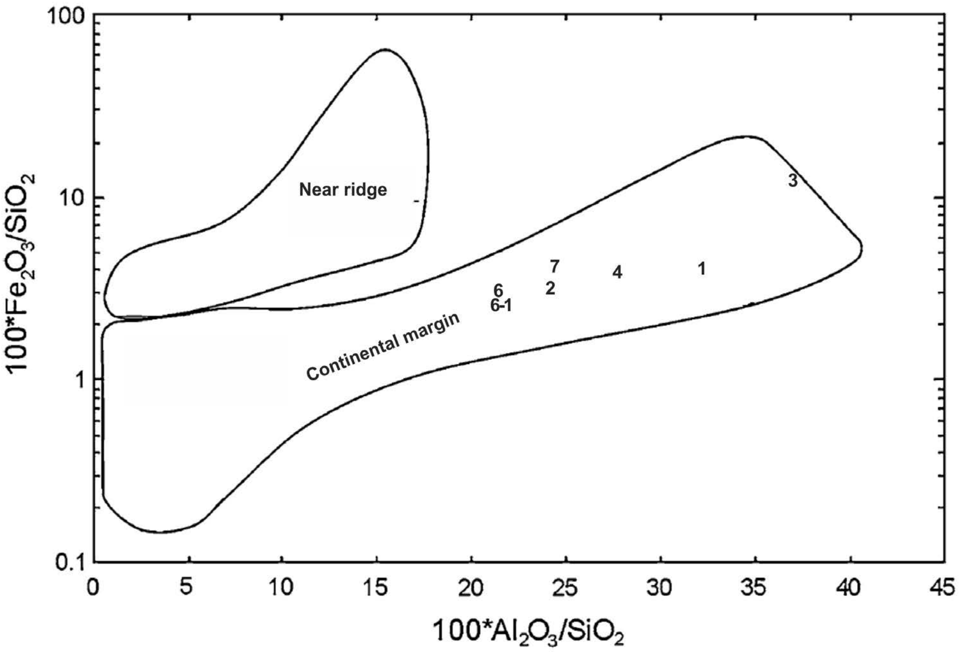

Fig. 8. Plot of investigated mudstone samples from Jersovec chert deposit in the discrimination diagram $100\times Fe_2O_3/SiO_2$ *vs.* $100\times Al_2O_3/SiO_2$ (after MURRAY, 1994).

According to $100\times Fe_2O_3/SiO_2$ - $100\times Al_2O_3/SiO_2$ discriminant diagram (Murray, 1994), depositional environment of the material is continental margin (Fig. 8). Exception is sample Je-05, which is placed outside the diagram due to its high Fe_2O_3 and low SiO_2 content.

All samples plotted on the discriminant diagram Fe_2O_3/TiO_2 - $Al_2O_3/(Al_2O_3+Fe_2O_3)$ (Fig. 9) also display the values typical for continental margin and old continental crust provenance (Murray, 1994; Girty et al., 1996).

The fine-grained clastics from the Jersovec are not hydrothermally altered as can be seen from the Fe_2O_3/TiO_2 *vs.* $Al_2O_3/(Al_2O_3+Fe_2O_3+MnO)$ diagram (Boström, 1973) where they plot close to the material of terrigenous to basaltic origin (Fig. 10).

The degree of weathering has been established by three different indices. The chemical index of alteration (CIA) – $Al_2O_3/(Al_2O_3+Na_2O+CaO+K_2O) \times 100$ (Nesbitt & Young, 1982) is on the average 79.4, indicating weathered material. Sample Je- 01 has the lowest index of alteration (CIA; 75.1), and sample Je-05 has the highest (83.2). The chemical index of weathering (CIW) – $Al_2O_3/(Al_2O_3+Na_2O+CaO) \times 100$ (Harnois, 1988) ranges from 87.4 (sample Je-01) to 95.5 (sample Je-07), with an average value of 93.3 demonstrating intense and prolonged weathering (Barbera

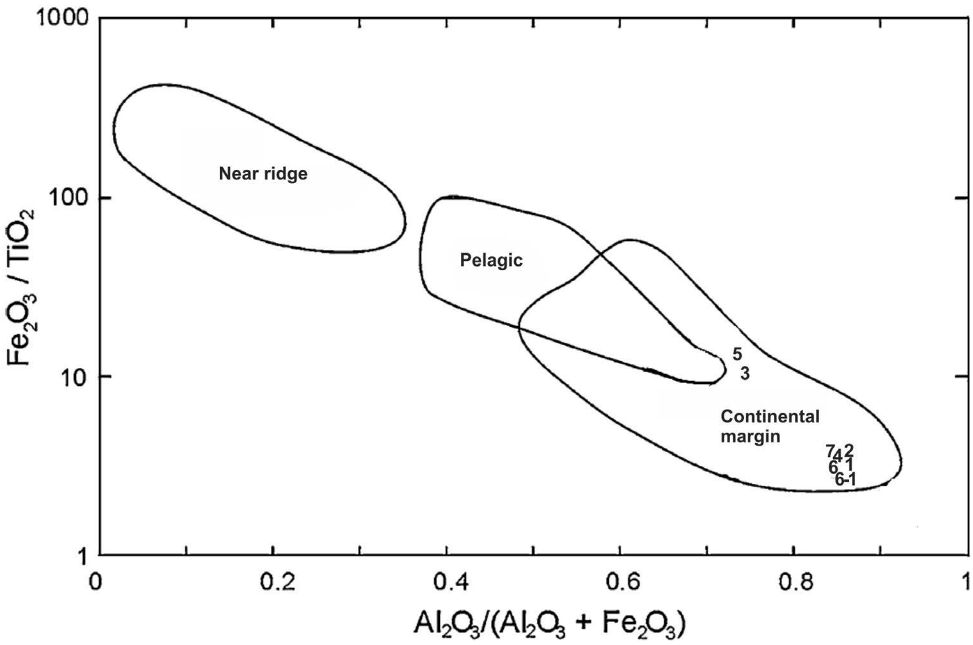

Fig. 9. Plot of the Jersovec mudstone samples in the Fe_2O_3/TiO_2 *vs.* $Al_2O_3/(Al_2O_3+Fe_2O_3)$ diagram (according to Murray, 1994; Girty et al., 1996).

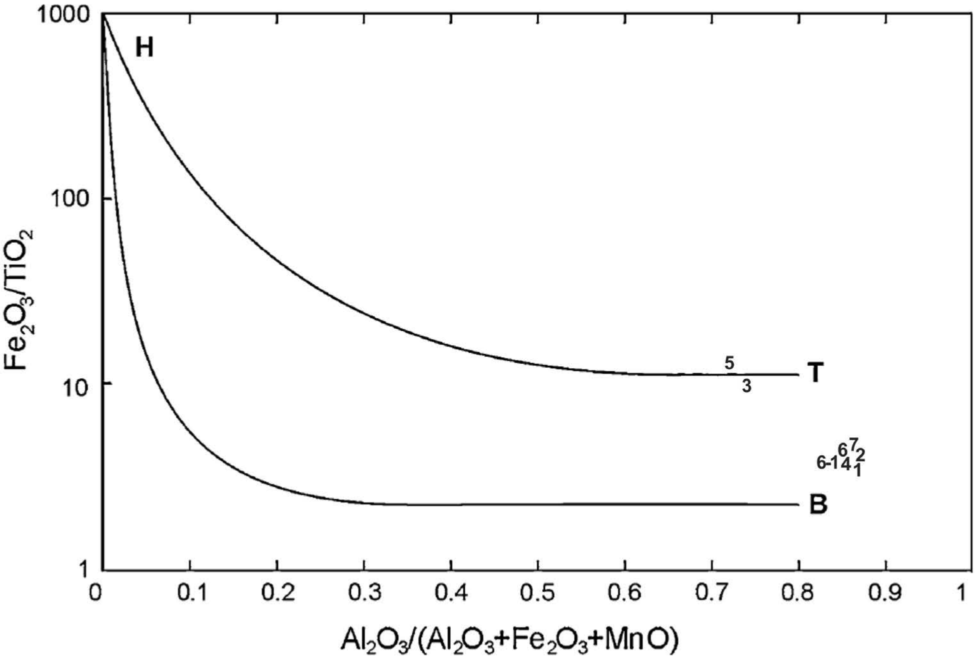

Fig. 10. Plot of the Jersovec mudstones in Fe_2O_3/TiO_2 *vs.* $Al_2O_3/(Al_2O_3+Fe_2O_3+MnO)$ discrimination diagram according to Boström (1973); abbreviations: T – terrigenous material, B – basaltic material; H – hydrothermal end-member

et al., 2006). The brown coloured samples Je-03 and Je-05 have also very high CIW values, 95.0 and 95.2 respectively. The average value of the ICV (index of compositional variability): $(Fe_2O_3+K_2O+Na_2O+CaO+MgO+TiO_2)/Al_2O_3$ (Cox et al., 1995) is 0.54, and points to compositionally mature sediments (Cullers & Podkovyrov, 2000; Barbera et al., 2006). Also, the rounded grains of some accessory minerals (i.e. zircon, ilmenite) point to terrigenous origin of the material.

The Jurassic bedded cherts from Izvir are the closest to the investigated area. Comparison of Jersovec mudstones with the Izvir shales shows similar geochemical characteristics. The differences are in higher content of K_2O in Izvir shales reflecting the presence of K-feldspar. In Izvir area, the mixing of marine and meteoric waters during late diagenesis caused alteration of K-minerals, which were already present in sediments, into K-feldspars (Skobe et al., 2013). This process has not been detected in Jersovec. According to geochemical analysis, the material from Izvir is of terrigenous and not volcanic origin. Sediments in Izvir area, which is also part of the transitional zone that formed by rifting of thinned (micro)continental margin (Rižnar, 2005), were deposited on a Tethyan passive margin due to rapid subsidence, originally as silica-rich carbonate beds intercalated with mud (Skobe et al., 2013). As is in the case of Jersovec mudstones, the hydrothermal origin is also excluded for Izvir shales (Skobe et al., 2013). The average chemical index of weathering (CIW) is 95.7 and is similar to Jersovec samples. It indicates an intense and prolonged source of weathering. Also, index of compositional variability (ICV) points to compositionally mature material (Skobe et al., 2013).

Conclusions

The fine-grained material from Jersovec chert deposit is macroscopically very similar, but different in colour, ranging from prevailing green (5GY 7/2, 5GY 8/1) to sometimes brown (5YR 5/6, 5YR 3/4). Nevertheless, mineral composition of all the samples is very similar. Quartz and clay minerals, that is illite/muscovite and minerals of chlorite group, dominate, but mineral ratios vary. Further, SEM/EDS analysis showed the presence of Ti-oxide (probably rutile), zircon and monazite in all investigated samples and chromite, ilmenite, xenotime, apatite and baryte in some of them. The average sizes of accessory minerals range from 3 to 20 µm. Larger grains of some minerals (e.g. ilmenite, zircon) are rounded due to transportation. The results of SEM/EDS analysis are strongly supported by geochemical results; the contents of SiO_2 and Al_2O_3 are the highest, followed by K_2O, MgO, TiO_2, CaO, Na_2O, P_2O_3, whereas Fe_2O_3 is variable. Two samples, Je-03 and Je-05, differ from others, as they are poorer in SiO_2 and enriched in Fe_2O_3 and some trace elements, i.e. As, Ba, Ni, Pb, Sr, U, V, REE, and Al_2O_3 and loss on ignition. Also, both samples differ from others macroscopically, as they are brown in colour. The colour and geochemical characteristics could indicate more intense weathering of the two samples as it is also proven by weathering indices. Based on the mineral compositions and grain sizes, all samples are mudstones.

According to the results of the geochemical analysis, discriminant diagrams show terrigenous origin of the mudstones from Jersovec. The material was deposited on the continental margin. The average indices of chemical alteration (CIA) and weathering (CIW) are 79.4 and 93.3, respectively. Both indicate an intense and long weathering. Weathering processes have been also confirmed by well-rounded minerals documented by SEM/EDS. The index of compositional variability (ICV; average value is 0.54) demonstrates the compositional maturity of the material. The similar results have been obtained in the clastics from the vicinity, near Izvir in Krško depression. Fine-grained material from both locations has comparable mineral and geochemical attributes, which point to terrigenous origin and the sedimentation on the continental margin. The difference is the presence of authigenic K-feldspar in Izvir samples as a result of later diagenetic processes. K-feldspars have not been detected in Jersovec samples.

Acknowledgements

We thank Kremen d.d. for enabling the access to the Jersovec quarry. Many thanks to Dr. Dragomir Skaberne and Dr. Aleksander Horvat for help with the fieldwork.

References

Amodeo, F. 1999: Il Triassico terminale - Giurassico del Bacino Lagonegrese. Studi stratigrafici sugli Scisti Silicei della Basilicata (Italia meridionale). Mémoires de Géologie, Lausanne, 33: 1–121, pls. 1–10.

Andreozzi, M., Dinelli, E. & Tateo, F. 1997: Geochemical and mineralogical criteria for the identification of ash layers in the stratigraphic framework of a foredeep; the Early Miocene Mt. Cervarola Sandstones, northern Italy. Chemical Geology, 137: 23–39, doi:10.1016/S0009-2541(96)00148-9.

Anthony, J.W., Bideaux, R.A., Bladh, K.W. & Nichols, M.C. 2009: The Handbook of Mineralogy [online]. Mineralogical Society of America. Internet: http://www.handbookofmineralogy.org/ (10.9.2016).

Baltuck, M. 1982: Provenance and distribution of Tethyan pelagic and hemipelagic sediments, Pindos Mountains, Greece. Sedimentary Geology, 31/1: 63–88, doi:10.1016/0037-0738(82)90008-2.

Barbera, G., Mazzoleni, P., Critelli, S., Pappalardo, A., Lo Giudice, A. & Cirrincione, R. 2006: Provenance of shales and sedimentary history of the Monte Soro Unit, Sicily. Periodico di Mineralogia, 75: 313–330.

Barrett, T.J. 1981: Chemistry and mineralogy of Jurassic bedded chert overlying ophiolites in the North Apennines, Italy. Chemical Geology, 34/3-4: 289–317, doi:10.1016/0009-2541(81)90118-2.

Barthelmy, D. 2010: The Mineralogy Database. Internet: http://webmineral.com/ (8.6.2016),

Baumgartner, P.O. 2013: Mesozoic radiolarites—accumulation as a function of sea surface fertility on Tethyan margins and in ocean basins. Sedimentology, 60/1: 292–318, doi:10.1111/sed.12022.

Boström, K. 1973: The origin and fate of ferromanganoan active ridge sediments. Stockholm Contributions in Geology, 27: 147–243.

Cox, R., Low, D.R. & Cullers, R.L. 1995: The influence of sediment recycling and basement composition on evolution of mudrock chemistry in the southwestern United States. Geochim Cosmochim Acta, 59: 2919–2940.

Cullers, R.L. & Podkovyrov, V.N. 2000: Geochemistry of the Mesoproterozoic Lakhanda shales in southern Yakutia, Russia: implications for mineralogical and provenance control, and recycling. Precambrian Research, 104/1-2: 77–93, doi: 10.1016/S0301-9268(00)00090-5.

Di Leo, P., Dinelli, E., Mongelli, G. & Schiattarella, M. 2002a: Geology and geochemistry of Jurassic pelagic sediments, Scisti silicei Formation, southern Apennines, Italy. Sedimentary Geology, 150/3-4: 229–246, doi:10.1016/S0037-0738(01)00181-6.

Di Leo, P., Giano, S.I. & Schiattarella, M. 2002b: Volcanoclastic layers in upper Triassic-Jurassic deep-sea sediments from the Lucanian Apennine, southern Italy: mineralogy, geochemistry, and palaeotectonic implications. Periodico di Mineralogia, 71: 49–63.

Girty, G.H., Ridge, D.L., Knaack, C., Johnson, D. & Al-Riyami, R.K. 1996: Provenance and depositional setting of Paleozoic chert and argillite, Sierra Nevada, California. Journal of Sedimentary Research, 66: 107–118, doi:10.1306/D42682CA-2B26-11D7-8648000102C1865D.

Halamić, J., Marchig, V. & Goričan, Š. 2005: Jurassic radiolarian cherts in north-western Croatia: geochemistry, material provenance and depositional environment. Geologica Carpathica, 56: 123–136.

Harnois, L. 1988: The CIW index: A new chemical index of weathering. Sediment Geol, 55/3-4: 319–322, doi:10.1016/0037-0738(88)90137-6.

Murray, R.W. 1994: Chemical criteria to identify the depositional environment of chert: General principles and applications. Sedimentary Geology, 90/3-4: 213–232, doi:10.1016/0037-0738(94)90039-6.

Nesbitt, H.W. & Young, G.M. 1982: Early Proterozoic climates and plate motions inferred from major element chemistry of lutites. Nature, 299: 715–717, doi:10.1038/299715a0.

Peh, Z. & Halamić, J. 2010: Discriminant function model as a tool for classification of stratigraphically undefined radiolarian cherts in ophiolite zones. J Geochem Explor, 107: 30–38, doi:101016/j.gexplo.2010.06.003.

Placer, L. 1999: Contribution to the macrotectonic sudivision of the border region between Southern Alps and External Dinarides. Geologija, 41: 223–255, doi:10.5474/geologija.1998.013.

Rižnar, I. 2005: Geology of the transitional area between outer and inner Dinarides, Eastern Slovenia. Ph.D. dissertation, University of Zagreb, Zagreb: 146 p, app. 5.

Skobe, S., Goričan, Š., Skaberne, D., Verbič T., Mišič, M. & Zupančič, N. 2013: K-feldspar rich shales from Jurassic bedded cherts in southeastern Slovenia. Swiss Journal of Geosciences, 106: 491–504, doi:10.1007/s00015-013-0147-3.

Šolar, V.S. 1991: Modifikacijske spremembe mineralov kremenice roženca iz nahajališča Jersovec. Magistrska naloga. Univerza Edvarda Kardelja, Ljubljana: 107 p.

GEOLOGIJA *60/2*, 235-256, Ljubljana 2017
https://doi.org/10.5474/geologija.2017.017

Nadgradnja ploskovnega erozijskega modela z območji erozije v strugah – primer občine Bohinj

Upgrade of the surface erosion model with the channel erosion areas – the Bohinj municipality case-study

Marko KOMAC[1] & Matevž PAVLIČ[2]

[1]FGG – UL, Jamova 2, Ljubljana, Slovenija; e-mail: m.komac@telemach-net
[2]Gecko - Geologija, Ekologija in Svetovanje d.o.o., Lilly Novy 3, Ljubljana, Slovenija; e-mail: matevz@geo-gecko.si

Prejeto / Received 1. 3. 2017; Sprejeto / Accepted 18. 10. 2017; Objavljeno na spletu / Published online 22. 12. 2017

Dedicated to Professor Mihael Ribičič on the occasion of his 70th birthday

Ključne besede: erozija, ploskovna, površinska, struge, model podvrženosti, Bohinj, Slovenija
Key words: erosion, surface, channels, susceptibility model, Bohinj, Slovenia

Izvleček

Erozija predstavlja pomemben eksogeni proces, ki je prisoten na skoraj vsakem delu Zemljinega površja in tudi slovensko ozemlje ni izjema. Stopnja erozije je močno odvisna od dejavnikov, vezanih na lastnosti površine kot so tip rabe tal, tip vegetacijskega pokrova in geomorfologija ter od dejavnikov, vezanih na podnebje kot sta padavinski režim in nihanja temperature. Prispevek obsega modeliranje mehanske erozije in transport delcev po površju s pomočjo vode, cilj pa je bil združiti splošno uveljavljeno metodologijo RUSLE, ki učinkovito modelira ploskovno erozijo z metodo ocene stopnje podvrženosti eroziji v strugah. Združeni metodi uspešno modelirata erozijo v izrazito goratih in kraških območjih. Za testno območje je bilo izbrano območje občine Bohinj, kjer so zaradi geomorfološke razgibanosti terena prisotni številni naravni površinski procesi, idealno za razvoj združenega modela erozijski h območij.

Abstract

Erosion is an important exogene process that can be found on almost all surfaces around the globe and Slovenian territory is no exception to the rule. The extent of the erosion is a result of various factors linked to the surface properties, such as land use type, vegetation type, and geomorphology and of the factors linked to the climate, such as the precipitation regime and the temperature oscilation. The paper focuses on the modelling of the mechanical erosion and the surface transport of particles due to surficial waters. The aim of the research was to combine the RUSLE surface erosion method with a model of gully erosion. The combined approach successfuly models the erosion in the mountainous and karst areas. Due to its vivid geomorphology that results in various natural surface proceses the area of Bohinj municipality was chosen as an ideal case study for testing the joint methodology.

Uvod

V znanostih, ki se ukvarjajo s procesi na Zemljinem površju, predstavlja erozija površinske procese, pri katerih pride s pomočjo delovanja vode ali vetra do mehanskega prenosa trdnih delcev kamnin ali tal, ali kemičnega prenosa raztopin z ene lokacije na drugo (Toy et al., 2002). Erozijski procesi se glede na vzrok in način transporta delcev delijo na ploskovno, rečno, obalno, kemično, ledeniško, poplavno in vetrno erozijo ter pobočne masne premike (Zachar, 1982; Toy et al., 2002). Prisotnost številnih strug na območju ocene stopnje erozivnosti, predstavlja za kvaliteno oceno le-te z modelom RUSLE precejšni izziv. Zhang et al. (2013) navajajo, da je v tem primeru ocena z modelom RUSLE pomanjkljiva in jo je zato treba dopolniti z modelom, ki upošteva tudi vpliv strug in ukrivljenosti terena. Feng et al. (2016) pa ugotavljajo, da je treba za dosego realnih rezultatov v goratih predelih del modela RUSLE, ki opisuje naklon in dolžino pobočja, umeriti. Dai et al (2017) in Zhang et al. (2017) navajajo, da lahko predstavljajo kraška območja velik izziv pri modeliranju površinskih pojavov kot posledica vode zaradi prisotnosti zaprtih depresij, kot so vrtače in uvale. Kraško oblikovano površje torej predstavlja določen izziv pri izdelavi ocene stopnje erozivnosti, saj je na kraških območjih površinski odtok minimalen in ne sledi pravilom površinskega odvodnjavanja. Odtok površinske vode je na kraških območjih usmerjen v notranjost pojava za razliko od nekraških rečnih sistemov, kjer se vode stekajo po površju in tvorijo »idelano« rečno mrežo. Ne glede na to dejstvo pa je površinska erozija prisotna tudi na kraškem terenu, a v manjšem obsegu (He et al., 1998; Kheir et al., 2008).

Na območju slovenskih Alp so stopnjo erozivnosti, oziroma količine erodiranega materiala v preteklosti ocenjevali Hrvatin et al. (2006), Komac & Zorn (2005 in 2007), Mikoš et al. (2006), Pintar et al. (1986), Komac et al. (2007), Zorn & Komac (2009), Zorn (2008) je opravil podrobno študijo erozijskih procesov v slovenski Istri, Ciglič et al. (2012) pa so se dotaknili tudi prisotnosti erozije na kraških območjih.

Med številne strokovne podlage za potrebe smotrnega urejanja prostora sodi tudi karta (model) erozijskih območij, ni pa določena metodologija za izdelavo take stokovne podlage. Na podlagi v nadaljevanju predstavljenega pristopa je bil izdelan model v merilu 1 : 25.000, ki se namesto na izračun količine erodiranega materiala osredotoča na določitev območij z večjo verjetnostjo pojavljanja erozije. Kot testno območje za razvoj metodologije, ki obsega združitev modela RUSLE in modela za določitev verjetnosti pojavljanja erozije v strugah, je bilo izbrano območje občine Bohinj.

Namen raziskave je bil modeliranje mehanske oziroma fizične erozije in transporta delcev po površju s pomočjo vode, cilj pa je bil združiti splošno uveljavljeno metodologijo RUSLE (Wischmeier & Smith, 1958, 1965, 1978), ki učinkovito modelira ploskovno erozijo z metodo ocene stopnje podvrženosti eroziji v strugah, ki je značilna za območja z večjimi nakloni površja.

Opis obravnavanega območja

Občina Bohinj leži v severo-zahodnem delu Slovenije v Julijskih Alpah in se razprostira na 333,73 km^2. Razpon nadmorskih višin v občini sodi med največje v državi, saj se le-te gibljejo med 462 in 2864 m, kar kaže na izredno geomorfološko razgibanost terena in posledično večjo verjetnost pojavljanja vseh oblik površinskih masnih premikov – zemeljskih plazov, skalnih podorov, drobirskih tokov in erozijskih pojavov, vezanih na naravne površinske procese. V tej raziskavi je bila obravnavana zgolj površinska erozija zaradi delovanja vode, modeliranje ostalih oblik površinskih masnih premikov pa zahteva drugačne pristope in ti niso bili cilj raziskave. Območje je toliko bolj problematično z vidika modeliranja površinskih procesov, ker je večinoma sestavljeno iz karbonatnih kamnin (več kot 96 %) (Buser, 1986; Jurkovšek, 1987). Posledično so prisotne oblike povečanega vertikalnega in podzemnega toka vode ter površinske kraške oblike, ki predstavljajo določen izziv za modeliranje v GIS-ih. Slika 1 prikazuje senčen model reliefa za območje občine Bohinj z dodanim kilometrskim pasom izven občine Bohinj in lokacije vremenskih postaj, s katerih so bili pridobljeni padavinski podatki.

Podnebje na območju Bohinja je tipično alpsko z maksimalno kumulativno količino letnih padavin med 1800 – 2900 mm, maksimalno dnevno količino padavin s povratno dobo desetih let med 232 in 298 mm (upoštevajoč podatke za meteorološke postaje Bohinjska Češnjica – 2002-2012, Stara Fužina – 1982-2002, Ukanc – 1975-1997, Vogel – 1982-2012 in Zgornja Sorica 1970-2016) ter maksimalno 30-minutno količino padavin s povratno dobo desetih let med 33 in 44 mm (upoštevajoč podatke za meteorološke postaje Bohinjska Češnjica – 2002-2012, Stara Fužina – 1982-2002, Ukanc – 1975-1997 in Vogel – 1982-2012) (ARSO, 2016a).

Geološka zgradba testnega območja je opisana v Osnovni geološki karti, List Tolmin in Videm (Buser, 1986) ter List Beljak in Ponteba (Jurkovšek, 1987), na kratko pa jo povzemata Grimšičar (1961) in Budkovič (1978). Večina kamnin pripada triasnim plastem (66,3 % površine), med katerimi revladujejo apnenci, apnenci z roženci, dolomitne plasti, prisotne pa so tudi prioklastične kamnine. Triasne plasti tvorijo domala vsa visokogorska območja in obkrožajo dolino reke Save Bohinjke. Kamnine jurske starosti zastopajo apnenci, podrejeno pa so prisotni skrilavi glinovci, jursko-kredni skladi pa so zastopani z biancone apnencem. Skupaj obsegajo triasne plasti 8,7 % ozemlja. Kredne plasti zastopajo plasti fliša in lapornega apnenca z vložki drugih kamnin (0,8 % površine). Terciarne plasti predstavljajo apnenčaste plasti

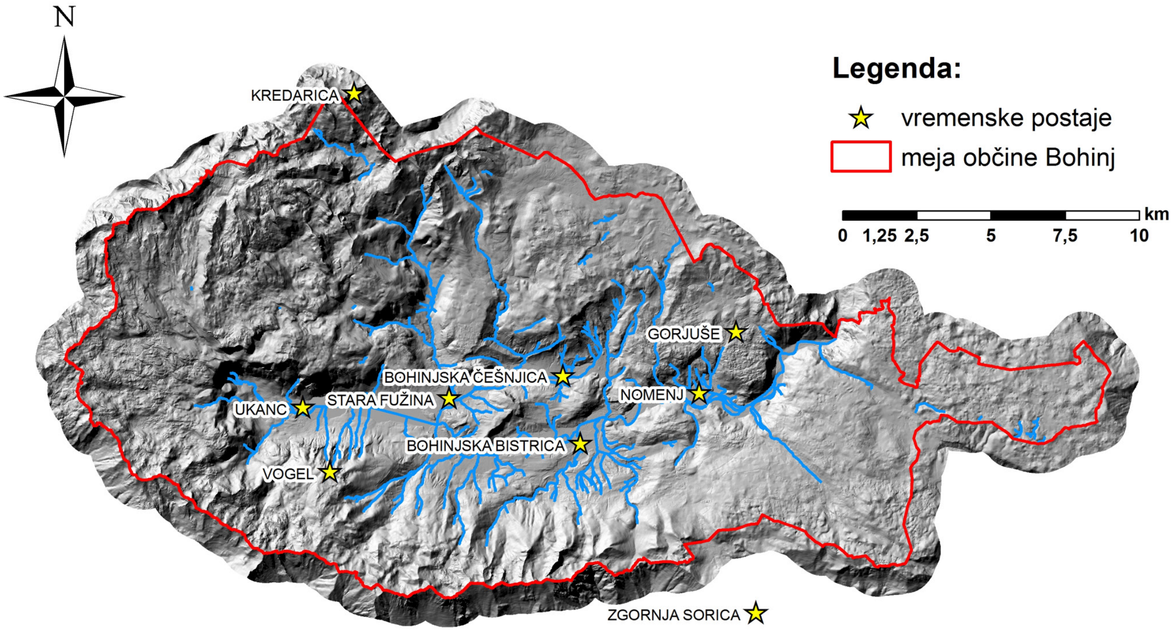

Sl. 1. Senčen model reliefa občine Bohinj, katere meja je označena z rdečo linijo. Rečna mreža je prikazana z modrimi linijami. Lokacijami bližnjih vremenskih postaj so prikazane z rumeno zvezdo.

Fig. 1. Shaded terrain model of the Bohinj municipality, delinated with the red line. River network is represented with the blue lines. The near weather stations' locations are marked with yellow stars.

ter gline in peščenjaki (1,7 % površine). Kvartarni starosti pripadajo številne sprijete in nesprijete morene, jezerski sedimenti, melišča, ter deluvialni in aluvialni nanosi (21,7 % površine). Manj kot en odstotek območja pokriva Bohinjsko jezero (0,9 % površine). Območje Alp in tudi bohinjske občine sekajo številni prelomi, predvsem v dinarski in njej prečni smeri, prisotni pa so tudi narivi. Vsi tektonski elementi dodatno negativno vplivajo na trdnost kamnin in posledično tudi nastajanje materiala, primernejšega za površinski transport. Prevladujoče karbonatne kamnine pogojujejo prisotnost kraških pojavov, katerih površinski tipi vplivajo na kakovost modela RUSLE, kot je bilo že omenjeno v uvodnem delu.

Pedološke in z njimi povezane vegetacijske značilnosti so eden izmed dejavnikov območja, ki vplivajo na stopnjo erozije. Na bolj ali manj nagnjenih pobočjih so zastopane rendzine na apnencu in dolomitu, z njimi se prepletajo rjava pokarbonatna tla. Tu se širijo bukovi in smrekovi gozdovi, značilen je tudi macesen; ob gozdni meji, ki sega od 1600 do 1800 m visoko, pa alpsko rušje. Gozd pokriva dna dolin, strma pobočja in visoke planote. V gozdovih so poleg gospodarske funkcije poudarjene varovalna, hidrološka, podnebna, zootopska, rekreacijska, estetska in druge ekološke vloge gozda. V najvišjih predelih, vrhovih, slemenih in strmih pobočjih so se razvili litosoli, na njih pa se razraščajo alpske vrbe, združba čvrstega šaša s triglavskim sviščem, združba okrogolistnega mošnjaka z julijskim makom (Lovrenčak, 1987).

Metodologija

Za izdelavo ocene stopnje ploskovne erozivnosti na območju občine Bohinj je bila izbrana metoda RUSLE. V preteklosti so na območju jugovzhodne Evrope nekateri avtorji uporabili Gavrilovičevo metodo oziroma njene variacije (Lazarević, 1968, 1985; Pintar et al., 1986; Zorn & Komac, 2009), drugi spet metodo USLE (Mikoš et al., 2006). V tem prispevku je bila testirana uporabnost RUSLE metode, ki pa je bila že od začetka ocenjena kot prekonzervativno za oceno stopnje erozivnosti na območjih z ekstenzivnim načinom kmetovanja, kot so pašniki (Dabney et al., 2014), na območjih z večjimi nakloni ter na kraško oblikovanem površju. Posledično je bil model RUSLE nadgrajen z modelom ocene erozije v strugah.

Za izdelavo modela (karte) erozivnosti je največ v uporabi metoda RUSLE (ang. Revised Universal Soil Loss Equation), ki temelji na njeni predhodnici USLE (ang. Universal Soil Loss Equation), obe pa sta na podlagi obstoječe metode Univerze v mestu Purdue razvila Wischmeier & Smith (1958, 1965, 1978), nadgradili pa so jo Foster et al. (2000 in 2001) in Lown et al. (2000). RUSLE je empirično zasnovan univerzalni model za izračun izgub zemljine, omogoča pa teoretični izračun erozije tal (ob kvalitetnih podatkih tudi mesečne ocene, lahko pa tudi oceno erozije ob posameznem nalivu). Tako model USLE, kot tudi model RUSLE definira enačba (1), ki omogoča izračun povprečne izgube tal (v t, kjer je 1 t = 1000 kg) na enoto površine (*A*):

$$A = R \times K \times L \times S \times C \times P \qquad (1)$$

kjer so: *A* – povprečna izguba tal na enoto površine (t ha^{-1} – tona na hektar); *R* – erozivnost padavin je dejavnik, ki temelji na vplivu energije padavin in odtoka le-teh (MJ ha^{-1} mm h^{-1}); *K* – erodibilnost različnih tipov tal je dejavnik, ki je odvisen od njihovih pedoloških lastnosti (t MJ^{-1} h mm^{-1}); *L* – dolžina pobočja je dejavnik, ki opisuje razmerje med izgubo tal pri dejanski in primerjalni dolžini, ki znaša 22,13 m (dejavnik nima enote); *S* – naklon pobočja je dejavnik, ki opisuje razmerje med izgubo tal pri dejanskem in primerjalnem 9 % naklonu (dejavnik nima enote); *C* – dejavnik vrednost erozije tal je odvisen od pokrovnost oziroma tipa rabe tal (dejavnik nime enote; vrednosti se gibljejo med 0 in 1, kjer največje vrednosti pripadajo golim območjem) in podaja razmerje med izgubo tal pri dejanski rabi in primerjalni rabi, ki jo predstavlja neobdelano polje; *P* – dejavnik kmetijskih zaščitnih ukrepov podaja razmerje med izgubo tal pri dejanski rabi območja za kmetijske/industrijske namene in primerjalni rabi, ki je orano polje (dejavnik nima enote; vrednosti se gibljejo med 0 in 1,3, kjer predstavljajo večjo vrednost območja s slabšimi zaščitnimi ukrepi). Vrednosti dejavnikov *L* in *S* se računajo sočasno, saj predstavljata združena dejavnika *L* in *S* tako imenovani topografski dejavnik (*LS* = *L* × *S*; v nadaljevanju označen kot *LS*), nenavadne mere – 22,13 m in 9 % naklon pa izhajajo iz pretvorbe anglo-saksonskega merskega sistema v ISO. Tudi ta dejavnik nima enote. V pristopu, ki je predstavljen v tem prispevku, dejanska vrednost povprečne izgube tal na enoto površine (A) ni bila izračunana, saj so bile vse vhodne spremenljivke nominalno ovrednotene glede na njihove dejanske vrednosti. Pravilna oznaka povprečne izgube tal na enoto površine (A) bi bila torej navidezna in temu primerno označena z »A'«:

$$A' = R' \times K' \times L' \times S' \times C' \times P' \qquad (2)$$

kjer vse vhodne spremenljivke predstavljajo enake lastnosti, kot so opisane zgoraj, a so njihove vrednosti poenostavljene na nominalno skalo.

Po metodologiji (R)USLE med erozivne dogodke sodijo vsi deževni dogodki, pri katerih se je v šestih urah akumuliralo vsaj 12 mm padavin oz. v 15 minutah vsaj 6 mm padavin (Wischmeier & Smith, 1978). Ker so natančni časovni podatki o intenzivnih padavinah prostorsko redki ali pa dostopni samo za omejeno časovno obdobje, je bila za potrebe ocene erozivnosti po metodologiji RUSLE uporabljena najboljša trenutno dostopna ocena erozivnosti padavin za Slovenijo (Petan, 2010).

Metoda RUSLE je splošno uveljavljena metoda ocene izgube tal zaradi erozije (Wischmeier & Smith, 1978; Renard et al., 1997). V slovenski prostor so metodo RUSLE med drugimi vpeljali ali jo razvijali za lokalne potrebe Petkovšek (2002), Maček (2006), Zorn et al. (2007), Petan et al. (2008a, 2008b), Petan (2010), Petan et al. (2010), Žabota (2015).

Pri vsakem od uporabljenih podatkov so bile določene vrednosti spremenljivk po uveljavljenih standardih (vrednosti *K*, *C* in *P* ter nominalne vrednosti *K*', *C*' in *P*'), vrednost *R* je bila povzeta iz modela erozivnosti padavin (Petan, 2010), vrednost LS pa je bila izračunana na podlagi enačbe (3):

$$LS = (1+m) \times \left(\frac{\lambda}{22{,}1}\right)^m \times \left(\frac{\sin(0{,}01745 \times \theta_{stp})}{0{,}09}\right)^n \qquad (3)$$

kjer je λ spremenljivka, odvisna od horizontalne projekcije dolžine pobočja in predstavlja zmnožek vrednosti funkcije »*FlowAccumulation*« ter osnovne velikosti celice v metrih; *m* je spremenljivka, odvisna od naklona pobočja, ki vpliva na erodibilnost tal; *22,1* je enota dolžine, ki sta jo določila (Wischmeier & Smith, 1978); θ naklon pobočja v stopinjah (vrednost 0,01745 omogoča pretvorbo stopinj v radiane); 0,09 je konstanta naklona pobočja (nakloni so podani v odstotkih in ne v stopninjah; 9 % = 0,09) in *n* je spremenljivka, odvisna od erodibilnost tal (Oliveira et al., 2013).

V literaturi je moč najti razpone vrednosti za spremenljivki *m* in *n* (Mitasova et al., 1996; Oliveira et al., 2013). Glede na omenjena vira sta kot najprimernejši ali najbolj značilni vrednosti za obdelane in travniške površine *m = 0,4* in *n = 1,4*. Spletni vir (Internet 1) povzema dognanja več raziskovalcev in priporoča vrednost *m* med 0,02 – 0,05 za nizke naklone, 0,04 – 0,71 za srednje naklone in 0,07 – 0,83 za velike naklone. Glede na opazno prevlado večjih naklonov pobočij v občini Bohinj je bila za vrednost spremenljivke *m* določena vrednost 0,4.

Spremenjljivke, uporabljene za izdelavo modela RUSLE, so bile razvrščene v nominalne razrede od 1 do n, kjer je spremenljivka n predstavljala število razredov vhodnega podatka. Vrednosti modela so bile izračunane na osnovi enačbe 2, nato pa razdeljene v pet razredov stopnje erozivnosti, kjer so večje dobljene vrednosti pomenile večjo stopnjo erozivnosti.

Drugi del modela za oceno stopnje erozivnosti je temeljil na oceni stopnje erozivnosti v strugah. Kot osnova za izračun stopnje erozivnosti je bila uporabljena hipotetična rečna mreža, izračunana na osnovi digitalnega modela višin. Mreža poleg strug površinskih tokov obsega še padnice po pobočjih in tako predstavlja območja gradientov (oziroma območja stekanja), po katerih poteka erozija. Vsakemu dobljenemu linijskemu elementu, torej osnovnemu – ravnemu gradniku mreže, je bila po principu Shreve-ja (1966) pripisana stopnja njegove pomembnosti, določena s številom manjših pritokov. Nadalje je bil vsakemu osnovnemu gradniku izračunan padec. Tako je bilo možno gradnike razvrstiti glede na stopnje podvrženosti erozivnosti po principu večje podvrženosti le-tej ob večjem padcu. Stopnja erozije za vsak gradnik je bila izračunana po enostavni enačbi Zingga (1940) (4), ki je tudi podlaga za izračun dejavnika *LS* v modelu RUSLE (Liu et al., 2001), kar dodatno argumentira združljivost obeh metod:

$$y = a \times x^b \quad (4)$$

kje je y stopnja erozije, a empirično pridobljena konstantna z vrednostjo 0,065, x naklon oziroma padec (gradient) toka vode in b empirično pridobljena konstantna z vrednostjo 1,48. Rezultat enačbe nima enote. Obstajajo tudi seveda številne druge enačbe za izračun stopnje erozije glede na naklon (npr. Chaplot & le Bissonnais, 2003; Assouline & Ben-Hur, 2006; Zhao et al., 2014; Zhang et al., 2015), ki pa upoštevajo še številne druge parametre, kot so intenziteta in trajanje padavin, usmerjenost brazd, natančen tip vegetacije in njena gostota, ki jih za dano območje ni bilo možno pridobiti ali izmeriti. Enačbe, ki določajo stopnjo erozije in ki so bile dobljene pri navedenih razikavah so posledično zelo specifične za testne lokacije, ki so jih raziskovalci uporabili za izračun sopnje erozije. Privzeto je bilo, da bi bila uporaba enačbe 4 (Zingg, 1940), ki predstavlja povprečenje stopenj erozije, najzaneslivejša za izbran pristop izračuna stopnje erozivnosti v strugah glede ne naklone le-teh.

Upraba hipotetične rečne mreže (ali navidezne mreže površinskih tokov) za izračun ocene stopnje erozivnosti v strugah temelji na navedbah raziskovalcev, ki so se s podobnim izzivom soočali v svojih raziskavah na kraških terenih z večjimi nakloni (npr. Zhang et al., 2013; Feng et al., 2016; Chen et al., 2017, Dai et al., 2017; Zhang et al., 2017). Protiargument bi seveda lahko bil, da je izostanek površinskih vodnih tokov na kraških območjih logičen in pričakovan, a je kljub temu treba upoštevati, da na strmejših pobočjih površinski odtok vode obstaja, pa čeprav na krajše razdalje in da večina tega ponikne v tla. Model erozije v strugah, ki je v tej raziskavi vpeljan kot nadgranja modela RUSLE, ne predstavlja dejanskega prenosa materiala po površini s pomočjo vodne erozije, temveč podaja območja, kjer je verjetnost erozije večja, pa čeprav je erozija na teh usmerjena v notranjost kraškega pojava ali na krajšo razdaljo. Nedvomno pa ima pri dolžini transporta materiala po površju veliko vlogo infiltracijska sposobnost kamnin (Kheir et al., 2008), a ta informacija ni bila na voljo in pri predstavljenem modelu ni bila vključena.

Številna literatura navaja več vrednosti naklonov pobočij oziroma padcev vodnega toka, pri katerih se začnejo opaznejši procesi erozije, večji del teh vrednosti pa se giblje med tremi in petimi stopinjami naklona, kar izraženo z odstotki pomeni okoli 10 % naklon. Tako Ebisemiju (1988, 1989) in Ebisemiju & Ado (1989) določata to vrednost na 3° – 5°, Panagos et al. (2015b) določajo to vrednost za izvajanje varovalnih ukrepov v kmetijstvu na 10 %, Floor (2016) in Pearce (1987) pa navajata 10 % naklon kot vrednost, pri kateri se erozija drastično poveča. Tudi spremenljivki *LS* ter *C* v modelu RUSLE temeljita na osnovni enoti z naklonom 9 % (Wischmeier & Smith 1958, 1965 in 1978). Posledično so bili elementi strug razdeljeni na štiri razrede z različnimi pogoji za izračun jakosti erozije, ki upoštevajo kombinacijo vrednosti naklona in pomembnost elementa (gradnika) po metodi Shreve-a (1966). Obe vrednosti sta bili združeni z namenom pridobitve ocene, ki upošteva oba dejavnika (tab. 1). Za gradnike, katerih naklon je bil večji od 4,5° (kar je identično naklonu 10 %, če so ti izraženi v odstotkih), je bila pri izračunu vrednosti erozije vzdolž tega gradnika uporabljena dejanska vrednost njegovega naklona (označuje jo spremenljivka x), za vse ostale naklone gradnikov pa je bila privzeta vrednost 4,5°. Rezultat predstavlja kombinacijo naklonov strug in hipotetične širine (jakosti) toka ter upošteva močnejšo vertikalno erozijo v strugah, ki je posledica večjega padca, in močnejšo lateralno erozijo, ki je posledica jakosti struge in je izražena z višjo vrednostjo po Shreve-u (1966). Prvi razred tako predstavlja segmente, ki ležijo na relativno položnem terenu in imajo malo pritokov (npr. manjši potoki z izviri pod vznožji pobočij). Drugi razred predstavlja segmente, ki ležijo na strmem terenu in imajo veliko pritokov (npr. večji gorski potoki ali rečice). Tretjemu razredu pripadajo segmenti, ki ležijo na relativno položnem terenu in imajo veliko pritokov (npr. večje reke). Četrtemu razredu pripadajo segmenti, ki ležijo na strmem terenu in imajo malo pritokov (npr. hudourniki ali padnice po pobočjih).

Tabela 1. Razredi za izračun jakost erozije v strugah, upoštevajoč pogoj naklona in pogoj Shreve-ja (1966), ki določa nivo pomembnosti posameznega elementa struge, določene s številom manjših pritokov.

Table 1. Classes based on which the channel erosion (“Erosion value (°)”) was claculated for each basic element. The channel erosion value was defined based on the slope condition and the Shreve (1966) condition that defines the contribution of each channel element and its side inflows.

#	Pogoj naklona/ Slope condition (°)	Pogoj po Shreve-ju / Shreve condition (1966)	Vrednost erozije / Erosion value
1	=<4,5	<100	$0{,}065 \times 4{,}5^{1{,}48}$
2	>4,5	=>100	$0{,}065 \times x^{1{,}48} \times$SHREVE
3	=<4,5	=>100	$0{,}065 \times 4{,}5^{1{,}48} \times$SHREVE
4	>4,5	<100	$0{,}065 \times x^{1{,}48} \times$SHREVE

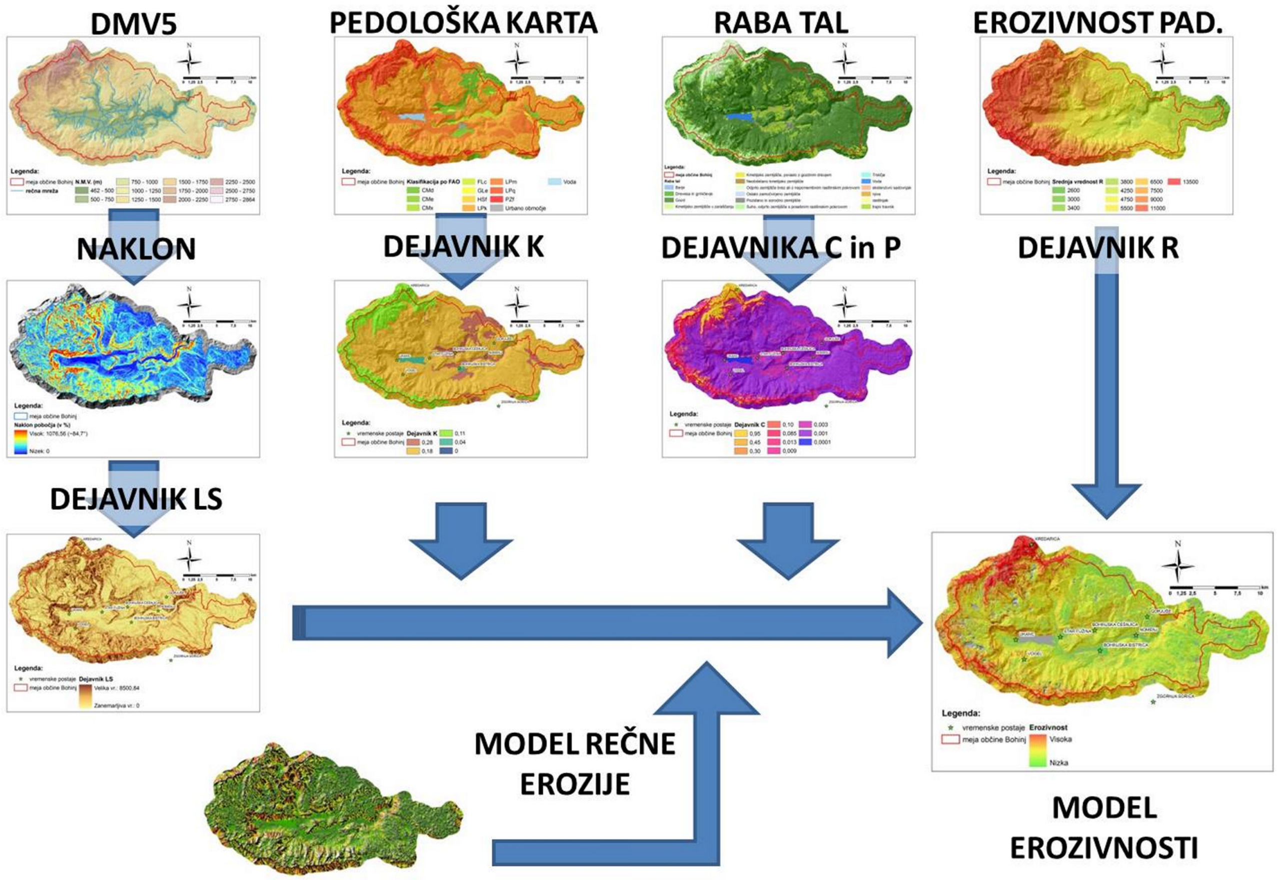

Sl. 2. Shema postopka izdelave modela (karte) erozivnosti na območju občine Bohinj.

Fig. 2. Derivation of the erosion model procedure spreadsheet, developed in the area of the Bohinj municipality. Input layer “DMV5” represents the digital elevation model with the 5 meters resolution, the layer “Pedološka karta” represents pedologic types map, the layer “Raba tal” represents the landuse coverage map, the layers “Erozivnost” and the “Dejavnik R”represent the rainfall-runoff erosivity factor, the layer “Naklon” represents the slope inclination information, the layer “Dejavnik K” represents the soil erodibility factor, the layer “Dejavnika C in P” represents the joined factor of the cover-management factor and the support practice factor, the layer “Erozivnost” represents the rainfall-runoff erosivity factor, the layer “Dejavnik LS” represents the joined factor of the slope inclination factor and the slope length factor, the layer “Model rečne erozije” represents the model of the channel erosion levels, and the layer “Model erozivnosti” represents the final product – the surface erosion model.

Izračun vrednosti dejavnikov v modelu RUSLE z uporabo GIS-sov so dokazali številni avtorji (Desmet & Govers, 1996; Fu et al., 2005; Lim et al., 2005; López-Vicente et al., 2008; Zhang et al., 2013; Feng et al., 2016; Chen et al., 2017, Dai et al., 2017; Zhang et al., 2017), zato je bil enak pristop izbran tudi za izdelavo modela (karte) erozivnosti na območju občine Bohinj, ki temelji na metodi RUSLE z dodanim korakom, ki upošteva tudi erozijo v strugah. Shema postopka izdelave modela (karte) je prikazana na sliki 2.

Uporabljeni podatki in določitev vrednosti spremenljivk

Za izdelavo modela so bili uporabljeni podatki kot jih določa model RUSLE, torej pedološka karta, karta tipov rabe tal, digitalni model višin ter karta erozivnosti padavin, za izračun erozije v strugah pa izpeljanke iz digitalnega modela višin – hipotetična rečna mreža ter lastnosti njenih osnovnih gradnikov (segmentov površinskega toka). V nadaljevanju so prikazani podatkovni sloji v tej raziskavi uporabljenih prostorskih podatkov, v opisu slike posameznega sloja pa je zraven podana tudi informacija o ločljivosti izvornega podatka.

Pedološka karta

Pedološka karte Slovenije v merilu 1 : 25.000 je bila pridobljena s spletnega portala Ministrstva za kmetijstvo, gozdarstvo in prehrano (GERK 2016). Slika 3 prikazuje pedološke značilnosti občine Bohinj, ki so osnova za določitev spremenljivke erodibilnosti tal (*K*) v modelu RUSLE in spremenljivkle *K*‘ v navideznem modelu RUSLE.

Pedološke enote na območju občine Bohinj so razdeljene na 134 ločenih homogenih enot, tabela 2 pa podaja porazdelitev prisotnih pedoloških tipov po klasifikaciji FAO – kode pedoloških enot (FAO 1988, 1990) glede na njihovo površino, delež površine enot, kvantifikacijo erodibilnosti (spremenljivka *K*) prisotnih pedoloških tipov na osnovi Kassama et al. (1992) in ocenjeno nominalno vrednost spremenljivke *K*, ki je predstavljala vhodni podatek za izračun modela RUSLE.

Raba tal

Raba tal z ločljivostjo orto-foto podob (1 m) je bila pridobljena s spletnega portala Ministrstva za kmetijstvo, gozdarstvo in prehrano (GERK 2016). Slika 4 prikazuje rabo tal v občini Bohinj.

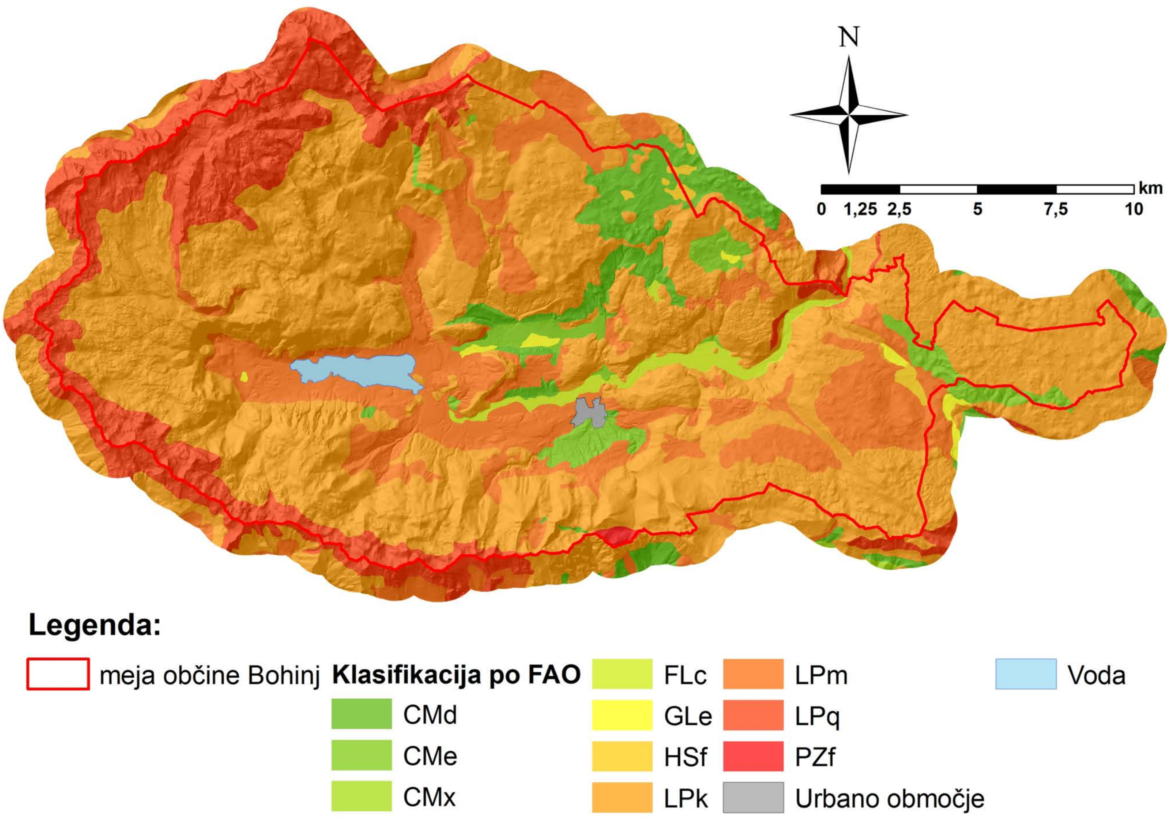

Sl. 3. Pedološka karta občine Bohinj (Izvorni podatek – sloj v merilu 1 : 25.000). Meja občine je označena z rdečo linijo.

Fig. 3. Pedologic map of the Bohinj municipality, delinated by the red line (the source data – layer's scale was the 1 : 25,000). The legend of the pedlogic types (Klasifikacija po FAO) is explained in the Table 2.

Tabela 2. Porazdelitev pedoloških tipov po FAO klasifikaciji (FAO opis, ki mu je dodano slovensko poimenovanje tipov tal) na območju občine Bohinj glede na število poligonov posameznega razreda FAO (št. poligonov), njihovo skupno površino (A, v ha) in delež površine v občini (A v %), stopnjo erodibilnosti tal (K) ter nominalno vrednost dejavnika stopnje erodibilnosti *(K')* (ta podatek je bil vhodni podatek za izračun navideznega modela RUSLE po enačbi 2).

Table 2. Distribution of the pedological types (after FAO) (official FAO pedological type abbreviation – "FAO description") in the area of Bohinj municipality. The type description is given in the column "FAO opis", the number of polygons for each type is given in the column "Št. poligonov", the area in the column "A (ha)", the area proportion in the column "A (%)", the level of the erodibility of the pedological type is given in the column *"K"* and its nominal value that was used for the calculation of the RUSLE model based on the equation 2 is given in the column *"K'"*.

FAO oznaka/ FAO label	FAO opis / Description	Št. poligonov / No. of Polygons	A (ha)	A (%)	*K*	*K'*
CMd	Distrična rjava tla / Dystric Cambisol	11	1193,76	3,58	0,28	4
CMe	Evtrična rjava tla /Eutric Cambisol	9	999,69	3,00	0,28	4
FLc	Karbonatna obrečna tla / Calcaric Fluvisol	3	504,06	1,51	0,28	4
GLe	Evtrični psevdoglej / Eutric Gleysol	5	106,07	0,32	0,18	3
HSf	Slabo razkrojena šotna tla / Fibric Histosol	6	98,018	0,29	0,28	4
LPk	Humusno akumulativna tla na karbonatni podlagi / Rendzic Leptosol	54	19910,16	59,66	0,18	3
LPm	Humusno akumulativna tla na karbonatni podlagi z moličnim horizontom / Mollic Leptosol	38	6221,95	18,64	0,18	3
LPq	Litični leptosol oz. kamnišče / Lithic Leptosol	5	3896,58	11,68	0,11	2
PZf	Železov podzol / Feric Podzol	1	55,79	0,17	0,28	4
Voda* / Water*	Vodna površina, morje, reke, * / Water surface, sea, river, lake*	1	313,34	0,94	0,04	1
Urbano območje* / Urban area*	Urbana površina, mesto, naselje * / Urban area, city, settlement*	1	73,06	0,22	0,04	1

*ni uradna FAO oznaka / not an official FAO type

Vrednost dejavnika erozije tal *C* ima v modelu RUSLE razpon med 0 in 1 ter je specifičen za vsako skupino tipov rabe tal. Kot primerjalni tip površine se upošteva gola površina (brez vegetacije), katere vrednost dejavnika *C* je enaka 1. Ta vrednost se zmanjšuje z večanjem gostote vegetacijskega pokrova in obliko rabe tal (npr. njiva, travnik, sadovnjak itd.). Dejavnik *C* je najverjetneje najpomembnejši dejavnik, na katerega lahko vpliva človek s svojimi odločitvami o zaščitnih ukrepih (Panagos et al., 2015a). Dejavnik *P* predstavlja stopnjo umetne zaščite rabe tal glede na primerjalni tip (brez) zaščte, ki ga predstavlja golo območje z linijskimi vzorci vzdolž padnice pobočja (npr. brazde ali podobni kanali). Umetni zaščitni ukrepi so na primer kolobarjenje, oblikovanje teras, oranje po plastnicah, ohranjanje strnišč, košnja itd. Raba tal je osnova za določitev spremenljivk vrednost erozije tal (*C*) in vrednost zaščitnega ukrepa (*P*) v enačbi RUSLE za izračun erozivnosti tal, oziroma njunih nominalnih vredosti *C'* in *P'*. Podatki o zaščitnih ukrepih na testnem območju niso bili dostopni, zato je bila za dejavnik *P* in *P'* privzeta splošna vrednost 1.

Tabela 3 podaja porazdelitev tipov rabe tal na območju občine Bohinj glede na njihovo površino, na delež površine in ocenjeno vrednost erozije tal – *C* (po Wischmeier & Smith, 1978). Kljub številnim različnim ocenam vrednosti spremenljivke *C*, se večina avtorjev izračunov erozivnosti tal (Fernandez et al., 2003; Adediji et al. 2010; Žabota, 2015; Gelagay & Minali, 2016) sklicuje na Wischmeier & Smith (1978), zato so bile njune ocene vključene v izračun erozivnosti za občino Bohinj.

Digitalni model višin

Digitalni model višin z ločljivostjo 1 m je bil pridobljen s portala ARSO (ARSO 2016b). Za potrebe izdelave modela in zaradi enostavnejšega upraljanja s podatki pa je bil model razredčen na ločljivost petih metrov (DMV 5 m). Ocenjeno je bilo, da je izbrana ločljivost dovolj kvalitetna za izdelavo želene ocene stopnje erozivnosti. Slika 5 prikazuje porazdelitev površine občine Bohinj glede na pasove nadmorskih višin z razponom 250 m. Taka razdelitev je bila izbrana zgolj v informativne namene in ni imela vpliva na nadaljnje modeliranje. Morfologija terena oziroma njegove fizične lastnosti, ki jih je možno izračunanti iz višinskih podatkov, so osnova za določitev spremenljivk dolžina pobočja (L) in naklon pobočja (S) v modelu RUSLE in posledično skupnega navideznega dejavnika pobočij (LS').

Tabela 3. Porazdelitev tipov rabe tal na območju občine Bohinj glede na njihovo površino, delež in ocenjeno vrednostjo spremenljivke C in nominalno vrednost spremenljivke C' (ta podatek je bil vhodni podatek za izračun navideznega modela RUSLE po enačbi 2).

Table 3. Distribution of the landuse types by GERK code ("#"). The landuse type description is given in the column "Landuse description", the area in the column "A (ha)", the area proportion in the column "A (%)", the level of the cover--management factor type is given in the column "C" and its nominal value that was used for the calculation of the RUSLE model based on the equation 2 is given in the column "C'".

#	Opis rabe tal / Description of landuse	A (ha)	A (%)	C*	C'
1100	Njiva / Field	51,3	0,15	0,085	6
1190	Rastlinjak / Orchard	0,04	0,00013	0,0001	1
1222	Ekstenzivni sadovnjak / Extensive orchard	56,2	0,17	0,013	5
1300	Trajni travnik / Permanent meadow	3078,0	9,22	0,003	3
1410	Kmetijsko zemljišče v zaraščanju / Agricultural land in overgrowth	173,0	0,52	0,450	9
1500	Drevesa in grmičevje / Trees and schrubs	208,2	0,62	0,009	4
1600	Neobdelano kmetijsko zemljišče / Non-cultivated agricultural land	40,0	0,12	0,300	8
1800	Kmetijsko zemljišče, poraslo z gozdnim drevjem / Agricultural land covered with trees	288,6	0,86	0,100	7
2000	Gozd / Forest	24382,2	73,06	0,001	2
3000	Pozidano in sorodno zemljišče / Built and similar areas	457,6	1,37	0,001	2
4100	Barje / Marsh	2,5	0,01	0,0001	1
4210	Trstičje / Rushes	2,0	0,01	0,0001	1
4220	Ostalo zamočvirjeno zemljišče / Other swamp land	0,3	0,0008	0,0001	1
5000	Suho, odprto zemljišče s posebnim rastlinskim pokrovom / Dry, open land with a specific plant cover	2997,0	8,98	0,013	5
6000	Odprto zemljišče brez ali z nepomembnim rastlinskim pokrovom / Open land without or with an insignificant plant cover	1213,6	3,64	0,950	10
7000	Voda / Water	422,2	1,27	0,0001	1

*Wischmeier & Smith (1978)

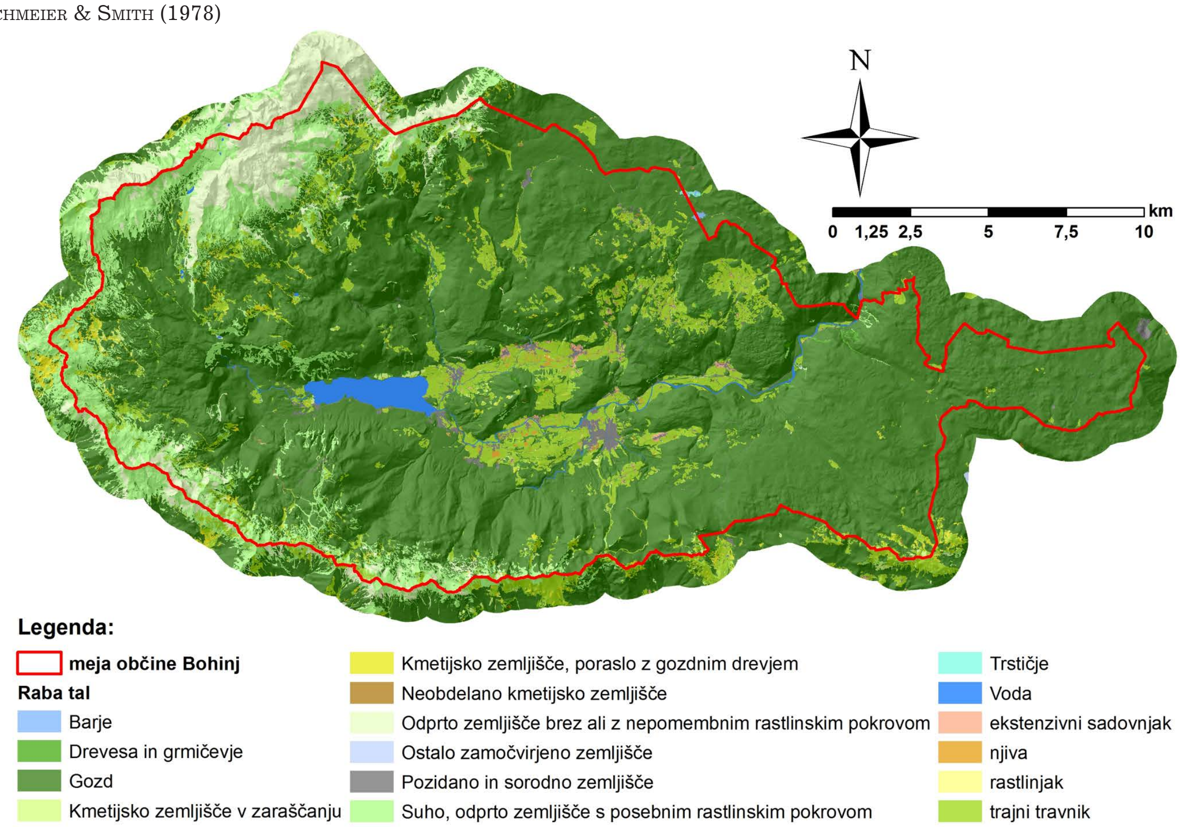

Sl. 4. Karta rabe tal na območju občine Bohinj (izvorni podatki imajo ločljivosti 1 m).

Fig. 4. Landuse coverage map of the Bohinj municipality, delinated with the red line (the source data – layer's resolution was 1 m). The legend for the landuse types is given in the Table 3.

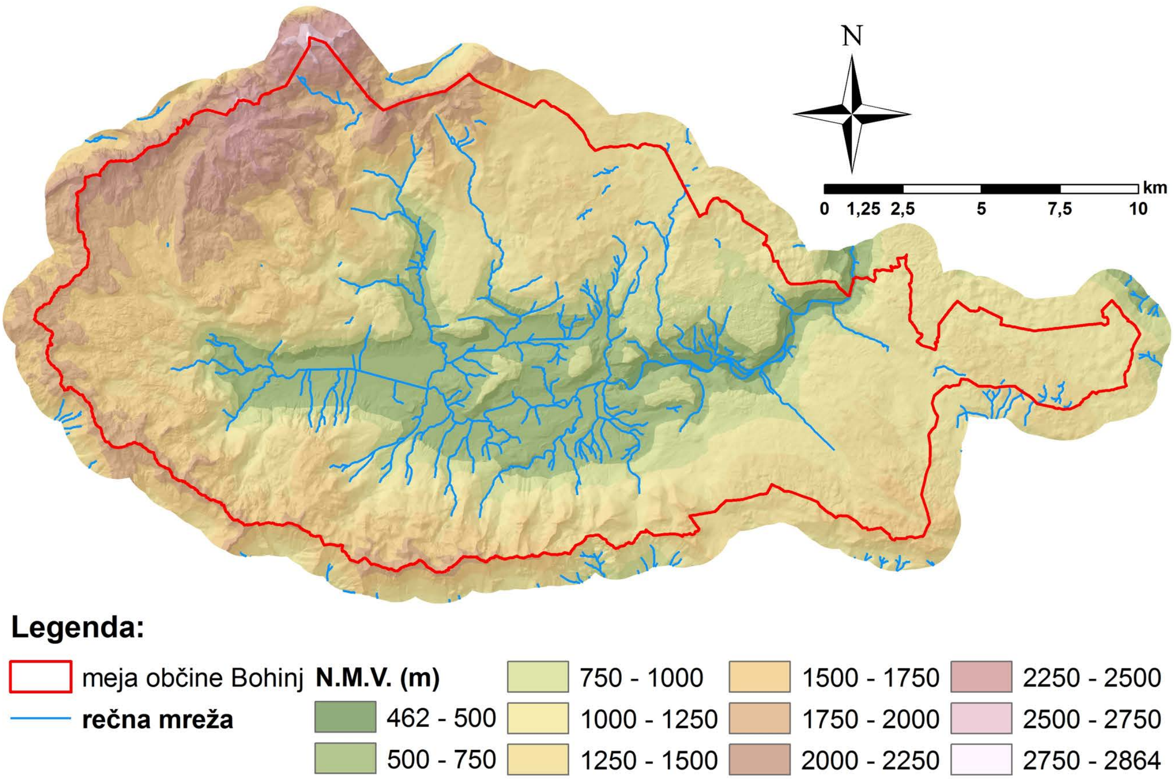

Sl. 5. Karta nadmorskih višin (v metrih) na območju občine Bohinj, katere meja je prikazana z rdečo linijo. Rečna mreža je prikazana z modrimi linijami. Izvorni podatek – sloj ima ločljivosti 1 m.

Fig. 5. Elevation map of the Bohinj municipality, delinated with the red line (the source data – layer's resolution was 1 m). Evelation data is represented in meters above sea level ("N.M.V. (m) ")and in classes by 250 meters. River network is represented with the blue lines.

Erozivnost padavin

Podatek o erozivnosti padavin je bil povzet po Petan (2010), ki je bil izdelan za območje celotne Slovenije. Oceno erozivnosti padavin je Petan (2010) izdelal na podlagi opravljenih meritev intenzitete padavin in porazdelitve padavinskih delcev iz izpeljanih eksponentnih regresijskih povezav med kinetično energijo in intenziteto padavin, ki so veljavne za submediteransko, subalpsko in zmerno celinsko podnebno območje Slovenije. Iz izpeljanih regresijskih povezav je določil erozivnost padavin za 31 lokacij v Sloveniji, ki so bile prostorsko in časovno reprezentativno porazdeljene. Karto prostorske porazdelitve erozivnosti padavin v Sloveniji je izračunal z metodo interpolacije. Ne glede na dejstvo, da je ta sloj slabše ločljivosti kot ostali uporabljeni sloji, je le-ta za območje občine Bohinj edini dostopen podatek o erozivnosti padavin, ki določa spremenljivko erozivnosti padavin (R) v modelu RUSLE in njeno nominalno vrednost R'. Slika 6 prikazuje porazdelitev vrednosti erozivnosti padavin na območju občine Bohinj. Tabela 4 prikazuje porazdelitev istih razredov na površino in njihove deleže. Ta podatek je najbolj podvržen napakam, predvsem zaradi nujne prostorske interpolacije točkovnih vrednosti.

Hipotetična rečna mreža

Za potrebe modeliranja erozije v strugah (rečne erozije) je bila iz digitalnega modela višin generirana hipotetična rečna mreža (sl. 7). Pred nadaljnjo obdelavo je ta sloj sestavljalo okoli 36.600 linijskih elementov, za potrebe analize pa so bili le-ti razdeljeni na posamične ravne segmente; skupaj jih je bilo okoli 153.000. Skupna dolžina hipotetične rečne mreže je znašala 3918,5 km, kar je za 7,5-krat več od dejanske rečne mreže.

Rezultati in diskusija

Izpeljanke prostorskih podatkov, ki so bile uporabljene kot vmesni podatki za izračun modela erozivnosti

Na osnovi vrednosti, ki so bile za vsak dejavnik določene na podlagi predhodnih raziskav oziroma obstoječe literature, so bile izdelane izpeljanke osnovnih prostorskih podatkov. Te so predstavljale vhodne podatke za izračun vmesnih modelov in končnega modela ocene stopnje erozivnosti.

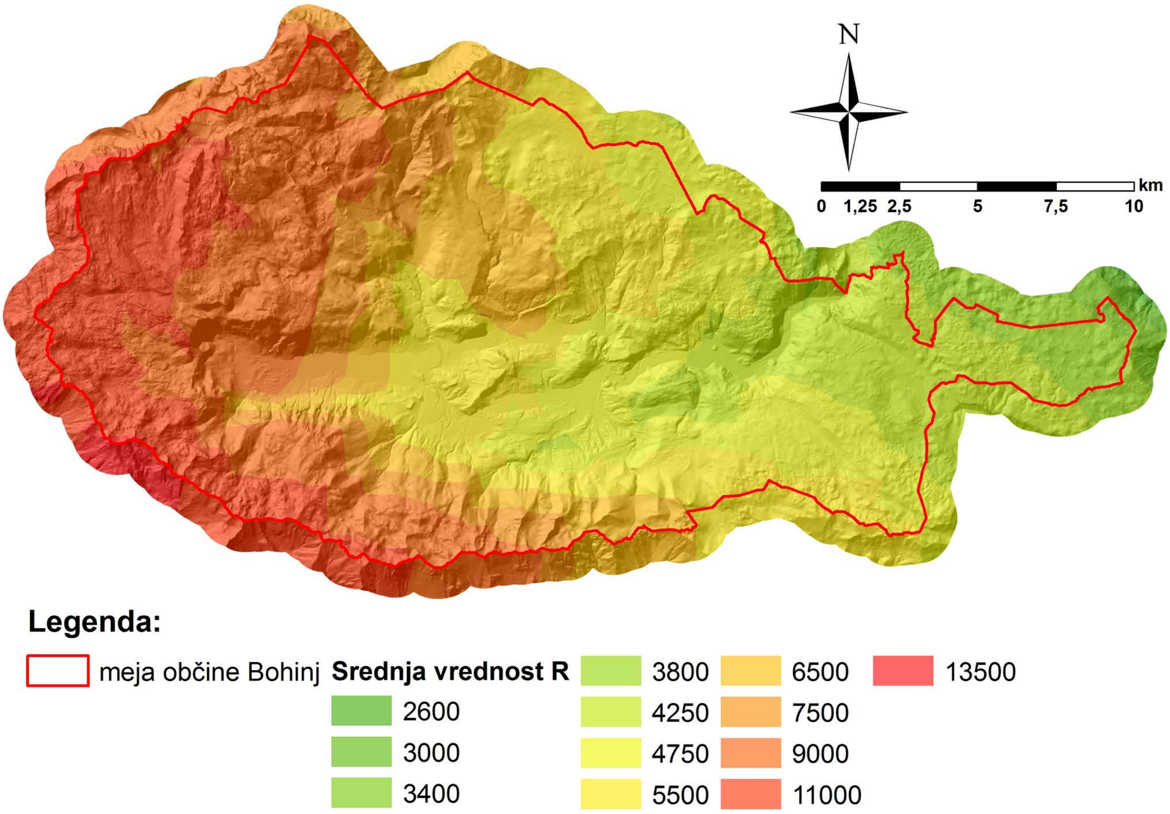

Sl. 6. Karta srednjih vrednosti erozivnosti padavin (izraženih v MJ ha-1 mm h-1) na območju občine Bohinj (izvorni podatki dejavnika vrednost erozivnosti padavin so imeli ločljivost 100 m).

Fig. 6. The map of the average value of the rainfall-runoff erosivity factor (in MJ ha-1 mm h-1) for the Bohinj municipality, delinated with the red line (the source data – layer's resolution was 100 m). The legend for the rainfall-runoff erosivity factor is given in the Table 4.

Tabela 4. Porazdelitev razredov erozivnosti na območju občine Bohinj glede na razrede razponov spemenljivke erozivnosti padavin in srednje vrednosti razreda, njihovo skupno površino, delež površine ter nominalno vrednost erozivnosti tal *R*' (ta podatek je bil vhodni podatek za izračun navideznega modela RUSLE po enačbi 2).

Table 4. Distribution of the rainfall-runoff erosivity factor (R Class range) in the area of Bohinj municipality. The medium value of a given class is presented in the column “Average value - *R* (MJ ha-1 mm h-1)”, the area in the column “A (ha)”, the area proportion in the column “A (%)”, and the rainfall-runoff erosivity factor nominal value that was used for the calculation of the RUSLE model based on the Equation 2 is given in the column *“R'”*.

Razpon vrednosti *R* v razredu / *R* class range (MJ ha^{-1} mm h^{-1})	Srednja vrednost *R* / Average value *R* (MJ ha^{-1} mm h^{-1})	A (ha)	A (%)	*R*'
3200 – 3600	3400	71,18	0,21%	1
3600 – 4000	3800	804,37	2,41%	2
4000 – 4500	4250	3774,57	11,31%	3
4500 – 5000	4750	5028,30	15,07%	4
5000 – 6000	5500	6192,33	18,56%	5
6000 – 7000	6500	4042,65	12,11%	6
7000 – 8000	7500	2743,08	8,22%	7
8000 – 10.000	9000	6414,06	19,22%	8
10.000 – 12.000	11.000	4276,66	12,81%	9
12.000 – 15.000	13.500	25,32	0,08%	10

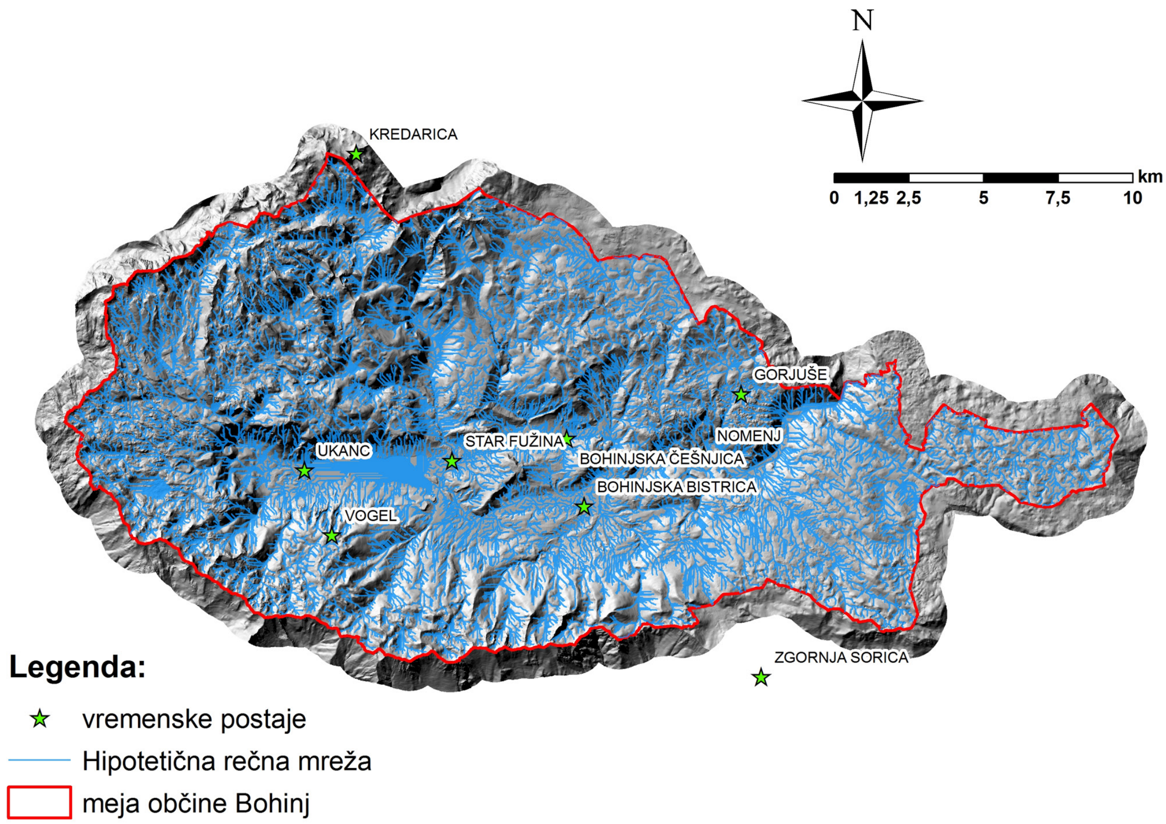

Sl. 7. Karta hipotetične rečne mreže za območje občine Bohinj (izvorni podatki – digitalni model višin – v ločljivosti 5 m).

Fig. 7. The map of the hypothetical river network (represented with blue lines) for the Bohinj municipality, delinated with the red line. The weather stations are presented with the green stars. The source data – layer's (digital elevation model) resolution was 5 m.

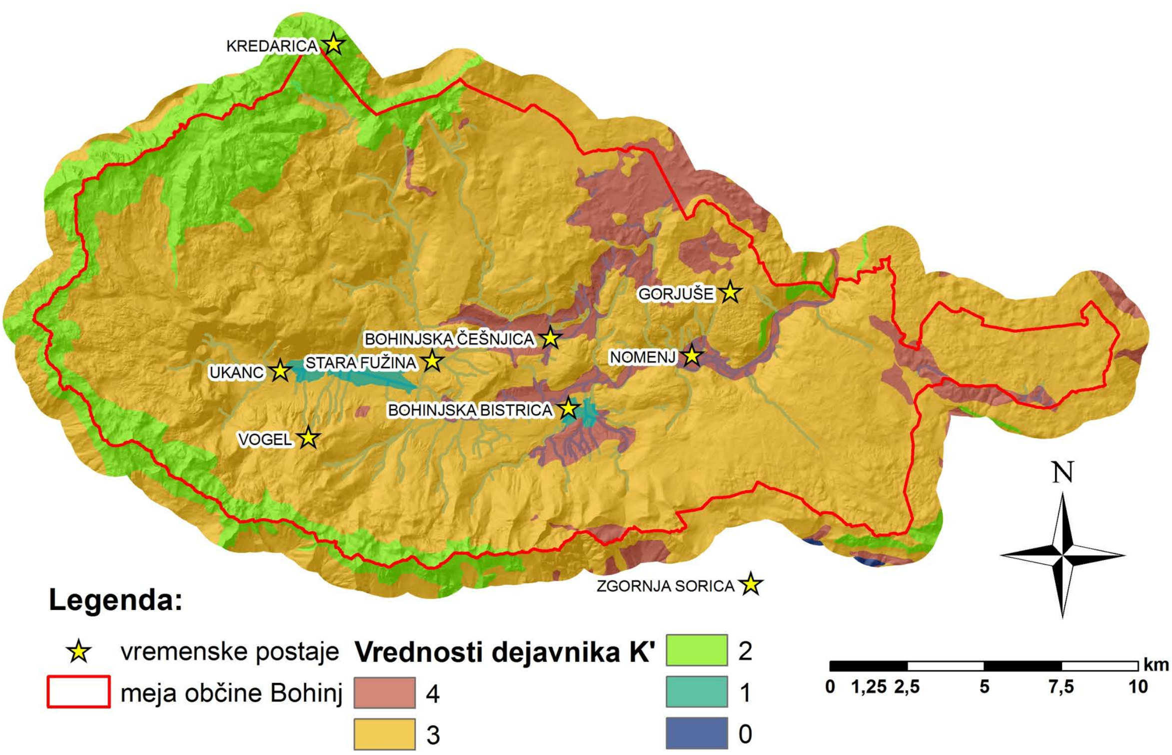

Sl. 8. Porazdelitev nominalnih vrednosti dejavnika stopnje erodibilnosti (K') na območju občine Bohinj glede na ocenjeno vrednost iz tabele 2 (izvorni podatki – pedološka karta – v ločljivosti1 : 25.000). Vremenske postaje so predstavljene z rumenimi zvezdami.

Fig. 8. The distribution map of the soil erodibility factor's nominal values (K'; "Vrednosti dejavnika K'") for the Bohinj municipality, delinated with the red line. The source data – layer's (pedlologic map) resolution was 1 : 25,000. The weather stations are represented with the yellow stars.

Nominalne vrednosti dejavnika stopnje erodibilnosti (K') za območje občine Bohinj, povzete iz tabele 2, so prikazane na sliki 8.

Nominalne vrednosti dejavnika erozije tal (C') za območje občine Bohinj, povzete iz tabele 3, so prikazane na sliki 9.

Vrednosti dejavnika zaščitni ukrepi (*P*) in njegove nominalne vrednosti *P'* so bile ocenjene na vrednost 1, kar pomeni, da so vsa območja podvržena enakim protierozijskim varovalnim ukrepom. To seveda ne pomeni, da ta podatek dejansko predstavlja dejansko stanje v občini Bohinj, temveč zgolj alternativo dejstvu, da informacije o dejanskem stanju zaščitnih ukrepov na obravnavanem območju ni bilo na voljo.

Za izračun RUSLE spremenljivke naklona in dolžine pobočja (*LS*) je bila iz digitalnega modela višin izračunana prostorska izpeljanka, ki opisuje naklon, ta pa predstavlja vhodni podatek za izračun spremenljivke *S*. Izpeljanka predstavlja prispevek površinskega toka vode za vsako celico (ang. *Flow Accumulation*) in predstavlja vhodni podatek za izračun spremenljivke *L*. Na osnovi enačbe 3 je bil izračunan dejavnik naklona in dolžine pobočja (*LS*). Slika 10 prikazuje razpon naklonov v občini Bohinj, izražen v odstotkih, kjer 100 % pomeni naklon 45°. Vrednosti naklonov, izraženih v odstotkih naklona, so bile razvrščene v štiri razrede: (1) nakloni do 5 % (<2,86°), (2) nakloni med 5 in 7,5 % (2,86° - 4,3°), (3) nakloni med 7,5 in 10 % (4,3° - 5,73°) ter (4) nakloni nad 10 % (>5,73°). Osnovna statistika prostorskega pojavljanja posameznih razredov pokaže, da z 88,2 % površine prevladuje četrti razred, s 5,9 % mu sledi prvi razred, nato pa skoraj identično z 2,95 % še preostala dva razreda naklonov. Taka porazdelitev naklonov je botrovala k izbiri večje vrednosti spremenljivke *m* (0,4) v enačbi za izračun spremenljivke naklona in dolžine pobočja (*LS*) (enačba 3), ki je prikazana na sliki 11, v tabeli 5 pa je podana porazdelitev razredov dejavnika naklona in dolžine pobočja (*LS*) vključno s površinami v hektarih, deleži površin razredov in nominalne vrednosti dejavnika *LS'*, ki so služile kot vhodni podatek za izračun navideznega modela RUSLE po enačbi 2.

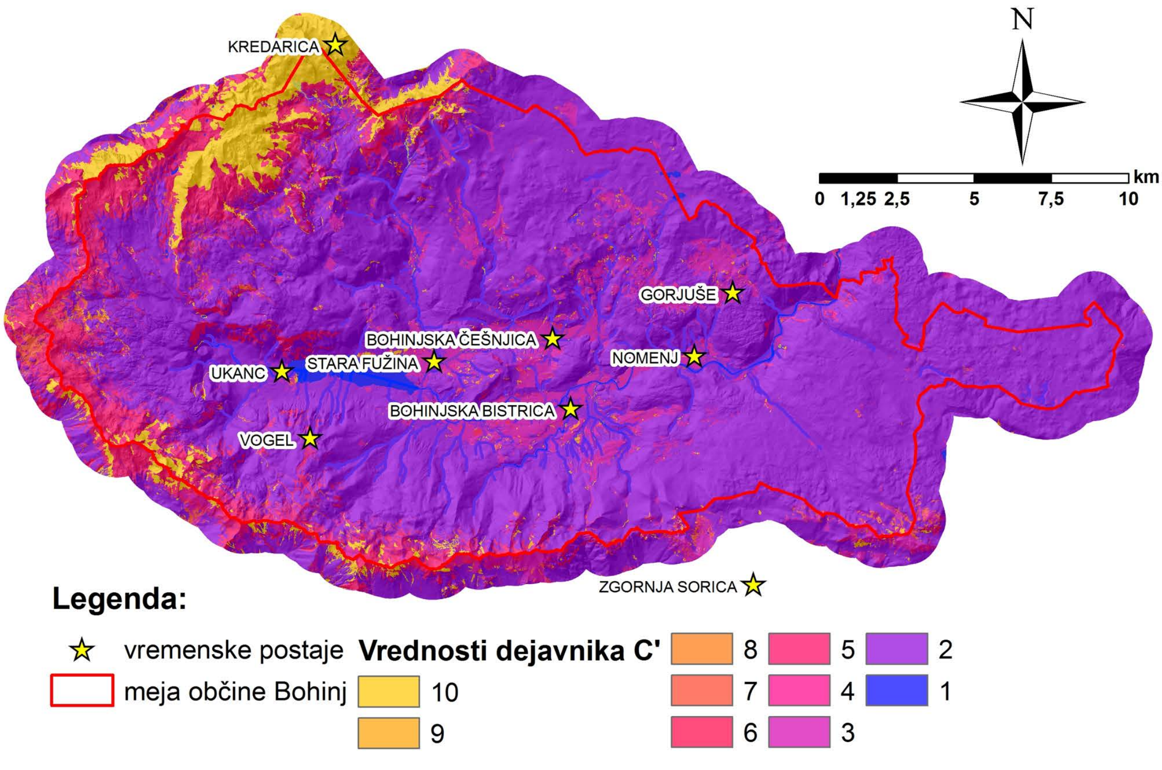

Sl. 9. Porazdelitev nominalnih vrednosti dejavnika erozije tal (C') na območju občine Bohinj glede na ocenjeno vrednost, ki jih podaja tab. 3 (izvorni podatki – raba tal – v ločljivosti 5 m). Rečna mreža je predstavljena z modrimi linijami, vremenske postaje pa z rumenimi zvezdami.

Fig. 9. The distribution map of the cover-management factor's nominal values (C') for the Bohinj municipality, delinated with the red line. The source data – layer's (landuse cover) resolution was 5 m. The river network is represented with the blue lines and the weather stations are represented with the yellow stars.

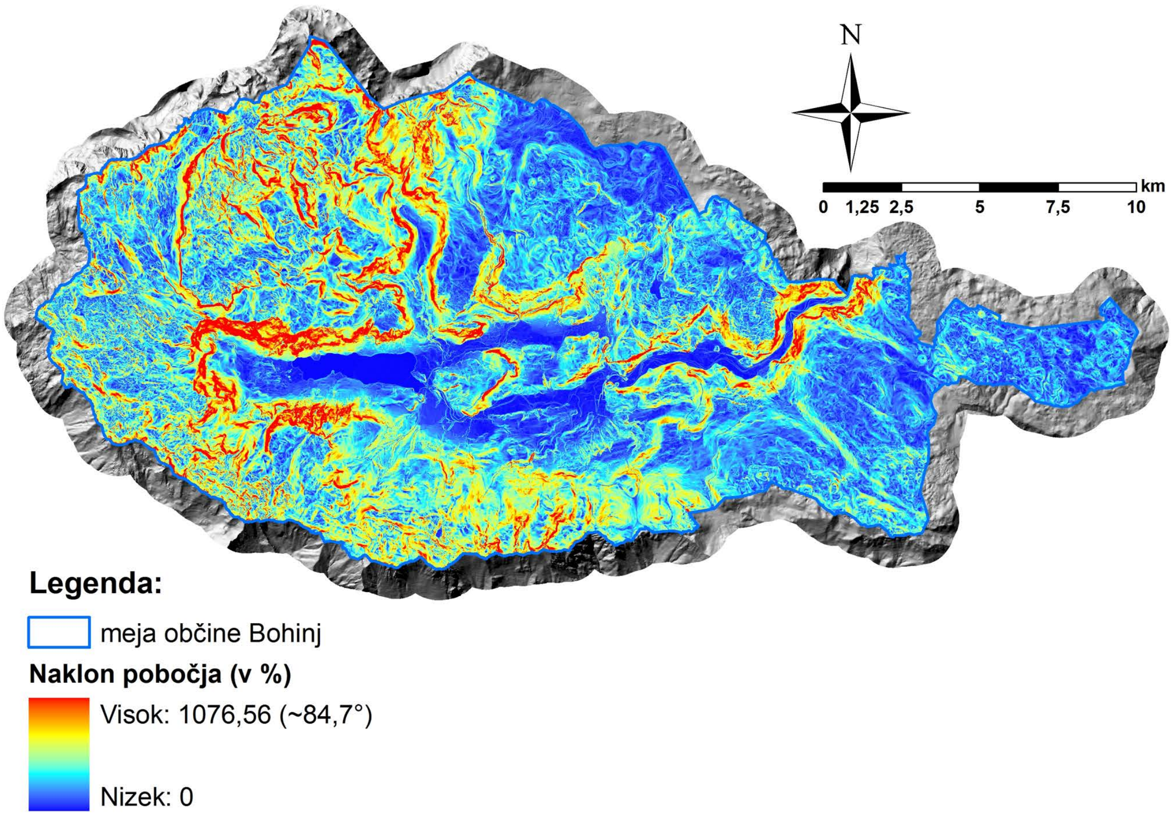

Sl. 10. Karta razponov naklonov na območju občine Bohinj. Nakloni so izraženih v %, kjer je 100 % naklon identičen 45°. Izvorni podatek – digitalni model višin – ima ločljivosti 5 m.

Fig. 10. The distribution map of the slope steepness ("Naklon pobočja") in percentages for the Bohinj municipality, delinated with the red line. The slopes inclination values that are given in % are ranging from flat ("Nizek: 0") to steep ("Visok: 1076,65 (~84,7°)) where 100 % equals the slope inclinaton of 45°. The source data – layer's (digital elevation model) resolution was 5 m.

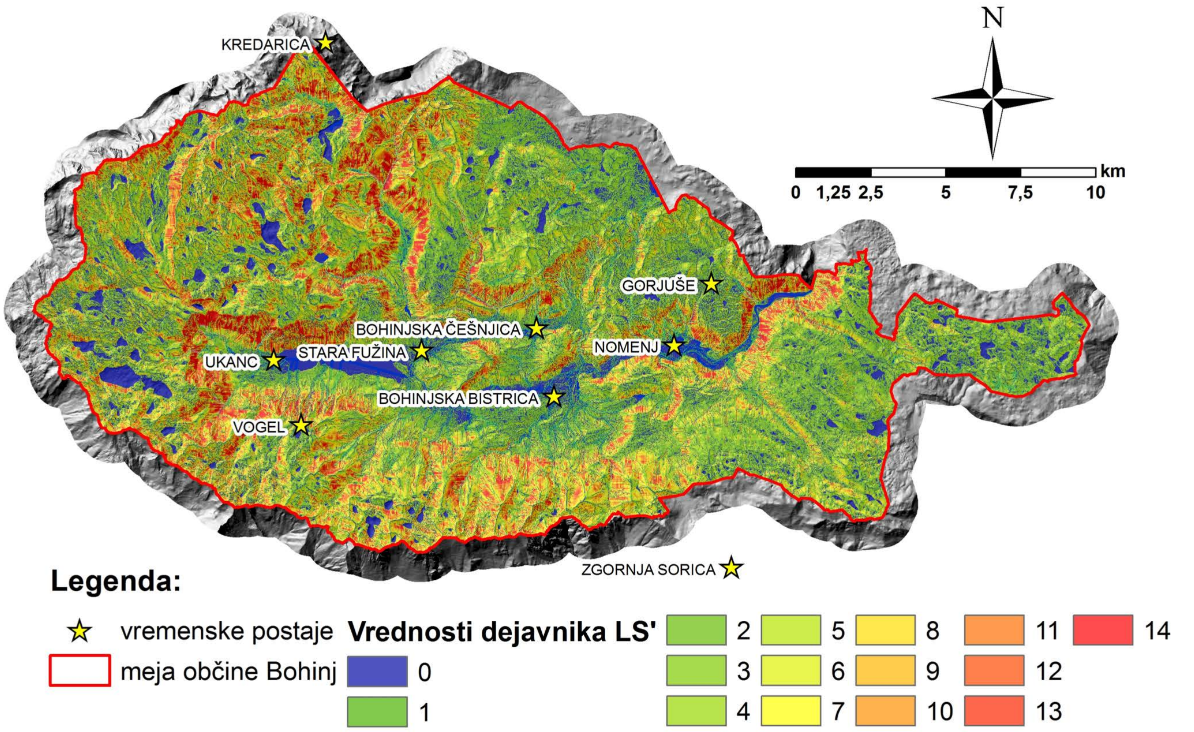

Sl. 11. Karta nominalnih vrednosti dejavnika naklona in dolžine pobočja (LS'), izračunanega na osnovi enačbe 3 za območje občine Bohinj (izvorni podatki digitalnega modela višin so imeli ločljivost 5 m).

Fig. 11. The distribution map of the slope steepness - slope length factor's nominal values (LS') for the Bohinj municipality, delinated with the red line. Factor is calculated based on the equation 3. The source data – layer's (digital elevation model) resolution was 5 m. The weather stations are presented with yellow stars.

Izračunana vrednost dejavnika *LS* / Calculated value of factor *LS*	A (ha)	A (%)	*LS'*
0-0,22	5338,983	16,0	0
0,22-2,46	2714,385	8,13	1
2,46-6,93	4807,315	14,4	2
6,93-11,4	3974,253	11,91	3
11,4-15,87	3170,405	9,5	4
15,87-20,34	2542,795	7,62	5
20,34-24,81	2094,31	6,28	6
24,81-29,28	1756,92	5,26	7
29,28-33,75	1476,745	4,43	8
33,75-38,23	1198,495	3,59	9
38,23-42,7	946,675	2,84	10
42,7-47,17	724,3325	2,17	11
47,17-51,64	536,9675	1,61	12
51,64-56,11	399,6725	1,2	13
56,11-8500,84	1690,355	5,07	14

Tabela 5. Porazdelitev razredov dejavnika naklona in dolžine pobočja (*LS*) s podanimi površinami, deleži razredov površin in normiranimi vrednostmi *LS'* (ta podatek je bil vhodni podatek za izračun navideznega modela RUSLE po enačbi 2).

Table 5. Distribution of the combined slope inclination and slope length factor (»Calculated value of factor *LS*«) in the area of Bohinj municipality. The area of a given class is presented in the column "A (ha)", the area proportion in the column "A (%)", and the combined slope inclination and slope langth factor nominal value that was used for the calculation of the RUSLE model based on the Equation 2 is given in the column "*LS'*".

Izračun jakosti erozije v strugah kot ga podaja tabela 1, je pokazal, da prevladuje četrti razred, kjer imajo segmenti naklone, večje od 4,5° in imajo obenem tudi vrednost po Shreve-ju (1966) manjšo od 100. Takih segmentov je slabih 55 %. Po deležu sledijo segmenti prvega razreda, torej tisti z nakloni, manjšimi od 4,5° in vrednost po Shreve -ju (1966) manjšo od 100. Delež teh segmentov je 37 %. Slabih pet odstotkov (4,9 %) predstavljajo segmenti tretjega razreda z nakloni manjšimi od 4,5° in vrednostjo po Shreve -ju (1966) večjo od 100. Najmanj (3,1 %) je segmentov drugega razreda, ki imajo naklone večje od 4,5° in vrednost po Shreve -ju (1966) večjo od 100.

Izračun posameznih modelov erozivnosti in združitev v skupni model erozivnosti

Vse do sedaj predstavljene spremenljivke (*K'*, *C'*, *P'*, *R'* in *LS'*), ki predstavljajo nominalne vrednosti izvornih spremenljivk, so bile uporabljene za izdelavo navideznega modela RUSLE. Vrednosti modela, ki so bile izračunane na osnovi enačbe 2 in so imele razpon od 0 do 5040, so bile razdeljene na pet razredov stopnje erozivnosti na podlagi klasifikacijske metode Natural Breaks (Jenks, 1967). Stopnja erozije je bila razvrščena v pet razredov, kjer številke predstavljajo vrednosti navideznega modela RUSLE in pripisano besedilo opis razreda stopnje erozivnosti: 0 = *zanemarljiva stopnja*; 1-273 = *majhna stopnja*; 274-735 = *srednja stopnja*; 736-1650 = *velika stopnja*; 1651-5040 = *zelo velika stopnja*). Slika 12 prikazuje model stopnje površinske erozivnosti po opisani metodi.

Rezultat izračune stopnje erozije v strugah je dal razpone vrednosti med 0,6 in 22,358, kjer večje vrednosti predstavljajo večjo stopnjo erozije. Z namenom zagotovitve normalne porazdelitve vrednosti so bile le-te logaritmirane. Nove vrednosti pa so bile razvrščene v 16 razredov z razponom ene četrtine standardnega odklona (SD) (sl. 13), nato pa je bilo vsakemu segmentu določeno vplivno območje desetih metrov na vsako stran. Na koncu je bila stopnja erozije v strugah razvrščena v štiri razrede: 1-3 = *majhna stopnja*; 4-6 = *srednja stopnja*; 7-10 = *velika stopnja*; 11-16 = *zelo velika stopnja*). Privzeto je bilo dejstvo, da v strugah ni zanemarljive erozije, saj je ta vedno prisotna.

Oba modela erozivnosti - navidezni model RUSLE, ki podaja ploskovno erozivnost in model stopnje erozije v strugah - sta bila združena v končni model erozivnosti po principu privzetja (naj)večje vrednosti stopnje erozije, torej maksimuma obeh modelov. Skupni model stopnje erozivnosti na območju občine Bohinj z ločljivostjo 5 × 5 m tako predstavlja največjo stopnjo erozivnosti za posamezno osnovno celico. Slika 14 prikazuje združen model, tabela 6 pa podaja porazdelitev razredov (stopenj) erozivnosti na območju občine Bohinj po površini in deležih površine. Vrednosti v modelu pomenijo sledeče stopnje erozije: 1 – Zanemarljiva; 2 – Majhna; 3 – Srednja; 4 – Velika; 5 – Zelo velika.

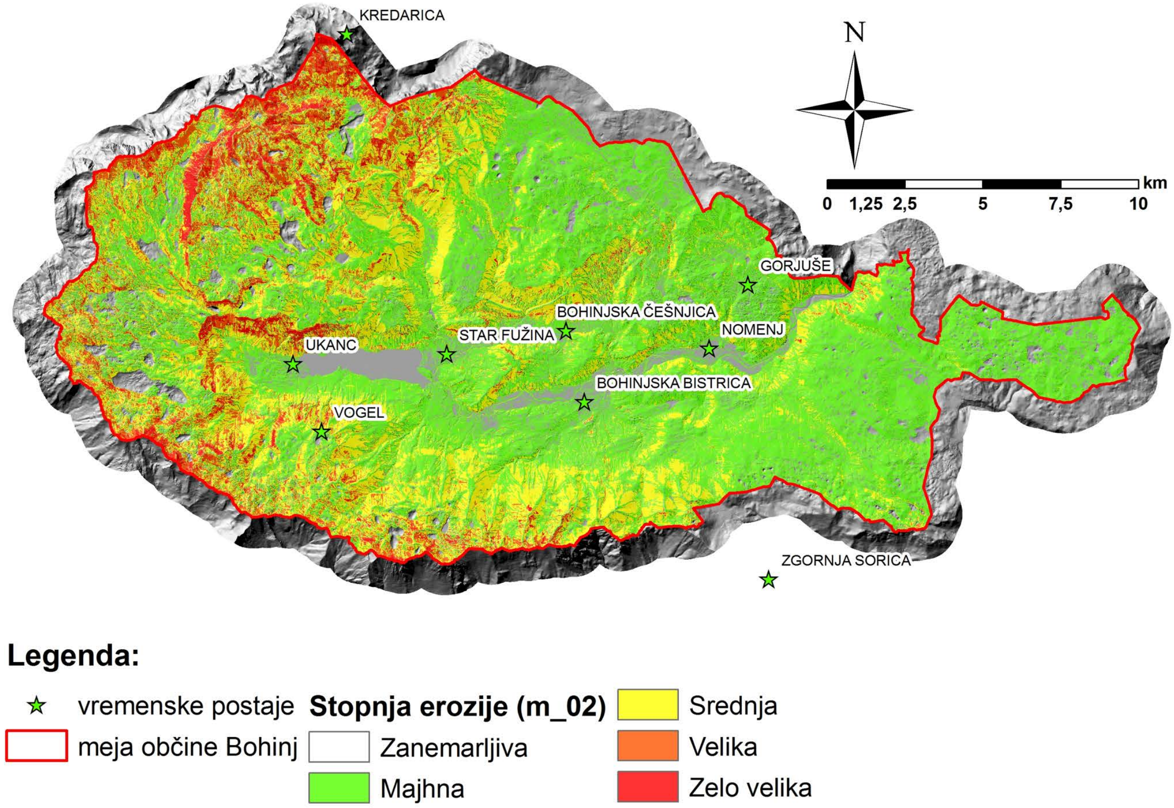

Sl. 12. Model stopnje površinske erozivnosti (model št. 2) na območju občine Bohinj, izdelan na osnovi metode RUSLE, ki pa je v kateri pa so bile namesto dejanskih vrednosti spremenljivk uporabljene njihove nominalne vrednosti.

Fig. 12. The surface erosion model ("Stopnja erozije") (model no. 2) for the Bohinj municipality, calculated based on the RUSLE method, but using nominational values of the input factors. The municipality is delinated with the red line. The weather stations are presented with green stars.

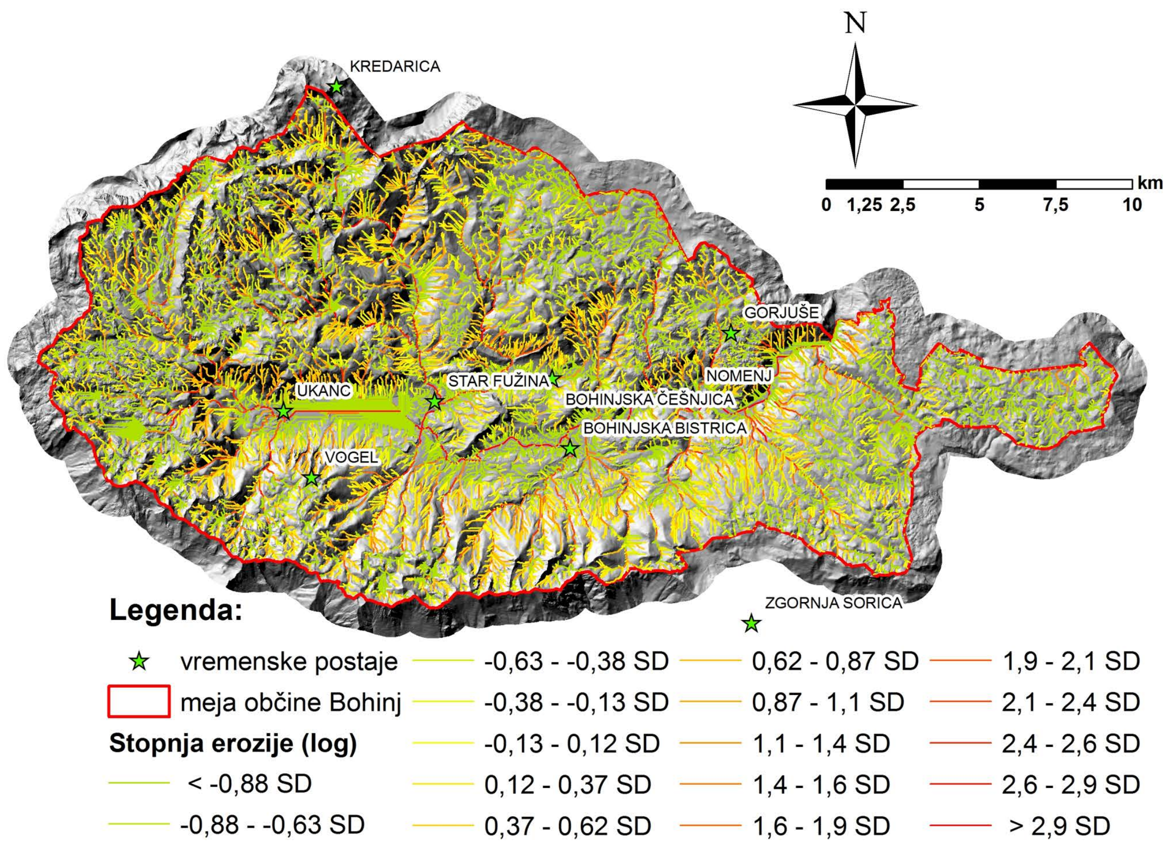

Sl. 13. Stopnja erozivnosti v strugah na območju občine Bohinj, razdeljena v razrede po četrtine standardnega odklona (SD).

Fig. 13. The model of the channel erosion level ("Stopnja erozije (log)") for the Bohinj municipality, divided into ¼ of the standard deviation values (SD). The municipality is delinated with the red line. The weather stations are presented with green stars.

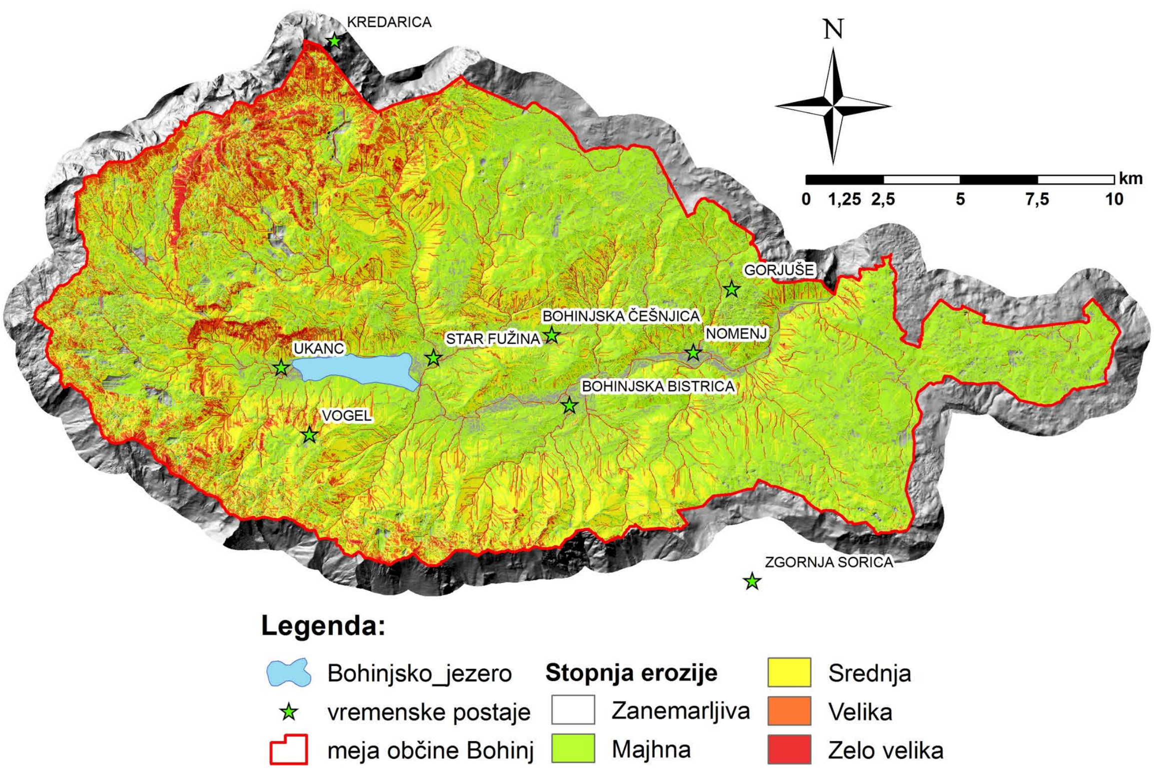

Sl. 14. Združen model stopnje erozivnosti na območju občine Bohinj (izvorni podatek ima ločljivost 5×5 m).

Fig. 14. Combined erosion model levels ("Stopnja erozije") for the Bohinj municipality. The municipality is delinated with the red line and the lake is with a blue area. The erosion levels are as follows: "Zanemarljiva" – Negligible; "Majhna" – Moderate; "Srednja" – Medium; "Velika" – Large; "Zelo velika" – Very large. The source data – layer's resolution is 5×5 m.

Tabela 6. Porazdelitev razredov (stopenj) erozivnosti na območju občine Bohinj kot jih določa model, prikazan na sliki 14.

Table 6. Distribution of the erosion level classes ("Erosion class") in the area of Bohinj municipality, as are presented in the Fig. 14. The number of input classes (based on the values of the model) for each erosion level class is given in the column "No. of classes", area of a given class is presented in the column "A (ha)", and the area proportion in the column "A (%)".

#	Razred (stopnja) erozije/ Erosion class	Št. razredov/ No. of classes	A (ha)	A (%)
1	Zanemarljiva / Negligible	0 – 1	3995,8	12
2	Majhna / Low	1 – 273	16306,5	48,9
3	Srednja / Medium	274 – 735	8641,2	25,9
4	Velika / High	736 – 1650	3230,4	9,7
5	Zelo velika / Very high	1651 – 5040	1204,1	3,6

Dobljeni model predstavlja zgolj teoretično napoved, saj na podlagi izračunov prikazuje območja, kjer je verjetnost erozivnosti večja, ne podaja pa kvantitativnih informacij o natančnosti modela in informacije o zanesljivosti napovedi stopenj erozije. Posledično je njegova teža predvsem informativnega značaja. Z vidika kakovostnega ovrednotenja količinskih vrednosti, je model pomanjkljiv in ga je zato treba ovrednotiti. Ena od možnosti je preverjanje erodiranih količin na terenu ter njihova primerjava z vrednostmi vhodnih spremenljivk. Možna metoda validacije modela je njegova primerjava s podatki, pridobljenimi s terenskim kartiranjem erozijskih območij, ki je bilo izvedeno v okviru iste raziskave.

Za predstavljen primer je bila izbrana primerjava s podatki terenskega kartiranja z metodo prekrivanja obeh modelov in z navzkrižno primerjavo ujemanja vrednosti stopenj erozije (tab. 7). Erozijske stopnje na karti, izdelani na podlagi terenskega kartiranja, se nekoliko razlikujejo od vrednosti izračunanega modela in vsebujejo sledeče razrede: A – Območja antropogene erozije; B – Območja erozijskih žarišč; C – Melišča; Č – Potencialna erozijska območja (nizka stopnja); D – Potencialna erozijska območja (srednja stopnja); E – Potencialna erozijska območja (velika stopnja); F – Potencialna erozijska območja (zelo velika stopnja); G – Vršaji. Kombinacije posameznih razredov (A – 4 & 5, B – 4 & 5, C – 4 & 5, Č – 2, D – 3, E – 4, F – 5, G – 2 & 3) predstavljajo razrede iz obeh izdelkov, ki predstavljajo identične stopnje erozije. Preseki teh razredov torej kažejo na nivo zanesljivosti napovedi erozivnosti.

Iz rezultatov prekrivanja, ki so prikazani v odstotkih porazdelitve površin razredov kartiranih na terenu (A – G) znotraj posameznih razredov modela erozivnosti (1 – 5) (tab. 7), je razvidno, da je ujemanje zelo dobro pri presekih razredov Č in 2 (93,5 %), ki predstavljata majhno stopnjo erozivnosti ter D in 3 (67,2 %), ki predstavljata srednjo stopnjo erozivnosti. Pri presekih razredov E in 4 (57,4 %), ki predstavljata veliko stopnjo erozivnosti ter F in 5 (53,3 %), ki predstavljata zelo veliko stopnjo erozivnosti, je ujemanje nekoliko slabše. Pri razredih D, E in F je opazen zamik stopnje erozivnosti proti manjši stopnji, kar bi lahko kazalo na nekoliko precenjeno razvrstitev območij glede na izračunano erozivnost v teoretičnem modelu. Območja antropogene erozije (A) se najbolje ujemajo z območji srednje stopnje erozivnosti v teoretičnem modelu, kar je do določene mere pričakovano glede na izogibanje človeških posegov na strmejših območjih in v strugah. Območja erozijskih žarišč (B) in območja melišč (C) se podobno ujemajo z območji zgornjih treh razredov stopnje erozivnosti v teoretičnem modelu, predvsem z razredom velike stopnje erozivnosti. To kaže na dobro napoved teoretičnega modela, ki pa bi ga bilo treba še izpopolniti, da bi se le-ta v največjih dveh razredih bolje ujemala s stanjem na terenu. Zelo dobro pokrivanje območij vršajev (G) s spodnjimi tremi razredi stopnje erozivnosti v teoretičnem modelu pa bi bilo možno interpretirati na dva načina. Lahko so vršaji obravnavani kot območja sedimentacije in dejanskega zmanjševanja erozivnosti, pri čemer je teoretični model dobro napovedal taka območja z nizko stopnjo erozivnosti. Če pa so vršaji obravnavani kot območja aktivne erozije, je teoretičen model zatajil in bi ga bilo treba v prihodnje z vidika teh erozijskih procesov temeljito dopolniti in nadgraditi.

Zaključki

Za območje občine Bohinj je bil izdelan kvalitativen teoretičen model erozivnosti, ki ne podaja frekvence ali količine erodiranega materiala, temveč zgolj določa območja z večjo stopnjo (oz. verjetnostjo) erozivnosti. Prednost predstavljenega modela je, da poleg splošno uporabljenega modela erozivnosti RUSLE, ki je usmerjen v izračun stopnje ploskovne erozivnosti, upošteva tudi stopnjo erozivnosti v strugah hribovitih (goratih) in zakraselih območij. Glavna pomanjkljivost predstavljenega modela je seveda njegova nezmožnost podajanja kvantitativne ocene, kot jo lahko ob kvalitetnih vhodnih podatkih podaja model RUSLE. Model pokaže območja večje erozivnosti na informativnem nivoju, zato je za integracijo v prostorske občinske načrte nujna terenska validacija vrednosti in ocena primernosti modela. V tem prispevku izvedena validacija je pokazala, da je teoretičen model dobro napovedal stopnje

Tabela 7. Porazdelitev deležev površin razredov (stopenj) erozivnosti kot so bili določeni na podlagi kartiranja (Erozija K; vrednosti prve vrstice) glede na razrede v tem prispevku predstavljenega modela (Erozija T; vrednosti prvega stolpca) za območje občine Bohinj. Opisi vrednosti stopenj "Erozija T" so podani v Tab. 6, opisi vrednosti stopenj "Erozija K" pa so: A – Območja antropogene erozije; B – Območja erozijskih žarišč; C – Melišča; Č – Potencialna erozijska območja (nizka stopnja); D – Potencialna erozijska območja (srednja stopnja); E – Potencialna erozijska območja (velika stopnja); F – Potencialna erozijska območja (zelo velika stopnja); G – Vršaji. Vse vrednosti so podane v odstotkih (deležih). Vrednosti, podane z odebeljenim besedilom, predstavljajo signifikantne vrednosti, tiste podane s poševnim besedilom pa mejno signifikantne vrednosti.

Table 7. Distribution of the area proportion of erosion level classes as defined by the field mapping approach ("Erosion K"; values in the first row) within the classes of the model developed based on the method that is presented in this paper ("Erosion T"; values in the first column) for the area of Bohinj municipality. Description for the erosion levels values of the model "Erosion T" are given in the Tab. 6, while the descriptions for the erosion levels values of the mapping approach "Erozija K" are: A – Areas of anthropogene erosion; B – Areas of erosion sources; C – Scree deposits; Č – Potential erosion area (Low); D – Potential erosion area (Medium); E – Potential erosion area (High); F – Potential erosion area (Very high); G – Alluvial/deposition fan. All values are given in percentage. Values, given in bold text represent significant values, and those represented with italic text represent marginally significant values.

	Erozija K / Erosion K (%)							
Erozija T / Erosion T	1	2	3	4	5	6	7	8
1	7,9	3,3	6,5	3,6	2,2	1,2	1,6	*26,7*
2	20,6	5,2	2,5	**93,5**	*28,9*	3,8	0,4	**41,5**
3	**45,3**	*31,1*	*24*	2,5	**67,2**	*36,3*	7,4	16,4
4	*21,3*	**38**	**44**	0,4	1,6	**57,4**	*37,3*	9,9
5	4,8	*22,4*	*23*	0,02	0,1	1,4	**53,3**	5,5
Vsota / SUM	100	100	100	100	100	100	100	100

erozivnosti zgolj za nekatere erozijske procese, za izboljšanje napovedi drugih erozijskih procesov pa bi bilo treba model izboljšati.

Nedvomno bi kvaliteto modela dodatno izboljšala informacija o infiltracijski sposobnosti kamnin na obravnavanem območju, zato je v prihodnje smiselno pridobiti in vključiti tudi ta podatek. Koristen bi tudi bil podatek o varovalnih ukrepih s strani človeka (dejavnik P v modelu RUSLE), vrsto, gostoto in kakovost vegetacije pa bi lahko izboljšala z vključitev vegetacijskega indeksa (NVDI), pridobljenega iz satelitskih podob.

Zahvale

Avtorja se želita zahvaliti občini Bohinj za delno financiranje raziskave. Zahvala gre tudi ARSO in MKGP za omogočanje javnega dostopa do prostorskih podatkov.

Literatura

Adediji, A., Tukur, A.M. & Adepoju, K.A. 2010: Assessment of Revised Universal Soil Loss Equation (RUSLE) in Katsina Area, Katsina State of Nigeria using Remote Sensing (RS) and Geographic Information System (GIS). Iranica Journal of Energy & Environment, 1/3: 255-264.

Arso 2016a: Portal meteo.si. Uradna vremenska napoved za Slovenijo Ministrstvo za okolje in prostor – Arhiv. Agencija Republike Slovenije za okolje, Ministrstvo za okolje in prostor. Internet: http://meteo.arso.gov.si/met/sl/app/webmet/ (15.10.2016).

Arso 2016b: Portal e-vode. Agencija Republike Slovenije za okolje, Ministrstvo za okolje in prostor. Internet: http://evode.arso.gov.si/ (15.10.2016).

Assouline, S. & Ben-Hur, A. 2006: Effects of rainfall intensity and slope gradient on the dynamics of interrill erosion during soil surface sealing. Catena, 66: 211–220.

Budkovič, T. 1978: Stratigrafija Bohinjske doline = The stratigraphic sequence of the Bohinj Valley. Geologija, 21/2: 239-244.

Buser, S. 1986: Osnovna geološka karta SFRJ 1 : 100.000, list Tolmin in Videm (Udine) (Basic geological map of Yugoslavia 1:100,000, sheet Tolmin and Udine). Zvezni geološki zavod, Beograd.

Chaplot, V.A.M. & le Bissonnais, Y. 2003: Runoff features for interrill erosion at different rainfall intensities, slope lengths, and gradients in an agricultural loessial hillslope. Soil Sci. Soc. Am. J., 67: 844–851.

Chen, H., Oguchi, T. & Wu P. 2017: Assessment for soil loss by using a scheme of alterative sub--models based on the RUSLE in a Karst Basin of Southwest China. Journal of Integrative Agriculture, 16/2: 377-388, doi:10.1016/S2095-3119(16)61507-1.

Ciglič, R., Hrvatin, M., Komac, B. & Perko, D. 2012: Karst as a criterion for defining areas less suitable for agriculture = Kras kot kazalnik za določanje manj primernih območij za kmetijstvo. Acta geographica Slovenica, 52/1: 61-98, doi:10.3986/AGS52103.

Dabney, S.M., Yoder, D.C. & Ferruzzi, G.G. 2014: Forage Harvest Representation in RUSLE2. Agron. J., 106: 151–167, doi:10.2134/agronj2013.0059.

Dai, Q., Peng, X., Yang, Z. & Zhao, L. 2017: Runoff and erosion processes on bare slopes in the Karst Rocky Desertification Area. Catena, 152: 218-226, doi:10.1016/j.catena.2017.01.013.

Desmet, P.J.J. & Govers, G. 1996: A GIS procedure for automatically calculating the USLE LS factor on topographically complex landscape units. Journal of soil and water conservation, J. Soil Water Conserv., 51: 427-433.

Ebisemiju, F.S. 1988: Gully morphometric controls in a laterite terrain, Guyana. Geo-Eco-Trop, 12/1-4: 41-59.

Ebisemiju, F.S. 1989: A Geomorphological Approach to Land Use Planning and Soil Conservatio. Journal of Environmental Management, 28: 327-336.

Ebisemiju, F.S. & Ado, E. 1989: A morphometric approach to gully analysis. Z.Geomorph. N.F. 33/3: 307-322.

Fao 1988, 1990. FAO-Unesco-ISRIC Soil Map of the World, Revised Legend (with corrections in the 1990 version). World Resources Report 60. FAO, Rim.

Feng, T., Chen, H., Polyakov, V.O., Wanga, K., Zhange, X. & Zhang, W. 2016: Soil erosion rates in two karst peak-cluster depression basins of northwest Guangxi, China: Comparison of the RUSLE model with ^{137}Cs measurements. Geomorphology, 253: 217-224, doi:10.1016/j.geomorph.2015.10.013.

Fernandez, C., Wu, J.Q., McCool, D.K. & Stöckle, C.O. 2003: Estimating water erosion and sediment yield with GIS, RUSLE, and SEDD. Journal of Soil and Water Conservation, 58/3: 128-136.

Floor, J. A. 2016: Soil erosion and conservation - part1. Internet: www.seafriends.org.nz/enviro/soil/erosion.htm (15.10.2016.)

Foster, G.R., Yoder, D.C., McCool, D.K., Weesies, G.A., Toy, T.J. & Wagner, L.E. 2000: Improvements in science in RUSLE2. Paper No. 00-2147. ASAE.

Foster, G.R., Yoder, D.C., Weesies, G.A. & Toy, T.J. 2001: The Design Philosophy Behind RUSLE2: Evolution of an Empirical Model. In: Ascough, J.C. II & Flanagan, D.C. (eds.): Soil Erosion Research for the 21st Century, Proc. Int. Symp. (3-5 January 2001, Honolulu, HI, USA), 95-98.

Fu, B.J., Zhao, W.W., Chen, L.D., Zhang, Q.J., Lü, Y.H., Gulinck, H. & Poesen, J. 2005: Assessment of soil erosion at large watershed scale using RUSLE and GIS: A case study in the Loess Plateau of China. Land Degrad. Dev., 16: 73-85.

Gelagay, H.S. & Minale, A.S. 2016: Soil loss estimation using GIS and Remote sensing techniques: A case of Koga watershed, Northwestern Ethiopia. International Soil and Water Conservation Research, 4/2: 126–136.

Gerk 2016: Podatkovni portal MKGP. Internert: http://rkg.gov.si/GERK/ (15.10.2016).

Grimšičar, A. 1961: O geoloških razmerah med Bohinjem in Triglavskimi jezeri = Geologic relationship berween Bohinj and Triglav lakes area. Geologija, 7: 283-285.

He, C., Xiong, K., Li, X. & Cheng, X. 1998: Karst geomorphology and its agricultural implications in Guizhou, China. Fourth International Conference On Geomorphology – Bologna, Italy 1997. Supplements of Geografia Fisica e Dinamica Quaternaria, Volume III. Torino.

Hrvatin, M., Komac, B., Perko, D. & Zorn, M., 2006: Slovenia. In: Soil erosion in Europe. Wiley, Chichester, 297-310.

Jenks, G.F. 1967: The Data Model Concept in Statistical Mapping. International Yearbook of Cartography, 7: 186–190.

Jurkovšek, B. 1987: Osnovna geološka karta SFRJ 1 : 100.000, list Beljak in Ponteba (Basic geological map of Yugoslavia 1:100,000, sheet Villach and Pontebba). Zvezni geološki zavod, Beograd.

Kassam, A.H., van Velthuizen, H.T., Mitchell, AJ.B., Fischer, G.W. & Shah, M.M. 1992: Agro-ecological land resources assessment for agricultural development planning. A case study of Kenya. Resources data base and land productivity. Technical Annex 2. Soil Erosion and Productivity. Land and Water Development Division, Food and Agriculture Organization of the United Nations and International Institute for Applied Systems Analysis, 59 p.

Kheir, R.B, Abdallah, C. & Khawlie, M. 2008: Assessing soil erosion in Mediterranean karst landscapes of Lebanon using remote sensing and GIS. Engineering Geology, 99/3-4: 239-254, doi:10.1016/j.geomorph.2015.10.013

Komac, B. & Zorn, M. 2005: Soil erosion on agricultural land in Slovenia - measurements of rill erosion in the Besnica valley. Acta geographica Slovenica, 45/1: 53-86.

Komac, B. & Zorn, M. 2007: Pobočni procesi in človek = Slope processes and man. ZRC Publishing, Ljubljana:217 p.

Komac, B., Zorn, M. & Gabrovec, M. 2007: Influence of land use changes on erosion in Slovene Alps. In: Man in the landscape across frontiers: landscape and land use change in Central European border regions: proceedings. Charles University, Prague: 221-234.

Lazarević, R. 1968: Erozija u slivu Gvozdačke reke – prilog metodici za izradu karte erozije = Erosion in the Gvozdačka reka river basin – supplement to the instructions for erosion map elaboration. Glasnik Srpskog geografskog društva, 49/2: 75-98.

Lazarević, R. 1985: Novi postupak za odredjivanje koeficijenata erozije (Z) = The new method for erosion coefficient determination – Z. Erozija – stručno-informativni bilten, 13: 54-61.

Lim, K. J., Sagong, M., Engel, B.A., Tang, Z., Choi, J. & Kim, K. 2005: GIS-based sediment assessment tool. Catena, 64: 61-80.

Liu, B.Y., Nearing, M.A., Shi, P.J. & Jia, Z.W. 2001: Slope length effects on soil loss for steep slopes. In: Scott, D.E., Mohtar, R.H. & Steinhard, G.C. (eds.): Sustaining the Global Farm. Selected papers from the 10th Interntional Soil Conservation Organisation Meeting (May 24-29, 1999), Purdue University, USA: 784-788.

López-Vicente, M., Navas, A. & Machín, J. 2008: Identifying erosive periods by using RUSLE factors in mountain fields of the Central Spanish Pyrenees. Hydrol. Earth Syst. Sci., 12: 523-535.

Lovrenčak, F. 1987: Zgornja gozdna meja v Julijskih Alpah in na visokih kraških planotah Slovenije = The upper forest line in the Julian Alps and in high Karst plateaus of Slovenia. Geografski zbornik, 26: 7-62.

Lown, J.B., Lyon, J.P. & Yoder, D.C. 2000: A Scientific Modeling Architecture to Simultaneously Meet Needs of Scientists, Programmers, Data Managers, and End-Users. Paper No. 003051. ASAE.

Maček, J. 2006: Analiza erozivnosti padavin na območju Kamniško–Savinjskih Alp. Diplomska naloga. UL, FGG, Vodarstvo in komunalno inženirstvo, Ljubljana:79 p.

Mikoš, M., Fazarinc, R. & Ribičič, M. 2006: Sediment production and delivery from recent large landslides and earthquakeinduced rock falls in the Upper Soča River Valley, Slovenia. Engineering geology, 86/2-3: 198-210.

Mitasova, H., Hofierka, J., Zlocha, M. & Iverson, R. 1996: Modelling Topographic Potential for Erosion and Deposition using GIS. International Journal of Geographical Information Systems, 10/5: 629-641.

Oliveira, P.T.S., Rodrigues, D.B.B., Alves Sobrinho, T., Panachuki, E. & Wendland, E. 2013: Use of SRTM data to calculate the (R) USLE topographic factor. Acta Scientiarum. Technology, 15: 507-513, doi:10.4025/actascitechnol.v35i3.15792.

Panagos, P., Borrelli, P. & Meusburger, K. 2015a: Estimating the soil erosion cover management factor at the European scale. Land Use Policy, 48: 38–50.

Panagos, P., Borrelli, P., Meusburger, K., van der Zandenc, E. H., Poesend, J. & Alewellb, C. 2015b: Modelling the effect of support practices (P-factor) on the reduction of soil erosion by water at European scale. Environmental Science & Policy, 51: 23–34.

Pearce, F.J. 1987: Complexity of the landscape. In: Halbach, D., Runge, C.F., Larson, W.E. (eds.): Making soill and water conservation work: scientific and policy perspectives, Aukeney, Iowa, Soil Conservation Society of America.

Petan, S. 2010: Meritve in prostorsko modeliranje erozivnosti padavin kot parametra erozije tal. Doktorska disertacija. UL, FGG, Oddelek za okoljsko gradbeništvo, Ljubljana: 205 p.

Petan, S., Padežnik, M., Zorn, M., Šraj, M., Vidmar, A., Mikoš, M. & Brilly, M. 2008a: Measurements and modelling of rainfall interception and soil erosion processes on the Dragonja experimental river basin. In: Morell, M. (ed.): Balwois: abstracts, Conference on Water observation and information system for decision support, 27-31 May 2008 Ohrid, Republic of Macedonia. Gradežen fakultet Skopje: 371-372.

Petan, S., Rusjan, S., Vidmar, A. & Mikoš, M. 2010: The rainfall kinetic energy-intensity relationship for rainfall erosivity estimation in the Mediterranean part of Slovenia. Journal of Hydrology, 391/3-4: 314-321, doi:10.1016/j.jhydrol.2010.07.031.

Petan, S., Zorn, M. & Mikoš, M. 2008b: Measurements of interrill soil erosion under different land use in Slovene Istria. In: Abstracts of the contributions of the EGU General Assembly 2008: Vienna, Austria, 13-18 April 2008, Vol. 10: 1 p.

Petkovšek, G. 2002: Kvantifikacija in modeliranje erozije tal z aplikacijo na povodju Dragonje. Doktorska disertacija. UL, FGG, Oddelek za gradbeništvo, Ljubljana: 205 p.

Pintar, J., Mikoš, M. & Verbovšek, V. 1986: Elementi okolju prilagojenega urejanja vodotokov: alternativa utesnjevanju živih naravnih procesov v toge objekte = Elements of the water management – an alternative to narrowing of live natural processes in rigid objects. In: Simonović, S. (ed.): Drugi kongres o vodama Jugoslavije. Jugoslovensko društvo za odvodnjavanje I navodnjavanje; Beograd: 800-814.

Renard, K.G., Foster, G.R., Weesies, G.A., McCool, D.K. & Yoder, D.C. 1997: Predicting soil erosion by water: a guide to conservation planning with the revised universal soil loss equation (RUSLE). Washington, DC, USDA ARS. Agricul. Handbook 703: 384 p.

Shreve, R. L. 1966: Statistical Law of Stream Number. Journal of Geology, 74: 17-37.

Toy, T.J., Foster, G.R. & Renard, K.G. 2002: Soil Erosion: Processes, Prediction, Measurement, and Control. John Wiley & Sons: 338 p.

Wischmeier, W.H. & Smith, D.D. 1958: Rainfall energy and its relationship to soil loss. Trans Am. Geophys. Union, 39: 285-291.

Wischmeier, W.H. & Smith, D.D. 1965: Predicting rainfall erosion losses from cropland east of the Rocky Mountains. Washington, DC, USDA ARS. Agricul. Handbook, 282: 47 p.

Wischmeier, W.H. & Smith, D.D. 1978: Predicting rainfall erosion losses. Washington, DC, USDA ARS. Agricul. Handbook, 537: 57 p.

Zachar, D. 1982: Soil erosion. Developments in Soil Science 10. Elsevier Scientific, Amsterdam: 547 p.

Zhang, Z., Sheng, L., Yang, J., Chen, X.A., Kong, L. & Wagan, B. 2015: Effects of Land Use and Slope Gradient on Soil Erosion in a Red Soil Hilly Watershed of Southern China. Sustainability, 7: 14309-14325, doi:10.3390/su71014309.

Zhang, H., Yang, Q., Li, R., Liu, Q., Moore, D., He, P., Ritsema, C.J. & Geissen, V. 2013: Extension of a GIS procedure for calculating the RUSLE equation LS factor. Comput. Geosci. 52: 177–188, doi:10.1016/j.cageo.2012.09.027.

Zhang, H., Yao, Z., Yang, Q., Li, S., Baartman, J.E.M., Gai, L., Yao, M., Yang X., Ritsema, C.J. & Geissen, V. 2017: An integrated algorithm to evaluate flow direction and flow accumulation in flat regions of hydrologically corrected DEMs. Catena, 151: 174-181, doi:10.1016/j.catena.2016.12.009.

Zhao, X.N., Huang, J., Wu, P.T., & Gao, X.D. 2014: The dynamic effects of pastures and crop on runoff and sediments reduction at loess slopes under simulated rainfall conditions. Catena, 119: 1–7.

Zingg, A.W. 1940: Degree and length ofland slope as it affects soil loss in runoff. AgricEng, 21: 59-64.

Zorn, M. 2008: Erozijski procesi v slovenski Istri = Erosion processes in Slovene Istria. ZRC Publishing, Ljubljana: 423 p.

Zorn, M. & Komac, B. 2009: Response of soil erosion to land use change with particular reference to the last 200 years (Julian Alps, Western Slovenia). Revista de geomorfologie, 11: 39-47.

Zorn, M., Miko, M., Petan, S. & Mikoš, M. 2007: Measurements of interrill erosion on flysch soil under different land use (SW Slovenia). In: Abstracts of the contributions of the EGU General Assembly 2007: Vienna, Austria, 15-20 April 2007, Vol. 9: 2 p.

Žabota, B. 2015: Ocenjevanje erozije prsti s pomočjo metode RUSLE. Geomix, 22/1: 52-56.

Internetni vir:

Internet 1: http://gis4geomorphology.com/ls-factor-in-rusle/ (15.10.2016)

GEOLOGIJA 60/2, 257-266, Ljubljana 2017

https://doi.org/10.5474/geologija.2017.018

REE-bearing minerals in Drava river sediments, Slovenia, and their potential origin

Minerali z redkimi zemljami v sedimentih reke Drave (Slovenija) ter njihov potencialni izvor

Aleš ŠOSTER[1], Janez ZAVAŠNIK[2], Mihael RAVNJAK[3] & Uroš HERLEC[1]

[1]University of Ljubljana, Faculty of Natural Sciences and Engineering, Department of Geology
Aškerčeva cesta 12, SI-1000 Ljubljana; e-mail: ales.soster@geo.ntf.uni-lj.si; uros.herlec@geo.ntf.uni-lj.si
[2]Jožef Stefan Institute, Center for Electron Microscopy and Microanalysis, Jamova cesta 39, SI-1000 Ljubljana; e-mail: janez.zavasnik@ijs.si
[3]Cesta na Roglo 21, SI-3214 Zreče; e-mail: mihael.ravnjak@gmail.com

Prejeto / Received 12. 10. 2017; Sprejeto / Accepted 6. 11. 2017; Objavljeno na spletu / Published online 22. 12. 2017

Key words: monazite, xenotime, microanalysis, REE, heavy minerals, Drava, Slovenija
Ključne besede: monacit, ksenotim, mikroanaliza, REE, težki minerali, Drava, Slovenia

Abstract

Monazite and xenotime are major ore minerals for rare earth elements (REE), Y, and actinides, a powerful tool for radiometric dating and indicators of the geological genesis of the parent rock. In this contribution, we present results of microanalysis of monazite and xenotime mineral grains found in heavy mineral sand fraction from Drava river. Investigated grains of monazite(-Ce) were found to be exhibiting varying concentrations of Th, indicating mixed hydrothermal (or greenschist-amphibolite grade) and igneous origin. Monazite was found to be isomorphically replaced by cheralite ($CaTh(PO_4)_2$) and subordinately by huttonite ($ThSiO_4$), forming monazite-cheralite and monazite-huttonite solid solution. Chemical composition and the degree of isomorphic replacement of monazite grains are indicating their source from rocks of Eclogite belt and Granatspitz massif in Tauern Window, Austria. On the other hand xenotime(-Y) shows consistent concentrations of Y while concentrations of associated heavy rare earth elements (HREE) vary, indicating the origin of mixed affinities.

Izvleček

Minerala monazit in ksenotim sta pomemben vir redkih zemelj, itrija in aktinidov. Lahko ju uporabimo tudi kot orodje za radiometrično datiranje (geokronologijo), ter kot indikator geneze matične kamnine. V prispevku predstavljamo rezultate mikroanalize zrn monacita in ksenotima zaznanih v frakciji težkih peskov reke Drave. Cerijev monacit ima spremenljive vsebnosti Th, kar kaže na njegov hidrotermalni izvor ali izvor iz metamorfnih (od faciesa zelenega skrilavca do amfibolitnega faciesa) in magmatskih kamnin. Rezultati mikroanalize monacita kažejo izomorfno nadomeščanje s ceralitom ($CaTh(PO_4)_2$) in v manjši meri s huttonitom ($ThSiO_4$), pri čemer tvorijo trdno raztopino. Kemijska sestava in stopnja izomorfnega nadomeščanja monacitnih zrn nakazujejo njihov izvor iz kamnin Eklogitnega pasu in masiva Granatspitz v Visokih Turah v Avstriji. V ksenotimu je najbolj zastopan element Y, ki ima v vseh zrnih enakomerne vsebnosti, medtem ko se vsebnosti težkih redkih zemelj (HREE) spreminjajo, kar kaže na izvor iz različnih geoloških okolij.

Introduction

Heavy mineral sand deposits or placers are waterborne deposits of minerals with high specific density, formed as a result of water flow dynamics, either by wave motion, long-term coastal currents or by unidirectional flow associated with rivers. The principal mechanism in the formation of heavy mineral deposits is a natural separation of low and high-density minerals in a manner where low-density minerals are removed by flowing medium thus concentrating high-density minerals (Robb, 2004). Placer deposits are known as a significant source of many industrially important minerals, i.e., diamond, gold, tantalite-columbite, cassiterite, rutile, ilmenite, uraninite, zircon and rare earth element (REE)-bearing minerals (Robb, 2004; Rao & Misra, 2009). Principal ore minerals mined for REE are monazite, bastnaesite, and xenotime (Voncken, 2016). Monazite is a phosphate mineral of light rare earth elements (LREE) with generalized formula $CePO_4$, which besides Ce contains variable proportions of La, Nd, and Pr. Based on predominant LREE incorporated in monazite a suffix is given to denote the most abundant auxiliary element (i.e., monazite(-Ce)) (Voncken, 2016). Monazite occurs as an accessory mineral in peraluminous granites, syenitic and granitic pegmatites, quartz veins, carbonatites, migmatites and paragneisses (Förster, 1998a; Breiter, 2016). Monazite is considered to be a major host of LREE and smaller fractions of Y, heavy rare earth elements (HREE), and actinides (Bea, 1996). Therefore it presents a powerful tool for monazite-based radiometric dating (Harrison et al., 1995; Zhu & O'nions, 1999; Schandl & Gorton, 2004; Grand'Homme et al., 2016). Xenotime, in contrast to monazite, beside Y contains also a significant amount of HREE, among which most commonly occurring are Dy, Yb, Er, and Gd while Tb, Ho, Tm, and Lu are occurring less often (Förster, 1998b; Švecová et al., 2016; Voncken 2016). Depending on its geological genetic environment, xenotime is considered to be a primary source of HREE and actinides and it is a common accessory mineral in many non-basic igneous rocks, most granitic rocks and granitic pegmatites where it accounts for significant fraction of Y and HREE of bulk rock composition (Bea, 1996; Förster, 1998b), while it is also present in migmatites and high-grade metamorphic rocks (Förster, 1998b). Minerals such as monazite and xenotime are considered to be of economic importance especially when enriched in actinides (i.e., U and Th) for their use in nuclear industry, however they may pose an environmental hazard due to increased natural radiation (Alam et al., 1999; Vassas et al., 2006; Rao & Misra, 2009). Regarding actinides, monazite is known to more often contain Th, while xenotime is more likely to contain U and also smaller amounts of Th (van Emden et al., 1997; Kim et al., 2009; Deer et al., 2013). This research aims to present the results of microanalysis performed on REE-bearing minerals from heavy mineral fraction of Drava river and to make an attempt to elucidate their potential provenance.

Geographical and geological background

Our case study area is situated near village Zlatoličje in NE Slovenia, along Drava river (Fig. 1a). River Drava has its source in Innichen (San Candido) in the Puster Valley of South Tyrol, Italy, and flows eastwards through East Tyrol and Carinthia regions in Austria into region Styria in Slovenia and further along Croatia-Hungary border, where it joins the Danube near the city of Osijek (Tockner et al., 2009). Along its path, it has a number of tributaries with their sources in Hohe Tauern, i.e., *Isel*, with its source beneath Grossvenediger (3674 m) joining Drava near Lienz and *Möll* with its source near Heiligenblutt below Großglockner (3798 m). Knowledge of drainage area and therefrom eroded rocks, of the

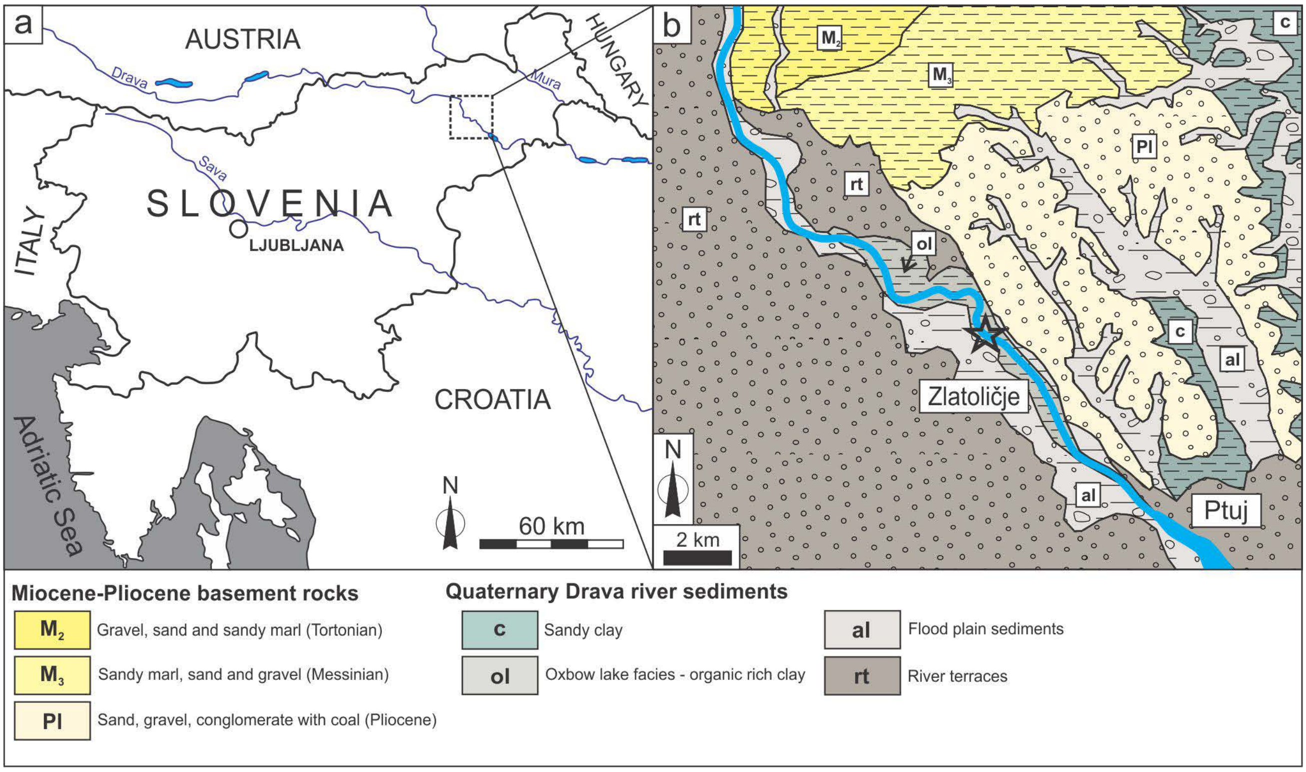

Fig. 1. Location of the study area (a) with detailed geological setting (b) (modified after Žnidarčič & Mioč, 1987).

river and its tributaries combined with in-detail chemical analyses of minerals, both from parent rock and sediments, is crucial for determining the provenance of the grains downstream. The region of Hohe Tauern, in detail discussed by Schimd et al. (2013) and Scharf et al. (2013), is considered to be the source of gold found in fluvial sediments of river Drava (Bermanec et al., 2014), therefore broader area of Hohe Tauern could also be considered as a source of minerals in heavy mineral sands.

In the area of our case study, fluvial sediments of river Drava are deposited onto Cenozoic basement mainly represented by Upper Miocene (Tortonian to Messinian) marlstones and sandstones paleogeographically a part of Central Paratethys and Pliocene sand, gravel and conglomerate with intermediate coal beds deposited in the Lake Pannon realm (Fig. 1b; Pleničar et al., 2009). The Quaternary period is represented by sediments of Drava reflecting changes in flow dynamics and migrating river channels, thus most common sediments are granulometrically heterogeneous gravel and sand of the river channel, floodplains sediments and organic clay of oxbow lake facies (Fig. 1b; Mioč & Žnidarčič, 1989; Pleničar et al., 2009).

Materials and methods

Field sampling

Sampling was conducted in the river bank gravel, in the river channel and in the distal parts of river bars to ensure a high yield of the heavy mineral fraction. Three bulk samples of initially 2 kg each, were washed to remove any plant detritus and clay particles. Bulk samples underwent manual gravitational separation, which was achieved by panning to obtain a relatively pure heavy mineral concentrate. Particles larger than 5 mm were removed manually. Heavy mineral concentrate was further processed by heavy liquid separation in which we used lithium meta-tungstate heavy fluid (LMT) with density [σ = 2.95 g/cm^3] to further remove light mineral grains. The remaining mineral grains were, for the needs of optical and electron microscopy, vacuum-cast into two component epoxy resin. Grinding and polishing were performed stepwise using silicon carbide 240 and 1200 grit for grinding and 9 μm, 3 μm and 1 μm diamond paste for polishing to high gloss finish.

X-ray diffraction analysis

Identification and quantification of major minerals forming bulk fluvial sediment and heavy mineral sands were performed using X-ray powder diffraction analysis (XRD, PW 3830/40, PANalytical B.V., Almelo, the Netherlands). Powdered samples were inserted into a holder with divergence slit for incident X-rays at 0.04° and 0.2 mm wide slit for diffraction path. Samples were analyzed in the angular span between 3° - 70° 2θ with step 3°2θ /60 s. Source of X-rays was copper anode with the generator set at 30 mA and 40 kV, producing radiation with λ=1.5406 Å. Quantification of entities was achieved using Rietveld refinement (goodness of fit: 2.085, R-expected: 13.95, R-profile: 19.97), individual FWHM function and Pseudo Voigt function. Identification of mineral structure was performed using ICSD Database FIZ Karlsruhe (Pan ICSD 2.x).

Optical microscopy and scanning electron microscopy

Identification of minerals, observation of morphology and grain size were performed by Zeiss Imager Z1.m polarizing optical microscope, additionally equipped with in-lens calibrated digital camera for accurate scaling. Scanning electron microscopy (SEM) was performed by using JEOL JSM-5800 with thermionic source under high vacuum (5x10^{-6} bar). Preliminary mineral identification was made using backscattered electron imaging (BEI), where relative contrast in the image is directly related to mean atomic number of the investigated sample. Semi-quantitative chemical analysis of the mineral grains was performed using Oxford Instruments energy-dispersive X-ray spectrometer (EDS, mod. 6841, Oxford Instruments Ltd.). The operating conditions for EDS analyses were 20 kV, 10 mm working distance and 0° tilt. Beam current was adjusted to yield a dead time of 20-30 %, while the live time was set at 60s. Data reduction was performed using atomic number-absorption-fluorescence matrix correction (ZAF). Prior to SEM observation samples were coated with few nm of amorphous carbon to improve the conductivity of the sample and prevent charging.

Results

Bulk fluvial sediment is uniformly composed of quartz, calcite, dolomite, chlorite, mica, plagioclase and traces of kaolinite and amphibole group minerals (Fig. 2a) as determined by XRD analysis. Bulk sediment samples with an initial

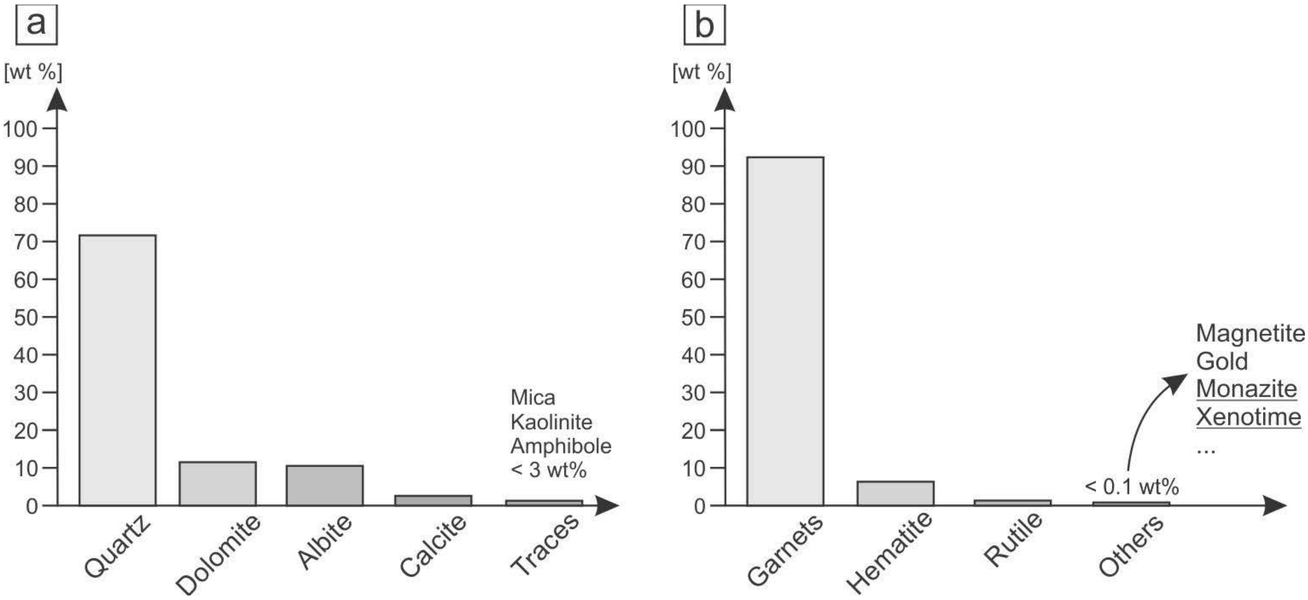

Fig. 2. Column diagram of the mineral composition of (a) bulk fluvial sediment and (b) heavy mineral fraction.

mass of 2 kg each, yielded 46.2 – 79.7 g of the heavy mineral fraction after final treatment with LMT. Heavy mineral sands are present in the fraction between 0.06 and 0.5 mm corresponding with very fine sand to coarse sand. Prevailing minerals in the heavy mineral fraction are garnets accounting for 92 wt%, followed by hematite (6.7 wt%) and rutile (0.7 wt%) (Fig. 2b). Besides aforementioned minerals also diopside, epidote, ilmenite, hematite, magnetite, gold, pyrite, sphalerite, barite, chalcopyrite, molybdenite, monazite and xenotime were identified using optical or scanning electron microscopy, which overall account for less than 0.1 wt% of heavy mineral fraction, which is below detection limit of XRD analysis (Fig. 2b).

Table 1. Relative concentrations of major oxides in monazite acquired by semi-quantitative EDS analysis given in wt%. Values marked by »*« represent formulae for 4 oxygen per formula unit (apfu).

	P_2O_5	La_2O_3	Ce_2O_3	Nd_2O_3	ThO_2	P*	La*	Ce*	Nd*	Th*
Mnz-1	27.44	23.56	35.16	10.07	3.76	0.953	0.356	0.527	0.147	0.035
Mnz-2	29.02	18.07	34.80	9.47	6.82	1.034	0.280	0.536	0	0.065
Mnz-3	30.36	19.08	33.52	9.34	6.44	1.016	0.278	0.485	0.132	0.058
Mnz-4	29.81	17.79	35.04	12.66	3.42	0.991	0.257	0.503	0.177	0.031
Mnz-5	32.05	18.01	33.42	11.72	3.92	1.032	0.252	0.465	0.159	0.034
Mnz-6	29.78	18.47	35.68	11.17	3.95	0.992	0.268	0.514	0.157	0.035
Mnz-7	29.04	19.50	34.96	11.51	3.71	0.977	0.285	0.508	0.163	0.034
Mnz-8	31.81	16.80	31.49	11.27	6.48	1.024	0.235	0.438	0.153	0.056
Mnz-9	28.32	17.61	33.29	11.50	7.82	0.966	0.262	0.491	0.165	0.072
Mnz-10	31.93	17.48	29.77	11.23	8.20	1.031	0.246	0.415	0.153	0.071
Mnz-11	30.27	18.62	33.95	10.82	4.47	0.997	0.267	0.483	0.150	0.040
Mnz-12	27.24	21.72	39.79	10.67	0	0.943	0.327	0.595	0.156	0
Mnz-13	29.24	18.31	34.16	13.09	4.32	0.983	0.268	0.496	0.186	0.039
Mnz-14	29.13	17.89	35.75	9.86	5.77	0.979	0.262	0.537	0.140	0.052
Mnz-15	28.46	19.36	36.54	11.72	3.12	0.968	0.287	0.496	0.168	0.029
Mnz-16	31.00	18.76	35.10	12.02	2.31	1.013	0.267	0.540	0.166	0.020
Mnz-17	29.26	17.02	37.33	12.29	2.77	0.980	0.248	0.488	0.173	0.025
Mnz-18	28.5	19.06	33.37	11.68	5.49	0.966	0.281	0.521	0.167	0.050
Mnz-19	28.92	18.68	35.29	10.94	4.95	0.968	0.278	0.522	0.158	0.046
Mnz-20	26.53	19.44	34.50	11.35	6.46	0.929	0.296	0.516	0.167	0.061
Mnz-21	31.26	14.42	36.59	12.53	4.43	1.020	0.205	0.452	0.172	0.039

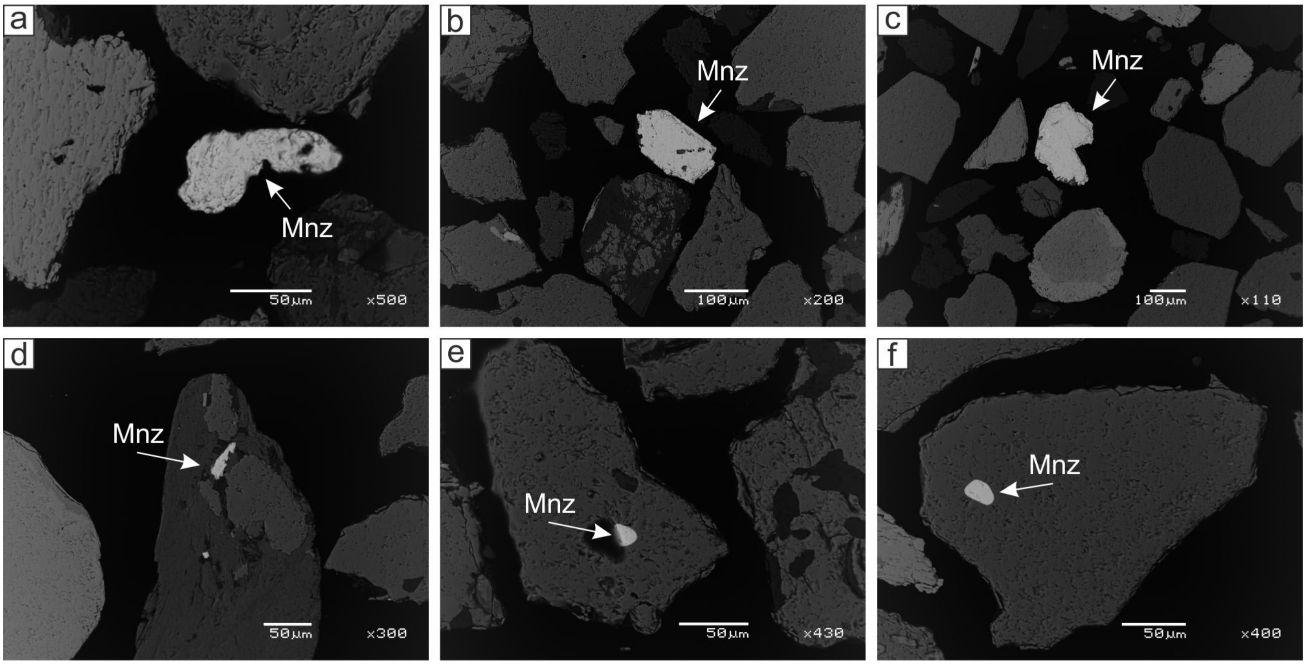

Fig. 3. SEM (BEI) images of monazite mineral grains (Mnz) in polished section of the heavy mineral fraction from Drava river. Monazite is occurring as individual liberated grains (a-c) or as inclusions in other minerals, i.e., quartz and garnet (d-f).

Monazite

Monazite is present as individual liberated grains or included within other mineral grains (i. e. epidote, garnet (var. Andradite) or diopside) measuring from 5 to 200 µm. Individual grains of monazite are elongated to complex and angular to subrounded (Figs. 3a-c), while monazites included within other minerals are predominantly equant and circular, characteristic of mineral inclusions (Figs. 3d-f). Semi-quantitative EDS analysis revealed that monazite contains Ce_2O_3 (28.49-33.97 wt%), La_2O_3 (12.29-20.09 wt%) and Nd_2O_3 (8.12-10.85 wt%) and smaller amounts of ThO_2 (0-7.20 wt%). Major oxide composition of investigated monazites is given in Table 1. Higher ThO_2 content was detected predominantly in individual liberated monazite grains, while in smaller grains included within aforementioned minerals, ThO_2 content was generally lower.

Xenotime

Grains of xenotime from heavy mineral fraction from Drava river are scarce and included within garnets (var. Spessartine) with individual grains measuring from 5 to 50 µm. Xenotime grains are elongated, sub-rounded or equant (Figs. 4a-c) which is characteristic of mineral inclusions. Semi-quantitative EDS analysis performed on xenotime grains showed that they contain Y_2O_3 (26.25-38.60 wt%) and Yb_2O_3 (3.91-12.47 wt%) accompanied by smaller quantities of other HREE, i.e., Dy_2O_3 (2.52-4.80 wt%) and Er_2O_3 (3.59-5.29 wt%). Major oxide composition of investigated xenotimes is presented in Table 2.

Table 2. Relative concentrations of major oxides in xenotime acquired by semi-quantitative EDS analysis given in wt%. Values marked by »*« represent formulae for 4 oxygen per formula unit (apfu).

	P_2O_5	Y_2O_3	Dy_2O_3	Er_2O_3	Yb_2O_3	P^*	Y^*	Dy^*	Er^*	Yb^*
Xtm-1	41.37	49.02	5.50	4.10	0	1.106	0.726	0.056	0.041	0
Xtm-2	52.46	33.34	0	0	14.20	1.260	0.444	0	0	0.123
Xtm-3	52.68	41.10	5.64	3.81	6.78	1.164	0.621	0	0.039	0.067
Xtm-4	38.80	44.22	2.89	6.05	4.45	1.083	0.684	0.031	0.063	0.045
Xtm-5	39.93	47.04	4.20	4.35	4.48	1.092	0.713	0.044	0.044	0.044

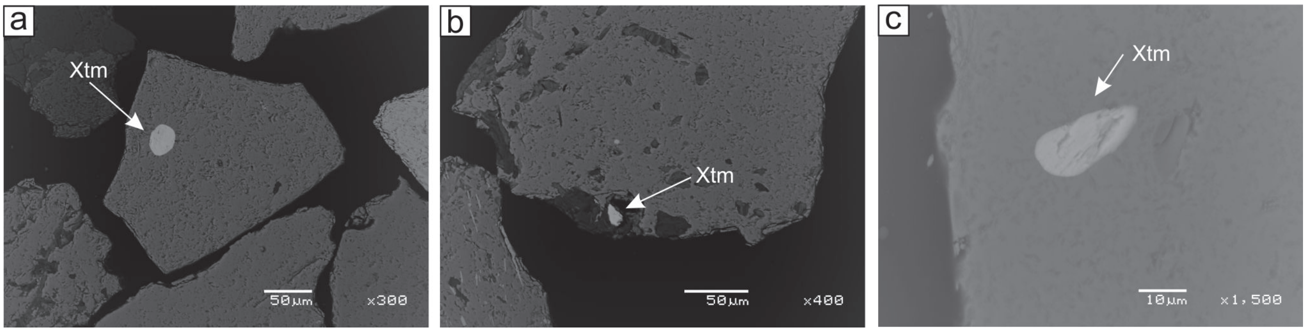

Fig. 6. Comparison of chemical composition (a) and the degree of isomorphic replacement in monazite (b) between studied Drava river monazites and monazites from Tauern Window and Pohorje Mts.

Discussion

Heavy mineral fractions of fluvial sediments from Drava river are predominantly composed of garnets, hematite, rutile and other minerals in traces (e.g., gold, monazite, xenotime, etc.) that account for less than 0.1 wt% of analyzed samples. Heavy mineral fraction is in size order of 0.06-0.5 mm corresponding with very fine to coarse sand and accounts for 2.3-4 wt% of bulk fluvial sediment.

Investigated monazites from Drava river show variable concentrations of REE and Th. Among REE, La, Ce, and Nd were identified in all analyzed samples, and their relationship can be summarized in the following manner based on their abundance in monazite: Ce > La > Nd. REE plotted in the ternary diagram show that majority of the analyzed grains are shifted towards Ce-rich corner thus indicating cerium monazite – monazite(-Ce) variety (Voncken, 2016) (Fig. 5a).

Monazite shows variable content of ThO_2 (0-7.20 wt%) of which highest concentrations were measured in larger isolated monazite grains. Detrital monazite texture, mode of occurrence and its geochemistry have been found to point toward its genetic environment, therefore, enabling separation of igneous monazite from its hydrothermal counterpart (Burnotte et al., 1989; Schandl et al., 1994; Wang et al., 1994). Schandl & Gorton (2004) demonstrated that hydrothermal monazite can be distinguished from igneous monazite by combining petrographic analyses with advanced electron microscopy techniques, performed on monazite mineral grains, and concluded that *hydrothermal* monazite (or greenschist-amphibolite metamorphic facies monazite) generally contains lower concentrations of ThO_2 (< 1 wt%), compared to *igneous* monazite, in which concentrations of ThO_2 were found to be significantly higher (3 – >5 wt%). Based on these facts it can be concluded that monazite in heavy mineral fraction from Drava river originates from two or more genetically different sources, hydrothermal (< 1 wt% ThO_2) and igneous (3 – >7.20 wt% ThO_2) source. Furthermore, monazite grains with highest ThO_2 concentrations are relatively larger and show high mineral liberation factor, indicating longer transport distance than their lower ThO_2 content counterparts.

In order to delineate possible intercrystalline substitution and intercrystalline partitioning behaviour of REE, Y, Th and U in monazite, composition of detrital monazites from Drava river was plotted in the diagram 4×(P+Y+REE) *versus* 4×(Si+Th+U), proposed by Harlov et al. (2008), which presents the degree of cheralite ($CaTh(PO_4)_2$) or huttonite ($ThSiO_4$) isomorphic substitution in monazite (Fig. 5b). Majority of the investigated detrital monazites from Drava river show slight or significant monazite-cheralite isomorphic substitution; some studied specimens even plotted above monazite-cheralite substitution line indicating the transition of monazite to cheralite. Only a small number of analyzed monazites plot near monazite-huttonite isomorphic substitution line. Observations using BEI image contrast did not show any huttonite or cheralite exsolutions within monazite, thus indicating they rather form solid solutions with monazite. Diagram of LREE versus U+Th+Pb (Fig. 5c) shows one primary field and another rather discrete. Fields are divided from each other by a virtual horizontal line at 0.84 LREE *apfu* (atoms per formula unit). Monazites in the primary field have a relatively high concentration of REE but somewhat lower concentrations of Th as their counterpart below 0.84 LREE *apfu*.

Xenotime grains show relatively consistent Y and variable HREE concentrations and lack presence of any actinides (i.e., U and Th). Among

HREE, Dy, Er, and Yb were identified in analyzed samples. The quantitative relationship between Y and HREE in xenotime can be summarized in the following manner: Y >> Yb > Dy ≥ Er. Due to the high relative abundance of Y (26.25-38.60 wt%) and low relative abundance of HREE (∑HREE: 8.39-14.19 wt%) investigated xenotime grains can be attributed to its Y-rich variety – xenotime(-Y).

The HREE+U versus Y diagram of *apfu* normalized values for xenotime (Fig. 5d) shows very scattered results, exhibiting relatively consistent concentrations of Y, while concentrations of HREE vary extensively. Lack of grouping and scattered results point towards the origin of xenotime from variable geological backgrounds (Guastoni et al., 2016).

Potential origin of monazite(-Ce) in Drava river fluvial sediments

Potential source of monazite(-Ce) from Drava river was estimated by comparing its chemical composition and the degree of monazite-cheralite and monazite-huttonite isomorphic substitutions, with monazite(-Ce) from three localities; two from Tauern Window (Finger et al., 1998; Hoschek, 2016) and one from Pohorje Mts. (Uher et al., 2014). In the work of Finger et al. (1998), samples of monazite were acquired from Granatspitz massif in Tauern Window, from S-type granite gneiss metamorphosed to amphibolite facies. Monazites, presented by Hoschek (2016), originate from Eclogite belt in Tauern Window, which is a thrust sheet between Venediger nappe and overlying Glockner nappe, consisting predominantly of Mesozoic metasediments and

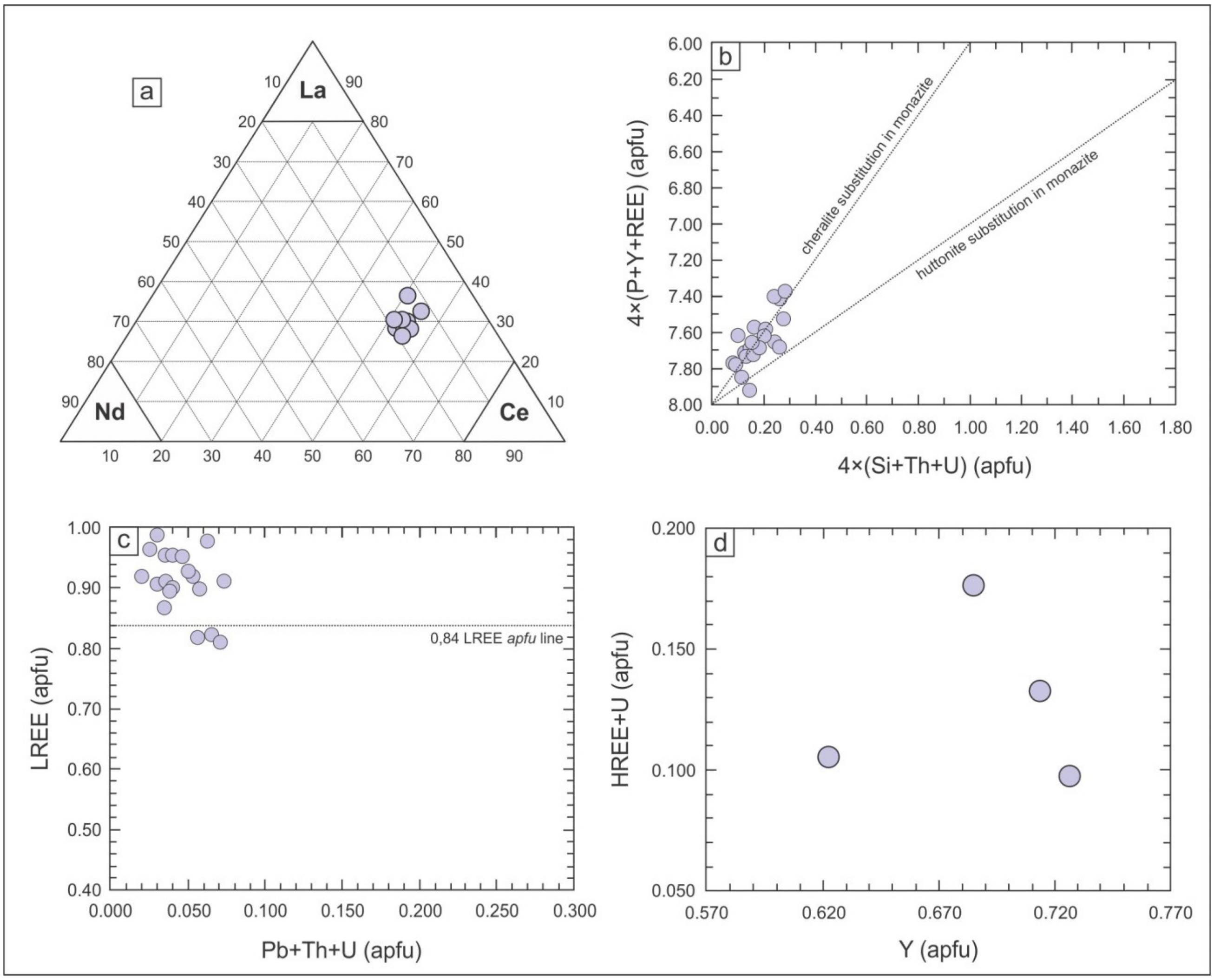

Fig. 5. Ternary diagram of Ce-La-Nd for investigated monazite (a) and diagrams of: 4×(P+Y+REE) versus 4×(Si+Th+U) apfu and (b) LREE versus Pb+Th+U apfu for investigated monazite (c) and HREE+U versus Y apfu normalized values of investigated xenotime grains (modified after HARLOV et al. (2008)) (d).

metabasites that were metamorphosed during Alpine plate collision. Monazites, presented by Uher et al. (2014), were acquired from granitic pegmatites emplaced in UHP rocks in Pohorje Mts, north-eastern Slovenia. Comparison of chemical composition of monazites from our case study with that of monazites from localities mentioned above are presented in the diagram Pb+Th+U *versus* LREE (Fig. 6a). The diagram shows three affinity fields marked in Roman numerals (I, II, III). The chemical composition of Drava monazites significantly corresponds with monazites originating from Eclogite belt and Granatspitz massif in Tauern Window. Affinity field (i), containing the majority of Drava monazites, corresponds greatly with monazites from Eclogite belt studied by Hoschek (2016), while monazites in affinity field (ii) correspond significantly with monazites from Granatspizt massif (Finger et al., 1998). Affinity fields (i) and (ii) are divided by 0.84 LREE *apfu* virtual horizontal line as established above based solely on Drava monazites. Monazites from Pohorje Mts. (Uher et al., 2014) on the other hand form a separate group (iii) below 0.70 LREE *apfu* which does not contain any of the investigated Drava river monazites. The degree of monazite-cheralite-huttonite isomorphic replacement is shown in 4×(Si+Th+U) *versus* 4×(P+Y+REE) (Fig. 6b). The diagram shows similarity in monazite-cheralite isomorphic replacements in studied Drava river monazites and monazites from Eclogite belt, while the degree of replacement in monazites from Granatspitz massif and Pohorje vary extensively, with only some points exhibiting a nearly similar degree of isomorphic substitution. Based on observed similarity in chemical composition and degree of monazite-cheralite isomorphic replacement, it can be concluded that majority of monazites, found in Drava fluvial sediments, are derived from localities in Tauern Window, among which rocks of Eclogite belt seem to be their most likely source.

Conclusions

1) Heavy minerals account for 2.3-4 wt% of bulk fluvial sediment of Drava river. Heavy minerals are present in a grain size fraction between 0.04 and 0.5 mm and predominantly consist of garnet group minerals, hematite, rutile and other minerals that account for less than 0.1 wt%.

2) Monazite is classified as monazite(-Ce) based on prevalent content of Ce compared to La and Nd. The variable content of Th in monazite suggests it originates from at least two different parent rocks or geological settings. The first group is *igneous* monazite where relative concentrations of ThO_2 are 3 – >7.20 wt% and second, *hydrothermal* or greenschist-amphibolite metamorphic grade monazite, with concentrations of ThO_2 < 1 wt%. Monazite was found to be forming monazite-cheralite and subordinate monazite-huttonite isomorphic replacements. No phase separation was observed using BEI, indicating solid solution relationship rather than mineral exsolution.

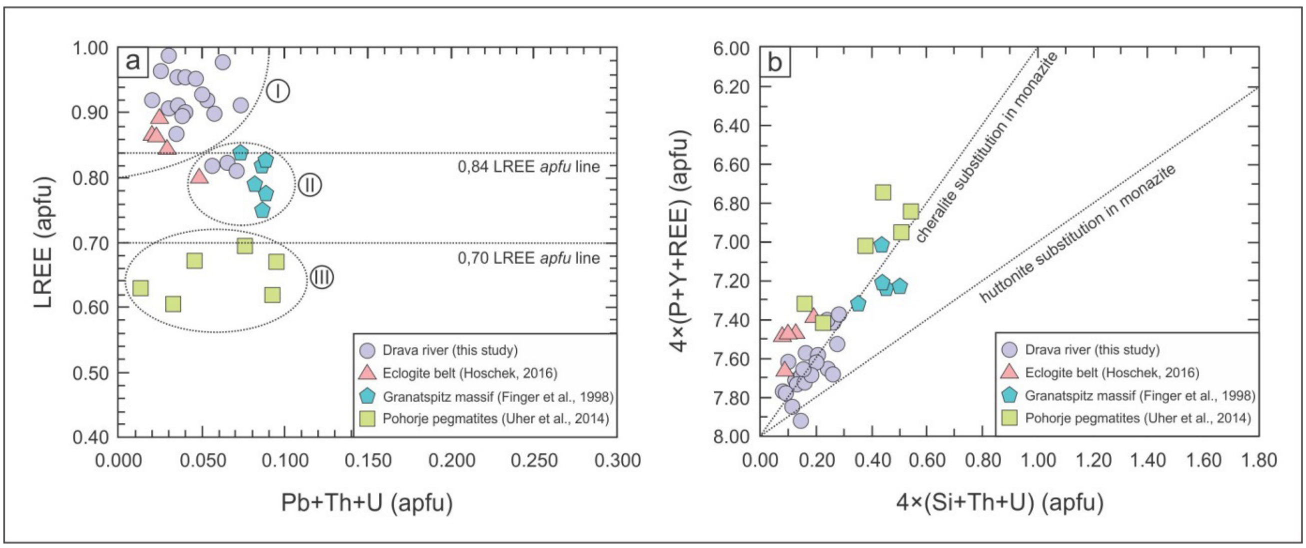

Fig. 6. Comparison of chemical composition (a) and the degree of isomorphic replacement in monazite (b) between studied Drava river monazites and monazites from Tauern Window and Pohorje Mts.

3) Based on relatively high abundance of Y compared to ∑HREE, xenotime grains from heavy mineral fraction from Drava river can be classified as xenotime(-Y), which most probably originates from various sources or geological backgrounds.

4) Chemical composition and degree of isomorphic replacement in Drava river monazite correspond significantly with monazites from Tauern Window, indicating the possible origin of monazite from Eclogite belt and subordinately from Granatspitz massif, while Pohorje Mts. can be disregarded as a potential source of monazite.

Acknowledgements

The authors acknowledge the financial support from the Slovenian Research Agency (research core funding contract No. 1000-17-0510; MR No. 39235) and Program group Geochemical and Structure processes (P1-0195). SEM/EDS analyses were performed at Centre for Electron Microscopy and Microanalysis (CEMM), Jožef Stefan Institute, Ljubljana, Slovenia. Authors would like to thank two anonymous reviewers for their detailed and constructive comments and suggestions improving the quality of the manuscript.

References

Alam, N. M., Chowdury, M. I., Kamal, M., Ghose, S., Islam, N. M., Mustafa, N. M., Miah, M. M. N. & Ansary, M. M. 1999: The ^{226}Ra, ^{232}Th and ^{40}K activities in beach sand minerals and beach soils of Cox's bazar, Bangladesh. Journal of Environmental Radioactivity, 46/2: 243-250, doi:10.1016/S0265-931X(98)00143-X.

Bea, F. 1996: Residence of REE, Y, Th and U in granites and crustal protoliths; implications for the chemistry of crustal melts. Journal of Petrology, 37: 521-552, doi:10.1093/petrology/37.3.521.

Bermanec, V., Palinkaš, L. Šoufek, M. & Zebec, V. 2014: Gold in the Drava and Mura rivers – Geological genesis and mineralogical analysis. Podravina, 13/25: 7-18.

Breiter, K. 2016: Monazite and zircon as major carriers of Th, U and Y in peraluminous granites: Examples from the Bohemian Massif. Mineralogy and Petrology, 110/6: 767-785, doi:10.1007/s00710-016-0448-0.

Burnotte, E., Pirard E. & Michel, G. 1989: Genesis of gray monazites: Evidence from the Paleozoic of Belgium Economic Geology, 84/5: 1417-1429, doi:10.2113/gsecongeo.84.5.1417.

Deer, W. A., Howie, R. A. & Zussman, J. 2013: An introduction to the rock-forming minerals, 3rd edition. The Mineralogical Society, London: 498 p.

Finger, F., Broska, I., Roberts, M. P. & Schermaier, A. 1998: Replacement of primary monazite by apatite-allanite-epidote coronas in an amphibolite facies granite gneiss from the eastern Alps. Am. Mineral., 83: 248-258, doi:10.2138/am-1998-3-408.

Förster, H. J. 1998a: The chemical composition of REE-Y-Th-U-rich accessory minerals in peraluminous granites of the Erzgebirge-Fichtelgebirge region, Germany, Part I: The monazite-(Ce)-brabantite solid solution series. American Mineralogist, 83: 259-272, doi:10.2138/am-1998-3-409.

Förster, H. J. 1998b: The chemical composition of REE-Y-Th-U-rich accessory minerals in peraluminous granites of the Erzgebirge-Fichtelgebirge region, Germany. Part II: Xenotime. American Mineralogist, 83: 1302-1315, doi:10.2138/am-1998-11-1219.

Grand'Homme, A., Janots, E., Bosse, V., Seydoux-Guillaume, A. M. & De Ascenção Guedes, R. 2016: Interpretation of U-Th-Pb in-situ ages of hydrothermal monazite-(Ce) and xenotime-(Y): evidence from a large-scale regional study in clefts from the western alps. Minereralogy and Petrology, 110/6: 787-807, doi:10.1007/s00710-016-0451-5.

Guastoni, A., Pozzi, G., Secco, L., Schiazza, M., Pennacchioni, G., Fioretti, A. M. & Nestola, F. 2016: Monazite-(Ce) and Xenotime-(Y) from an LCT, NYF Tertiary pegmatite field: Evidence from regional study in the Central Alps (Italy and Switzerland). The Canadian Mineralogist, 54: 863-877, doi:10.3749/canmin.1600021.

Harrison, T. M., McKeegan, K. D. & Le Fort, P. 1995: Detection of inherited monazite in the Manaslu leucogranite by ^{208}Pb/^{232}Th ion microprobe dating: Crystallization age and tectonic implications. Earth and Planetary Science Letters, 133: 271-282, doi:10.1016/0012-821X(95)00091-P.

Harlov, D. E., Procházka, V., Förster, H. J. & Matejka, D. 2008: Origin of monazite-xenotime-zircon-fluorapatite assemblages in peraluminous Melechov granite massif, Czech Republic. Mineralogy and Petrology, 52/2: 191-219, doi:10.1007/s00710-008-0003-8.

Hoschek, G. 2016: Phase relations of the REE minerals florencite, allanite, and monazite in quartzitic garnet–kyanite schist of the

Eclogite Zone, Tauern Window, Austria. European Journal of Mineralogy, 28: 735-750, doi:10.1127/ejm/2016/0028-2549.

Kim, Y., Yi, K. & Cho, M. 2009: Parageneses and Th-U distributions among allanite, monazite, and xenotime in Barrovian-type metapelites, Imjingang belt, Central Korea. American Mineralogist, 94: 430-438, doi:10.2138/am.2009.2769.

Mioč, P. & Žnidarčič, M. 1989: Basic Geological map of SFRY, Interpretation of map sheet Maribor and Leibnitz. Federal Geological Survey Beograd, Beograd: 69 p.

Pleničar, M., Ogorelec, B. & Novak, M. 2009: The Geology of Slovenia. Geological Survey of Slovenia, Ljubljana: 612 p.

Rao, N. S. & Misra, S. 2009: Sources of Monazite sand in Southern Orissa beach placer, Eastern India. Journal of the Geological Society of India, 74: 357-362, doi:10.1007/s12594-009-0140-7.

Robb, L. 2004: Introduction to Ore-Forming processes. Wiley-Blackwell, Oxford: 373 p.

Schandl, E. S., Gorton, M.P. & Davis, D. V. 1994: Albitization at 1700 ± 2 Ma in the Sudbury - Wanapitei Lake area, Ontario: implications for deep-seated alkalic magmatism in the Southern province. Canadian Journal of Earth Sciences, 31/3: 597-607, doi:10.1139/e94-052.

Schandl, E. S. & Gorton, M. P. 2004: A textural and geochemical guide to the identification of hydrothermal monazite: Criteria for selection of samples for dating epigenetic hydrothermal ore deposits. Economic Geology, 99/5: 1027-1035, doi:10.2113/gsecongeo.99.5.1027.

Švecová, E., Čopjaková, R., Losos, Z., Škoda, R., Nasdala, L. & Cícha, J. 2016: Multistage evolution of xenotime(-Y) from Písek pegmatites, Czech Republic: An electron probe micro-analysis and Raman spectroscopy study. Mineralogy and Petrology, 110/6: 747-765, doi:10.1007/s00710-016-0442-6.

Tockner, K., Uehlinger, U. & Robinson, C. T. 2009: Rivers of Europe. Academic press, London: 728 p.

Uher, P., Janák, M., Konečný, P. & Vrabec, M. 2014: Rare-element granitic pegmatite of Miocene age emplaced in UHP rocks from Visole, Pohorje Mountains (Eastern Alps, Slovenia): accessory minerals, monazite, and uraninite chemical dating. Geologica Carpathica, 65/2: 131-146, doi:10.2478/geoca-2014-0009.

van Emden, B., Thornber, M. R., Graham, J. & Lincoln, J. L. 1997: The incorporation of actinides in monazite and xenotime from placer deposits in Western Australia. The Canadian Mineralogist, 35/1: 95-104.

Vassas, C., Pourcelot, L., Vella, C., Carpena, J., Pupin, J. P., Bouisset, P. & Guillot, L. 2006: Mechanisms of enrichment of natural radioactivity along beaches of Camargue, France. Journal of Environmental Radioactivity, 91/3: 146-159, doi:10.1016/j.jenvrad.2006.09.002.

Voncken, J. H. L. 2016: The Ore Minerals and Major Ore Deposits of the Rare Earths. In: Voncken, J. (ed.): The Rare Earth Elements, Springer International Publishing, 15-52.

Wang, J., Tatsumoto, M., Li, X., Premo, W.R. & Chao, E. C. T. 1994: A precise ^{232}Th- ^{208}Pb chronology of fine-grained monazite age of Bayan Obo REE-Fe-Nb ore deposit, China. Geochim. Geochimica et Cosmochimica Acta, 58/15: 3155-3169, doi:10.1016/0016-7037(94)90043-4.

Zhu, X. K. & O'Nions, R. K. 1999: Monazite chemical composition: some implications for monazite geochronology. Contributions to Mineralogy and Petrology, 137/4: 351-363, doi:10.1007/s004100050555.

Žnidarčič, M. & Mioč, P. 1987: Basic geological map of SFRY. L 33-56, Maribor and Leibnitz 1:100.000. Federal Geological Survey, Beograd.

GEOLOGIJA 60/2, 267-277, Ljubljana 2017
https://doi.org/10.5474/geologija.2017.019

Application of environmental tracers to study the drainage system of the unsaturated zone of the Ljubljansko polje aquifer

Uporaba naravnih sledil za študij drenažnega sistema nezasičene cone vodonosnika Ljubljanskega polja

Branka TRČEK

University of Maribor, Faculty of civil enginering, Transportation Engineering and Architecture, Smetanova ulica 17, SI-2000 Maribor, Slovenia; e-mail: branka.trcek@um.si

Prejeto / Received 17. 12. 2016; Sprejeto / Accepted 8. 11. 2017; Objavljeno na spletu / Published online 22. 12. 2017

Dedicated to Professor Miran Veselič the occasion of his 70th birthday

Key words: Urban intergranular aquifer, unsaturated zone, drainage system, environmental tracers
Ključne besede: urbani medzrnski vodonosnik, nezasičena cona, drenažni sistem, naravna sledila

Abstract

The groundwater recharge processes were investigated in the unsaturated zone of the Ljubljansko polje intergranular aquifer. The study based on application of environmental tracers. The monitoring of the drainage system was established at an urban lysimeter consisting of artificial and autochthonous sediment layers. Groundwater was sampled with the suction cups instaled at depths of 0.3, 0.6, 1.2, 1.8, 3.0 and 4.0 m. The results pointed out the most important factors that control the hydrodynamic processes and solute transport in the study site where the soil cover and vegetation are missing. The physico–chemical and isotopic properties of sampled groundwater indicated that the clayey layers have an important role in the hydraulic behaviour of the unsaturated zone. As a consequence of a piston effect the event and pre-event water concentrate above these layers causing lateral flow. A vertical breakthrough of this water into lower layers of the unsaturated zone could occur through preferential paths during intensive precipitation events in dependence on pre-accumulated water volumes. Under such conditions groundwater residence time is about 2 months in the unsaturated zone 3 m below the surface.

Izvleček

V nezasičeni coni vodonosnika Ljubljanskega polja z medzrnsko poroznostjo smo proučevali tok podzemne vode v urbanem lizimetru. Monitoring drenažnega sistema zgornjega dela nezasičene cone, ki jo gradijo plasti avtohtonih in nanešenih sedimentov, je slonel na uporabi naravnih sledil. Podzemno vodo smo vzorčevali s keramičnimi sesalnimi svečkami, vgrajenimi v globinah 0,3; 0,6; 1,2; 1,8; 3,0 in 4,0 m. Rezultati so izpostavili najpomembnejše faktorje, ki nadzirajo hidrodinamične procese in prenos snovi na raziskovanem območju, kjer sta horizont tal in vegetacija odsotna. Fizikalno–kemijske in izotopske lastnosti vode so pokazale, da imajo plasti, ki vsebujejo glinen material, pomembno vlogo pri hidravličnih lastnostih raziskovanega območja. Kot posledica batnega efekta se nova padavinska voda in predhodno uskladiščene vode skoncentrirajo nad omenjeno plastjo in pridobijo lateralno komponento toka. Vertikalen preboj vode v nižje plasti nezasičene cone se pojavi po prednostnih poteh le v obdobju intenzivnih padavinskih dogodkov v odvisnosti od volumna predhodno uskladiščene vode. V nezasičeni coni, 3 m pod površjem, je povprečen zadrževalni čas podzemne vode pod takimi pogoji okoli 2 meseca.

Introduction

Groundwater is extensively used worldwide for domestic, industrial, and agricultural purposes. Generally, aquifers contribute at least 25 % to the city drinking water supply (Gleick, 2002), but as much as 75 % in Europe (Sampat, 2000) and 95 % in Slovenia (Uhan & Krajnc, 2003). Groundwater is renewing if the climate does not change dramatically or it is not degraded by inappropriate use. Better understanding of groundwater flow and contaminant transport mechanisms could essentially contribute to protection of this natural resource.

Groundwater from a sandy–gravel aquifer is an invaluable drinking water resource for the Ljubljana city (Slovenia), as well as for the Union Brewery, which is located within an industrial-

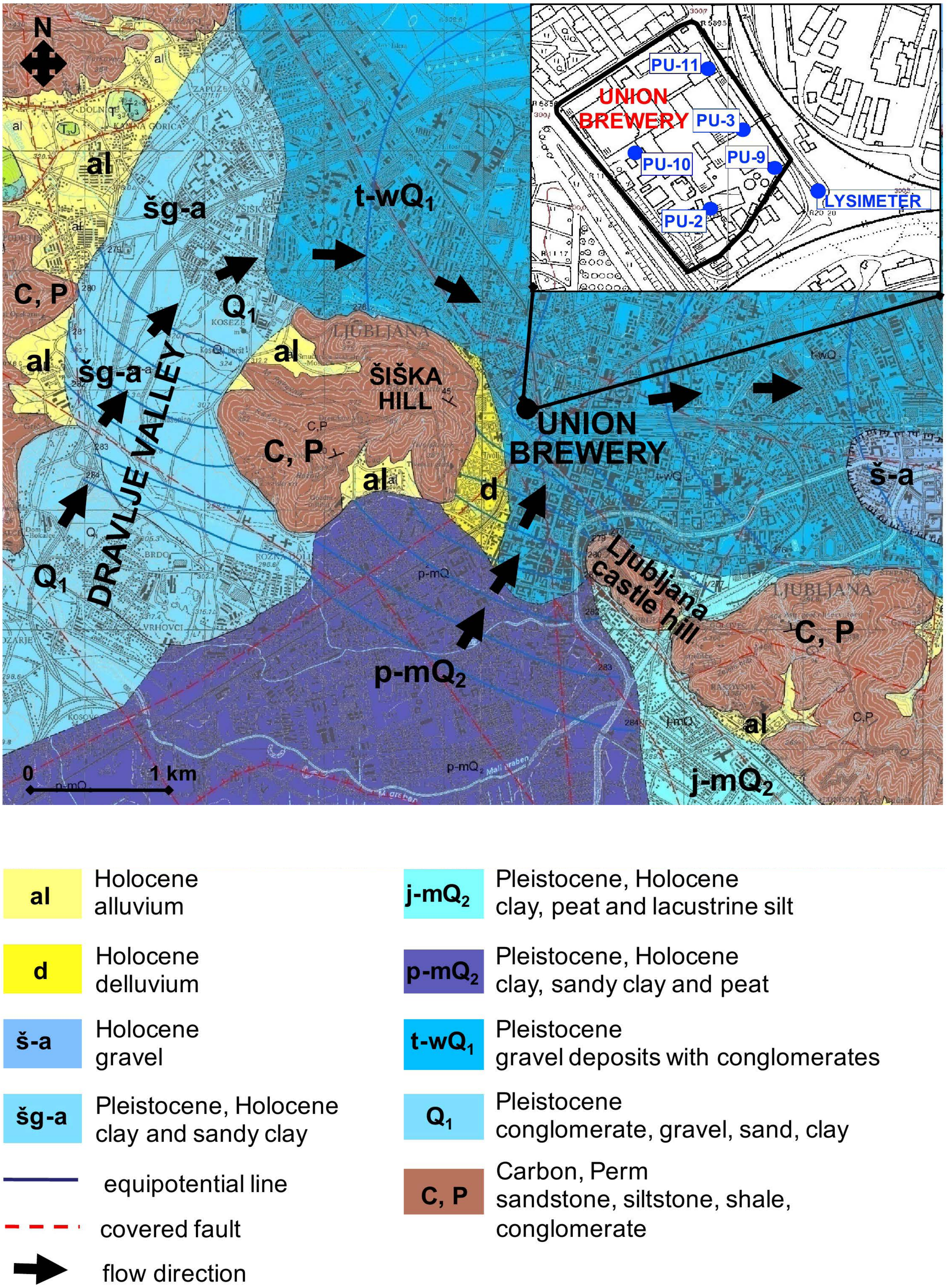

Fig. 1. Study area (PU-X observation well).

Sl. 1. Raziskovalno območje (PU-X opazovalna vrtina).

ized area near the centre of Ljubljana. A large sector of the aquifer recharge area is highly urbanized, which represents a great risk for the groundwater quality. The brewery exploits quality groundwater from the lower part of the aquifer that is bounded by an impermeable barrier from the upper part that is contaminated. Chemical analyses of groundwater samples from the brewery vicinity indicated the local contamination with herbicides, chlorides and some urban contaminants derived from traffic, industry and waste water systems (Trček et al., 2010; Vižintin et al., 2009). In regard with the implementation of the sustainable groundwater management the extensive studies of groundwater flow and solute transport were performed in the period from 2000 to 2014 in the catchment area of the Union Brewery groundwater resources (Juren et al., 2003; Trček, 2005, 2006; Trček & Juren, 2007; Trček et al., 2010, 2013; Vižintin et al., 2009). Their main research goal was the assessment and prediction of groundwater flow and the contaminant directions through the unsaturated and saturated zone of the urban intergranular aquifer. The quality and quantity monitoring was conducted in numerous observation wells within the brewery and in its vicinity (some of them are illustrated in Fig. 1), as well as at the urban lysimeter (Fig. 1), which is a topic of this paper.

To understand groundwater flow and solute transport mechanisms in urban aquifers a comprehensive study of the urban water cycle components and impacts of urbanisation should be integrated (Vižintin et al., 2009). Different land-uses in urban areas significantly affect the infiltration and recharge characteristics. The complex urban groundwater recharge patterns were investigated with a help of lysimeters in the Ljubljansko polje intergranular aquifer. The lysimetry enable accurate measurements of water flow and water balance parameters, and can be used for investigating hydrological and hydrogeochemical processes in the aquifer unsaturated zones (Meissner et al., 2007; von Unold & Fank, 2008).

Since 2000 active researches were performed at the lysimeter station in the Ljubljana Kleče Water Pumping station (Zupanc et al., 2005, 2012). The water balance components were investigated in monolith lysimeters consisted from 2-m deep layers of sandy gravel sediments covered by the autochthon soil and vegetated by grass. In time of high water usage of vegetation only subsequent substantial precipitation events directly result in water flow towards lower layers (Zupanc et al., 2012). At the same time, gravely layers of the deeper parts of the unsaturated zone have little or no capacity for water retention, and in the event that water line leaves top soil, water flow moves downwards fairly quickly. Zupanc et al. (2012) stressed that the low water retention of the aquifer sediments showed susceptibility of the aquifer to groundwater pollution.

The lysimeter of the Union Brewery differs a lot from the one in the Ljubljana Kleče Water Pumping station. It consists from boreholes that penetrate a much larger sector of the aquifer unsaturated zone (Fig. 2). It was constructed in the industrialized area, adjacent to the brewery (Fig. 1) where the soil and the upper sediment layers were removed during construction processes and nowadays some artificial sediments cover the aquifer. Moreover, there is no vegetation in the lysimeter vicinity. Hence, the Union Brewery lysimeter represents a polygon to study the typical urban infiltration conditions. This article presents the study of the lysimeter drainage system that based on environmental tracers. The sampled water δ^{18}O served as a leading parameter for hydrodynamic investigations of the unsaturated zone in the urban intergranular aquifer.

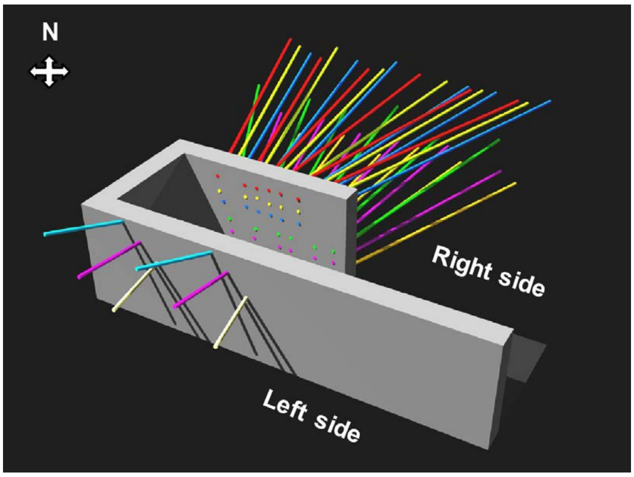

Fig. 2. Scheme of the lysimeter construction.
Sl. 2. Shema kostrukcije lizimetra.

Study area

The Union brewery is located in the Ljubljana city at an altitude of 300.3 m asl. The Ljubljana area is a large tectonic depression, surrounded by hills and mountains. It was formed in Plio–Quaternary by the sequential subsiding. Its northern part is named Ljubljansko polje. It is filled by fluvial deposits that form the so called Ljubljansko polje aquifer. The deep Holocene and Pleistocene sediments are very heterogeneous. The upper layers consist mostly of sands and gravels and the lower ones mostly of conglomerates, which is reflected in the aquifer hydrodynamic parameters (Auersperger et al., 2005; Bračič Železnik et al., 2005; Vižintin et al., 2009). Lenses of the low permeable clay and sandy–clay layers locally divide the aquifer into two parts – the upper and lower aquifer, as it is the case in the Union Brewery area, where the unsaturated zone is 20 m deep on average, while the aquifer depth is approximately 90 m. The effective porosity ranges between 5 % and 12 % in the study area and the groundwater velocity between 5 and 19 m/day (Trček et. al., 2010).

The urban lysimeter of the Union Brewery was designed in the upper unsaturated zone of the sandy–gravel aquifer (Fig. 1). 36 boreholes were drilled into the right and left walls of the construction, which is 8.5 m deep in NE and SW directions, respectively (Fig. 2). The boreholes are up to 8 m long. They are located under the industrial railway tracks on right side of the lysimeter and beneath the asphalt surface on the left lysimeter side. By the beginning of January 2003, the lysimeter was completely equipped with the UMS recording and sampling system (Juren et al., 2003). Tensiometers, TDR probes and suction cups were installed into the ends of boreholes.

The boreholes of the right lysimeter side were included into discussed study. They are distributed in six columns (1–6) and six levels (I–VI) at depths of 0.3, 0.6, 1.2, 1.8, 3.0 and 4.0 m (Figs. 2 and 3). The boreholes are named by their distribution: RI-1, RI-2, RVI-5 and RVI-6.

A detailed geological cross-section of the ends of the boreholes is illustrated in Figure 3. The boreholes penetrate four layers: sandy gravel, silt–sandy gravel, clayey silt–sandy silt with gravel grains and gravel with sand and silt. The upper three layers are artificial. The fourth layer is autochthon and consists of fluvial deposits. The boreholes of levels I, II, and III end in artificial layers, the boreholes of the level IV end close to the contact with the autochthon layer, while the boreholes of levels V and VI end in the autochthon layer.

Methods

The monitoring of the drainage system of the aquifer unsaturated zone was performed in 18 observation points on right side of the Union Brewery lysimeter: RI-1 to RIII-6 (Fig. 3). Groundwater was sampled with suction cups that are distributed at depths of 0.3, 0.6, 1.2, 1.8, 3.0 and 4.0 m. In addition, precipitation was monitored and sampled near the entrance to the lysimeter.

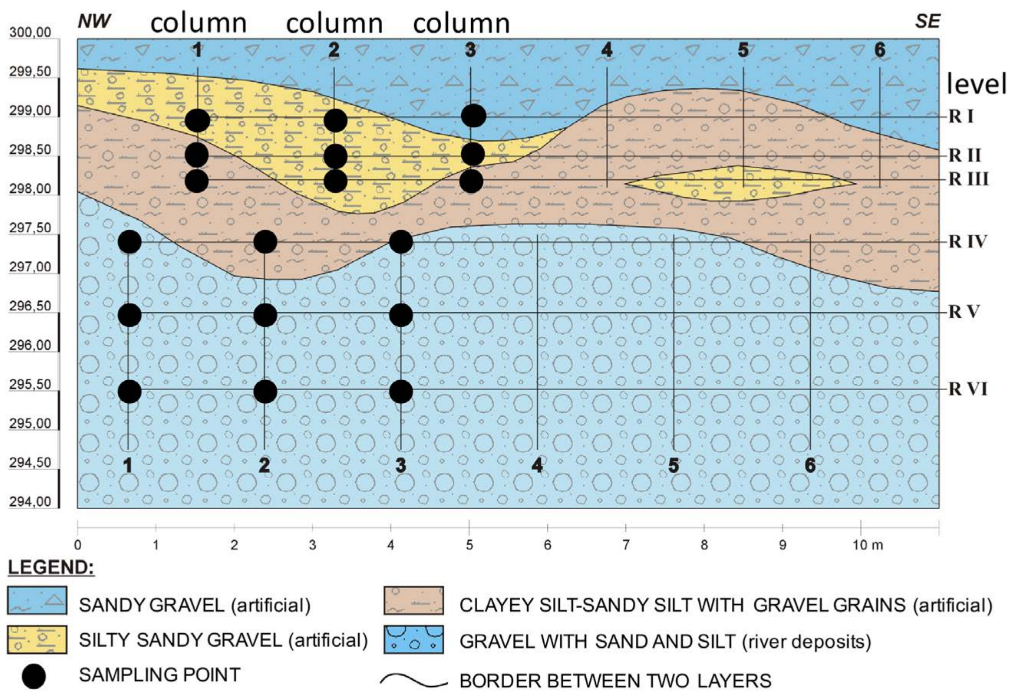

Fig. 3. Geological cross-section of the right side of the lysimeter at the end of boreholes, with sampling points indicated (modified after Juren et al., 2003)

Sl. 3. Geološki prerez s konca vrtin na desni strani lizimetra z označenimi vzorčnimi mesti (prirejeno po Juren et al., 2003).

In the period from 2004 to 2014 continuous measurements of water balance and physico–chemical water parameters (T, pH and specific electroconductivity - SEC) have been performed and water has been sampled temporarily for chemical and isotopic investigations. Water was sampled and preserved based upon the method described by Clark & Fritz (1997). Isotopic analyses of stable isotopes of H and O were made in Laboratory Centre for Isotope Hydrology and Environmental Analytics, Joanneum Research, Graz, Austria. The oxygen isotopic composition ($\delta^{18}O$) of water was measured by the classic CO_2 – H_2O equilibrium technique (Epstein & Mayeda, 1953) with a fully automated device adapted from Horita et al. (1989) coupled to a Finnigan DELTAplus Mass Spectrometer. Deuterium ($\delta^{2}H$) was measured in a continuous flow mode by chromium reduction using a ceramic reactor slightly modified from Morrison et al. (2001). Stable oxygen isotopic ratios are reported relative to the VSMOW (Vienna–SMOW) standard with an overall precision of 0.1 and 1 ‰, respectively.

The stable isotope ^{18}O was applied to investigate the urban recharge process. The study based on isotopic variations in precipitation as the predominant groundwater source. After infiltration of precipitation into the unsaturated zone the physical processes of diffusion, dispersion, mixing and evaporation alter the groundwater isotopic composition (Clark & Fritz, 1997; Hoefs, 1997). The stable isotope content of water was considered conservative, because the processes took place under low–temperature and low–circulation conditions and the relative amount of water involved in chemical reactions remained limited (Clark & Fritz, 1997; Hoefs, 1997).

The sampled water $\delta^{18}O$ together with hydrometric data provided information on the movement and mixing of water masses. Precipitation infiltrates and recharges the aquifer, where it is mixed with pre–stored groundwater, which results in the input signal attenuation indicated in a lowering of the isotopic variation amplitude. Owing to different mixing and homogenisation stages, groundwater has different $\delta^{18}O$ throughout the unsaturated zone and with that different amplitude of the isotopic seasonal variation. These differences were applied for the determination of groundwater residence time seeing that the longer residence time, the lower is the amplitude of groundwater isotopic seasonal variation.

The isotopic sampling was performed in the long–term (monthly/seasonally) and short–term protocol during significant precipitation events. In the period 2004–2007 the water was sampled in daily, weekly or monthly intervals, while only the seasonal sampling followed by 2010. The detailed sampling focused on the investigation of preferential flow on right side of the lysimeter. The snow $\delta^{18}O$ with significant low values was applied as a signal to trace the distribution of snowmelt water through heterogeneous sediment layers of the unsaturated zone (Fig. 3).

Isotopic data were statistically processed with a help of the classical method of weighted averages (McDonnell et al., 1990):

$$\delta^{18}O = (\sum^{n}_{i=1} P_i \delta_i{}^{18}O) \,/\, (\sum^{n}_{i=1} P_i) \qquad (1)$$

$\delta^{18}O$ – weighted average of the oxygen isotopic composition of precipitation/sampled water,
P_i – precipitation amount/water volume of the sample (i),
$\delta_i{}^{18}O$ – oxygen isotopic composition of the sample (i).

Results and discussion

Data of sampled water $\delta^{18}O$ and SEC measurements during snowmelt events in the period 2004–2010 indicated that this relatively slow but concentrated infiltration generated a recharge process with a prevailing vertical flow component in the lysimeter levels, I, II and III. The result is in accordance with findings at the lysimeter station in the Ljubljana Kleče Water Pumping station (Zupanc et al., 2012) considering the absence of retention due to the soil and vegetation activities. However, $\delta^{18}O$ and SEC data evidenced the so-called piston effect at the lysimeter level III – the following precipitation events displaced the pre-stored snowmelt water, which resulted in the attenuation of the isotopic response at the lysimeter lower layers. The analysis of $\delta^{18}O$ and SEC measurements during storm events indicate that the intensive rain infiltration could lead to a breakthrough of water that was pre-stored in the lysimeter upper levels (I, II and III) into the lysimeter lower levels through preferential paths. The responses were dependant on the pre-accumulated water volumes.

The discussed characteristics of recharge and discharge processes in the urban unsaturated zone are presented through isotopic analyses from 2005 when the sampling frequency was the highest (Fig. 4). The lysimeter responses to the snowmelt event in March and to the storm events at the beginning of April, at the end of August and at the beginning of September were studied. 25 cm of snow was melted in the middle of March, while the maximal daily precipitation amounts during investigated storm events were 46, 42 and 71 mm, respectively (Fig. 4).

The isotopic response to the snowmelt was fast and intensive in the level I. Nevertheless, the maximal response was observed almost two weeks after the event beginning (Fig. 4). The similar situation was evidenced in the level III, but with a greater delay. The peak isotopic response of this level was registered after high precipitation at the beginning of April that displaced the pre-event water, which reflects the piston effect. The mentioned rain event pushed water of low $\delta^{18}O$ from the lysimeter upper levels also to levels IV, V and VI (Fig. 4). However, their impact on the parameter oscillation was much lower. The process was not intensive, but resulted in a characteristic $\delta^{18}O$ decrease. In the beginning of June the lowest $\delta^{18}O$ was indicated in the sampling point RV-2. It most probably reflects the snowmelt influence that has an approximately two months' shift. In September the highest $\delta^{18}O$ value was monitored at the sampling point RV-3, after the intensive rainy period. It is presumed that the August precipitation temporally saturated the lysimeter upper part above the clayey silt–sandy silt and gravel layer (Fig. 3), while the September rain generated a water breakthrough into the lysimeter lower level RV-3 through the preferential paths.

The statistical characteristics of water $\delta^{18}O$ sampled in the period 2004–2010 are graphically illustrated with boxplots in Figure 5. The distributions of data sets significantly distinguish among themselves. Precipitation values range between -3 and -18 ‰, whilst the groundwater values vary between -6 and -16 ‰. The means that as well as the spread of $\delta^{18}O$ data for various lysimeter sampling points differ significantly, which most probably reflect different residence times of the seepage water. A comparison with precipitation indicates that $\delta^{18}O$ ranges of groundwater for the upper three levels are the highest, reflecting the intensive groundwater dynamics and short residence times. The similarity between the precipitation and level I boxplots is

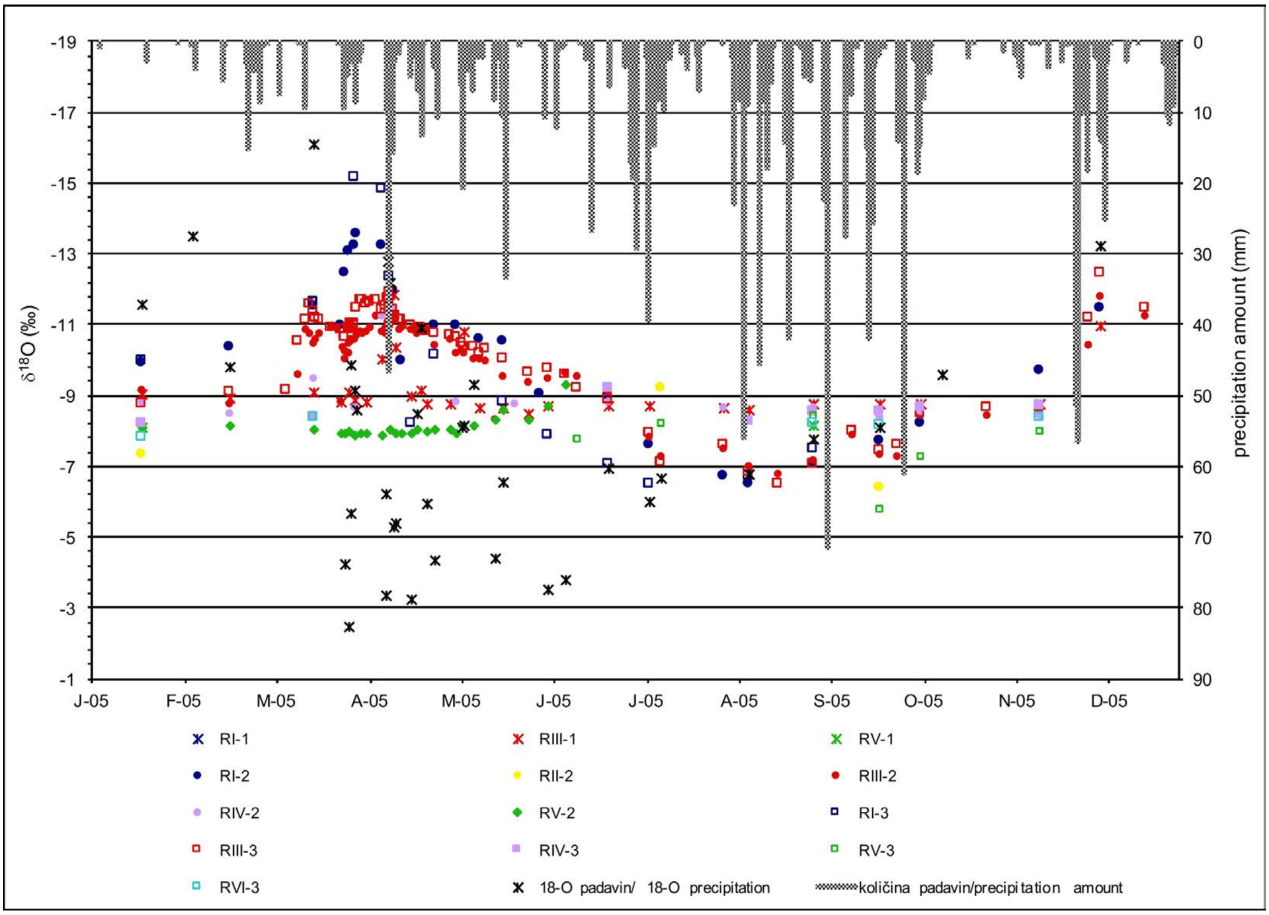

Fig. 4. Time-trend plot of water oxygen isotopic composition sampled at the lysimeter in 2005.
Sl. 4. Časovno nihanje izotopske sestave kisika v vodi, vzorčeni v lizimetru leta 2005.

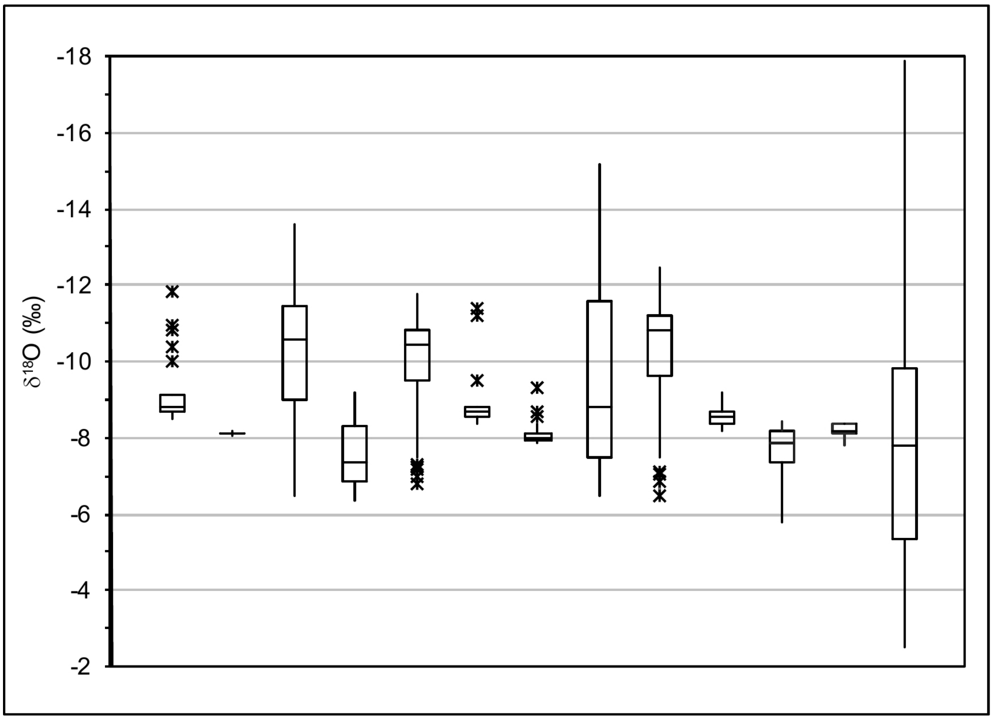

Fig. 5. Boxplots of water oxygen isotopic composition sampled at the lysimeter in the period 2004–2010.

Sl. 5. Škatlasti diagrami izotopske sestave kisika v vodi, vzorčeni v lizimetru v obdobju 2004–2010.

expected, because this level lies only 0.3 m below the surface. On the other hand, the parameter variation is much more attenuated at the lysimeter lower levels (IV, V and VI), which reflects less intensive dynamics and longer groundwater residence times.

The outside values that are marked with asterisks in Figure 5 point out the unusual isotopic composition of sampled water. Considering findings related to Figure 4 and the fact that the outside values are not characteristic for levels I and II it is presumed that the discussed values reflect vertical recharge processes in the intergranular aquifer that occur through preferential paths during important hydrological events. The outside values in the negative direction refer to winter precipitation with the lowest δ^{18}O and vice versa, the values in the positive direction refer to summer precipitation with the enriched isotopic composition.

To get better insight into the lysimeter drainage system the weighted averages of δ^{18}O data were calculated (eq. 1) for the period 2005–2009. They are listed in Table 1 together with average annual discharge volumes of lysimeter sampling points. The bulk of water was discharged at the level III as sampling points RIII-2 and RIII-3 discharged the highest volumes. The two sampling points are located near the contact between two structurally different layers: silt–sandy gravel and underlying clayey silt–sandy silt with gravel grains. The hydraulic conductivity of the upper layer is higher than that of the lower layer, which indicates that greater volumes discharged from the level III result from the development of a lateral flow component near this level and that only important hydrological events generate a vertical breakthrough of water from the level III into the lysimeter lower layers.

Table 1. Weighted averages of lysimeter water oxygen isotopic composition, average annual discharge volumes of lysimeter sampling points and precipitation amount in the study site in the period 2005–2009.

Tabela 1. Tehtana povprečja izotopske sestave kisika v vzorčevanih vodah lizimetra, povprečni letni dotok vode vzorčnih mest v lizimetru in letna količina padavin na raziskovalnem območju v obdobju 2005–2009.

	δ^{18}O weighted averages / Tehtano povprečje δ^{18}O (‰)	Annual discharge volume / Letni dotok vode (l)	Annual precipitation amount / Letna količina padavin (mm)
RIII-1	-9.30	2.8	
RV-1	-8.17	0.1	
RI-2	-9.46	2.0	
RII-2	-7.75	0.1	
RIII-2	-9.61	1047	
RIV-2	-9.82	1.8	
RV-2	-8.15	3.6	
RI-3	-8.01	1.0	
RIII-3	-9.61	1605	
RIV-3	-8.59	0.4	
RV-3	-7.62	0.4	
RVI-3	-8.22	0.3	
Precipitation / Padavine	-8.79		1353

Weighted averages of the sampled water $\delta^{18}O$ could be interpreted with a help of Tables 2 and 3 that present seasonal weighted averages of sampled water $\delta^{18}O$ and seasonal portions of the sampling point discharged volumes respectively. The sampling points with lower $\delta^{18}O$ averages from the one of precipitation were mostly recharged in winter when the precipitation $\delta^{18}O$ was the lowest, while the sampling points with higher $\delta^{18}O$ averages from the one of precipitation were mostly recharged in summer or autumn when the precipitation $\delta^{18}O$ was high. In addition, the discharge regime of sampling points (Tab. 3) reflects dependence between the preferential and laminar flow regime.

Table 2. Seasonal weighted averages of lysimeter water oxygen isotopic composition (‰) in the period 2005–2009.

Tabela 2. Sezonska tehtana povprečja izotopske sestave kisika v vzorčevanih vodah lizimetra (‰) v obdobju 2005–2009.

	Winter / Zima	Spring / Pomlad	Summer / Poletje	Autumn / Jesen
RIII-1	-9.76	-9.28	-8.70	-8.75
RV-1	-8.17	-9.02	-8.16	-8.21
RI-2	-10.79	-11.03	-7.04	-8.39
RII-2	-7.35	-8.97	-9.21	-6.38
RIII-2	-10.62	-10.55	-7.41	-8.80
RIV-2	-9.34	-11.04	-8.69	-8.44
RV-2	-8.11	-8.19	-7.32	-8.20
RI-3	-10.45	-10.09	-6.98	-8.91
RIII-3	-10.71	-10.91	-7.72	-9.38
RIV-3	-8.34	-8.11	-8.61	-8.64
RV-3	-8.24	-7.74	-8.36	-7.13
RVI-3	-8.11	-7.82	-8.20	-8.26
Precipitation / Padavine	-13.67	-7.04	-6.95	-8.65

Table 3. Seasonal discharge volumes of the lysimeter sampling points (%) in the period 2005–2009.

Tabela 3. Sezonski dotok vode vzorčnih mest v lizimetru (%) v obdobju 2005–2009.

	Winter / Zima	Spring / Pomlad	Summer / Poletje	Autumn / Jesen
RIII-1	45	20	20	15
RV-1	48	0.1	53	0.1
RI-2	35	21	23	22
RII-2	9	0.2	45	45
RIII-2	37	26	23	14
RIV-2	46	36	9	9
RV-2	51	49	0.1	0.1
RI-3	7	26	68	0.1
RIII-3	44	8	29	19
RIV-3	12	0.1	54	34
RV-3	0.2	11	34	54
RVI-3	17	0.1	20	63
Precipitation / Padavine	21	34	20	26

The presented results indicate the existence of a perched aquifer near the lysimeter above the clayey silt–sandy silt with gravel grains (Fig. 3). The comparison analysis between isotopic and hydrometric data demonstrated that the extension of the perched accumulation and of a subsequent discharge to the lysimeter lower levels depends on the water saturation and are not correlated with precipitation amounts.

It is well known that low permeability clayey layers give rise to perched aquifer conditions to the north and to the east of the Permo–Carboniferous outcrop of the Šiška hill (Auersperger et al., 2005; Bračič Železnik et al., 2005; Trček et. al., 2010, 2013; Vižintin et al., 2009). In the brewery area the clayey lances are distributed in the unsaturated and saturated zone of the aquifer (Trček et. al., 2010, 2013; Vižintin et al., 2009). The observation well PU-9 that is 50 m distant from the lysimeter (Fig. 1) includes layers of clayey sediments at depths of 3, 19 and 28 m. To verify the lysimeter results the isotopic interpretation of the unsaturated zone hydraulic behaviour was transferred to SEC data that are available on a much greater extend for the lysimeter and for the wider study area. Figure 6 presents the hourly oscillation of groundwater SEC data in the observation well PU-9 approximately 10 m below the groundwater table (at a depth of 30 m) in the period 2005–2014. SEC data are not correlated with groundwater table (R^2 = 0.58). Nevertheless, the increase of SEC values is most often connected with the rise of groundwater table, which reflects the displacement of pre-stored water in the aquifer. It is presumed that groundwater with higher SEC values is stored above the upper clayey lances and it is discharged to the aquifer lower parts during hydrological events. The reverse process connected with the inflow of event water is rare (Fig. 6).

The described recharge mechanism is important for understanding transport of contaminant loads in the investigated aquifer in a vertical direction. It is in agreement with estimates of groundwater residence time. The average age of PU-9 groundwater determined with the $^3H/^3He$ dating technique is estimated to 4 years (Trček et. al., 2013), which supports the presented results. Based on $\delta^{18}O$ data groundwater residence time is about 2 months below the first clayey lance at depth of 3 m.

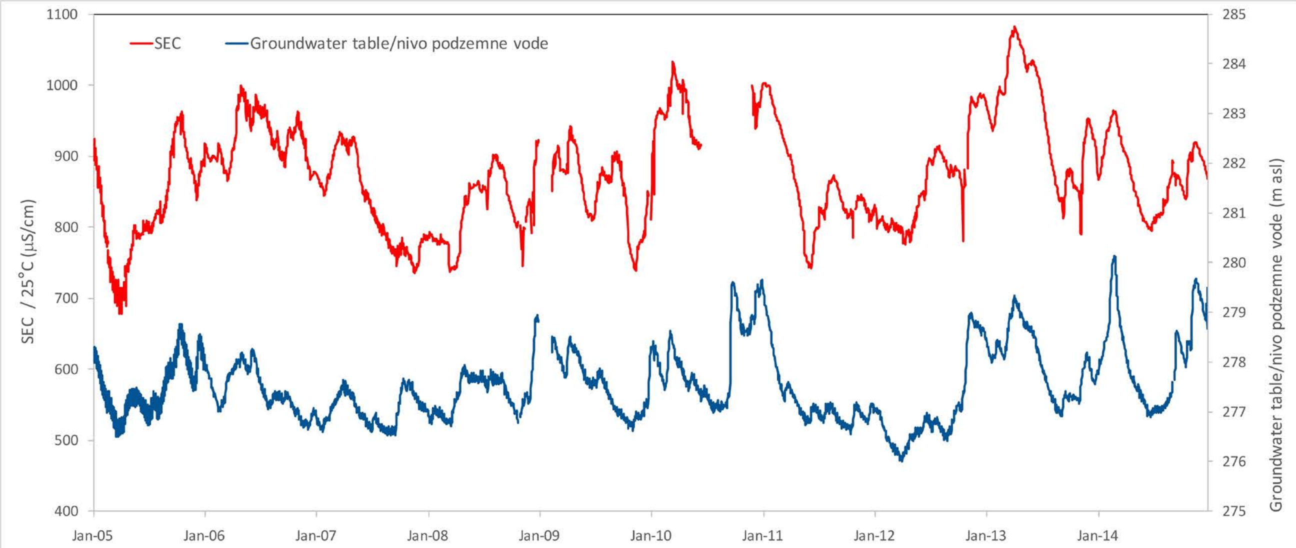

Fig. 6. Hourly oscillation of groundwater electroconductivity in the piezometer PU-9 in the period 2005–2014.
Sl. 6. Urno nihanje elektroprevodnosti podzemne vode v piezometru PU-9 v obdobju 2005–2014.

Conclusions

The vertical seepage of measured parameters in groundwater of the Ljubljansko polje aquifer was observed in numerus investigations (Auersperger et al., 2005; Bračič Železnik et al., 2005; Vižintin et al., 2009). The presented results pointed out the most important factors that control the hydrodynamic processes and solute transport in the aquifer unsaturated zone without the soil cover, which is a typical phenomenon in urban areas. Hence, the vegetation has no impact on infiltration and recharge processes and water/solutes are not affected with the soil attenuation factors. The results indicated that layers of clayey sediments have an important role in the hydraulic behaviour of the study site due to the lower hydraulic conductivity that allows the formation of perched aquifers. It is presumed that the recharge process above these layers is a consequence of the piston effect. The recharged pre-event and event water concentrate above them, which results in a development of a lateral flow component. A vertical breakthrough of this water into lower layers of the unsaturated zone and into the saturated zone could occur through preferential paths during intensive precipitation events in dependence on pre-accumulated water volumes. Under such conditions groundwater residence time is about 2 months in the unsaturated zone 3 m below the surface and about 4 years 10 m below the water table at a depth of 30 m (Trček et. al., 2013).

The lateral flow component has an important role in the protection of groundwater of the Ljubljansko polje aquifer. However, the role of vertical flow is quite the opposite, because it is the main factor controlling contaminant transport towards the drinking water resources. Hence, the main goal of future investigations is directed to transport studies of contaminant loads in the investigated aquifer in a vertical direction.

Uporaba naravnih sledil za študij drenažnega sistema nezasičene cone v urbanem okolju

(Povzetek)

Pivovarna Union izkorišča kvalitetno podzemno vodo pleistocenskega medzrnskega vodonosnika. Precejšen del napajalnega območja vodonosnika je urbaniziran, kar predstavlja veliko tveganje za onesnaženje vodnega vira pitne vode. Da bi se vzpostavilo sonaravno gospodarjenje s podzemnim vodnim virom, se je izvajala obsežna študija toka podzemne vode in prenosa snovi na območju vodnega telesa pivovarne v obdobju 2000-2014 (Juren et al., 2003; Trček, 2005, 2006; Trček & Juren, 2007; Trček et al., 2010, 2013; Vižintin et al., 2009).

Hidravlični procesi nezasičene cone so se proučevali v urbanem lizimetru, v neposredni bližini pivovarne (sl. 1 in 2). Monitoring drenažnega sistema zgornjega dela nezasičene cone, ki ga gradijo plasti avtohtonih in nanešenih sedimentov (sl. 3), je slonel na uporabi naravnih sledil. Podzemna voda se je vzorčila na 18 opazovalnih točkah (RI-1 do RIII-6), s keramičnimi sesalnimi svečkami, vgrajenimi v globinah 0,3; 0,6; 1,2; 1,8; 3,0 in 4,0 m (sl. 2 in 3). Od leta 2004 naprej so se

izvajale zvezne meritve vodne bilance vzorčnih mest in fizikalno-kemijskih parametrov vode (T, pH in specifična elektroprevodnost), medtem ko se je vzorčila voda za kemijske in izotopske raziskave v posameznih fazah.

$\delta^{18}O$ vzorčenih vod predstavlja vodilni parameter hidrogeološke študije. Med pomembnimi padavinskimi dogodki so se proučevali procesi polnjenja in praznjenja nezasičene cone. Posebno pozornost je treba nameniti podatkom detajlnega vzorčenja topljenja snega, ki je nastopilo sredi marca (sl. 4). Le to je povzročilo, da so bile izmerjene dva tedna kasneje najnižje vrednosti $\delta^{18}O$ v vodah zgornjega nivoja lizimetra, 0,3 m pod površjem. Podobno situacijo opazimo tudi na nivoju III, le da je bil tam maksimalem odziv kasnejši. Povzročile so ga intenzivne padavinah na začetku aprila, ki so izpodrinile predhodno uskladiščeno vodo iz višjih nivojev, kar odseva batni efekt. Te padavine so potisnile vodo z nižjo $\delta^{18}O$ iz višjih nivojev lizimetra tudi v nivoje IV, V in VI, vendar je bil njihov vpliv na nihanje parametra precej nižji. Na začetku junija je bila izmerjena najnižja vrednost $\delta^{8}O$ v vzorčnem mestu RV- 2, ki najverjetneje odseva vpliv topljenja snega z dvomesečnim zamikom. Septembra, po obilnem deževnem obdobju, ki se je pričelo konec avgusta, pa je bila zabeležena najvišja vrednost $\delta^{18}O$ v vzorčnem mestu RV-3. Predpostavljamo, do so te padavine po prednostnih poteh povzročile preboj vode z višjo $\delta^{18}O$, ki je bila predhodno uskladiščena v višjih nivojih lizimetra.

Statistične lastnosti $\delta^{18}O$ vzorčenih vod so prikazane grafično s škatlastimi diagrami na sliki 5. Glede na padavine imajo vode zgornjih nivojev lizimetra (I, II in III) največje razpone vrednosti, kar odseva intenzivno dinamiko in s tem kratek zadrževalni čas. Nihanje parametra je veliko bolj dušeno v spodnjem delu lizimetra (nivoji IV, V in VI), kar odseva manj intenzivno dinamiko in daljši zadrževalni čas.

Letne in sezonske tehtane vrednosti $\delta^{18}O$ vzorčnih mest so razvidne iz tabel 1 in 2. Dodatno tabeli 1 in 3 prikazujeta še deleže letnega oziroma sezonskega dotoka vode v vzorčna mesta. Iz tabel je mogoče razbrati, da največja količina vode priteka v vzorčna mesta na nivoju III. Predvideva se, da je to posledica razvoja lateralne komponente toka podzemne vode v bližini kontakta s plastjo sedimentov, ki ima različno strukturo in vključuje tudi glinen material (sl. 3). Posledično se spremeni tudi hidravlična prevodnost, zato le pomembnejši hidrološki dogodki povzročijo vertikalni preboj vode iz nivoja III v nižje nivoje lizimetra.

Rezultati raziskav v urbanem lizimetru Pivovarne Union so izpostavili najpomembnejše faktorje, ki nadzirajo hidrodinamične procese na raziskovanem območju, kjer sta prst in vegetacija odsotna. Fizikalno-kemijske in izotopske lastnosti vode so pokazale, da imajo zaglinjene plasti pomembno vlogo pri hidravličnem obnašanju raziskovanega območja (sl. 4 in 6). Kot posledica batnega efekta se nova padavinska voda in predhodno uskladiščene vode skoncentrirajo nad omenjeno plastjo in pridobijo lateralno komponento toka. Vertikalen preboj vode v nižje plasti nezasičene cone se pojavi po prednostnih poteh le v obdobju intenzivnih padavinskih dogodkov v odvisnosti od volumna predhodno uskladiščene vode. V nezasičeni coni, 3 m pod površjem, je povprečen zadrževalni čas podzemne vode pod takimi pogoji okoli 2 meseca, medtem ko je v zasičeni coni, v globini 30 m, okoli 4 leta.

Urbani lizimeter Pivovarne Union predstavlja odličen poligon za proučevanje specifičnih infiltracijskih in napajalnih procesov v urbanem okolju. Vertikalna komponenta toka podzemne vode ima poglavitno vlogo pri nadzoru prenosa onesnaženja proti virom pitne vode, zato je glavni cilj nadaljnih raziskav proučevanje vertikalne obremenitve podzemne vode z onesnaževali.

Acknowledgement

The author would like to acknowledge the Union Brewery, the European Commission under the Fifth Framework Program and Knet Water, for the financial support of the studies.

References

Auersperger, P., Čenčur Curk, B., Jamnik, B., Janža, M., Kus, J., Prestor, J. & Urbanc, J. 2005: Dinamika podzemne vode. In: Rejec Brancelj, I., Smrekar, A. & Kladnik, D. (eds.): Podtalnica Ljubljanskega polja. Geografija Slovenije, 10: 39–61.

Bračič Železnik, B., Pintar, M. & Urbanc, J. 2005: Naravne razmere vodonosnika. In: Rejec Brancelj, I., Smrekar, A. & Kladnik, D. (eds.): Podtalnica Ljubljanskega polja. Geografija Slovenije, 10: 17–26.

Clark, I. & Fritz, P. 1997: Environmental Isotopes in Hydrogeology, Lewis Publishers: 342 p.

Epstein, S. & Mayeda, T. 1953: Variation of O^{18} content of waters from natural sources. Geochimica et Cosmochimica Acta, 4/5: 213–224, doi:10.1016/0016-7037(53)90051-9.

Gleick, P. 2002: The biennial report on freshwater resources. The World's Water 2002–2003, Washington DC, Island Press: 97-148.

Hoefs, J. 1997: Stable isotope geochemistry. 4th edition. Springer-Verlag, Berlin-Heidelberg: 168 p.

Horita, J., Ueda, A., Mizukami, K. & Takatori, I. 1989: Automatic δD and δ^{18}O analyses of multi-water samples using H_2 and CO_2-water equilibration methods with a common equilibration set-up. Applied Radiation and Isotopes, 40/9: 801–805, doi:10.1016/0883-2889(89)90100-7.

Juren, A., Pregl, M. & Veselič, M. 2003: Project of an urban lysimeter at the Union brewery, Ljubljana, Slovenia. RMZ - Materials and Geoenvironment, 50/3: 153–156.

McDonnell, J.J., Bonell, M., Stewart, M.K. & Pearce, A.J. 1990: Deuterium variations in storm rainfall: Implications for stream hydrograph separation. Water Resources Research, 26/3: 455–458, doi:10.1029/WR026i003p00455.

Meissner, R., Seeger J., Rupp H., Seyfarth M. & Borg H. 2007: Measurement of dew, fog, and rime with a high precision gravitation Lysimeter. Journal of Plant Nutrition and Soil Science, 170: 335–344, doi:10.1002/jpln.200625002.

Morrison, J., Brockwell, T., Merren, T., Fourel, F. & Philips, A.M. 2001. On-line high-precision stable hydrogen isotopic analyses on nanoliter water samples. Analytical Chemistry, 73/15: 3570–3575, doi:10.1021/ac001447t.

Sampat, P. 2000: Groundwater shock: the polluting of the world's major freshwater stores. World Watch, 10–22.

Trček, B. 2005: Investigations of flow system and solute transport at an urban lysimeter at Union Brewery, Ljubljana, Slovenia. RMZ – Meterials and Geoenvironment, 52/4: 685–696.

Trček, B. 2006: Isotopic investigations in the area of the Union brewery water body. Geologija, 49/1: 103–112, doi:10.5474/geologija.2006.008

Trček, B. & Juren, A. 2007: Flow and solute transport monitoring at an urban lysimeter of Union brewery, Ljubljana, Slovenia. In: Howard, K.W.F. (ed.): Urban groundwater - meeting the challenge: selected papers from the 32nd International Geological Congress (IGC), Florence, Italy. Taylor & Francis, London: 19–28.

Trček, B., Petauer, D., Leis, A., Harum, T. & Juren, A. 2010: Sustainable management of the Union Brewery groundwater resources, Ljubljana (Slovenia). Steirische Beiträge zur Hydrogeologie, 57: 71–85.

Trček, B, Auersperger, P., Leis, A. & Sültenfuss, J. 2013: Risk assesment of an urban aquifer based on environmental tracers. Geologija, 56/1: 97–106, doi:10.5474/geologija.2013.008.

Uhan, J. & Krajnc, M. 2003: Podzemna voda. In: Uhan, J. & Bat, M. (eds.): Vodno bogastvo Slovenije. ARSO, Ljubljana: 55-66.

Vižintin, G., Souvent, P., Veselič, M. & Čenčur Curk, B. 2009: Determination of urban groundwater pollution in alluvial aquifer using linked process models considering urban water cycle. Journal of Hydrology, 377/3–4: 261–273, doi:10.1016/j.jhydrol.2009.08.025.

Von Unold, G. & Fank, J. 2008: Modular design of field lysimeters for specific application needs. Water, Air & Soil Pollution, 8/2: 233–242, doi:10.1007/s11267-007-9172-4.

Zupanc, V., Bračič-Železnik, B. & Pintar, M. 2005: Water balance assessment for lysimeter station based on Water Pumping Station Kleče in Ljubljana. Acta Agriculturae Slovenica, 85/1: 83–90.

Zupanc, V., Nolz, R., Cepuder, P., Bračič-Železnik, B. & Pintar, M. 2012: Determination of water balance components with high precision weighing lysimeter in Kleče. Acta Agriculturae Slovenica, 99/2: 165–173, doi:10.2478/v10014-012-0016.

GEOLOGIJA *60/2*, 279-295, Ljubljana 2017
https://doi.org/10.5474/geologija.2017.020

Upper Carnian Clastites from the Lesno Brdo Area (Dinarides, Central Slovenia)

Zgornjekarnijski klastiti z območja Lesnega Brda (Dinaridi, osrednja Slovenija)

David GERČAR[1], Ajda KOCELI[2], Andreja ZALOŽNIK[3] & Boštjan ROŽIČ[4]

[1]Doslovče 2, 4274 Žirovnica, SI-1000 Slovenia; e-mail: gercar.david@gmail.com
[2]Podvin 205, SI-3310 Žalec, Slovenia
[3]Cesta na Gorenje 3, SI-3214 Zreče, Slovenia
[4]Faculty of Natural Sciences and Engineering, University of Ljubljana, Aškerčeva 12, SI-1000 Ljubljana, Slovenia

Prejeto / Received 8. 5. 2017; Sprejeto / Accepted 22. 11. 2017; Objavljeno na spletu / Published online 22. 12. 2017

Key words: External Dinarides, Lesno Brdo, Carnian, Tuvalian clastites, carbonate concretions

Ključne besede: Zunanji Dinaridi, Lesno Brdo, karnij, tuval, klastični sedimenti, karbonatna konkrecija

Abstract

This paper presents a detailed study of the Tuvalian clastic member in the Lesno Brdo Area in Central Slovenia (External Dinarides). The member represents the uppermost part of the mixed siliciclastic – carbonate Carnian succesion that overlays the carstified emersion surface on top of the “Cordevolian” limestone and dolomite. The Tuvalian member is composed of red and violet sandy mudstone and marlstone that are interbedded with sandstone and gravelly sandstone. Calcite concretions are common, particularly in mudstone and marlstone. The succession was deposited on the flood plain, where fine-grained flood sediments are interrupted by medium- to coarse-grained crevasse splay sandstone and cross-stratified gravely sandstone of the small river channels. Alternatively, this succession could have been deposited in the distal zone – terminal splay/fan sediments. According to paleogeographic subdivison we suggest that the provenance area was located to the south, where carbonates, volcanoclastites/vulcanites as well as clastites were eroded.

Izvleček

V pričujočem članku je opisana litološka sestava t.i. tuvalskega klastičnega člena iz okolice Lesnega Brda v osrednji Sloveniji. Člen predstavlja zgornji del paketa karnijskih karbonatnih in klastičnih kamnin, ki prekrivajo kraško-erozijsko diskordanco na vrhu »cordevolskega« apnenca in dolomita. Tuvalski klastični člen sestavljajo rdeči do vijoličasti rahlo peščeni muljevci, oziroma laporovci, z vmesnimi plastmi apnenčevih polilitičnih peščenjakov in prodnatih peščenjakov. Predvsem drobnozrnati različki kamnin vsebujejo kalcitne konkrecije. Zaporedje je bilo odloženo na poplavni ravnici, kjer prevladujoče drobnozrnate poplavne sedimente prekinjajo vmesne plasti srednje do debelozrnatih peščenjakov prebojnih pahljač in navzkrižno laminiranih prodnatih peščenjakov manjših rečnih korit. Alternativno bi se to zaporedje lahko odložilo na območju zaključnih vršajev. Glede na takratno paleogeografijo sklepamo, da je bilo izvorno območje sedimenta na jugu, kjer so bile razgaljene in erodirane predvsem karbonatne, vulkanoklastične in tudi klastične kamnine.

Introduction

The Middle and Upper Triassic in the External Dinarides is dominated by thick dolomite and subordinate limestone successions that are, following the Carnian regional emersion and the formation of bauxite, interrupted by mixed clastic-carbonate series (Dozet, 1979; Jelen, 1990; Dozet, 2004; Celarc, 2004, 2008; Dozet, 2009; Čar, 2010). In the Lesno Brdo Area, located 15 km southwest of Ljubljana, the succession is composed of the lower clastic member, a middle limestone member and an upper clastic member Julian in age, overlain by carbonate and siliciclastic members that are Tuvalian in age. So far, only the Julian beds with rich bivalve macrofauna and microfossils have been investigated in this part of the succession (Jelen, 1990). Oblak (2001) also analysed the foraminiferal assemblage in the Julian limestone member. Up above, the Carnian succession passes into the Norian-Rhaetian Main Dolomite (Grad & Ferjančič, 1974; Jelen, 1990).

With the exception of the paleontological work in the Julian carbonate rocks, the thick succession of younger clastics was poorly studied. In this paper, we present a sedimentological analysis of the Tuvalian clastic member, the succession of which is well exposed along the road that connects the villages of Lesno Brdo and Drenov Grič with the village of Zaklanec.

Geological Setting

Structurally, the Lesno brdo area belongs to the External Dinarides (Fig. 1), more precisely to the Hrušica Nappe, which are characterized by a post-Eocene Dinaric thrusting phase with compression running in the northeast-southwest direction (Placer, 1999, 2008). In central and western Slovenia, the External Dinarides are composed predominantly of thick carbonate successions interbedded by Ladinian volcanoclastics and Carnian siliciclastics (Buser, 2010). The Carnian succession in the Lesno Brdo – Drenov grič area was investigated by Jelen (1990) (Figs. 2 and 3). According to his stratigraphic subdivision, the Carnian succession of the area starts with "Cordevolian" grey coarse-sparry dolomite and micritic limestone with an erosional unconformity on top. Above follow the Julian lower clastic member, Julian middle limestone member, and Julian upper clastic member (Jelen, 1990). The lowermost member is deposited on the macro-paleorelief; bauxite is locally present on its base (Dozet, 1979; Celarc, 2008; Ogorelec, 2011). The Tuvalian succession starts with the carbonate member composed of various limestones and terminates with the Tuvalian clastic member, which was investigated and presented herein. Jelen (1990) described this member as massive and shaley mudstone, violet-red multi-coloured sandstone and conglomerate with quartz pebbles. Upwards, it passes through transitional beds into the Norian-Rhaetian Main Dolomite.

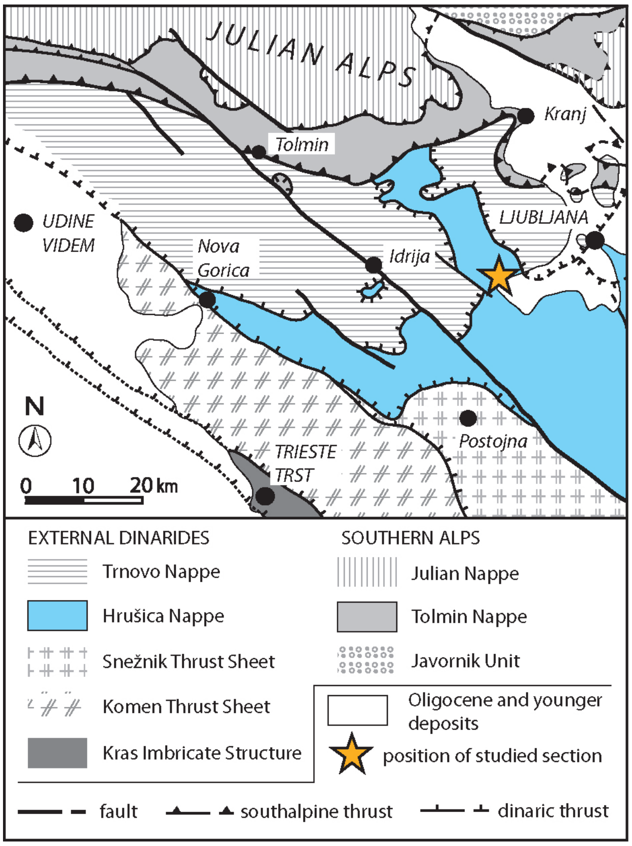

Fig. 1. Macrotectonic emplacement of the investigated area (modified from: Placer, 2008).

Methods

The sedimentological section at 1:50 scale was logged along the road that connects the villages of Lesno Brdo and Drenov grič with the village of Zaklanec (E 14°19'25", N 46°0'15"). During the logging, samples of coarse-grained clastites were taken with the aim of making thin sections and samples of fine-grained clastites for the XRD and geochemical analysis. Apart from host-rock samples, several samples of carbonate concretions were taken, from which two thin sections were made. On one such sample XRD and geochemical analysis was performed.

The nomenclature of clastics is based on their structure (for example: gravelly sandstone) and the naming of their composition-based classification (for example: quartz-polilithic gravelly sandstone).

The mineral compositions of three samples of fine-grained clastites and one sample of carbonate concretions were determined using a Panalytical PW 3830/40 XRD device, which uses a PW 1820 goniometer and a PW3830 X-ray generator, with copper tube PW 2273/20 under an electric current of 30 mA and a voltage of 40 kV. Difractograms were analysed with use of X'pert HighScore Plus software, together with the PAN - ICSD database for mineral determinations. For the geochemical analysis we used a Thermo Niton XL3t 900S-He Series Analyzer XRF device. For the elemental analysis a "mining" filter was used.

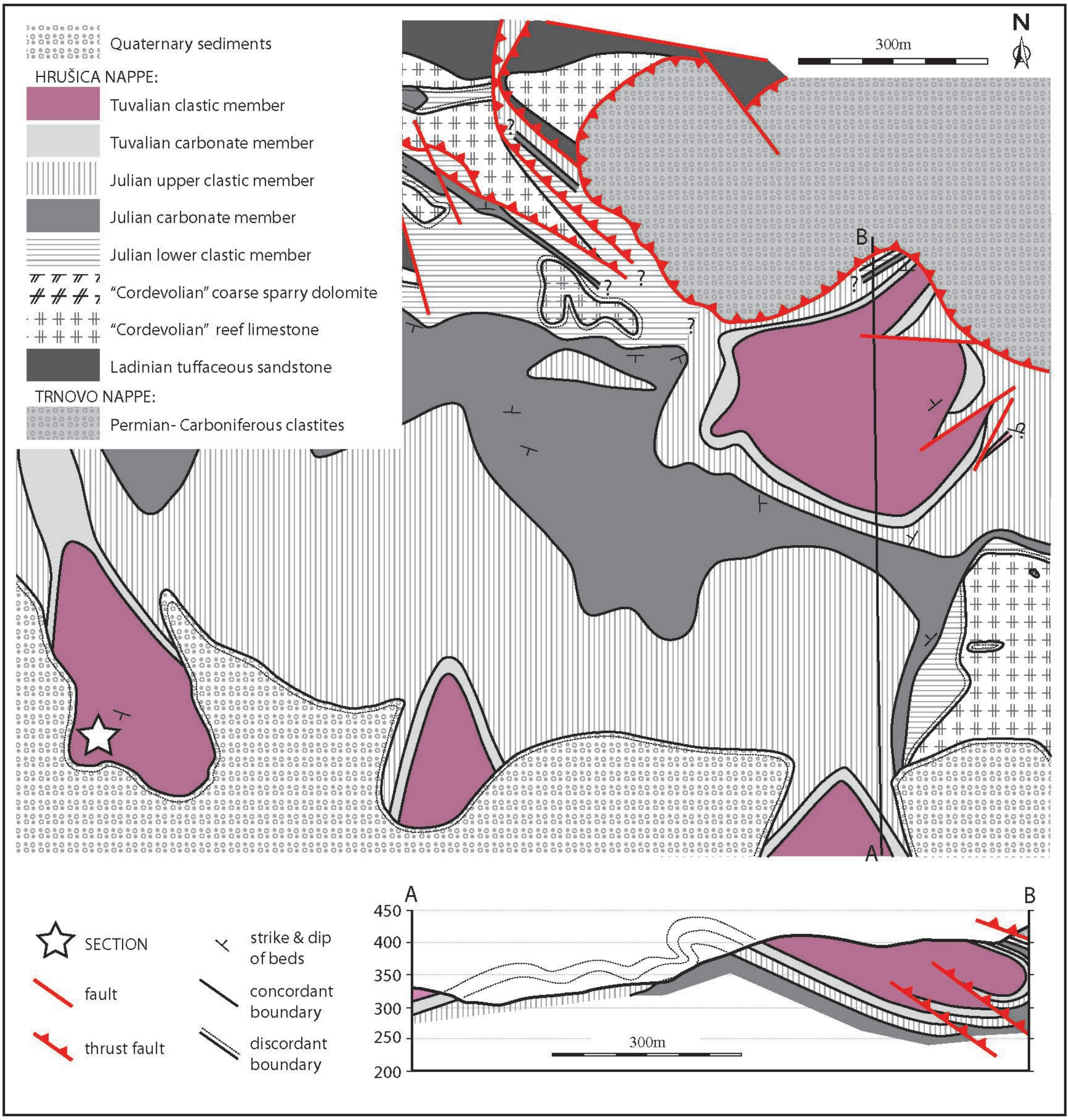

Fig. 2. Geological map and cross-section of the surrounding area and the location of the investigated section marked by a star (modified from: Jelen, 1990).

Description of Lesno Brdo section

The overall thickness of the section is 39 meters, with minor covered intervals between the 12th and 14th meter of the section (Fig. 3). The beds dip 20 degrees south–southwest. Through the entire section slightly sandy mudstone and marlstone prevail, which are coloured red and violet, but sporadic grey to greyish-green intervals also occur. The lower 15 meters of the section contain interbedded sandstone and gravelly sandstone, up to 60 cm thick (Fig. 4a). These beds are also coloured, mostly red and violet. Sandstone is deposited mostly in channels several meters wide and often exhibits cross lamination. An interbed between the 10th and 11th meter of the section shows clear normal grading. The number of gravelly-sandy interbeds decreases upwards along the section. Similarly, a lower sand content in the marlstone/mudstone is observed. Carbonate concretions are common largely in the lower 8 meters of the section. They appear in fine-grained as well as coarser- grained rocks. Upwards they occur only sporadically – locally between the 15th and 22th meter, and at the 26th and 38th meter of the section.

Fig. 3. Carnian succession of the Dinaric Carbonate Platform at Lesno Brdo (modified from: JELEN, 1990) with an investigated section of the Tuvalian clastic member.

Microfacies of the clastites

From the coarse-grained clastites we provide description of gravelly sandstones and fine- to medium-grained sandstones (Figs. 4b-e), and sandy mudstones/marlstones are described separately. Herein, we emphasise that the transitions between the described varieties are gradual.

(Quartz) carbonate lithic and poly-lithic gravelly to slightly gravelly sandstone

Most samples contain up to 60 % of grains, which are bounded by a fine-grained matrix (Fig. 4b) and in some rare cases, also by drusy mosaic and bladed calcite cements. The grain-size varies between 0.1 and 6 mm, with up to 30 % of grains larger than 2 mm. Two grain-size classes prevail – the first between 0.2 and 0.5 mm, and the second approximately 1.5 mm. Rocks are medium- to well-sorted, in some cases also poorly sorted. Grains are predominantly subrounded to subangular, and are in point, concavo-convex and occasionally sutured contacts and immature to semi-mature in texture. Beds are often normally graded.

The composition remains almost unchanged along the entire studied section, but we do find some minor variations, predominantly in the quantitative relationship between particular grain-types. The most common are carbonate lithoclasts, among which recrystallized micritic to microsparitic limestones with common partial replacement by opaque minerals, probably iron oxides, prevail. Some grains are entirely composed of opaque minerals. The surroundings of such grains (crystals) often show a red zoning coloring. Rarer but still present are darker micritic lithoclasts, which often appear in irregular shapes. Locally, the margins of these lithoclasts show silification, and some also show micritic coverings. Next in terms of abundance are quartz grains, grains of opaque mineral, feldspars and micas. Above the 10^{th} meter of the section lithoclasts of granitoid volcanic rocks are also common. Quartz grains can be subdivided into the following groups: A) monocrystal quartz grains, B) simple polycrystal quartz grains, and C) microcrystal quartz grains with or without mica. In most cases, such grains are likely recrystallized matrixes of granitoid volcanic rocks, whereas some grains could also be chert lithoclasts.

Among the cements, the most common are intergranular drusy mosaic and bladed calcitic cements. Corrosive carbonate cements, which substitute and obliterate the primary structure of quartz grains, are also present.

Quartz poly-lithic and carbonate lithic fine-to medium-grained sandstone

Samples contain some 60 % of grains, with intergranular spaces filled largely by a fine-grained matrix and in rare cases, also by drusy mosaic and bladed calcite cements. Grain-size varies between 0.05 mm and 2 mm, where most grains fall into size-classes of around 0.1 mm and 0.5 mm. Rocks are medium- to well-sorted, whereas grains are mostly subangular to subrounded. Grains are predominantly in concavo-convex and point contacts, while some grains are also floating. Rock texture is immature to semi-mature.

The composition is similar to the previously described gravelly sandstones, with a quantity of the carbonate lithoclasts. Owing to their smaller grain size the grains that can be definitely described as granitoid volcanics are also less common.

Quartz poly-lithic sandy mudstone or marlstone

The sample is composed of 35 % of grains in a fine-grained matrix. Most grains fall within the size-class of mud, and only some 30 % grains are between 0.06 and 0.4 mm in size. Grains are predominantly subrounded and floating, but rare point and concavo-convex contacts also appear. The studied sample is poorly sorted and immature in texture.

Among the grains the monocrystal quartz grains and carbonate lithoclasts prevail. Other, less frequent grains belong to polycrystal quartz, opaque mineral, feldspars micas and very rare lithoclasts of granitoid volcanic rock.

Microfacies of calcitic concretions

Concretions are composed of calcite (see also next chapter) and occur predominantly in fine-grained clastites (Figs. 5a-5b) in the lower part of the section, and rarely also present higher up. The outer margins of the concretions form irregular/nodular surfaces. Concretions consist mostly of fine-crystaline microsparite, whereas the size of crystals increases gradually and irregularly towards their interiors. These include rare, unreplaced quartz grains. Concretions are dissected by variously oriented fractures that

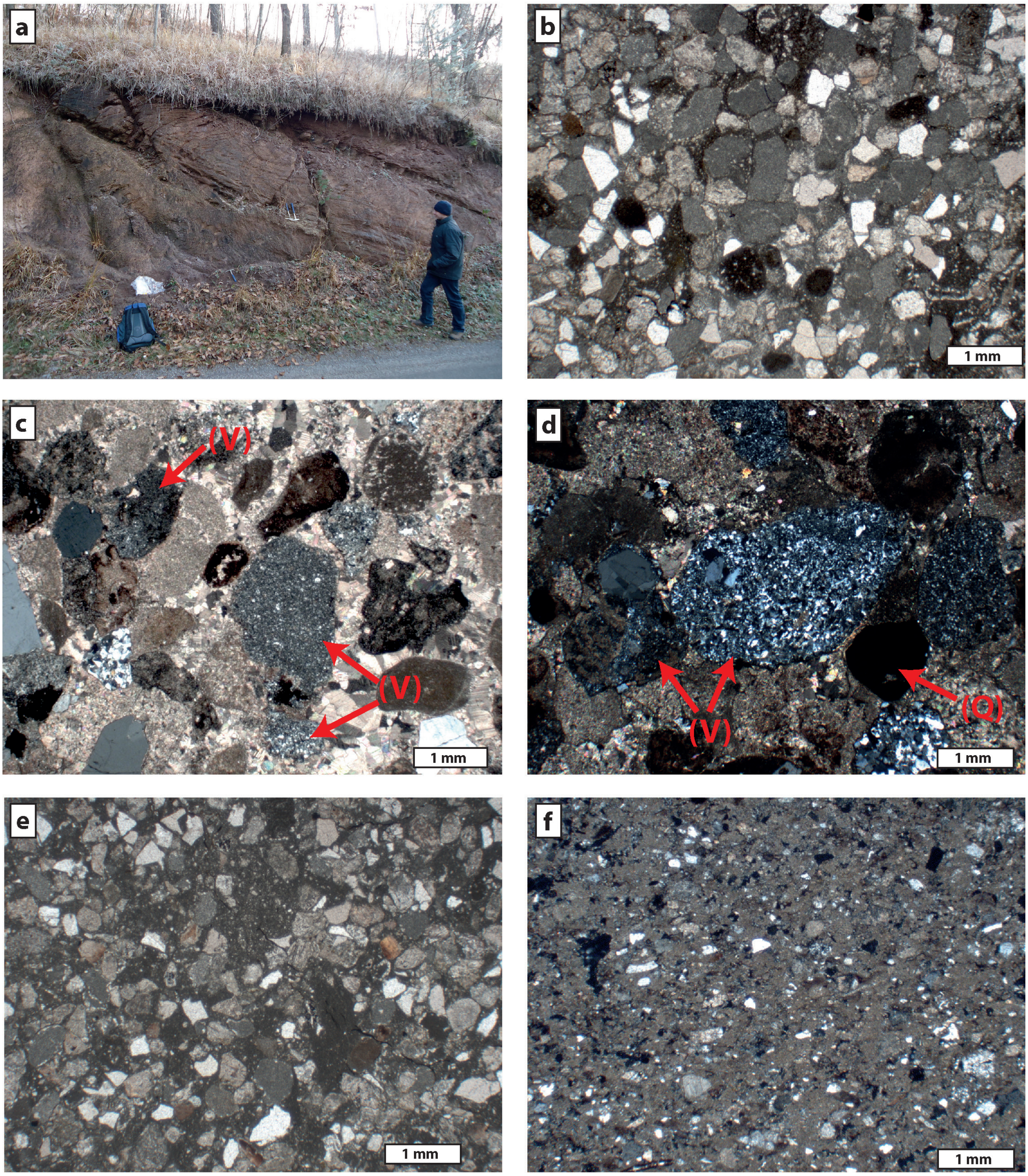

Fig. 4. Facies of the Tuvalian clastic member at Lesno Brdo. **a**) Lower part of the section in which sandy marlstone is interbedded with channels of gravelly sandstone. **b**) Medium- grained sandstone with quartz grains and carbonate lithoclasts. **c**) medium- to coarse-grained sandstone with various carbonate lithoclasts, quartz grains and lithoclasts of vulcanics (V); some carbonate grains contain opaque mineral (cross-polarized light). **d**) Pebbly sandstone with lithoclasts of vulcanics (V) with microcrystalline matrix and quartz and feldspar phenocrysts; various carbonate lithoclasts are also present; in the lower--right corner of the micrograph a monocrystal quartz grain is marked (Q) (cross-polarized light). **e**) Fine- to medium-grained sandstone composed predominantly of carbonate lithoclasts and monocrystal quartz grains; at margins of particular carbonate grains thin monocrystal quartz occurs. **f**) Sandy siltstone in which some grains up to 0.2 mm are visible – mostly quartz, carbonate lithoclasts and some lithoclasts of vulcanics (cross-polarized light).

form a complex network. They are filled predominantly by mosaic sparite, and in the marginal parts the surrounding sediment can be infiltrated in them. Sparite-filled fractures can occur also on the contact surface between concretion and sediment. Cement in this enveloping fracture is prismatic, with individual crystals oriented perpendicular to the concretion margin. This structure appears younger with respect to other fractures, as it also cuts parts where sed-

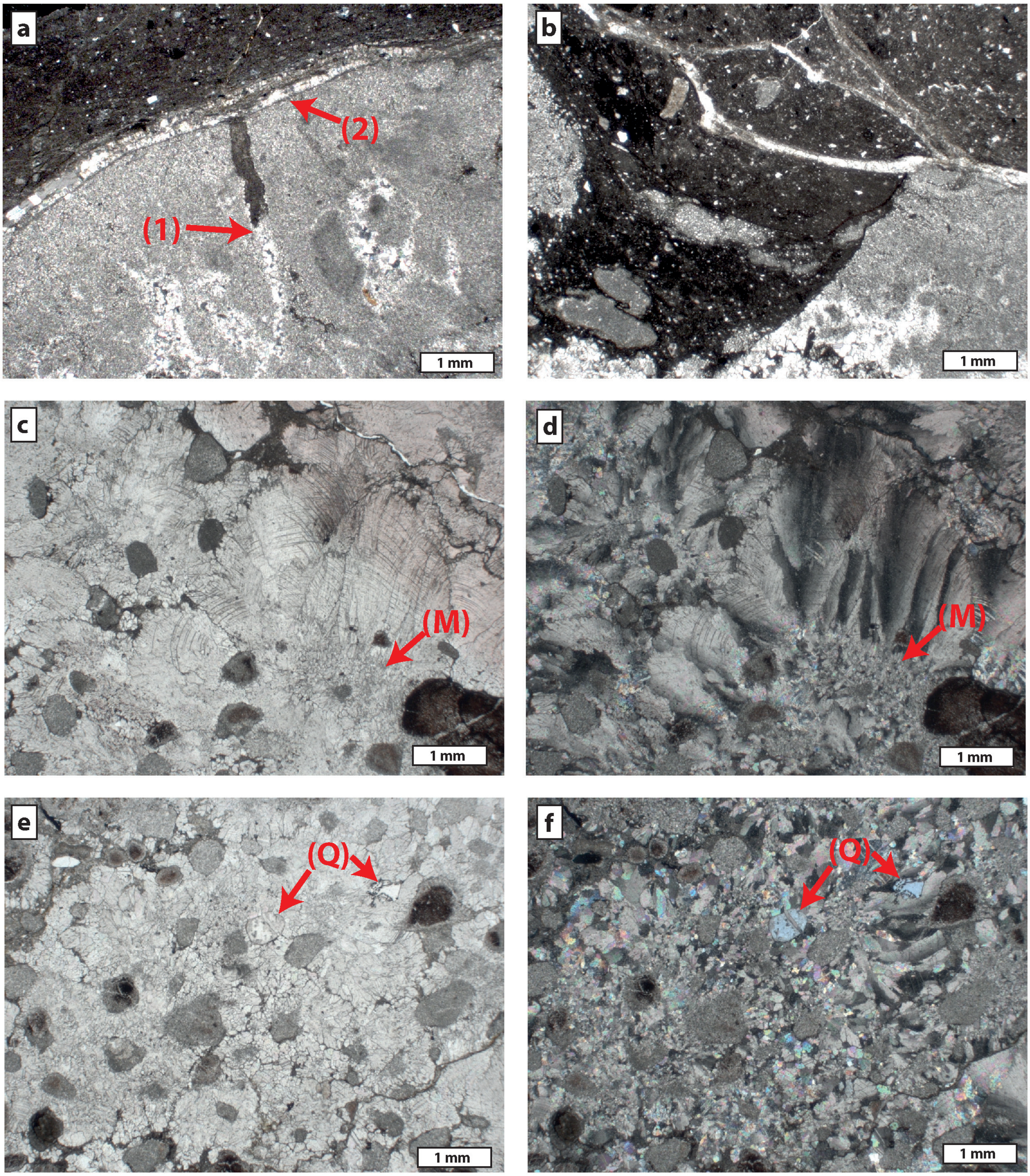

Fig. 5. Facies of the Tuvalian clastic member at Lesno Brdo. **a**) Concretion from mudstone/marlstone composed of microsparite, but irregular enlargement of crystals towards the center is also visible; in the center is a fracture filled mostly with mosaic cement (1), whereas in the marginal part it is infiltrated by sorrounding sediment; a younger generation of fractures (2) runs parallel to the margin of the concretion and is filled with prismatic cement. **b**) Concretion from mudstone/marlstone: signs of compaction – bending of laminae in the surrounding sediment and the younger generation of fractures in the part where the sediment is embedded deeper into the concretion **c**) Concretion from sandstone: larger carbonate lithoclasts are still visible, whereas the fine-grained fraction is replaced by radiaxial bladed cement; mosaic cement (M) is also present **d**) Figure 5c under cross-polarized light. **e)** Concretion from sandstone with recognisable carbonate lithoclasts as well as quartz grains; (Q) grains are bounded mostly by mosaic cement. **f)** Figure 5e under cross-polarized light.

iment infiltrates the fractures. The surrounding sediment is sandy mudstone, which on irregular contact with concretion shows signs of intense compaction, such as bended laminas and dissolution seams in the vicinity of the contact.

Calcite concretions occur rarely also in the more coarse-grained clastites (Figs. 5c-5f) and show more complex internal composition. In such concretions the primary texture and their composition only partially are still visible. Most recognizable are quartz grains and carbonate grains impregnated with opaque mineral. Some other carbonate grains are also visible, but they are mostly recrystallized into microsparite. In parts of the thin-section where the primary packing was denser, the intergranular space is filled with mosaic cement. In parts with looser primary packing the intergranular spaces are made of very coarse-crystalline radiaxial bladed calcite cement. The transition between the described textural types of concretion is gradual.

Mineral and geochemical composition

Mineralogical analysis was elaborated on three samples of fine-grained clastites and one sample of carbonate concretion. Clastites were sampled at approximately the 4th, 24th and 37th meter of the sections (samples: LB3,8; LB24,0 in LB37,2). The composition of samples taken from the fine-grained clastites is uniform. Samples contain five main minerals: quartz, calcite, hematite, alkaline plagioclase, and muscovite/illite (Fig. 6). Carbonate concretion, taken at approximately the 16th meter of the section (sample: LB15,7), is predominantly composed of calcite, whereas some quartz reflections/peaks were also detected.

Geochemical analysis was made on the same samples as were used for mineralogical analysis. Table 1 one presents concentrations of the main elements (in percentages), whereas Table 2 presents the concentrations of oxides of main elements.

The samples of fine-grained clastites (LB3,8; LB24,0 in LB37,2) show a higher volume of silicium bound to SiO_2 (quartz varieties and silicates). This is followed by calcium as a part of calcite and dolomite. The particularly lower magnesium content indicates the greater presence of calcite with respect to dolomite. Samples also contain iron as part of Fe_2O_3 (hematite). It is visible on the macro level as well as microscopically as a typically red colour of rocks/grains. Samples also contain some aluminium, which is bound in alumosilicates and potassium that is connected to the presence of the muskovite/illite. All three samples contain similar amount-values of their main constitutive elements.

Like fine-grained clastites, the results of mineralogical and geochemical content profiles also correspond to the carbonate concretion sample (Table 1 and Table 2), where the most common elements are calcium and silicon or, written in oxide-form, CaO and SiO_2.

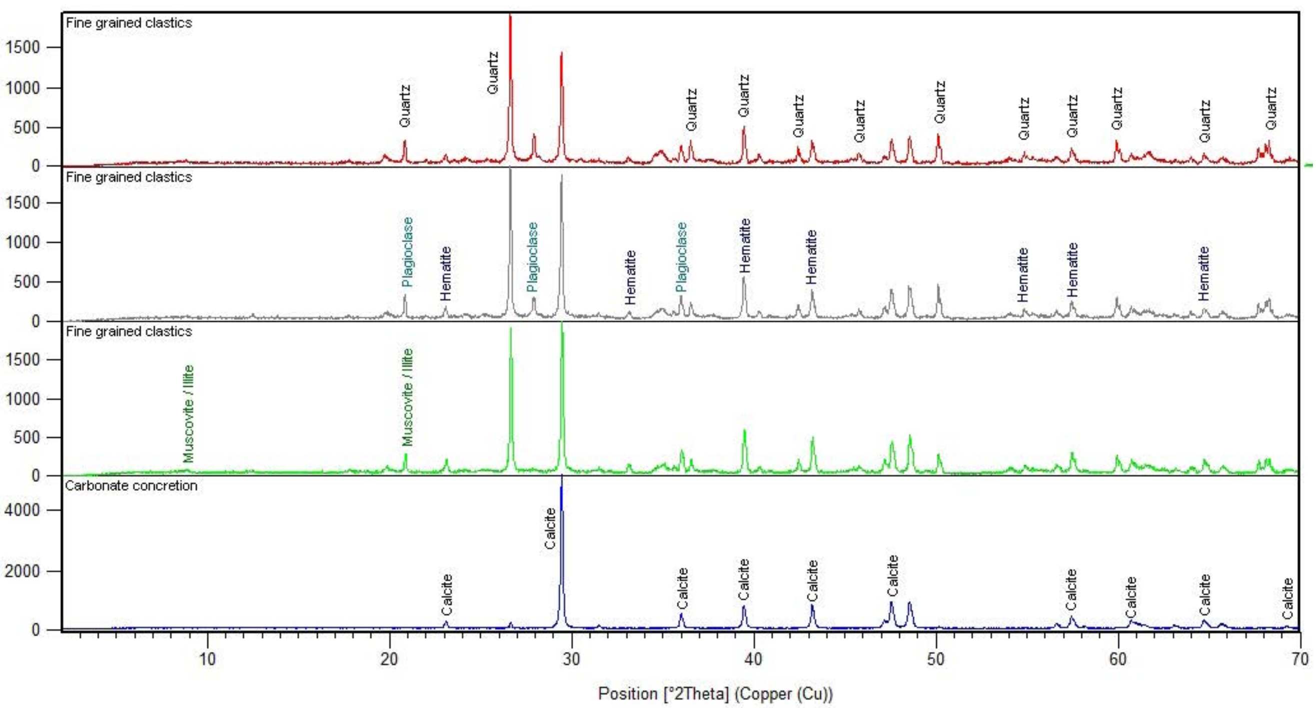

Fig. 6. Diffractograms of fine-grained clastics (upper three) and carbonate concretion (below).

Table 1. Concentration (as percentages) of main-group elements of fine-grained clastics (three upper) and carbonate concretion (below).

Element	Ca	K	Ti	Al	Mg	Si	Fe
LB 3.8	8.56	3.08	0.26	8.44	0.92	22.93	2.83
LB 24.0	14.18	2.24	0.20	6.84	1.14	18.21	2.81
LB 37.2	12.26	2.14	0.23	6.79	0.97	19.74	2.77
LB 15.7	35.86	0.14	0,03	0.89	0.95	2.99	0.63

Table 2. Percentages of main-group element oxides of fine-grained clastics (three upper) and carbonate concretion (below).

Oxide	SiO_2	Al_2O_3	Fe_2O_3	MgO	CaO	K_2O	TiO_2
LB 3.8	49.06	15.94	4.05	1.53	11.97	3.71	0.43
LB 24.0	38.95	12.93	4.01	1.90	19.84	2.70	0.34
LB 37.2	42.24	12.84	3.96	1.61	17.16	2.57	0.38
LB 15.7	6.39	1.68	0.91	1.57	50.17	0.17	0.05

Sedimentary analysis of Lesno Brdo section

The studied succession is composed exclusively of clastic rocks, where fine-grained clastics (sandy mudstones/marlstones) prevail and are interbedded with (quartz) poly-lithic sandstones and gravelly sandstones. The composition of clastics is indicative of continental sedimentation, whereas facies, structure and texture emplace the studied section in an alluvial environment, most probably a floodplain. Fine-grained clastics are suspension sediments of flood events; thin-bedded and structureless sandstones can be described as crevasse-splay deposits, whereas channelized and sometimes cross-laminated gravelly sandstones can be interpreted as deposits of either crevasse-channels or small meandering river channels (Skaberne, 1995; Bridge, 2003; Miall, 2006; Aslan, 2013).

An arid climate, which is typical for the Upper Carnian (Breda et al., 2009; Kiessling, 2010), is indicated in the studied section by a characteristic red to violet rock colour, which is a consequence of the presence of iron in oxide form (hematite), and by the presence of carbonate concretions (Alonso-Zarza, 2003; Khalaf, 2007; Moussavi-Harami, 2009; Breda & Preto, 2011). Given the pronounced arid conditions, the studied section could alternatively be interpreted as terminal fan deposits of a dryland river system with a diminishing discharge down-flow, causing a transition from a channelized to an unconfined flow (Nichols & Fisher, 2003).

Like the sedimentation on terminal fans, was interpreted a comparable Travenanzes Formation of the Dolomites was interpreted (Breda et al., 2009; Breda & Preto, 2011; Preto et al., 2015), where based on the overall analysis of far-better exposed Tuvalian rocks the authors presented a comprehensive sedimentological/facies model (Fig. 7). The southernmost facies zone A, in which also the Lesno Brdo studied section could be emplaced, is characterized by meandering dry-land rivers concluding in terminal fans. This zone passes through sabkhas and tidal flats of facies zone B to facies zone C with restrictive lagoons and sub-tidal marine environments. The Travenanzes Formatian is also characterized by the presence of carbonate concretions, mostly dolocretes. Preto and colleagues (2015) consider a dolomite as a primary diagenetic mineral. In contrast to carbonate concretions of the Travenanzes Formation, at Lesno brdo these are composed of calcite. In the future, it would be worthwhile making additional geochemical and mineralogical analyses with the aim of defining their formation more precisely.

The direction of transport cannot be distinguished from the data on the Lesno Brdo section, but taking into consideration the paleogeographic reconstruction of the Upper Triassic, where the deep marine Slovenian Basin was located to the north (Buser, 1989; Gale, 2010; Gale at al., 2012; 2016), we conclude that the sediment source-area was generally located to the south (present-day orientation). The composition of sediments indicates that in the hinterland, i.e. the provenance area of clastites, outcropping rocks were carbonates, volcanoclastites/vulcanites and possibly also clastites. Some grains, like those composed of coarse sparite or opaque mineral, could be of pedogenic origin. An intense pedogenesis and formation of carbonate and iron concretions occurred on the dried flood plain, which was followed by deflation, fragmentation of these into smaller grains, and redeposition by wind within a series of diverse sub-environments (Breda & Preto, 2011).

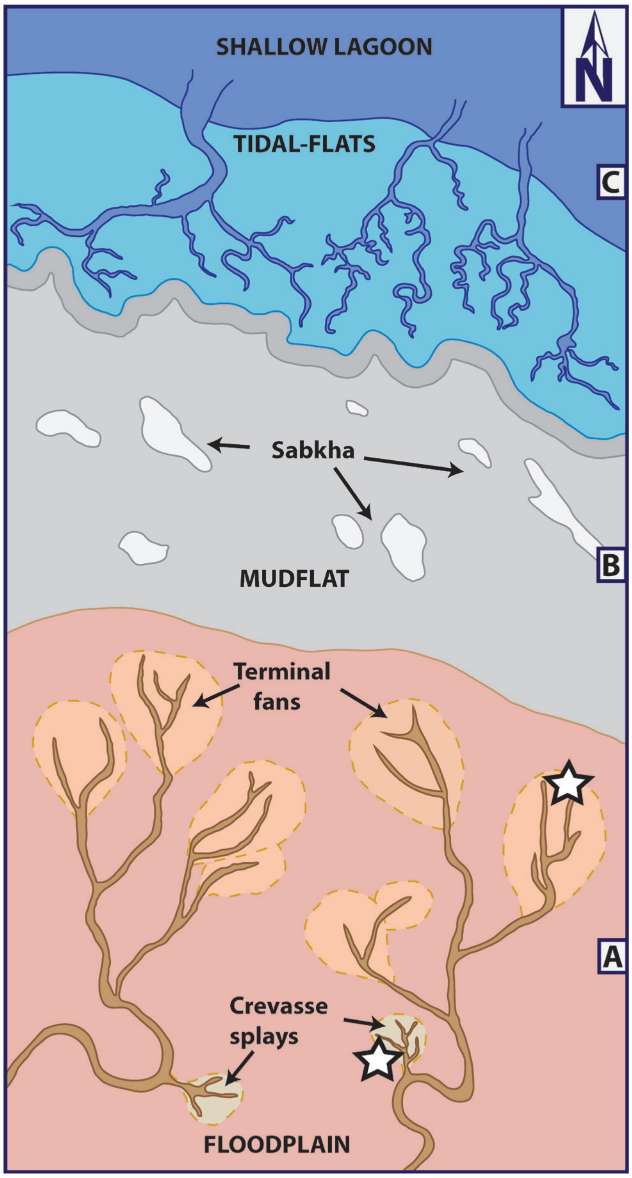

Fig. 7. Schematic paleoenvironmental reconstruction of the Travenanzes Formation (modified from Breda & Preto, 2011) A = aluvial plain with river channels, terminal fans, crevasse splays and a flood plain; B = Mudflat and coastal sabkha; C = Carbonate tidal flats and shallow lagoons. The stars mark the two most likely locations of the Lesno Brdo area.

Conclusions

The studied upper Carnian (Tuvalian) succession from the Lesno Brdo area consists of red and violet slightly sandy mudstone and marlstone, which are interbedded with sandstone and gravelly sandstone. Facies association is typical for sedimentation of flood plain deposits interrupted by medium- to coarse-grained sediments of crevasse splay or terminal fans, and less commonly of small-scale river channels. The composition indicates that in the (south-located) source area carbonate, volcanoclastic and siliciclastic rocks were eroded, while some grains could be of pedogenic origin.

Correlation with the sedimentological model of Tuvalian strata from the Dolomites in Italy (Travenanzes Formation) puts our section within facies zone A, which is characterized by sediments from flood plains, meandering river beds, crevasse splays and terminal fans. The presence of hematite and carbonate (calcite) concretions indicates an arid continental climate during the process of deposition.

Acknowledgments

This investigative research was financially supported by pedagogical funds from the Department of Geology and funds from the Geochemical and Structural Processes research group. We sincerely thank Dragomir Skaberne for consultations with him about microfacies. Unknown reviewers are acknowledged for their thorough review of the manuscript, and Ema Hrovatin and Miran Udovč for all of their technical support.

References

Alonso-Zarza, A. M. 2003: Palaeoenvironmental significance of palustrine carbonates and calcretes in the geological record. Earth-Science Reviews, 60: 261-298.

Aslan, A. 2007: Fluvial Environments: Sediments. In: Elias, S.A. (ed.): Encyclopedia of Quaternary Science. Royal Holloway, University of London: 672–685.

Breda, A. & Preto, N. 2011: Anatomy of an Upper Triassic continental to marginal marine system: the mixed siliciclastic – carbonate Travenanzes Formation (Dolomites, Northern Italy). Sedimentology, 58: 1613-1647.

Breda, A., Preto, N., Roghi, G., Furin, S., Meneguolo, R., Ragazzi, E., Fedele, P. &

Gianolla, P. 2009: The Carnian pluvial event in the Tofane Area (Cortina D'Ampezzo, Dolomites, Italy). Geo. Alp, 6: 80-115.

Bridge, J.S. 2003: Rivers and Floodplains: Forms, Processes, and Sedimentary Record. Wiley-Blackwell: 504 p.

Buser, S. 1989: Development of the Dinaric and Julian carbonate platforms and the intermediate Slovenian basin (NW-Yugoslavia). In: Carulli, G.B., Cucchi, F. & Radrizzani, C.P. (eds.): Evolution of the Karstic carbonate platform: relation with other periadriatic carbonate platforms. Mem. Soc. Geol. Ital., 40: 313-320.

Buser, S. 1996: Geology of western Slovenia and its paleogeographic evolution. In: Drobne, K., Goričan, Š. & Kotnik, B. (eds.): The role of Impact Processes in the Geological and Biological Evolution of Planet Earth. International workshop, ZRC SAZU: 111-123.

Celarc, B. 2004: Problematika »cordevolskih« apnencev in dolomitov v slovenskih Južnih Alpah. Geologija, 47/2: 139-149, doi:10.5474/geologija.2004.011

Celarc, B. 2008: Karnijski boksitni horizont na Kopitovem griču pri Borovnici – ali je v njegovi talnini »pozabljena« stratigrafska vrzel? Geologija, 51/2: 147-152, doi:10.5474/geologija.2008.015

Čar, J. 2010: Geološka zgradba idrijsko-cerkljanskega hribovja. Tolmač h Geološki karti idrijsko-cerkljanskega hribovja med Stopnikom in Rovtami v merilu 1:25.000 = Geological Structure of the Idrija - Cerkno hills : explanatory book to the Geological map of the Idrija - Cerkljansko hills between Stopnik and Rovte 1:25.000. Geološki zavod Slovenije, Ljubljana: 127 p.

Dozet, S. 1979: Karnijske plasti južno in zahodno od Ljubljanskega barja, Carnian beds south and west of the Ljubljana Moor. Geologija, 22: 55-70.

Dozet, S. 2004: O Karnijskem oolitnem železnatem boksitu Kopitovega griča ter o plasteh v njegovi talnini in krovnini, On Carnian oolitic iron bauxite of the Kopitov grič and on beds in its foot- and hanging walls. RMZ – materiali in geookolje, 51/4: 2191-2208.

Dozet, S. 2009: Mohorje Formation, Souther Slovenia, Mohorska formacija, južna Slovenija. Geologija, 52/1: 11-20, doi:10.5475/geologija.2009.002.

Grad, K. & Ferjančič, L. 1974: Osnovna geološka karta SFRJ. L33-65, list Kranj 1:100 000. Beograd: Zvezni geološki zavod.

Folk, R. L. 1980: Petrology of Sedimentary Rocks. Hemphill Publishing Company, Austin: 182 p.

Gale, L. 2010: Microfacies analysis of the Upper Triassic (Norian) "Bača Dolomite": early evolution of the western Slovenian Basin (eastern Southern Alps, western Slovenia). Geologica Carpathica, 61/4: 293-308, doi:10.2478/v10096-010-0017-0.

Gale, L., Kolar-Jurkovšek, T., Šmuc, A. & Rožič, B. 2012: Integrated Rhaetian foraminiferal and conodont biostratigraphy from the Slovenian Basin, eastern Southern Alps. Swiss journal of geosciences, 105/3: 435-462, doi:10.1007/s00015-012-0117-1.

Gale, L., Skaberne, D., Peybernes, C., Martini, R., Čar, J. & Rožič, B. 2016: Carnian reefal blocks in the Slovenian Basin, eastern Southern Alps. Facies, 62/4: 1-15, doi:10.1007/s10347-016-0474-8.

Jelen, B. 1990: Karnijska školjčna favna na Lesnem brdu in njen paleobiološki pomen, The Karnian bivalves (Mollusca) from Lesno brdo, Slovenia, NW Yugoslavia and their paleobiological significance. Geologija, 31, 32: 11-127.

Khalaf, F.I. 2007: Occurrences and genesis of calcrete and dolocrete in the Mio-Pleistocene fluviatile sequence in Kuwait, northeast Arabian Peninsula. Sedimentary Geology, 199: 129-139.

Kiessling, W. 2010: Reef expansion during the Triassic: Spread of photosymbiosis balancing climatic cooling. Palaeogeography, Palaeoclimatology, Palaeoecology, 290: 11-19.

Miall, A.D. 2006: The Geology of Fluvial Deposits: Sedimentary Facies, Basin Analysis and Petroleum Geology. Springer, Berlin: 582 p.

Moussavi-Harami, R., Mahboubi, A., Nadjafi, M., Brenner, R.L. & Mortazavi, M. 2009: Mechanism of calcrete formation in the Lower Cretaceous (Neocomian) fluvial deposits, northeastern Iran based on petrographic, geochemical data. Cretaceous Research, 30: 1146-1156.

Nichols, G.J. & Fisher, J.A. 2007: Processes, facies and architecture of fluvial distributary system deposits. Sedimentary Geology, 195: 75-90.

Oblak, K. 2001: carnian Foraminifera from the Kucler quarry at Lesno Brdo (Slovenia). Geologija, 44/2: 305-316, doi:10.5474/geologija.2001.022.

Ogorelec, B. 2011: Mikrofacies mezozojskih karbonatnih kamnin Slovenije. Geologija, 54/2

– dodatek/supplement: 1-136, doi:10.5474/geologija.2011.011.

Placer, L. 1999: Contribution to the macrotectonic subdivision of the border region between Southern Alps and External Dinarides, Prispevek k makrotektonski rajonizaciji mejnega ozemlja med Južnimi Alpami in Zunanjimi Dinaridi. Geologija, 41: 223-255, doi:10.5474/geologija.1998.013.

Placer, L. 2008: Principles of the tectonic subdivision of Slovenia: Osnove tektonske razčlenitve Slovenije. Geologija, 51/2: 205-217, doi:10.5474/geologija.2008.021.

Preto, N., Breda, A., Dal Corso, J., Spötl, C., Zorzi, F. & Frisia, S. 2015: Primary dolomite in the Late Triassic Travenanzes Formation, Dolomites, Northern Italy: Facies control and possible bacterial influence. Sedimentology, 62: 697-716, doi:10.1111/sed.12157.

Skaberne, D. 1980a: Predlog klasifikacije in nomenklature klastičnih sedimentnih kamnin. 1. del, Predlog granulometrijske klasifikacije in nomenklature. Rudarsko-metalurški zbornik, 27/1, 21-46.

Skaberne, D. 1980b: Predlog klasifikacije in nomenklature klastičnih sedimentnih kamnin. 2. del, Predlog klasifikacije po sestavi. Rudarsko-metalurški zbornik, 27/2-3, 205-233.

Skaberne, D. 1995: Rečni sistemi in njihovi sedimentacijski modeli. Geologija, 37, 38: 251-269, doi:10.5474/geologija.1995.010

Zgornjekarnijski klastiti z območja Lesnega Brda (Dinaridi, osrednja Slovenija)

Uvod

Srednje in zgornjetriasno zaporedje na območju Zunanjih Dinaridov predstavljajo predvsem debeli horizonti dolomitov in podrejeno apnencev, katere v karniju po regionalni emerziji in tvorbi boksitov prekinja mešana serija klastičnih in karbonatnih kamnin (Dozet, 1979; Jelen, 1990; Dozet, 2004; Celarc, 2004, 2008; Dozet, 2009; Čar, 2010). Na območju Lesnega Brda, 15 km jugozahodno od Ljubljane, zaporedje predstavljajo julski spodnji klastični člen, julski srednji apnenčevo – lapornati člen, julski zgornji klastični člen, tuvalski karbonatni člen in tuvalski klastični člen. Do sedaj je bila podrobno raziskana le školjčna združba julskih plasti (Jelen, 1990). Oblak (2001) je pozneje v julskem apnenčevo – lapornatem členu določila še foraminiferno združbo. Karnijske kamnine navzgor postopno prehajajo v Glavni dolomit (Grad & Ferjančič, 1974; Jelen, 1990).

Z izjemo omenjenih paleontoloških analiz, predvsem julskih karbonatov, debelo zaporedje klastičnih plasti nad njimi ni bilo deležno podrobnih geoloških raziskav. V članku predstavljamo sedimentološko analizo tuvalskega klastičnega člena, katerega zaporedje je lepo razgaljeno v useku ob cesti, ki povezuje Drenov Grič in Zaklanec.

Geološka umestitev

Raziskovano ozemlje pripada geotektonski enoti Zunanjih Dinaridov (sl. 1), natančneje Hrušiškemu pokrovu, za katero je značilna posteocenska dinarska narivna tektonska faza s kompresijo v smeri severovzhod – jugozahod (Placer, 1999, 2008). Zunanje Dinaride v zahodni in osrednji Sloveniji sestavljajo predvsem debelo zaporedje mezozojskih karbonatnih kamnin, katero v ladiniju in karniju prekinjajo intervali vulkanoklastične in klastične sedimentacije (Buser, 1989, 1996). Karnijsko zaporedje je na območju Lesnega Brda in Drenovega Griča proučeval Jelen (1990) (sl. 2-3). Po njegovi razdelitvi se karnijsko zaporedje ožjega območja začne s »cordevolskimi« sivimi zrnatimi dolomiti in mikritni apnenci. Nad erozijsko diskordanco ležijo julski spodnji klastični člen, srednji apnenčevo – lapornati člen in zgornji klastični člen (Jelen, 1990). Prvi člen je odložen na makropaleoreliefu. Na sami bazi so lokalno prisotni boksiti (Dozet, 1979; Celarc, 2008; Ogorelec, 2011). Tuvalsko zaporedje se začne s karbonatnim členom, katerega sestavljajo raznoliki apnenci, zaključi pa se s tuvalskim klastičnim členom, v katerem se nahaja naš raziskani profil. Jelen (1990) je ta člen opredelil kot masivne in skrilave muljevce, vijolično-rdeče pisane apnenčeve peščenjake in konglomerate s prodniki kremena. Navzgor klastično karnijsko zaporedje preko prehodnih plasti preide v norijsko – retijski glavni dolomit.

Sl. 1. Geotektonska umestitev območja raziskav (prirejeno po Placer, 2008). Glej angleški del prispevka.

Sl. 2. Geološka karta in prerez ožjega območja z lokacijo raziskanega profila označeno z zvezdo (prirejeno po Jelen, 1990). Glej angleški del prispevka.

Metode

Detajlni sedimentološki profil je bil posnet v merilu 1:50 v useku ob cesti, ki povezuje Lesno Brdo, oziroma Drenov grič in Zaklanec (E 14°19'25", N 46°0'15"). Ob snemanju profila so bili nabrani vzorci debelozrnatih kamin, iz katerih so bili narejeni petrografski zbruski, in vzorci drobnozrnatih kamnin, na katerih je bila izvedena rengtenska in kemijska analiza. Poleg tega smo nabrali tudi nekaj vzorcev karbonatnih konkrecij, iz katerih sta bila narejena dva petrografska zbruska. Na enem vzorcu konkrecije je bila prav tako izvedena rentgenska in kemijska analiza. Poimenovanje kamnin temelji na strukturi (npr. prodnati peščenjak) in imenovanju glede na klasifikacijo po sestavi (npr. kremenov polilitični prodnati peščenjak), kot predlaga Skaberne (1980a, b). Mineralna sestava treh vzorcev drobnozrnatih kamnin in enega vzorca konkrecije je bila določena z rentgensko praškovno difrakcijsko metodo (XRD) na napravi Panalytical PW 3830/40. Naprava deluje z goniometrom PW 1820 in generatorjem PW3830, z bakreno cevjo PW 2273/20 pri jakosti toka 30 mA in napetosti 40 kV. Difraktograme smo rešili s pomočjo programa X'pert HighScore Plus, z nameščeno PAN - ICSD podatkovno bazo za določevanje mineralov. Kemijska analiza je bila narejena z rentgensko fluorescenčno spektroskopijo (XRF) na napravi Thermo Niton XL3t 900S-He Series Analyzer. Za merjenje elementne sestave sedimenta je bil uporabljen način »mining«.

Opis profila Lesno Brdo

Skupna debelina raziskanega zaporedja znaša 39 m, z vmesnim pokritim delom med 12. in 14. m (sl. 3). Plasti vpadajo približno proti jugu z vpadom 200/20°. V zaporedju prevladujejo rdeči do vijoličasti peščeni muljevci in laporovci s posameznimi plastmi bolj sivkaste do sivo-zelene barve. Predvsem v prvih 15 m so pogoste do 60 cm debele plasti rdečih do vijoličnih peščenjakov in prodnatih peščenjakov, prav tako prevladujoče rdeče do vijoličaste barve (sl. 4a). Ti peščenjaki so večinoma odloženi v kanalih, širokih do nekaj metrov in imajo pogosto izraženo navzkrižno laminacijo. Plast med 10. in 11. m ima zelo dobro izraženo postopno zrnavost. Številčnost prodnato – peščenih plasti se navzgor po profilu zmanjša, prav tako se niža vsebnost peščene komponente znotraj muljevcev, oziroma laporovcev. Predvsem v prvih 8 m so zelo pogoste kalcitne konkrecije velikosti med 0,5 in 4 cm. Pojavljajo se tako v drobno, kot tudi debelejše zrnatih različkih kamnin. Višje nastopajo le še poredko – lokalno med 15. in 22. m, ter v plasteh nad 26. in nad 38. m profila.

Sl. 3. Shematski stratigrafski stolpec karnijske stratigrafije pri Lesnem Brdu (prirejeno po Jelen, 1990) z umeščenim detajlnejšim sedimentološkim profilom tuvalskega klastičnega člena. Glej angleški del prispevka.

Mikrofacies klastičnih kamnin

Iz bolj debelozrnatih klastičnih različkov podajamo opis prodnatih peščenjakov in drobno do srednjezrnatih peščenjakov (sl. 4b-4e), posebej pa opis peščenih muljevcev oziroma laporovcev. Pri tem poudarjamo, da so prehodi med opisanimi različki postopni.

(Kremenovi) karbonatno litični in polilitični prodnati do malo prodnati peščenjaki

Večina vzorcev vsebuje do 60 % zrn, ki so vezana z drobnozrnato osnovo (sl. 4b), redkeje tudi z medzrnskim druzimozaičnim in stebričastim kalcitnim cementom. Velikost zrn se giblje med 0,1 in 6 mm, do 30 % zrn je večjih od 2 mm. Prevladujoča sta dva velikostna razreda zrn, velikosti med 0,2 in 0,5 mm in približno 1,5 mm. Sortiranost kamnine je srednja do dobra, v posameznih primerih tudi slaba. Prevladujoča oblika zrn je polzaobljena do pologlata, kontakti so točkovni, konkavno konveksni in lahko tudi stiliolitski. Struktura je nezrela do polzrela. Plasti so pogosto normalno postopno zrnate.

Sestava zrn in razmerje med njimi se skozi celoten profil skorajda ne spreminjata, a vseeno so prisotna manjša odstopanja predvsem v količinskih odnosih posameznih vrst zrn. Najpogostejši so karbonatni litoklasti, med katerimi prevladujejo rekristalizirani mikritni do mikrosparitni klasti, v katerih je pogosto prisoten nepresevni mineral – najverjetneje železov oksid. Posamezna zrna so v celoti sestavljena iz nepresevnega minerala. Okolica takih zrn (kristalov) je pogosto conarno rdeče obarvana. Manj pogosti so temnejši mikritni litoklasti, pogosto nepravilnih oblik. Lokalno so ti klasti okremenjeni po robovih. Posamezni karbonatni litoklasti imajo tudi mikritne obloge. Naslednja po pogostosti so zrna kremena, sledijo zrna nepresevnih mineralov, glinencev, sljud in od 10. m zaporedja višje tudi pogosti klasti granitoidnih predornin. Kremenova zrna bi lahko uvrstili v naslednje skupine: A) monokristalna kremenova zrna, B) preprosta polikristalna kremenova zrna in C) mikrokristalni kremen z ali brez lističev sljude; najverjetneje gre za rekristalizirano steklasto osnovo granitoidnih predornin, del teh zrn bi lahko bil tudi roženec.

Med cementi so najpogostejši medzrnski druzimozaični in stebričasti kalcitni cement. Pojavlja se tudi kalcitni korozivni cement, ki nadomešča kremen in s tem zabriše primarno strukturo kremenovih zrn ter otežuje njihovo natančno opredelitev.

Kremenovo polilitični in karbonatno litični drobno do srednje zrnati peščenjaki

Vzorci vsebujejo okoli 60 % zrn, katera povezuje drobnozrnata osnova, redkeje tudi medzrnski druzimozaični in stebričasti kalcitni cement. Velikost zrn se giblje med 0,05 in 2 mm, s tem da večina zrn sodi v velikostni razred od 0,1 do 0,5 mm. Sortiranost kamnine je srednja do dobra, oblika zrn predvsem pologlata do polzaobljena. Kontakti so večinoma konkavno-konveksni in točkovni, najdemo pa tudi lebdeča zrna. Struktura kamnine je nezrela do polzrela.

Sestava je podobna kot v predhodno opisanih prodnatih peščenjakih, s tem da se zniža vsebnost karbonatnih litoklastov. Zaradi manjše zrnavosti je manjša tudi vsebnost zrn, ki jih lahko nedvoumno opredelimo kot litoklaste granitoidnih predornin.

Kremenov polilitični peščeni muljevec, oziroma laporovec

Kamnino sestavlja do 35 % zrn v drobnozrnati osnovi. Večino zrn sodi v velikostni razred mulja, le okoli 30 % zrn je velikih od 0,06 do 0,4 mm. Zrna so večinoma polzaobljena in lebdeča, prisotni so le posamezni točkovni in konkavno – konveksni kontakti. Sortiranost kamnine je slaba, struktura nezrela.

Med zrni prevladujejo zrna monokristalnega kremena in drobni karbonatni litoklasti. Prisotna so tudi posamezna polikristalna zrna kremena, nepresevni minerali, glinenci, sljude in zelo redki litoklasti granitoidne predornine.

Sl. 4. Faciesi tuvalskega klastičnega člena pri Lesnem Brdu. **a**) Spodnji del profila, kjer peščeni laporovec prekinjajo kanali prodnatih peščenjakov. **b**) Srednje zrnati peščenjak z zrni kremena in karbonatnimi litoklasti. **c**) Srednje do debelo zrnati peščenjak z raznovrstnimi karbonatnimi litoklasti, zrni kremena in litoklasti predornin (V); posamezna karbonatna zrna vsebujejo nepreseven mineral. (X-Nikoli). **d**) Prodnati peščenjak z litoklasti predornin (V) z mikrokristalno osnovo, ter vtrošniki kremena in glinencev; prisotni so tudi raznovrstni karbonatni litoklasti. V spodnjem desnem delu je vidno zrno monokristalnega kremena (Q) (X-Nikoli). **e**) Drobno do srednje zrnati peščenjak, katerega sestavljajo predvsem karbonatni litoklasti in zrna monokristalnega kremena. Ob robovih posameznih karbonatnih litoklastov se pojavlja droben mikrokristalen kremen. **f**) Rahlo peščen muljevec, kjer so vidna posamezna do 0,2 mm velika zrna – večinoma kremen, karbonatni litoklasti in posamezni klasti predornin (X-Nikoli). Glej angleški del prispevka.

Mikrofacies kalcitnih konkrecij

Konkrecije so kalcitne sestave (glej tudi naslednje poglavje) in se pojavljajo predvsem v drobnozrnatih klastitih (sl. 5a-5b) v spodnjemu delu profila, redke pa tudi višje. Zunanji robovi konkrecij tvorijo nepravilno/gomoljasto površino. Konkrecije sestavlja predvsem drobnokristalni mikrosparit. Velikost kristalov se proti notranjosti konkrecij postopoma in nepravilno veča. V konkrecijah so vidna tudi redka zrna nenadomeščenega kremena. Konkrecije so razpokane z mrežo različno usmerjenih razpok, ki so večinoma zapolnjene s sparitnim mozaičnim cementom, na zunanji delih konkrecij pa je lahko v njih infiltriran obdajajoči sediment. Sparitne žilice se lahko pojavljajo tudi na stiku med konkrecijo in sedimentom. Cement v tej obdajajoči žilici je prizmatski, s posameznimi kristali orientiranimi pravokotno na rob konkrecije. Ta tekstura je očitno mlajša od preostalih razpok, saj poteka tudi preko dela kjer sediment infiltrira v razpoke. Obdajajoči sediment je peščeni muljevec, ki na stiku z nepravilno površino konkrecije kaže močne znake kompakcije, kot so povijanje lamin ali pojavljanje disolucijskih šivov v bližini stika.

Kalcitne konkrecije se redko pojavljajo tudi v debeleje zrnatih klastitih (sl. 5c-5f). Te kažejo bolj kompleksno notranjo zgradbo. V njih je še vedno vidna prvotna struktura in deloma sestava sedimenta. Najlepše so vidna zrna kremena in karbonatna zrna impregnirana z nepresevnim mineralom. Vidna so tudi nekatera preostala karbonatna zrna, ki so praviloma prekristaljena v mikrosparit. V delih preparata, kjer je prvoten zlog kamnine bolj gost, se med zrni pojavlja mozaični cement. V delih z bolj redkim primarnim zlogom pa prostore med zrni tvori zelo debelo kristalen radialno – žarkovit stebričast kalcitni cement. Prehod med obema opisanima strukturnima tipoma konkrecij je postopen.

Sl. 5. Faciesi tuvalskega klastičnega člena pri Lesnem Brdu. **a**) Konkrecija iz plasti muljevca/laporova, sestavljena iz mikrosparita. Vidno je tudi nepravilno večanje velikosti kristalov proti notranjosti konkrecije. V sredini je razpoka (1), ki je v večji meri zapolnjena z mozaičnim cementom. V obrobnem delu konkrecije je vanjo infiltriran obdajajoči sediment. Mlajša generacija razpok (2) je vzporedna z robom konkrecije in zapolnjena s prizmatskim cementom. **b**) Konkrecija iz plasti muljevca/laporova z znaki kompakcije – povijanje lamin v obdajajočem muljevcu in mlajših generacij razpok na mestu, kjer se sediment zajeda v konkrecijo. **c**) Konkrecija iz peščenjaka: ohranjena so večja karbonatna litoklastična zrna, bolj drobnozrnato frakcijo prvotnega sedimenta pa zamenjuje radialno – žarkovit stebričast cement. Prisoten je tudi mozaični cement (M). **d**) Slika 5c pod navzkrižnimi Nikoli. **e**) Konkrecija iz peščenjaka: prepoznavna so karbonatna litoklastična zrna in tudi zrna kremena(Q). Zrna povezuje predvsem mozaični cement. **f**) Slika 5e pod navzkrižnimi Nikoli. Glej angleški del prispevka.

Mineraloška in geokemična analiza

Naredili smo minerološko analizo treh vzorcev drobno zrnatih klastičnih kamnin in enega vzorca karbonatne konkrecije. Vzorci klastitov so bili vzeti na približno 4., 24. in 37. m profila (LB 3,8; LB24,0 in LB37,2). Mineralna sestava drobnozrnatih klastitov je podobna. Vsebujejo pet glavnih mineralov: kremen, kalcit, hematit, kisli plagioklazi in muskovit/ilit (sl. 6). Vzorec konkrecije, ki je bil vzet približno na 16. m profila (LB15,7), sestavlja predvsem kalcit in v manjši meri kremen. Na istih vzorcih kot mineraloška analiza je bila opravljena tudi geokemična analiza. Tabela 1 prikazuje koncentracijo glavnih prvin (v odstotkih), Tabela 2 pa deleže oksidnih oblik glavnih prvin.

V vzorcih drobnozrnatih klastitov (LB 3,8; LB24,0 in LB37,2) je največji delež silicija, ki se veže v SiO_2 (kremenovi različki in ostali silikati). Količinsko mu sledi kalcij, ki gradi minerala kalcit in dolomit. Manjša vsebnost magnezija, nam kaže večinsko pojavljanje kalcita in ne dolomita. V vzorcih je tudi železo, ki se veže v Fe_2O_3 (hematit). V vzorcih je tudi nekaj aluminija, ki se veže v alumosilikate, in kalija, ki je vezan na prisotnost muskovita/ilita. Vsi trije vzorci imajo zelo podobne količinske vrednosti glavnih prvin.

Podobno kot pri drobnozrnatih klastitih se ujemajo rezultati rentgenske in kemijske analize tudi pri vzorcih karbonatne konkrecije (Tabela 1 in Tabela 2), kjer sta najbolj pogosta elementa kalcij in silicij, oziroma CaO in SiO_2 zapisano v oksidnih oblikah.

Sl. 6. Difraktogrami drobnozrnatih klastiov (trije zgornji) in karbonatne konkrecije (spodaj). Glej angleški del prispevka.

Tabela 1. Koncentracija (v procentih) glavnih prvin drobnozrnatih klastitov (trije zgornji) in karbonatne konkrecije (spodaj).

Element	Ca	K	Ti	Al	Mg	Si	Fe
LB 3,8	8,56	3,08	0,26	8,44	0,92	22,93	2,83
LB 24,0	14,18	2,24	0,20	6,84	1,14	18,21	2,81
LB 37,2	12,26	2,14	0,23	6,79	0,97	19,74	2,77
LB 15,7	35,86	0,14	0,03	0,89	0,95	2,99	0,63

Tabela 2. Deleži (v procentih) oksidnih oblik glavnih prvin drobnozrnatih klastitov (trije zgornji) in karbonatne konkrecije (spodaj).

Oxide	SiO_2	Al_2O_3	Fe_2O_3	MgO	CaO	K_2O	TiO_2
LB 3,8	49,06	15,94	4,05	1,53	11,97	3,71	0,43
LB 24,0	38,95	12,93	4,01	1,90	19,84	2,70	0,34
LB 37,2	42,24	12,84	3,96	1,61	17,16	2,57	0,38
LB 15,7	6,39	1,68	0,91	1,57	50,17	0,17	0,05

Sedimentacijska analiza raziskanega profila

Raziskano zaporedje sestavljajo izključno klastične kamnine, kjer prevladujejo zelo drobnozrnati klastiti (peščeni muljevci oziroma laporovci), le te pa prekinjajo posamezne plasti (kremenovo) polilitičnih peščenjakov in prodnatih peščenjakov. Sestava klastitov kaže na kontinentalno sedimentacijsko okolje, medtem ko facielna združba, struktura in teksture umeščajo raziskano zaporedje v aluvijalno okolje, natančneje poplavno ravnico. Drobnozrnate klastite interpretiramo kot sediment, odložen iz suspenzije ob poplavnih dogodkih. Tankoplastnate peščenjake brez opaznih tekstur lahko interpretiramo kot sediment prebojnih pahljač, kanalizirane in občasno navzkrižno laminirane prodnate peščenjake pa kot sedimente rečnih korit manjših meandrirajočih rek (Skaberne, 1995; Miall, 1996; Bridge, 2003; Aslan, 2013).

Aridna klima, ki je značilna za večji del zgornjega karnija (Breda et al., 2009; Kiessling, 2010) se v raziskanem zaporedju odraža po tipično rdeči do vijoličasti barvi kamnin, ki je posledica prisotnosti železa v oksidni obliki (hematit), in po prisotnost karbonatnih konkrecij (Alonso-Zarza, 2003; Khalaf, 2007; Moussavi-Harami, 2009; Breda & Preto, 2011). Upoštevajoč izrazito aridno klimo, bi opazovano zaporedje alternativno lahko umestili tudi v zaključne (terminalne) vršaje (Nichols & Fisher, 2003), katerih nastanek bi bil v tem primeru najverjetneje posledica nizke vodne bilance zaradi česar reke niso dosegle morja. Podobno, s sedimentacijo na zaključnih vršajih interpretirajo tudi primerljivo klastično zaporedje Travenanzes formacije iz Dolomitov (Breda et al., 2009; Breda & Preto, 2011; Preto et al., 2015), kjer so na podlagi analize bolje razgaljenih tuvalskih kamnin izdelali celosten sedimentacijski/faciesni model (sl. 7). Njihova rekonstrukcija paleookolja je razdeljena na tri faciesne cone. Najbolj južno faciesno cono A, v katero bi lahko umestili tudi zaporedje pri Lesnem Brdu, opredeljujejo meandrirajoče reke v puščavskem okolju, ki se končujejo z zaključnimi vršaji. Ta faciesna cona proti severu, preko sabk in plimskih ravnic faciesne cone B, prehaja v faciesno cono C z restriktivnimi lagunami – podplimsko morsko okolje. Tudi za Travenanzes formacijo je značilna prisotnost karbonatnih konkrecij, predvsem v obliki dolokretov. Preto in sodelavci (2015) domnevajo, da je dolomit primaren. Za razliko od karbonatnih konkrecij Travenanzes formacije so le te na Lesnem Brdu kalcitne sestave. V prihodnje bi bilo vredno opraviti dodatne mineraloške in kemijske raziskave, s čimer bi lahko natančneje opredelili njihovo genezo.

Smer transporta na podlagi podatkov iz profila ni mogoče določiti, vendar pa glede na paleogeografsko porazdelitev v zgornjem triasu, kjer proti severu prehajamo v globokomorski Slovenski bazen (Buser, 1989; Gale, 2010; Gale at al., 2012; 2016), lahko zaključimo da je bilo izvorno območje sedimenta zagotovo nekje na jugu (današnja orientacija). Sestava sedimentov kaže, da so bile v zaledju, torej na izvornemu območju klastitov, razgaljene karbonatne, vulkanoklastične in verjetno tudi klastične kamnine. Nekatera zrna imajo lahko tudi pedogen izvor, kjer je na izsušeni poplavni ravnici prišlo do intenzivne pedogeneze in tvorbe karbonatnih in železovih konkrecij. V dolgih sušnih obdobjih je sledila fragmentacija le teh v sparitna zrna in zrna iz neprosojnega minerala, deflacija, ter vetrni transport med različnimi podokolji (Breda & Preto, 2011).

Sl. 7. Shematska rekonstrukcija paleookolj Travenanzes formacije (prirejeno po Breda & Preto, 2011) A = aluvialna ravnica z rečnim koritom, prebojnimi pahljačami, zaključnimi vršaji in poplavno ravnico; B = blatna ravnica in sabke; C = karbonatna plimska ravnica in plitve lagune. Zvezdi označujeta najbolj verjetni lokaciji območja raziskav. Glej angleški del prispevka.

Zaključki

Proučeno zgornjekarnijsko (tuvalsko) zaporedje pri Lesnem Brdu po večini sestavljajo rdeči do vijoličasti rahlo peščeni muljevci oziroma laporovci z vmesnimi plastmi peščenjakov in prodnatih peščenjakov. Faciesna združba je značilna za poplavno ravnico, kjer prevladujoče drobnozrnate poplavne sedimente prekinjajo vmesne plasti srednje do debelozrnatih sedimentov prebojnih ali zaključnih pahljač, redkeje manjših rečnih korit. Po sestavi klastitov sklepamo, da so bile na južno ležečem izvornem območju erodirane predvsem karbonatne, vulkanoklastične in tudi klastične kamnine, obenem pa imajo določena zrna verjetno tudi pedogen izvor.

Pri korelaciji s sedimentacijskim modelom tuvalskega zaporedja (Travenanzes formacija) v italijanskih Dolomitih uvrščamo opisano zaporedje v faciesno cono A, katero opredeljujejo sedimenti poplavne ravnice, rečnih korit, prebojnih pahljač in zaključnih vršajev (Breda et al., 2009). Prisotnost hematita in karbonatnih (kalcitnih) konkrecij, kažeta na aridno klimo v času sedimentacije.

Zahvala

Raziskava je financirana deloma iz pedagoških sredstev Oddelka za geologijo in deloma iz raziskovalnega programa št. P1-0195(B) (Geokemični in strukturni procesi), katerega je sofinancirala Javna agencija za raziskovalno dejavnost Republike Slovenije iz državnega proračuna. Iskreno se zahvaljujemo Dragomirju Skabernetu za pomoč pri določanju klastičnih mikrofaciesov. Za skrben pregled rokopisa se zahvaljujemo neznanima recenzentoma, Emi Hrovatin in Miranu Udovču pa za vso tehnično podporo.

Literatura

Glej angleški del prispevka.

GEOLOGIJA 60/2, 297-307, Ljubljana 2017

https://doi.org/10.5474/geologija.2017.021

Origin of planation surfaces in the hinterland of Šumljak sedimentary bodies in Rebrnice (Upper Vipava Valley, SW Slovenia)

Nastanek reliefnih izravnav v zaledju sedimentnih teles Šumljak na Rebrnicah (Zgornja Vipavska dolina, SW Slovenija)

Tomislav POPIT

University of Ljubljana, Faculty of Natural Sciences and Engineering, Department of Geology, Privoz 11, SI-1000 Ljubljana; e-mail: tomi.popit@geo.ntf.uni-lj.si

Prejeto / Received 28. 9. 2017; Sprejeto / Accepted 30. 11. 2017; Objavljeno na spletu / Published online 22. 12. 2017

Key words: planation surface, steep scarp, slope deposit, scree deposit, fossil landslide
Ključne besede: reliefna izravnava, strmi robovi, pobočni sediment, melišče, fosilni plaz

Abstract

The Rebrnice area forms the north eastern slopes of the Upper Vipava Valley and is located between Karst plateau to the southwest and the Nanos plateau to the northeast. The Rebrnice slopes are geomorphologically defined by a thrust front of Mesozoic carbonates over Tertiary flysch deposits and are characterised by a variety of polygenetic landslides (being the most prominent geomorphological features). Among them, the three Šumljak sedimentary bodies of fossil landslides (approximately 0.56 km² in area) comprise carbonate gravels and breccia. The most distinctive geomorphological element is the planation surface of the carbonate breccia blocks positioned in the hinterland of the Šumljak sedimentary bodies. Another feature is the presence of local escarpments (steep scarps) defining the border between the planation surface in the hinterland and sedimentary bodies.

Our research suggests that the whole area in the hinterland of the Šumljak sedimentary bodies form part of a deep-seated rotational landslide formed of carbonate breccia. On the basis of the dipping of the breccia beds, in particular parts of the rotational blocks, the rotation can reach up to 60°. Planation surfaces developed above the curved, sliding plane in the central part and/or slightly outer part of the landslide. Steep scarps on the external parts of the planation surface represent the main scarps of the Šumljak sedimentary bodies. We propose that these bodies originated from the remobilization of material accumulated in outer parts of large-scale rotational slides and its transportation further downslope, mostly by rock avalanches.

Izvleček

Območje Rebrnic predstavlja severnovzhodna pobočja Zgornje Vipavske doline, ki se nahajajo med kraško planoto na jugozahodu in Nanosom na severovzhodu. Topografijo območja Rebrnic opredeljuje čelo narivnega robu mezozojskih karbonatov, ki so narinjeni na terciarne kamnine fliša, kontakt pa prekrivajo kvartarni pobočni sedimenti, med katerimi so najpomembnejši fosilni in recentni poligenetski plazovi. Med fosilnimi plazovi izstopajo tudi tri sedimentna telesa Šumljak (velikosti 0,56 km²), sestavljena iz karbonatnega grušča in breče in imajo specifične geomorfološke značilnosti. Najbolj značilen geomorfološki element so planarne (izravnane) površine blokov karbonatnih breč v zaledju sedimentnih teles Šumljak in prisotnost lokalnih morfoloških stopenj v obliki strmih robov, ki opredeljujejo mejo med izravnano površino v zaledju in sedimentnim telesom.

Raziskave kažejo, da je celotno območje v zaledju sedimentnih teles Šumljak lahko del globokih rotacijskih plazov karbonatnih breč. Na podlagi plastnatosti breče na posameznih delih rotacijskih blokov, ugotavljamo, da so bloki rotirali do 60°. Izravnana površina je razvita predvsem v osrednjem delu planarnih površin, na zunanjih delih izravnav pa se pojavljajo strmi robovi, ki predstavljajo glavne odlomne robove sedimentnih teles Šumljak. Menimo, da so telesa, predvsem v zgornjem delu pobočja nastala kot posledica remobilizacije materiala z zunanjih delov velikih rotacijskih palzov, kjer se je material nato v obliki kamninskih plazov transportiral nižje po pobočju.

Introduction

A large accumulation of carbonate gravel, that formed by different transport mechanisms and deposition processes, is positioned under the head of the thrust contact in the Rebrnice area. The spatial distribution of sedimentary bodies within the quaternary slope deposit and the type of deposition processes can be directly influenced by the regional structural, lithological, hydrological and geochemical conditions. Studies of these elements are supplementing our understanding of the gravitational events that were triggered throughout the north and north-eastern parts of Vipava Valley (Kočevar & Ribičič, 2002; Logar et al., 2005; Fifer Bizjak & Zupančič-Valant, 2007; 2009; Placer, 2007; Jež, 2007; Placer et al., 2008; Mikoš et al., 2009; Lenart & Fifer Bizjak, 2010; Petkovšek et al., 2011; Popit & Verbovšek, 2013; Mikoš et al., 2014; Pulko et al., 2014; Košir et al., 2015; Martín Pérez et al., 2016; Popit et al., 2017; Verbovšek et al., 2017a; 2017b). The structure and composition of the sedimentary bodies are extremely complex but this is not visible at ground level, where carbonate gravels prevail. This surface feature is still useful for distinguishing the mass-movement, sedimentary bodies from the primary flysch base rock (Popit et al., 2013, Popit et al., 2016; Popit, 2016).

The present work deals with the form and structure of a planation surface in the hinterland of the three Šumljak sedimentary bodies (SB1, SB2 and SB3) in the Rebrnice slope area. These approximately horizontal, planar surfaces are well-expressed and unusual for this area which is why there is interest in researching their origin.

General geological setting

In tectonic terms, the investigated area is part of a south west verging, Eocene to Oligocene fold-and-thrust structure in the External Dinarids (Placer, 1981; 1998). The Šumljak sedimentary bodies are located in the upper part of the Vipava Valley, which belongs to three different nappes (from structurally lowest to highest): The Komen Thrust Sheet, the Snežnik Thrust Sheet and the Hrušica Nappe (Fig. 2). The Topography of the studied area is defined by the Hrušica Nappe, which comprises Mesozoic (Cretaceous and Jurassic) limestone that has been thrusted over the Paleocene and Eocene flysch deposits of the Snežnik and Komen thrust sheets (Fig. 2); these have also been folded and fractured. The overlying carbonate rocks are intensively fractured along the thrust contacts and within wide zones of NW–SE trending strike-slip faults (the Predjama, Vipava and Raša faults) that cut the thrust contact (Placer, 1981; 1998; 2008; Čar & Gospodarič, 1988; Janež et al., 1997).

The upper part of the slope of the Vipava Valley is marked by steep carbonate cliffs, while the lower parts of the slope are more gently sloping and are composed of flysch bedrock covered by Quaternary slope deposits. The latter represent an array of composite, fan-shaped, sedimentary bodies with diverse composition, internal structures and textures, which indicate a complex depositional history and polyphase genesis (Popit and Košir, 2010; Popit et al., 2013; Popit, 2016, Novak et al., 2017).

Methods

The mapping of the sedimentary bodies and their hinterland is based on geological field mapping and analysis of shaded digital terrain models (DTMs) that were obtained by airborne laser scanning with a resolution of 1 × 1 m. The basic elements used for the visual interpretation of the shaded digital terrain model (Fig. 1) were texture, shape and tint (cf. Podobnikar, 2003; 2005; Oštir, 2006). An additional aid was a map of surface roughness, made using the Height Variability Method (Ruszkiczay-Rüdiger et al., 2009) and this proved to be the most useful of all the methods used for the quantification and visualisation of deposits with different sedimentary composition and genesis (Popit & Verbovšek, 2013; Popit et al., 2016).

The results of the Height Variability Method are presented in Fig. 5B and Fig. 7B, and they represent the difference between the highest and the lowest elevations. The casts of colours were divided roughly into three levels: low, medium and high variability of slopes. Areas marked in light to dark pink correspond to smooth surfaces (e.g. the bottom of the Upper Vipava Valley), the blue-green areas correspond to intermediate values (between smooth and rough surfaces), and the yellow-brown areas correspond to rough surfaces (e.g. Nanos cliff) (Figs. 5 and 7). Colour visualisation was found to be a useful way of illustrating the areas with low and/or high slope variability (Popit & Verbovšek, 2013; Popit et al., 2016). Based on both methods (geological mapping and surface roughness analyses), specific geomorphological and geological features were interpreted.

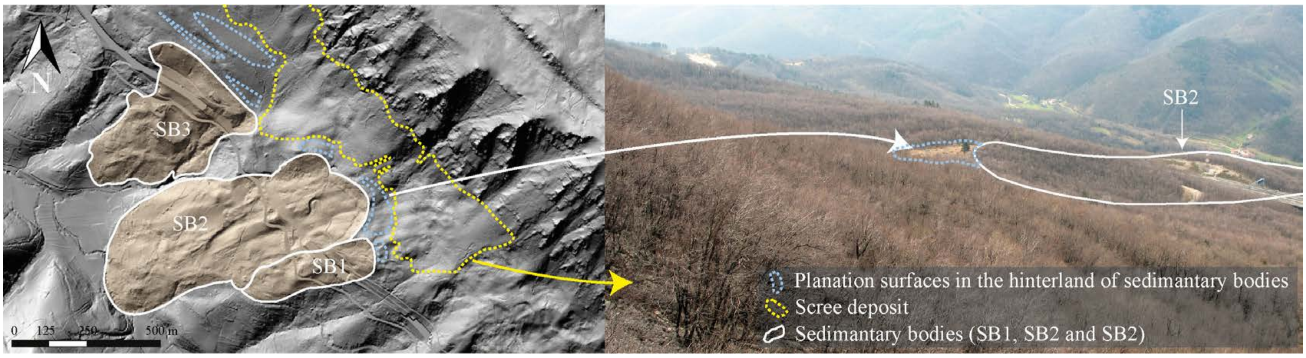

Fig. 1. (A) Shaded digital elevation model of the Šumljak sedimentary bodies (SB1, SB2 and SB3) and locations of planation surfaces in the hinterland and scree deposits. (B) View to Šumljak 2 sedimentary body (SB2) and its planation surface in the hinterland.

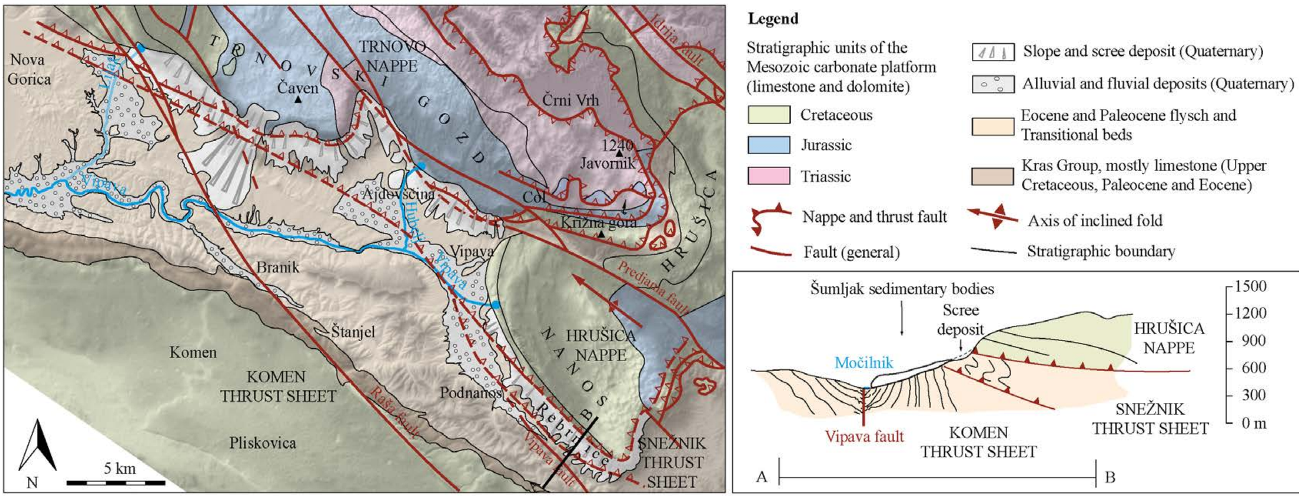

Fig. 2. Simplified geological map and cross-section of the Upper Vipava Valley and the Nanos Plateau. Compiled from Buser, (1973; 1986), Placer (1981; 2008), Janež et al. (1997) and others.

Šumljak sedimentary bodies and geology of their hinterland

Over the entire Rebrnice area, there are 11 isolated sedimentary bodies (of very complex genesis and composition), covering areas of between 0.09 km^2 and 0.50 km^2. The total surface area of the bodies in the Rebrnice area is approximately 2.8 km^2 (Popit, 2016; Jemec Auflič et al., 2017). In total, the surface of the Šumljak sedimentary bodies is approximately 0.58 km^2 and this represents 21 % of the surface area of all sedimentary bodies in the Rebrnice area.

The surface area of SB1 is 0.095 km^2. The difference between the height of the lowest and the highest edge of the sedimentary body is more than 160 m (Fig. 3). The surface area of SB2 is 0.332 km^2. The height difference between the lowest edge of the sedimentary body in Dolenje Žvanuti village, near Lozice, and the upper edge of the body is more than 230 m (Fig. 3). The surface area of SB3 is 0.156 km^2 and the difference between the lowest and the highest edge of the sedimentary body is 165 m.

Just above the scarps of the direct hinterland of the Šumljak sedimentary bodies, the morphology flattens out to planation surfaces. The baserock of these surfaces is composed of carbonate breccia (Figs. 6A and B), which occurs in bedding or in lenses (usually up to 1 m thick). It originated from the partial lithification of scree material. The dip direction and dip angle of the beds are different, depending on their position on the slope (see below). Near the carbonate cliff in the upper part of the slope, the dip angles of breccia beds are parallel or nearly parallel to the directions of the slope. In the middle part of the slope, the dip angles of the beds are sub-horizontal and in the lower parts of the slope the carbonate breccia beds dip towards the slope (Fig. 6). In the upper part of the slope (on the north-eastern side), the planation surface is bounded by recent scree aprons which follow the line of the carbonate Nanos cliff.

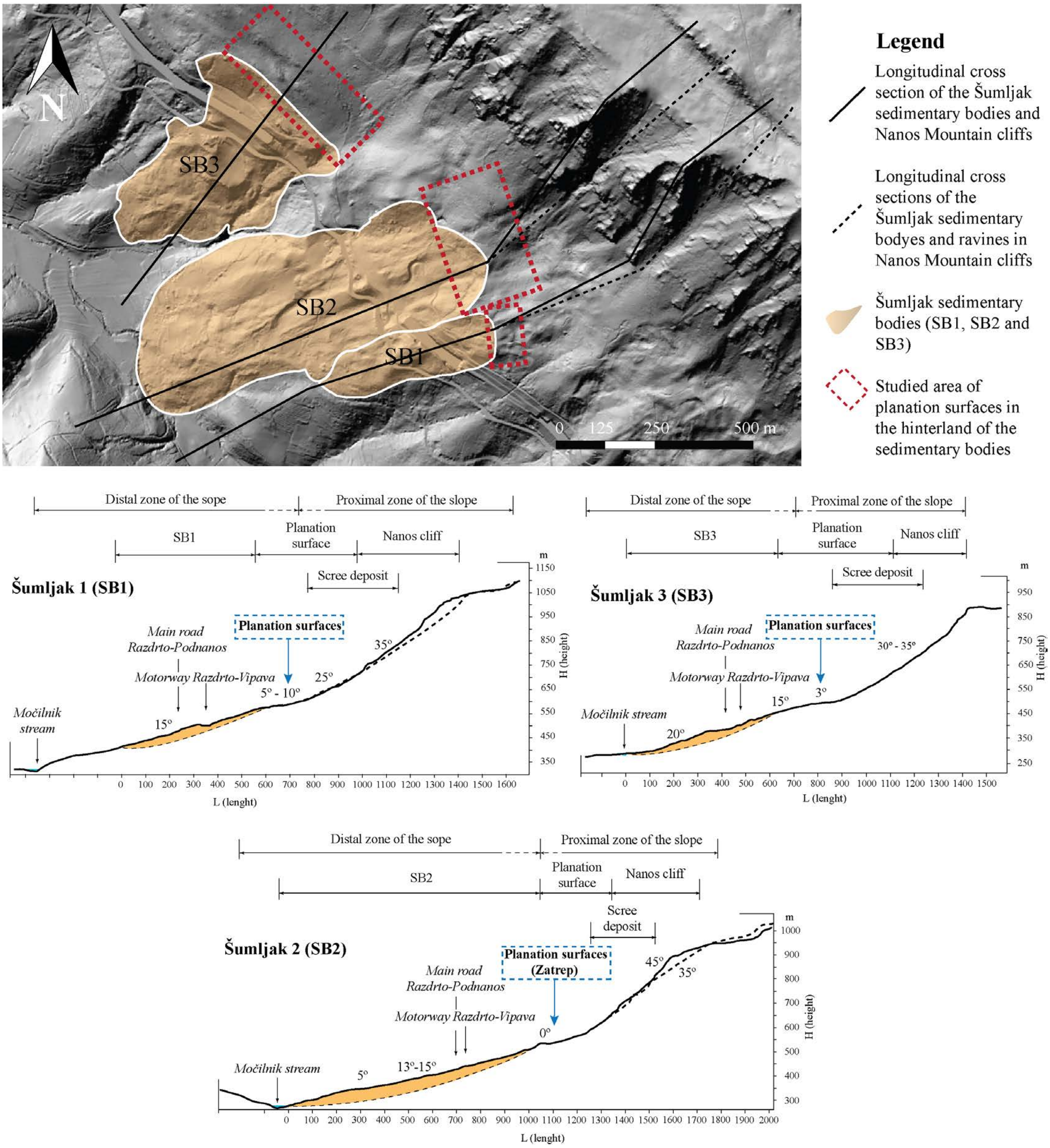

Fig. 3. The longitudinal profiles across Šumljak sedimentary bodies (SB1, SB2 and SB3) and location of the study area.

Geomorphometric analysis in the hinterland of Šumljak sedimentary bodies

By visual analysis of the DTMs and height variability map (Figs. 4, 5A and 5B) it can be identified that the Šumljak sedimentary bodies and their immediate surroundings represent areas with different surface roughness. It was found that carbonate gravels (which, in most cases, cover the individual sedimentary body surfaces) have a height variability and consequently represents an area with a high degree of surface roughness. By contrast, the hinterland of the Šumljak sedimentary bodies shows a low degree of height variability and the surface in this part is smooth. The transition from sedimentary bodies to hinterland is marked by steep scarps. Along the slope in the hinterland of the Šumljak sedimentary bodies, we distinguished three different areas with diverse morphology; from the bottom of the slope to the top, these are: *steep scarps*, *planation surfaces* and *scree deposits*.

Steep scarps

In the upper edge of the sedimentary bodies, on the boundary with the planation surfaces, we recognized steep, convex and strait scarps formed of carbonate breccia. The values of the surface roughness of the steep, convex scarps on the top of SB2 are very high. The convexity of the scarps also occurs in the upper part of SB1, whereas in the hinterland of SB3 they only appear as a few straight lines (Fig. 4). The strait lines of the SB3 hinterland is also recognized on the height variability map (Figs. 4 and 5), where approximately parallel, narrow bands extend over the upper part of SB3 and resemble a stepped feature in the hinterland of the sedimentary body.

Planation surface

In the hinterland of the Šumljak sedimentary bodies, above the Nanos cliff and below the steep scarps, there are large areas of carbonate breccia with extremely low roughness, named planation surfaces (Fig. 4). The largest uniform planation surface, named "Zatrep", is in the hinterland of SB2 and extends for approximately 0.03 km^2. SB1 is the smallest of the sedimentary bodies (Fig. 2) and, therefore, the planation surface in the hinterland of this body is also the smallest in area. The hinterland of SB3 is more complex. The shaded digital terrain model and the height variability map indicate the location of levelled edges (at the boundary between height and low surface roughness) (Fig. 5). Belts of high surface roughness can be easily recognized in the straight scarps mentioned above. Individual smooth surfaces between the scarps, represent three separated planation surfaces in the hinterland of SB3, forming a stepped structure.

The largest planation surface in the hinterland of SB3 is also the highest and extends to approximately 0.005 km^2 while the planation surfaces in the lower part of the slope are smaller, elongate and parallel to the steep scarps. In some parts in the hinterland of SB3, it was possible to recognize the dip direction and dip angle of the carbonate breccia strata. Measurable outcrops were mainly located close to, or just above, the steep scarps (Figs. 6A and 6B). The dip direction of the carbonate breccia strata, outcropping at the highest altitude closest to the Nanos cliff, is 230/30 (Fig. 6C, steep scarp 1). The next outcrop of carbonate breccia, detected lower down the slope on the secondary steep scarp, has a dip direction 210/20 (Fig. 6C, steep scarp 2), while the lowest lying breccia is dipping to the northeast (azimuth = 50°) with a relatively large dip angle of 25° (Fig. 6C, steep scarp 3).

Scree deposits

Scree deposits are located below the carbonate cliffs present in the uppermost part of the slope. Depending on the specific lithological and structural predisposition of the Nanos cliff, the deposits are deposited in talus cone shapes or scree

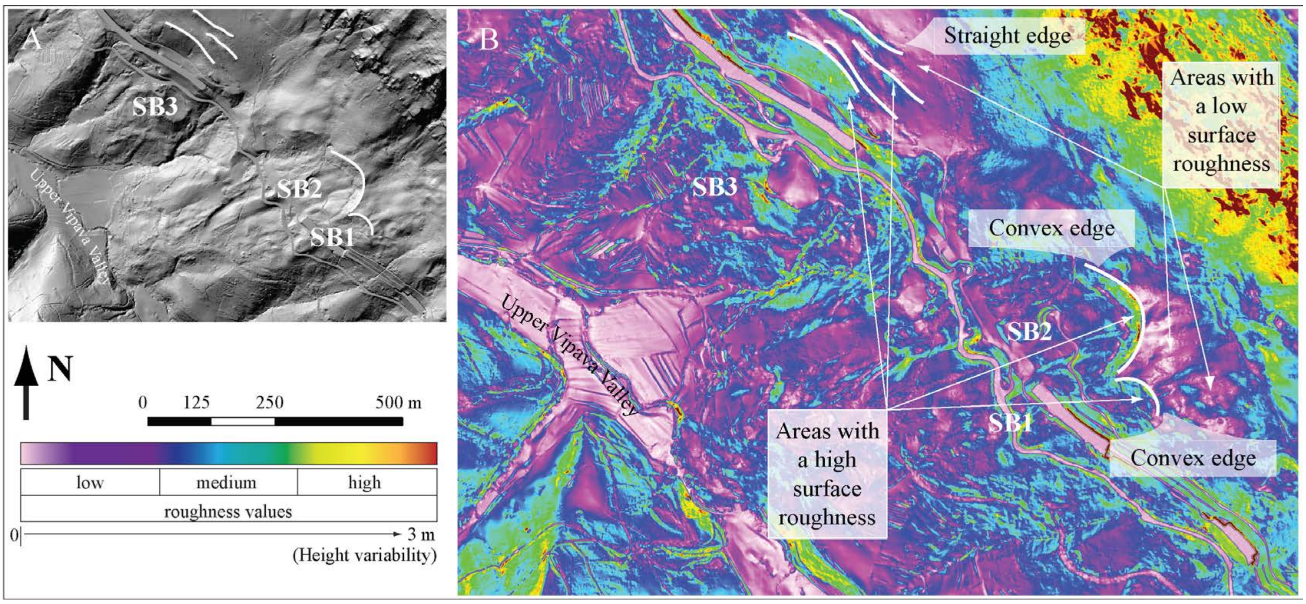

Fig. 4. (A) Shaded, digital terrain models (DTMs) with a resolution of 1 × 1 m, obtained by airborne laser scanning in the areas of SB1, SB2 and SB3 indicating the location of the convex and straight scarps. (B) A height variability map with the convex and straight scarps marked on SB1, SB2 and SB3. The upper arrows indicate an individual area with a very low surface roughness attributed to planation surfaces and the lower arrows indicate areas with high surface roughness, which are bound to individual convex scarps.

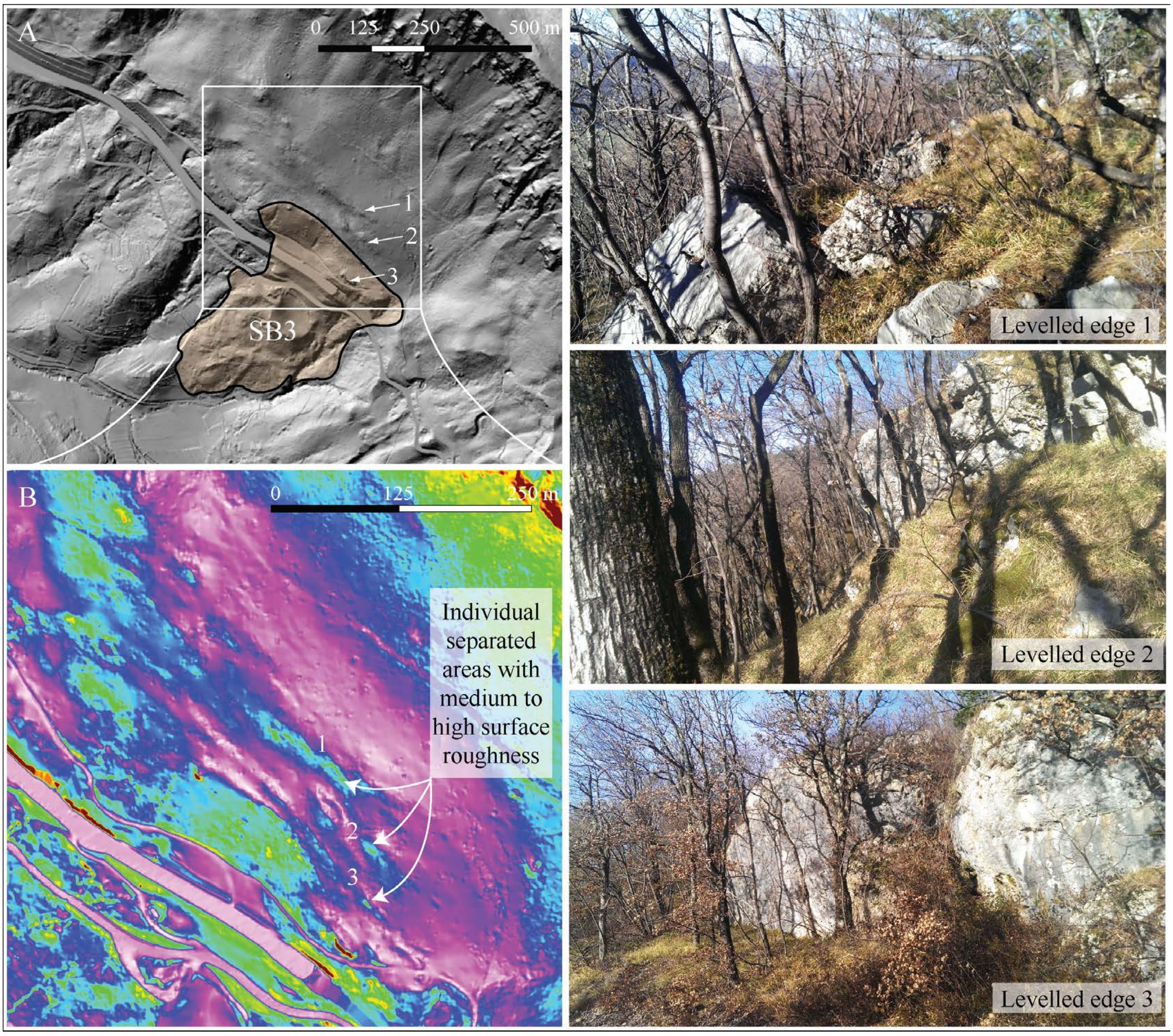

Fig. 5. (A) Shaded digital terrain model of the broad area of SB3 and indicated location of levelled edges (boundary between height and low surface roughness). (B) On the height variability map, belts with a high height variability are well recognized showing the steep scarps, forming a stepped structure in the hinterland of the Šumljak 3 sedimentary bodies. The scarps and individual rupture surfaces that were recorded in the field are shown on the right.

sheets (Popit et al., 2014a). On the basis of their spatial distribution, we were able to separate two levels of scree deposit, separated by the primary outcrop of Mesozoic limestone. The upper level scree deposits are smaller and accumulate on individual primary outcrops at their lower edges, while the scree deposits in the lower level are larger and distinctly cone-shaped (Fig. 7). The slope angles of the scree deposits appear to be between 33° and 45°.

Discussion

In the hinterland of the steep scarps of the SB1 and SB2 planation surfaces, carbonate breccia is observed, continuing almost to the foothills of the Nanos cliff (Fig. 8). We interpret the formation of these planation surfaces as being the result of a deep-seated rotational slide, where the carbonate breccia block and poorly lithified scree deposits rotated along the sliding surface that originated on the contact with the underlying weathered flysch base rocks and/or muddy mass-flow deposits.

Downslope, the planation surfaces pass through the steep scarps into the Šumljak sedimentary bodies. The Šumljak sedimentary body SB2 is characterised by a recognisable convex edge that is incised in carbonate breccia. We interpreted it as being the main scarp of the rock avalanche in SB2 (Fig. 4), that was triggered in the accumulated material at the outer margin of a large-scale, deep-seated rotational slide. Today, remobilized material forms the cover of SB2 in the upper part of the sedimentary feature.

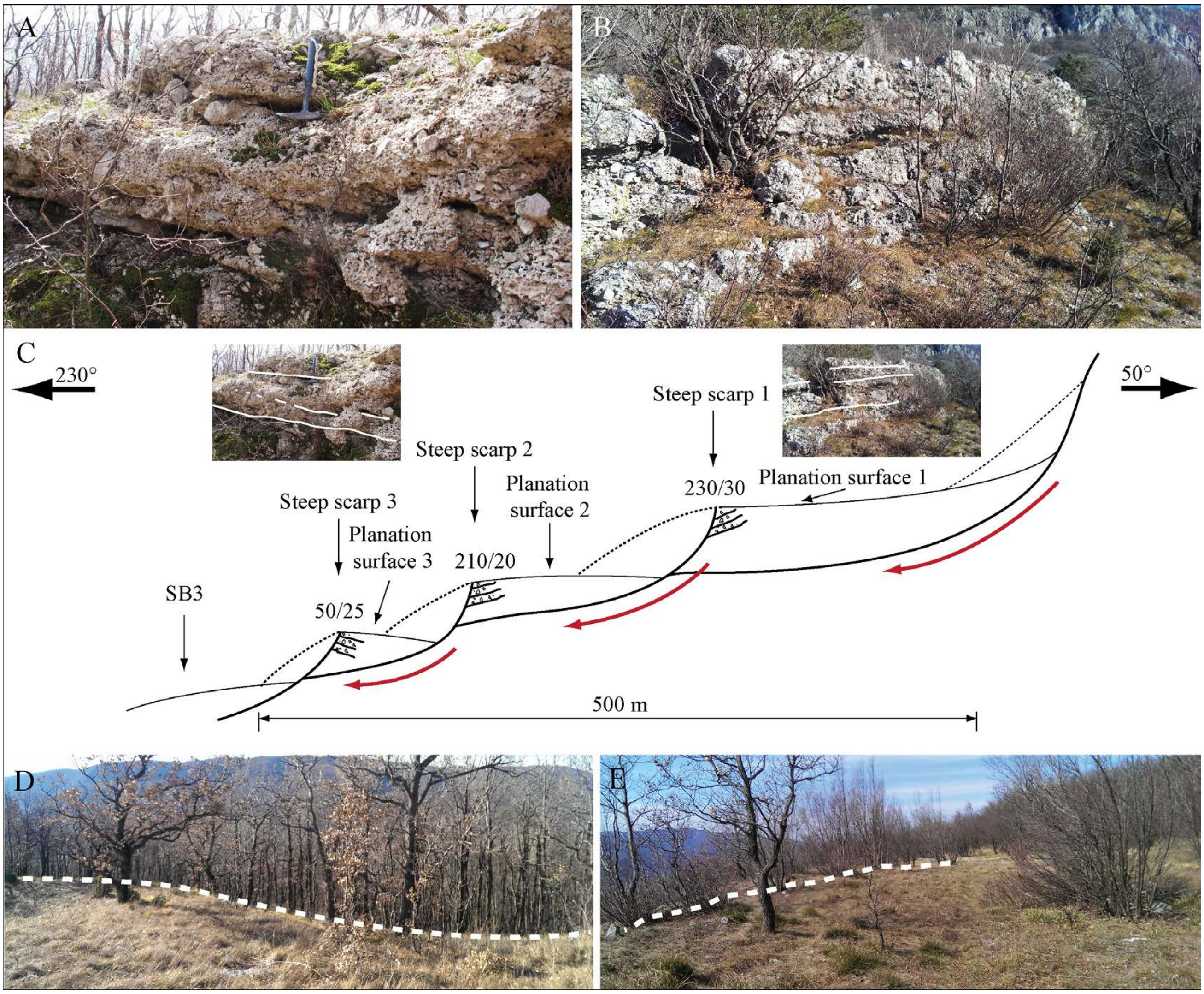

Fig. 6. Examples of planation surfaces and steep scarps which are connected to SB3. (A and B) Bedding of slope breccia in the upper parts of the steep scarps 1 and 3. (C) The slope breccia at scarp 1 (in the highest altitude and the nearest to Nanos cliff) has a bedding orientation of 230/30; at scarp 2, the orientation of beddings is 210/20 and the orientation of bedding of the breccia of the lowest-lying scarp (scarp 3) is 50/25. (D) The dashed line indicates the upper steep scarp 1 and (E) steep scarp 3.

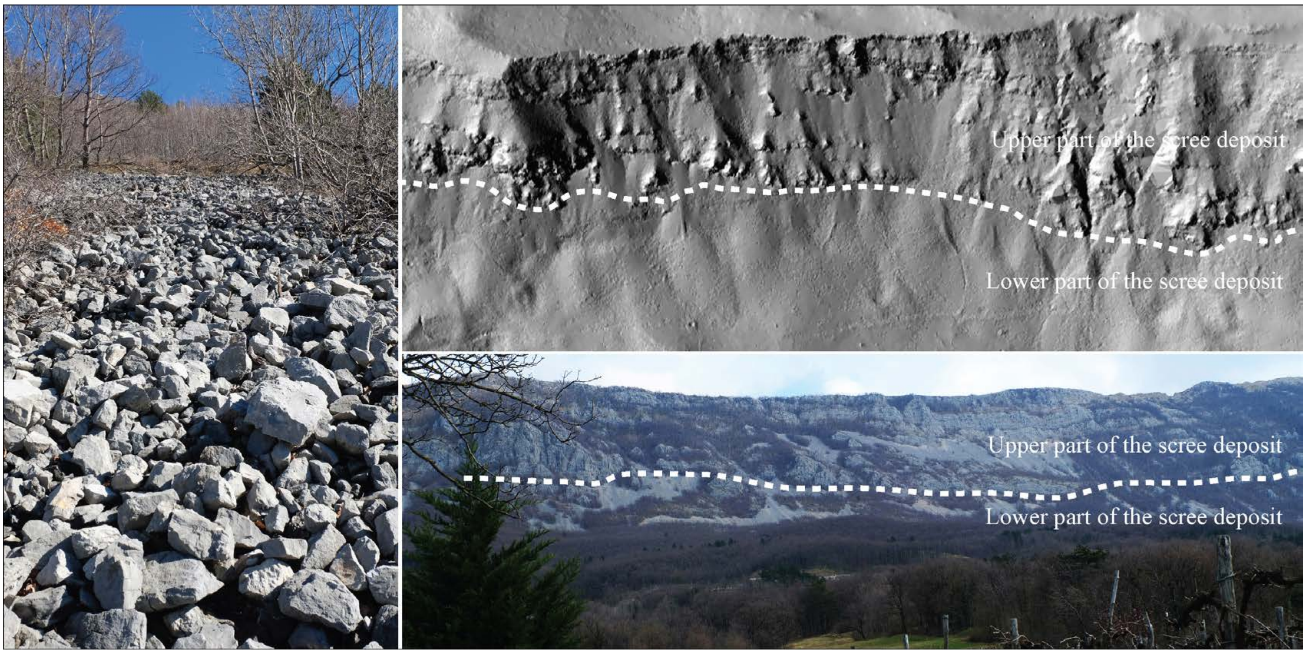

Fig. 7. Two positions of the scree deposits (talus cone and scree sheets) in the Rebrnice area. The photograph of the scree deposit (left figure) was taken in the upper part of the Nanos cliff.

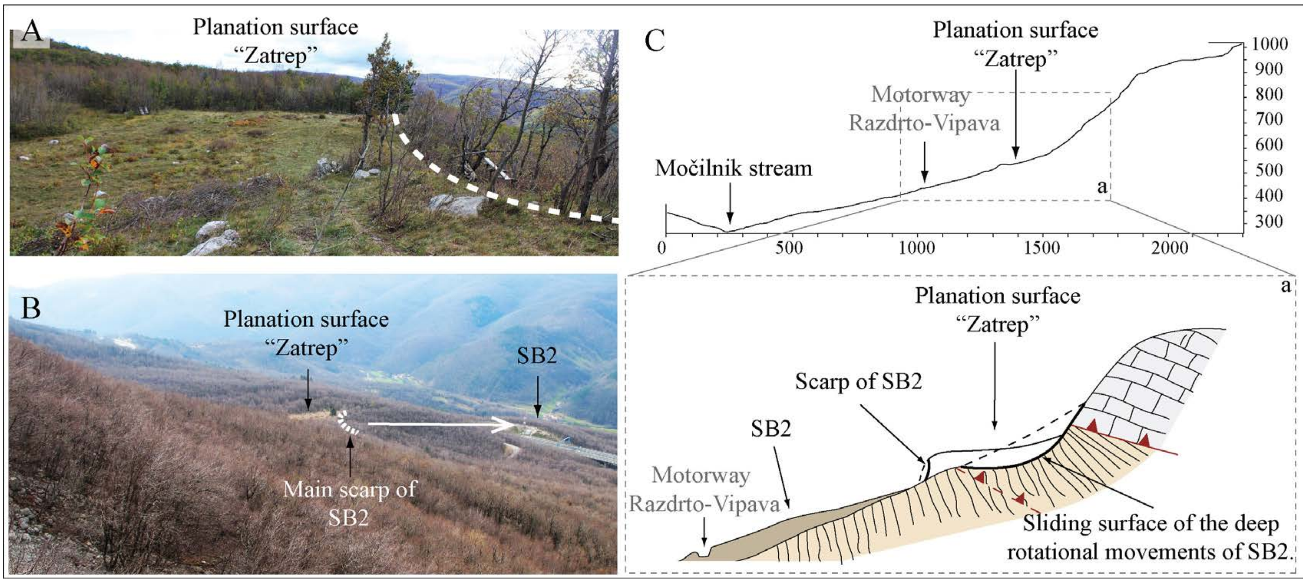

Fig. 8. (A) The example of the "Zatrep" planation surface and main scarp behind SB2. The dashed lines indicate the upper scarp. (B) The white arrow shows the direction of transport of material and is at right angles to the scarp. (C) Schematic longitudinal profiles through SB2 and (D) Flat surface resulting from the rotating block of carbonate breccia. A new steep scarp was formed in the toe of the rotational block, due to deep rotational movements along the sliding surface of the block in SB2.

The same observations are reported from deep-seated landslides, where a steep scarp often forms at the outer part of the sliding mass (Amudsen et al., 2010). The main direction of extension of the convex edge at SB2 is approximately perpendicular to the direction of transport (i.e. the direction of the lateral edges of the sediment body) but with a smaller deviation in the case of SB2 (8.2°) and a slightly larger one in the case of SB1 (20.5°). This is one of the typical properties of steep scarps (Van Den Eeckhaut et al., 2012a; 2012b) and can be identified in the Rebrnice area.

In the case of SB3, the overall architecture and depositional evolution is more complex. It was possible to identify at least three scarps that are approximately parallel to each other and laterally 'wedge out' (Figs. 5 and 6). By our interpretation, this step-like sequence is formed by the same large-scale mechanism that operated in the case of SB1 and SB2, i.e. a deep-seated rotational landslide, which developed into a rock avalanche in the lower slopes. Additionally, above the steep scarp, two parallel scarps occur which signify multiple, rotational landsliding that successively developed at the outer part of the large-scale, rotational landslide. The architecture of these landslides corresponds well to so-called 'diminishing' landslides, where the volume of the moving mass gradually decreases (cf. Cruden & Varnes, 1996). The planation surfaces between the individual scarps can be attributed to the different rotation of individual carbonate breccia blocks. Individual breccia blocks slipped down the slope and, at the same time, rotated towards the slope. Stairstepped patterns of displaced backward-rotated blocks, also called reverse slopes (Van Den Eeckhaut, 2011).

A deep-seated rotational slide is further indicated by the variation of dips within the breccia beds. The dip direction and dip angle of the breccia beds, which forms the base-rock of the planation surface, depends on their spatial position. Upward, near the Nanos carbonate cliff, the slope and the dip angles of breccia beds are parallel or nearly parallel to the directions of the slope. In the middle section, the dip angles of the bedding are subhorizontal and, in the lower parts of the planation area just above the lowest scarp, the carbonate breccia beds dip towards the slope (Fig. 6). If the dip angle in the lower part of the rotary block (50/25°) is reversed back to its primary orientation of between 210/35° and 230/35° (i.e. the inclination of the recent scree and breccia layers in the highest part of the slope) then the total rotation is approximately 60° (25° + 35°).

Conclusion

The planation surface in the hinterland of the Šumljak sedimentary bodies is a morphological expression of a deep-seated rotational landslide that developed along a line of transect from the Nanos carbonate cliffs to the less-steep, lower Rebrnice slopes and it is marked by flysch base rocks. The rotational slides are composed mostly of a well-stratified, carbonate breccia, originating from the partial lithification of scree deposits. Dipping of the breccia beds in particular segments of the rotational blocks in SB3, indicates that the overall rotation can reach up to 60°. The planation surfaces occur in the lower parts of the landslides, where the dipping of the breccia beds is rotated from being 35° parallel to the slope to becoming subhorizontal (or even up to 25°) towards the slope. The lower margin of the planation surface is defined by steep scarps that are the result of the subsequent debris and/or rock avalanches. The material that accumulated in the lower parts of the rotational landslide, was remobilised and transported further downslope, where it also covered older mass-movement deposits, created by a variety of previous transport mechanisms and depositional processes. All of the mass-movement deposits below the steep scarps now comprise the internally complex Šumljak sedimentary bodies.

Acknowledgements

The fieldwork in the study area was performed through an “Innovative scheme for co-funding doctoral study by encouraging cooperation in order to address current economic and social challenges – generation 2010 University of Ljubljana (European Social Fund and Republic of Slovenia, Ministry of Higher Education, Science and Technology)”. The fieldwork in the Rebrnice area was also performed by the Ivan Rakovec Institute of Palaeontology ZRC SAZU in the framework of the Project of Geological Monitoring of the Razdrto-Vipava Motorway Section, funded by DARS Motorway Company in the Republic of Slovenia. The author acknowledges financial support from the Slovenian Research Agency (research core funding No. P1-0195(B)). I would like to thank both reviewers for their insightful comments on the paper, as these comments led me to an improvement of the work.

References

Amundsen, J., Johnson, S., Rouse, K. & Wang, H. 2010: Using LiDAR-derived DEM’s to delineate and characterize landslides in Northern Kentucky and Hamilton County, Ohio: str. 1-26. http://www.trishock.com/academic/pdf/lidar_landslides.pdf (22. 5. 2013.)

Buser, S. 1973: Osnovna geološka karta SFRJ 1:100 000. Tolmač lista Gorica. Zvezni geološki zavod Beograd: 50 p.

Buser, S. 1986: Osnovna geološka karta SFRJ 1:100 000. List Gorica. Zvezni geološki zavod Beograd.

Čar, J. & Gospodarič, R. 1988: Geološka zgradba in nekatere hidrološke značilnosti bruhalnika Lijaka = Geological setting and some hydrological properties of the Lijak effluent. Acta Carsologica, 17:13–32.

Cruden, D. M. & Varnes, D. J. 1996: Landslide types and processes. In: Turner, A.K & Schuster, R.L (eds.): Landslides investigation and mitigation. Transportation research board, US National Research Council. (Special Report 247, Chapter 3), Washington, D.C.: 36–75.

Fifer Bizjak, K. & Zupančič-Valant, A. 2007: Rheological investigation for the landslide Slano Blato near Ajdovščina (Slovenia). Geologija, 50/1: 121-129, doi:10.5474/geologija.2007.010.

Fifer Bizjak, K. & Zupančič-Valant, A. 2009: Site and laboratory investigation of the Slano blato landslide. Engineering geology 105/3-4: 171-185, doi:10.1016/j.enggeo.2009.01.006.

Janež, J., Čar, J., Habič, P. & Podobnik, R. 1997: Vodno bogastvo Visokega krasa: Ranljivost kraškepodzemnevode Banjšic, Trnovskega gozda. Nanosa in Hrušice. Geologija d.o.o, Idrija.

Jemec Auflič, M., Jež, J., Popit, T., Košir, A., Maček, M., Logar, J., Petkovšek, A., Mikoš, M., Calligaris, C., Boccali, C., Zini, L., Reitner, J. & Verbovšek, T. 2017: The variety of landslide forms in Slovenia and its immediate NW surroundings. Landslides: journal of the international consortium on landslides, 14/4:1537-1546, doi:10.1007/s10346-017-0848-1.

Jež, J. 2007: Vzroki in mehanizem zemeljskega plazenja na Rebrnicah v Vipavski dolini. Geologija, 50/1: 55–63, doi:10.5474/geologija.2007.005.

Kočevar, M. & Ribičič, M. 2002: Geološke, hidrogeološke in geomehanske raziskave plazu Slano blato. Geologija, 45/2: 427–432, doi:10.5474/geologija.2002.043.

Košir, A., Popit, T. & Verbovšek, T. 2015: The Selo landslide: A long runout rock avalanche? In: Rožič, B. (ed.): 22. posvetovanje slovenskih geologov = 20th Meeting of Slovenian Geologists, Ljubljana, November 2015. Razprave, poročila, Geološki zbornik 23. Univerza v Ljubljani, Naravoslovnotehniška fakulteta, Oddelek za geologijo, Ljubljana: 92–95.

Lenart, S. & Fifer Bizjak, K. 2010: Particularities of Stože and Lokavec landslides - special laboratory tests for landslides modeling. WSEAS transactions on environment and development, 6/5: 355-364.

Logar, J., Fifer Bizjak, K., Kočevar, M., Mikoš, M., Ribičič, M. & Majes, B. 2005: History and present state of the Slano Blato landslide. Natural Hazards and Earth System Sciences, 5:447-457, doi:10.5194/nhess-5-447-2005.

Martín-Pérez, A., González-Acebrón, L., Košir, A. & Popit, T. 2016: Sandstone diagenesis, salt-induced weathering and landslide formation: the case of Slano Blato Landslide, Slovenia. In: 32nd IAS International Meeting of Sedimentology, 23-25 May 2016, Marrakech. Gent: International Association of Sedimentologists.

Mikoš, M., Petkovšek, A. & Majes, B. 2009: Mechanisms of landslides in over-consolidated clays and flysch. Activity scale and targeted region: national. Landslides, 6/4: 367-371, doi:10.1007/s10346-009-0171-6.

Mikoš, M., Sodnik, J., Petkovšek, A., Maček, M. & Majes, B. 2014: WCoE: Mechanisms of Landslides in Over-Consolidated Clays and Flysch and IPL-151 Project: Soil Matrix Suction in Active Landslides in Flysch-The Slano Blato Landslide Case. In: Sassa, K., Canuti, P. & Yin. Y. (eds.): Landslide Science for a Safer Geoenvironment, Springer Netherlands, Dordrecht, 143-148, doi:10.1007/978-3-319-04999-1_16.

Novak, A., Verbovšek, T. & Popit, A. 2017: Heterogeneously composed Lozice fossil landslide in Rebrnice area, Vipava Valley. Geologija, 60/1: 145-155, doi:10.5474/geologija.2017.011.

Oštir, K. 2006: Daljinsko zaznavanje. Inštitut za antropološke in prostorske študije, ZRC-SAZU, Ljubljana: 250 p.

Petkovšek, A., Fazarinc, R., Kočevar, M., Maček, M., Mejes, B. & Mikoš, M. 2011: The Stogovce landslide in SW Slovenia triggered during the September 2010 extreme rainfall event. Landslides, 8/4: 499-506, doi:10.1007/s10346-011-0270-z.

Placer, L. 1981: Geologic structure of southwestern Slovenia. Geologija, 24/1: 27–60.

Placer, L. 1998: Contribution to the macrotectonic subdivision of the border region between Southern Alps and External Dinarides. Geologija, 41: 223-255, doi:10.5474/geologija.1998.013.

Placer, L. 2007: Vzroki nastajanja recentnih in subrecentnih plazov na Rebrnicah - geohazard z vidika kompleksnosti geoloških procesov. In: Horvat, A. (ed.): 18. posvetovanje slovenskih geologov = 18th Meet ing of Slovenian Geologists. Geološki zbornik 19, Univerza v Ljubljani, Naravoslovnotehniška fakulteta, Ljubljana: 82-84.

Placer, L. 2008: Vipavski prelom = Vipava fault (Slovenia). Geologija, 51/1: 101–105, doi:10.5474/geologija.2008.011.

Placer, L., Jež, J. & Atanackov, J. 2008: Structural aspect of the Slano blato landslide (Slovenia). Geologija, 51/2: 229-234, doi:10.5474/geologija.2008.023.

Podobnikar, T. 2003: Kronologija izdelave digitalnega modela reliefa Slovenije. Chronology of Digital Terrain Model production of Slovenia. Geodetski vestnik, 47/1-2: 47–54.

Podobnikar, T. 2005: Production of integrated digital terrain model from multiple datasets of different quality. International journal of geographical information science, 19/1: 69-89.

Popit, T. 2016: Transport mechanisms and depositional processes of Quaternary slope deposit in Rebrnice area. Doctoral dissertation: Faculty of Civil and Geodetic Engineering and Faculty of Natural Science and Engineering, Ljubljana: 341 p.

Popit, T. & Košir, A. 2010: Kvartarni paleoplazovi na Rebrnicah. In: Košir, A., Horvat, A., Zupan Hajna, N. & Otoničar, B. (eds.): 3. Slovenski geološki kongres, Bovec, 16.-18. september 2010. Postojna: Znanstvenoraziskovalni center SAZU, Inštitut za raziskovanje krasa; Paleontološki inštitut Ivana Rakovca, Ljubljana: 39-40.

Popit, T. & Verbovšek, T. 2013: Analysis of surface roughness in the Sveta Magdalena paleo-landslide in the Rebrnice area Analiza hrapavosti površja fosilnega plazu Sveta Magdalena na območju Rebrnic. RMZ - Materials and geoenvironment, 60/3: 197-204.

Popit, T., Košir, A. & Šmuc, A. 2013: Sedimentological characteristics of Quarternary deposits of the Rebrnice slope area (SW Slovenia). In: Knjiga sažetka: 3. Znanstveni skup Geologija kvartara u Hrvatskoj s međunarodnim sudjelovanjem, povodom 130 godina rođenja akademika Marijana Salopeka i u spomen znanstvenici Maji Paunović na 10. obljetnicu smrti, Zagreb, 21–23. 3. 2013. Zagreb, HAZU: 45.

Popit, T., Supej, B., Kokalj, Ž. & Verbovšek, T. 2016: Primerjava metod za geomorfometrične analize hrapavosti površja na primeru Vipavske doline = Comparison of methods for geomorphometric analysis of surface roughness in the Vipava valley. Geodetski vestnik: glasilo Zveze geodetov Slovenije, 60/2: 227-240, doi:10.15292/geodetski-vestnik.2016.02.227-240.

Popit, T., Jež, J. & Verbovšek, T. 2017: Mass movement processes of Quaternary deposits in the Vipava Valley, SW Slovenia. In: Mikoš, M., Casagli, N., Yin, Y. & Sassa, K. (eds.): Advancing culture of living with landslides. Volume 4 Diversity of landslide forms. Cham: Springer. Cop.: 571-580, doi:10.1007/978-3-319-53485-5_66.

Pulko, B., Majes, B. & Mikoš, M. 2014: Reinforced concrete shafts for the structural mitigation of large deep-seated landslides: an experience from the Macesnik and the Slano blato landslides (Slovenia). Landslides, 11/1: 81–91, doi:10.1007/s10346-012-0372-2.

Ruszkiczay-Rüdiger, Z., Fodor, L., Horváth, E. & Telbisz, T. 2009: Discrimination of Fluvial, Eolian and Neotectonic Features in a Low Hilly Landscape: A DEM-based Morphotectonic Analysis in the Central Pannonian Basin, Hungary. Geomorphology, 104/ 3–4: 203–217.

Van Den Eeckhaut, M., Poesen, J., Gullentops, F., Vandekerckhove, L. & Hervás, J. 2011: Regional mapping and characterization of old landslides in hilly regions using LiDAR-based imagery in Southeren Flanders. Quaternary Research, 75/3: 721-733.

Van Den Eeckhaut, M., Kerle, N., Poesen, J. & Hervás, J. 2012a: Identification of vegetated landslides using only a lidar-based terrain model and derivatives in an object-oriented environment. In: Raul Querioz Feitosa et al., (ed.): Proceedings of the 4th GEOBIA, May 7-9, 2012 - Rio de Janeiro – Brazil, 211-216.

Van Den Eeckhaut, M., Kerle, N., Poesen, J. & Hervás, J. 2012b: Object-oriented identification of forested landslides with derivatives of single pulse LiDAR data. Geomorphology, 173–174: 30–42.

Verbovšek, T., Kočevar, M., Benko, I., Maček, M. & Petkovšek, A. 2017a: Monitoring of the Stogovce landslide slope movements with GEASENSE GNSS probes. 4th World Landslide Forum proceedings by Springer Nature publishing, SW Slovenia. In: Mikoš, M, Arbanas, Ž., Yin, Y. & Sassa, K. (eds.): Advancing Culture of Living with Landslides. Advances in Landslide Technology, 3/311-319, doi:10.1007/978-3-319-53487-9_35.

Verbovšek, T., Košir, A., Teran, M., Zajc, M. & Popit, T. 2017b: Volume determination of the Selo landslide complex (SW Slovenia): integrating field mapping, ground penetrating radar and GIS approaches. Landslides, 14/3:1265-74, doi:10.1007/s10346-017-0815-x.

GEOLOGIJA *60/2*, 309-327, Ljubljana 2017
https://doi.org/10.5474/geologija.2017.022

Research of the geological and geothermal conditions for the assessment of the shallow geothermal potential in the area of Ljubljana, Slovenia

Raziskave geoloških in geotermalnih razmer za oceno potenciala plitve geotermalne energije na območju Ljubljane, Slovenija

Mitja JANŽA, Andrej LAPANJE, Dejan ŠRAM, Dušan RAJVER & Matevž NOVAK

Geološki zavod Slovenije, Dimičeva ulica 14, SI-1000 Ljubljana, Slovenia;
e-mails: mitja.janza@geo-zs.si, andrej.lapanje@geo-zs.si, dejan.sram@geo-zs.si,
dusan.rajver@geo-zs.si, matevz.novak@geo-zs.si

Prejeto / Received 7. 11. 2017; Sprejeto / Accepted 8. 12. 2017; Objavljeno na spletu / Published online 22. 12. 2017

Key words: shallow geothermal energy, hydrogeology, groundwater temperature, thermal conductivity
Ključne besede: plitva geotermalna energija, hidrogeologija, temperatura podzemne vode, toplotna prevodnost

Abstract

Shallow geothermal energy is a renewable source of energy. Using it provides benefits for climate, health and economy. A prerequisite for its efficient and sustainable use is the knowledge of its potential as well as the barriers that limit its use. The paper presents the preliminary results of research carried out within the GeoPLASMA-CE project for the assessment of the shallow geothermal potential in the area of the City of Ljubljana. By compiling existing geological data and field work, a detailed geological map of the study area was elaborated. The spatial distribution of thermal conductivity was estimated with measurements of thermal conductivity on 47 representative samples of 18 lithostratigraphic units and field measurements in unconsolidated sediments at 12 localities. The measured values range between 0.63 and 5.18 $Wm^{-1}K^{-1}$. Continuous groundwater temperature measurements in 17 observation wells with depth to 118 m show relatively small temperature changes over time of 5 months. The measured values on the Ljubljansko polje range between 10.6 °C and 14.6 °C, while in the Ljubljansko barje the temperature increases up to 15.6 °C. Multi-level groundwater temperature measurements in 9 observation wells indicate three different conditions: both negative and positive temperature gradients and a constant temperature in different depths of the aquifer, which reflects the deeper geothermal or hydrogeological conditions and the anthropogenic impact.

Izvleček

Plitva geotermalna energija je obnovljiv vir energije. Njena raba omogoča ugodne učinke na podnebje, zdravje in gospodarstvo. Pogoj za učinkovito in trajnostno rabo geotermalne energije je poznavanje potenciala, kakor tudi ovir, ki omejujejo njeno rabo. V članku smo predstavili prve rezultate raziskav za oceno plitvega geotermalnega potenciala na območju mesta Ljubljana, ki se izvajajo v okviru projekta GeoPLASMA-CE. Z usklajevanjem obstoječih geoloških podatkov in terenskimi raziskavami je bila izdelana natančna geološka karta. Prostorska porazdelitev toplotne prevodnosti kamnin (18 litostratigrafskih enot) je ocenjena z meritvami na 47 reprezentativnih vzorcih in s terenskimi meritvami nekonsolidiranih sedimentov na 12 lokacijah. Izmerjene toplotne prevodnosti kamnin so v razponu med 0,63 in 5,18 $Wm^{-1}K^{-1}$. Zvezne meritve temperature podzemne vode v 17 opazovalnih vrtinah do globine 118 m kažejo relativno majhne spremembe v 5 mesečnem obdobju. Izmerjene vrednosti na Ljubljanskem polju so v razponu med 10,6 °C in 14,6 °C, na Ljubljanskem barju pa naraščajo do 15,6 °C. Temperature podzemne vode izmerjene na različnih globinah v 9 vrtinah kažejo tri različne razmere: negativni in pozitivni temperaturni gradient ter konstantno temperaturo v različnih globinah vodonosnika, kar odraža globlje geotermalne ali hidrogeološke razmere ter antropogeni vpliv.

Introduction

Shallow geothermal energy

Geothermal energy is the energy stored in the form of heat beneath the surface of the solid Earth (RES Directive, 2009). It originates internally from the Earth's core and mantle, from where it is transferred to the surface by the heat flow, and externally from solar radiation, which heats the upper ground. The fluctuation of the air temperature causes an annual variation of the ground temperature. Due to a high thermal inertia of the ground material, the amplitude of these variations diminishes with depth until the amplitude reaches a depth where it remains constant (Fig. 1). This temperature is often called the undisturbed ground temperature (Ouzzane et al., 2015). In Central Europe, a constant temperature around 10 °C is expected in a depth of 20 m (Internet 1; Strgar et al., 2017). Down to depths of 300 or 400 m, which are often referred to as the limit of shallow geothermal energy (Prestor et al., 2017), the temperature of the subsurface ranges between 2 and 20 °C in Central Europe and is similar or slightly higher in Slovenia (Rajver et al., 2006).

Due to the low temperature level, the direct use of shallow geothermal energy is limited. Heat pumps enable the extraction of heat energy from the ground and shallow subsurface, concentrating it and using it to supply heat and domestic hot water (Buckley et al., 2015). The same system can be used to cool a building by removing surplus heat energy and storing it under the ground. The most efficient systems carry out both functions. In general, there are two types of geothermal or ground source heat pump (GSHP) installations: closed loop and open loop systems (Internet 1). Closed loop systems use pipes that are either installed vertically down to several hundred meters (borehole heat exchangers – BHE), horizontally in depths of 1 to 2 meters (collectors), or in foundation piles of buildings. Closed loop systems use a fluid (a mixture of water and a refrigerant) that continuously circulates in the pipes, absorbs heat from the ground and transfers it via a heat exchanger to the heat pump, which raises the temperature up to 60 °C (Internet 1). For cooling, the process is reversed. Open loop systems use groundwater directly as a heat source. Groundwater is pumped from an extraction well, used by the heat pump and, afterwards, reinjected into an injection well.

The utilization of shallow geothermal energy has certain advantages compared to other renewables: it allows for the highest savings in comparison to conventional energy sources; it is available everywhere at any time, independent of weather conditions; and its exploitation has the lowest environment impact (Gemelli et al., 2011). Drawbacks are a higher initial cost, and limited availability of trained technicians and contractors (Kumar et al., 2015).

The heating and cooling of buildings account for approximately 40 % of the global energy consumption (Nejat et al., 2015); therefore, geothermal heat pump systems present one of the key technologies for reducing fossil fuel consumption and emissions that are hazardous to climate and air quality.

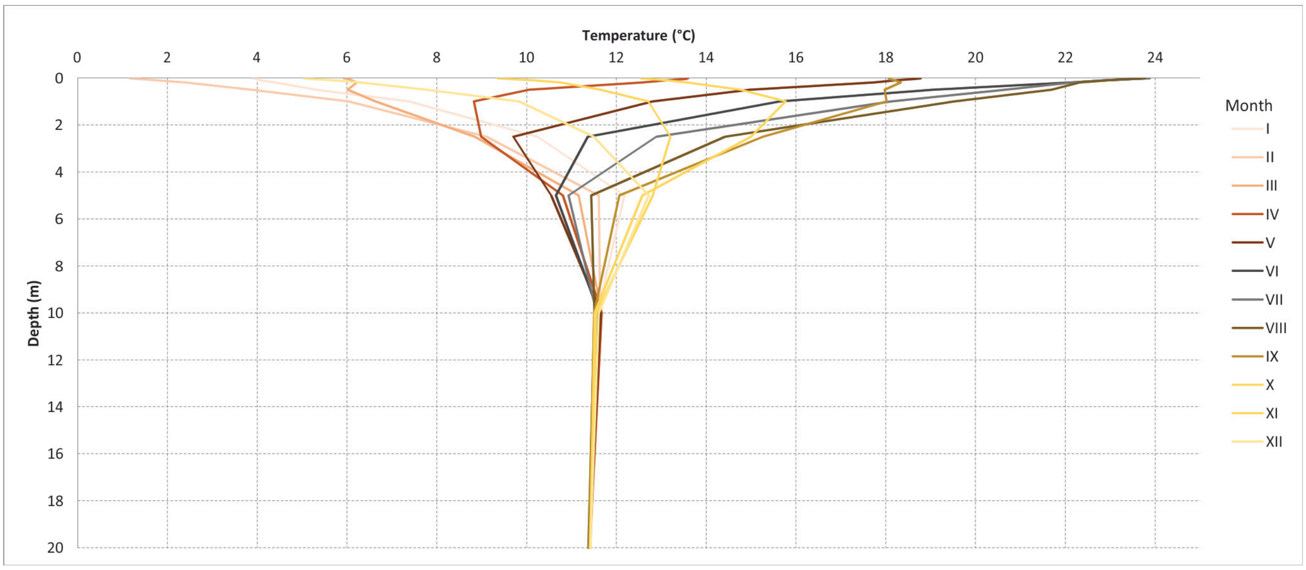

Fig. 1. Seasonal ground temperature distributions (adapted after Strgar et al., 2017).

The current utilization of shallow geothermal energy

The direct utilization of all geothermal energy is applied in at least 82 countries (Lund & Boyd, 2015). The installed thermal power for direct utilization at the end of 2014 equaled 70,329 MW_t, and the thermal energy used was 587,786 TJ/yr (163,287 GWh/yr), which was about a 38 % increase over 2010. GSHPs have the highest share among all the direct use categories, approximately 55 %, and it is assumed their share will continue to rise. Greater progress has been observed in the shallow geothermal energy use also in Slovenia, where, according to the status as of 31 Dec. 2015 (Rajver et al., 2016), the number of all GSHP units was around 9,350 with an installed capacity of 136.64 MW_t and a total energy consumption of 732.1 TJ/yr (203.36 GWh), compared to the status in 2010, when some 4,800 units were in operation. The great majority of units are typically of 11 to 12 kW rated power. About 47 % of them were open loop systems with 322.8 TJ of annual used shallow geothermal energy from groundwater; 46 % were closed loop systems with horizontal collectors with 230.4 TJ of annual used energy; and 7 % were vertical closed loop systems (BHEs) with 47.3 TJ of annual used energy from shallow subsurface.

Assessment of the shallow geothermal potential

Efficient use of shallow geothermal energy requires solid knowledge of natural conditions. The design of GSHP systems has to adapt to them, thus geological and geothermal data (rock type and hardness, ground thermal characteristics, groundwater occurrence) is of essential importance (Sanner, 2010). It is acquired by field investigation (geological mapping, rock sampling, investigations of hydrogeological, geochemical and geothermal conditions in the subsurface, etc.) and by laboratory measurements (thermal parameters of rock samples, etc.). The visualization of data in the form of geological/geothermal maps and their upgrade into geothermal potential maps can be very supportive in the planning of geothermal installations and can contribute to the fostering of their implementation. Methods for the estimation of the shallow geothermal potential and its integration into local energy plans and strategies are currently being developed within the projects GeoPLASMA-CE (Internet 1) and GRETA (Internet 2).

In the City of Ljubljana, a coal and biomass powered district heating system covers most of the densely populated area and distributes heat to 74 % of all households (COL, 2012). Natural gas is the complementary source of heating. The share of geothermal energy use for heating and cooling is very low. To achieve the environmental goals related to an increased share of renewable energy in the final energy consumption and reduction of the greenhouse gas emissions as set forth in the Sustainable Energy Action Plan of the City of Ljubljana (COL, 2012), the improvement of the energy efficiency and intensification of research and introduction of new technologies for the utilization of renewable energy sources are planned. The local heat and cold production is a sector in which the largest share (65 %) of the greenhouse gas emissions reduction can be achieved. In this respect, shallow geothermal energy will have an important role. The objective of the planned activities, part of which is presented in this study, is to quantify the shallow geothermal potential and provide geoscientific information that could be integrated into development strategies and help to foster the use of shallow geothermal energy.

In this paper, the research results of the geological and geothermal conditions for the assessment of the shallow geothermal potential in the area of the City of Ljubljana are presented. The harmonization of existing geological data/maps was performed to create a basis for spatial distributions of geological units (3D model) and thermal properties of the shallow subsurface in the study area. Using the harmonized geological map, 47 representative samples of lithological units were taken, their thermal parameters (thermal conductivity and diffusivity) measured, and a map of thermal conductivities elaborated. For assessing the geothermal potential of the groundwater, a monitoring network with temperature loggers in 17 observation wells was established and 5 months of measurements obtained. The presented investigations and results are part of the workflow for mapping the shallow geothermal potential developed within the GeoPLASMA-CE project (Hofmann et al., 2017), which will be implemented in six pilot areas (including the presented study area) across central Europe.

The study area

The study area covers 275 km² (Fig. 2) and corresponds to the administrative area of the City of Ljubljana (COL). The central flat urbanised area is surrounded by a hilly hinterland and divided by hills (Golovec, Grajski hrib and Rožnik) in the middle on the Ljubljansko polje (Ljubljana Field) and the Ljubljansko barje (Ljubljana Marsh).

Geologic setting

The geological structure of the study area is extremely diverse regarding both the lithology and age of the geological units. This is due to the tectonic collage of several paleogeographic units represented today in three geotectonic units. The largest part of the area belongs to the External Dinarides with the transition into the Internal Dinarides to the east and north. In the north-western corner, the Dinarides border the Southern Alps. Characteristic for the External Dinarides is the thrust and nappe structure that became accomplished in the Upper Eocene to the post-Eocene times. In the study area territory, only the Hrušica and Trnovo nappes can be recognized with certainty in the area's western rim (Placer, 2008). There, the Trnovo nappe is the highest structural unit of the External Dinarides. The Carboniferous-Permian siliciclastic rocks in the north-eastern part of the nappe west of the Ljubljana basin undoubtedly lie on the Mesozoic mostly carbonate beds of the lower Hrušica nappe unit. On the contrary, the Carboniferous-Permian clastic rocks of the Litija anticline in the Sava folds east of the Ljubljana basin lie consistently below the Mesozoic beds. The Carboniferous-Permian clastites of the Trnovo nappe and Litija anticline then come into contact in the area of the Ljubljana basin, although they belong to different structural units. In the Sava folds nappe structure, units occur that lie structurally above the Trnovo nappe. The contact of the two tectonic settings is the Želimlje fault, which passes over the central part of the External Dinarides along the eastern rim of the Ljubljansko barje and the western rim of Ljubljana basin (Placer, 1998a, b, 2008).

Along the north-western rim of the study area, deep-marine rocks belonging to the Slovenian basin paleogeographic unit are overthrust on the Trnovo nappe (Placer, 2008).

In the wider territory of the study area, the recent continuing tectonic activity with deformations is evidenced in geodetic and geomorphologic data (e.g. Rižnar et al., 2005; Jamšek Rupnik, 2013; Jamšek Rupnik et al., 2013; Moulin et al., 2016).

Pre-Quaternary basement

The most widespread lithological unit of the pre-Quaternary basement is represented by the Carboniferous-Permian siliciclastic rocks which build the predominant part of the rim of the Ljubljana basin with the largest extent to the east

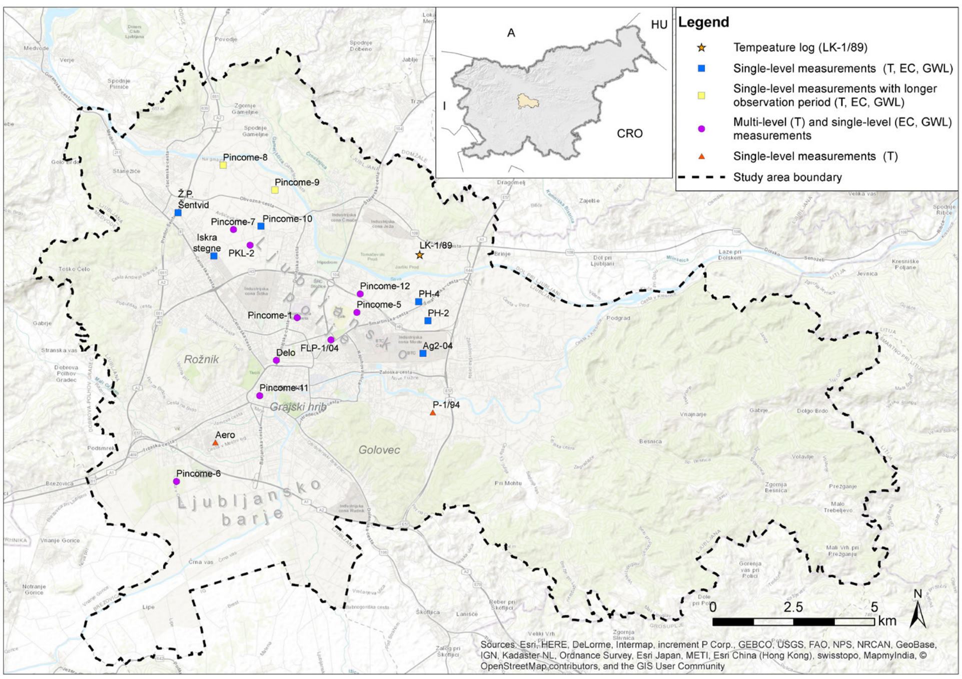

Fig. 2. Study area and monitoring network (T, EC, GWL denote temperature, electric conductivity and groundwater level measurements).

in the Sava folds. These rocks are also the oldest in the study area. Quartz sandstone and lithic quartz sandstone strongly prevail over quartz conglomerate, siltstone and shale. In the lithostratigraphic succession of these rocks, three superpositional units were distinguished (Mlakar, 1987; Mlakar et al., 1993). Due to the absence of fossils, up till now only the rocks of the middle sandstone subunit have been dated and attributed to the Late Carboniferous (Namurian-Westphalian A and Westphalian A) based on fossil plant remains found between Ljubljana (Grajski hrib, Golovec) and Polšnik near Litija (Kolar-Jurkovšek & Jurkovšek, 1985, 2002, 2007).

The only other unit that also occurs to a larger extent is the Middle to Upper Triassic (Ladinian to Carnian) dolomite of the Schlern formation. This whitish, coarse grained late diagenetic dolomite, usually non-bedded (massive) and heavily tectonized, builds the south-eastern rim of the study area.

All other lithostratigraphic units of the pre-Quaternary basement cover only smaller areas. The Middle Permian Gröden formation is composed of alternating quartz sandstone, conglomerate, siltstone and shale, all of them of characteristic reddish or greyish colour. Only in the area of Podmolnik, interbeds of dolomite occur. The Lower Triassic Werfen formation is lithologicaly very heterogenous with alternation of marly limestone and dolomite, marlstone, sandstone and shale. The lower part of the Middle Triassic (Anisian) comprises thickly bedded dolomite, while Ladinian is again heterogeneous. Thin-bedded limestone, with chert laminae and nodules intercalated with marlstone, dominates over shale, marlstone, green tuff and tuffite. Lithologically very similar is the Upper Carnian (Julian-Tuvalian) unit, but with lesser marlstone and volcaniclastic beds and more sandstone. The upper part of the Upper Triassic (Norian-Rhaetian) is represented with two thick-bedded carbonate units, the Main dolomite and the Dachstein limestone, respectively. Similar to the latter, but with oolithic layers and breccia horizons, is the Lower Jurassic (Liassic) limestone, occurring only in Podutik. On the slopes of Šmarna gora and Rašica occur Lower Cretaceous (Aptian-Cenomanian) deeper marine flysch rocks, namely shale, marlstone, sandstone, reddish limestone and limestone breccia with intercalations of conglomerate.

Quaternary sedimentary fill

The central and the most densely populated territory of the study area lies in the neotectonic basin with extensive and thick accumulations of Pleistocene and Holocene fluvial sediments. The foundations for the up-to-date subdivision of Quaternary sedimentary fill in the Ljubljana basin were laid by Kuščer (1955) who subsequently studied the influence of tectonics on sedimentation (Kuščer, 1991). Žlebnik (1971, 1993) considered the Quaternary fill of the Ljubljansko polje (the Ljubljana Field), the northern and central parts of the Ljubljana basin, as glaciofluvial and divided it into four units, namely the Older, Middle and Younger conglomeratic fill, and the latest gravel fill. The chronology of their origin relies mostly on the results of pollen analyses from finer sediments, indicating that most of the sediments are of Würmian age or younger (Šercelj, 1965, 1966). Absolute datings (Vidic & Lobnik, 1997; Vidic, 1998) later upgraded the chronology in the broader area of the Ljubljana basin, which resulted in the division of sedimentary fill into three chronostratigraphic units dating ≤ 62 ka, 450–980 ka, and 1.8 Ma, respectively. The two samples of sandy silt with gravel that covers the wider surroundings of Podutik were dated by employing the OSL method as Late Rissian or Rissian - Würmian interglacial age (Bavec & Pohar, 2009).

The extensive area of the Ljubljansko barje in the south-western part of the Ljubljana basin is filled with lacustrine and paludal sediments. The tectonic model of the Ljubljansko barje is not satisfactorily understood, but a rapid subsidence in Quaternary is an established fact. The sedimentary succession in general thickens from the west and in the north-east of the Ljubljansko barje. According to borehole data, the maximum thickness is around 170 m (Mencej, 1990), although the results of geoelectric surveys also indicate depths surpassing 200 m (Ravnik, 1965). In the bottom part there are gravels, sandy gravels and silty gravels of varying thicknesses, followed upward by a sequence of fluvial, lacustrine and paludal sediments exceeding 100 m in places. The variability of sediments indicates tectonically and climatically affected changes of the sedimentation regime, well-documented and dated for a large part of the Quaternary. Palynologic analyses of sediment indicate an almost continuous sedimentation during the interval from the start of the Mindelian glacial (approx. 650 ka) into the Holocene, when it was terminated by the deposition of organogenic lake clay and, in places, with the formation of peat bog (Šercelj, 1965, 1966; Bavec & Pohar, 2009).

Hydrogeology

The thick accumulation of Pleistocene and Holocene fluvial sediments in the Ljubljansko polje area is highly permeable and contains significant quantities of groundwater, which is the main resource exploited for the public water supply of the City of Ljubljana. The Ljubljansko polje aquifer is unconfined, recharged mainly from the Sava River and partly from rainfall (Janža, 2015). The recharge from the Sava River is intensive in the north-western part of the Ljubljansko polje; in the eastern part, groundwater is drained into the river. Groundwater flow in the western part is directed from the river towards the south and south-east, and in the eastern plain towards the east and north-east. Groundwater flow velocity is high, estimated up to 20 m/day (Janža et al., 2005). The unsaturated zone is on average 25 m and the saturated zone up to 70 m thick. The fluctuation of the groundwater table in observation wells is the highest in the north-eastern part (up to almost 10 m) and decreases towards the central and eastern part, where the difference between high and low groundwater table is around 2 m.

The Ljubljansko barje is composed of alternating fluvial and lacustrine deposits with a heterogeneous composition. The top clay layer in the northern part of the Ljubljansko barje is 4 m thick. A heterogeneous and low permeable upper Pleistocene aquifer, about 2 meters thick, is situated below. It is separated by another thick clay layer from the lower Pleistocene aquifer that consists of gravel and contains groundwater of good quality. The latter is a confined or semi-confined aquifer with artesian to subartesian conditions (Janža et al., 2017).

Deep geothermal conditions

In the study area, the geothermal gradient down to 1000 m depth is between 15 and 28 mK/m. In the 1801 m deep LK-1/89 borehole, drilled almost completely through clastic rocks (claystone to mudstone, siltstone and sandstone) of Car-

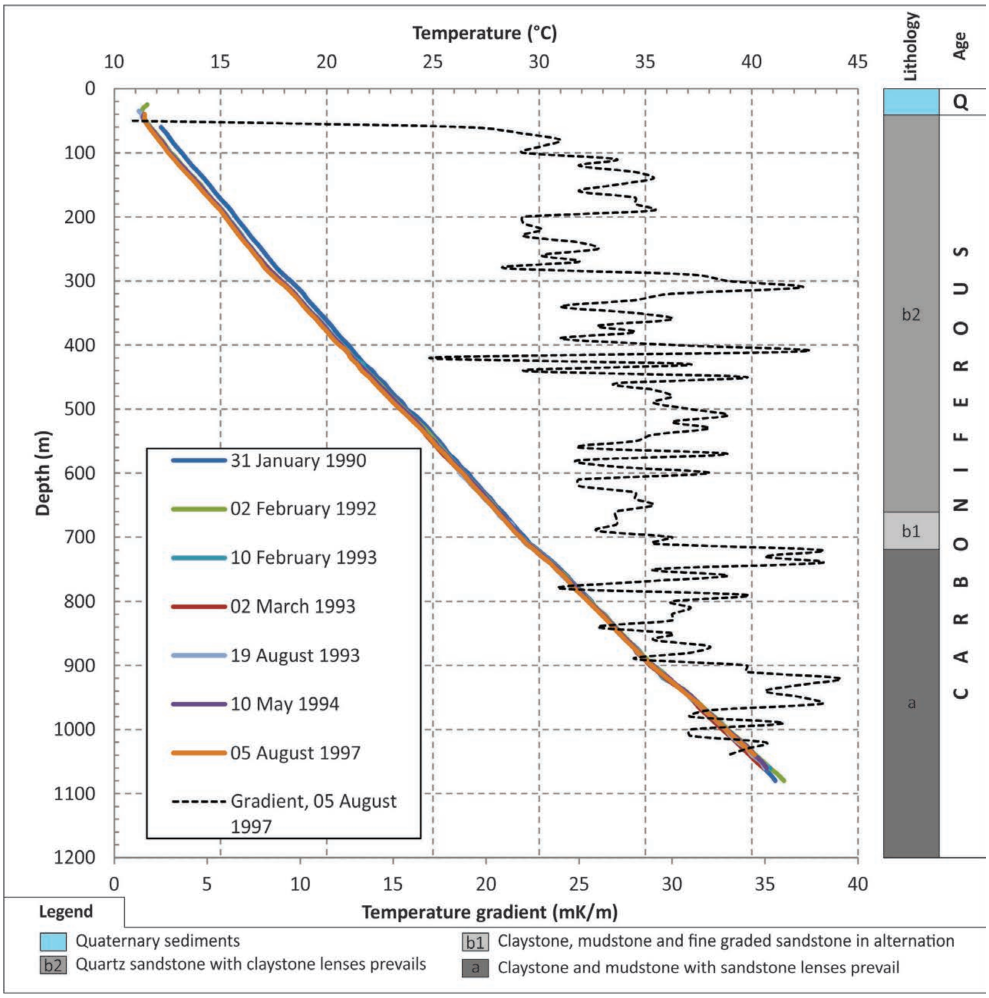

Fig. 3. Temperature logs and geothermal gradient determined in LK-1/89 borehole. Geological column is simplified after Kranjc et al. (1989).

boniferous-Permian age near Nadgorica (Fig. 2), temperature logging was performed eight times in a period 1990 to 1997 (Fig. 3). With the last logging in 1997, 38.8 °C was measured at 1000 m depth. Slightly higher geothermal gradients are in lowlands of the study area, especially south and southwest of Ljubljana in the Ljubljansko barje, where temperature logging was carried out in 21 shallow boreholes. In this southern part of the study area, none of the examined boreholes was deeper than 370 m. But geophysical research there in the period 1988–1993 indicated the existence of local positive geothermal anomaly in the Quaternary low permeable sediments, which is probably a consequence of a thermal convection zone in the carbonate rocks, mostly dolomite of Triassic age, just below the Quaternary sediments (Živanović & Rajver, 2004).

The surface heat-flow density (HFD) was determined in the past 30 years at localities of ten boreholes in a wider study area. In nine boreholes, the rock samples were cored, and thermal conductivity was measured using mostly the devices with transient hot wire method (Prelovšek & Uran, 1984; Prelovšek et al., 1982). The HFD values, corrected for topographic effect, range from 60 to 135 mW/m^2. However, the highest values (100 to 135 mW/m^2) are influenced by the mentioned thermal convection zone (between Vnanje Gorice and Trnovo), while outside of this zone, the values range between 86 and 96 mW/m^2, which are 40 to 57 % higher than the rest of Slovenia (Rajver & Ravnik, 2002) and 33 to 49 % higher than the continental (European) average (Čermák, 1979; Hurtig et al., 1992; Majorowicz & Wybraniec, 2011).

Methods

The harmonization of the geological map and an update of the pre-Quaternary bedrock

The basis for 3D geological modeling and for the determination of the sampling localities for the measurement of thermal parameters was the Basic Geological Map of SFR Yugoslavia 1:100,000 which cover the study area with four sheets, namely: Kranj (Grad & Ferjančič, 1974), Ljubljana (Premru, 1983), Postojna (Buser et al., 1967), and Ribnica (Buser, 1969). The newer and revised Geological Map of Slovenia 1:250,000 (Buser, 2009) was used for emendations and harmonization, while several maps of larger scales were used for fine tuning and adjusting the model to the data from the boreholes (e.g. Novak, 2000).

The pre-Quaternary very low permeability base of the Ljubljansko polje aquifer and the northern part of the Ljubljansko barje aquifer (Mencej, 1990; Kristensen et al., 2000) was updated using new data from the boreholes (Janža et al., 2017).

Measurements of thermal parameters

The evaluation of the conduction and absorption of heat in the Earth's upper crust requires knowledge of the thermal properties of the ground material. Heat transmission in the Earth occurs principally by conduction and secondarily by convection and radiation (Robertson, 1988; Kappelmeyer & Haenel, 1974; Beck, 1988).

Measurements of the thermal parameters of rocks and hard soil

For the evaluation of the thermal parameters of the rocks, it was necessary to sample many different types of rock in the field. In the field, the main lithostratigraphic units which cover larger areas and their most common lithological varieties were sampled in several localities. Altogether, 47 samples from 18 solid rock units were collected. The measurements of thermal conductivity (TC) and thermal diffusivity (TD) on compact rocks and also on hard soil (e.g. clays and similar soils that are not too soft) were performed in the laboratory using Thermal Conductivity Scanner (TCS), produced by TCS Lippmann and Rauen GbR (Popov et al., 2017, Fig. 8). The TC and TD measurements were carried out on 47 rock samples with 86 rock pieces. All these rock pieces were measured to obtain better representative mean values of the thermal properties of rocks for each lithological unit. The samples were wrapped in plastic bags, and those assigned in Table 1 as "saturated" were put in water over night, others were put in water for one or two hours, but their surface was left to dry out just before the scanning.

The optical scanning technology is based on the scanning of the plane or cylindrical surface (along the cylinder axis) of a studied sample with a focused, mobile and continuously operated heat source in combination with infrared temperature sensors (Popov et al. 1999; 2012). The determination of thermal conductivity values is based on the comparison of excessive temperatures of standard samples (having a known thermal conductivity λ_R) with excessive temperatures of one or more unknown samples being under heating by the movable concentrated heat source. The thermal conductivity of unknown samples is calculated as a result of a comparison of the excessive temperatures using the standard thermal conductivity values. For the TCS method, a low tolerance is prescribed for the flatness of the sample surface (+/- 0.5 mm), and hence, almost all the samples were first cut with a circular saw to cope with this requirement. The simultaneous measurements of TC and TD use a 2-channel type of temperature sensor measuring two temperatures after heating at spots located some mm apart.

Measurements of the thermal parameters of soft soil

Field measurements of the thermal parameters, the TC and thermal resistivity, of the softer or unconsolidated and porous sediments were carried out at 12 localities (3 lithological units). They were performed with the use of the KD2 Pro thermal properties analyzer (Decagon Devices, 2016), which is especially dedicated for soft and loose sediments (Fig. 4). Typically, the probe for measuring TC and thermal resistivity consists of a 6 cm (optionally 10 cm) long needle with a heater and temperature sensor inside. More recently, the heater and temperature sensors have been placed in separate needles, both 3 cm long and 6 mm apart. Within such a dual probe, the analysis of the temperature versus time relationship for the separated probes yields information on TD and volumetric specific heat capacity along with TC and thermal resistivity. All four thermal parameters were measured at 7 of the mentioned 12 localities.

Groundwater temperature measurements

Groundwater temperature has been continuously measured on 17 locations (Fig. 2). Single-level (8 locations) and multi-level measurements (9 locations) (Fig. 5) have been performed with GSR 120 NTG loggers (15 pcs) (Internet 3) and HOBO temperature loggers (44 pcs) (Internet 4). Along with the temperature measurements, GSR 120 NTG loggers also enable measurements of the water level and the electrical conductivity of the groundwater. Loggers were installed in May 2017 and set up to record measurements at one hour intervals. The spatial distribution of measurement locations was designed in a way to capture the influence of the factors which presumably affect the groundwater temperature in the study area (e.g. recharge from the Sava River and the urban area heat island).

Results and discussion

The harmonized geological map and the updated pre-Quaternary bedrock

The harmonized geological map of the study area (Fig. 6) and an updated interpretation of the pre-Quaternary bedrock (Fig. 7) are presented in the following text.

Fig. 4. Field measurement of the thermal parameters with the KD2 Pro meter.

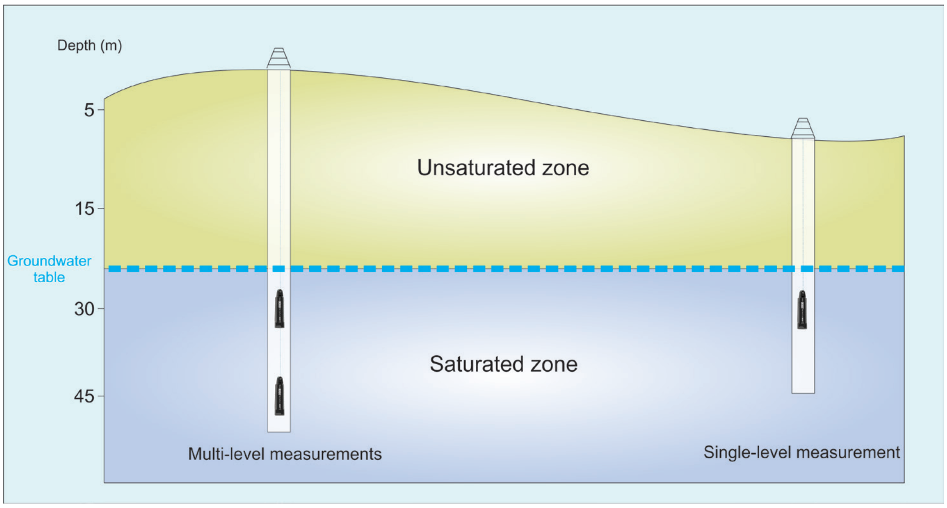

Fig. 5. Scheme of multi-level and single-level measurements in observation wells.

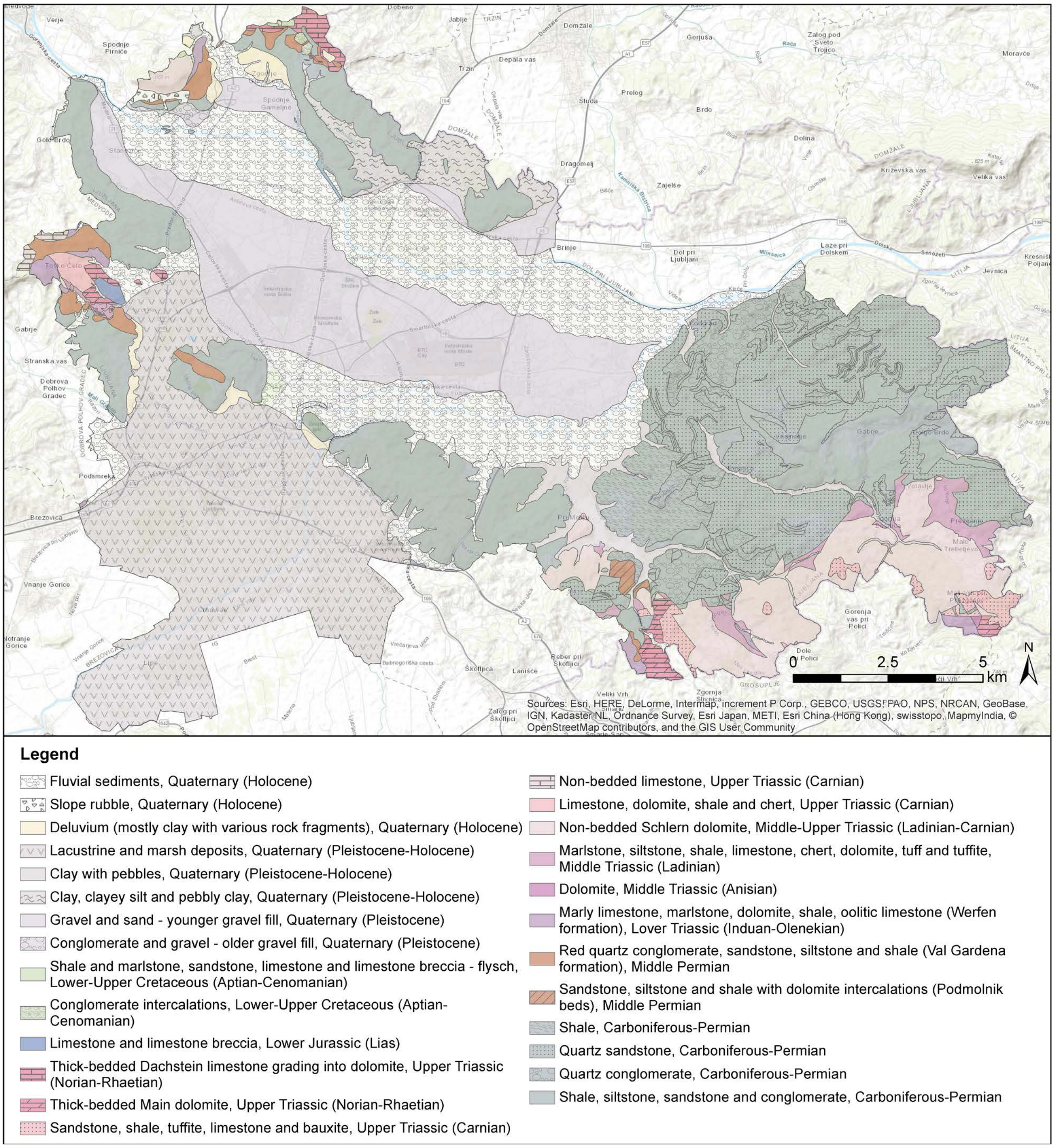

Fig. 6. The harmonized geological map of the study area.

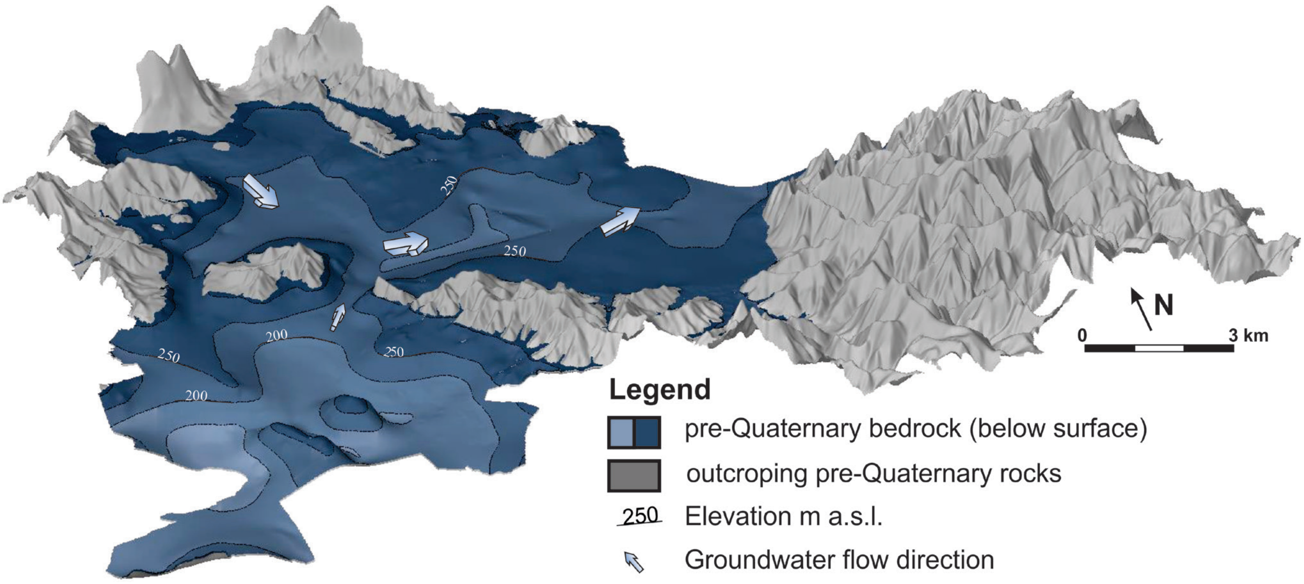

Fig. 7. 3D model of pre-Quaternary bedrock (5 × vertical exaggeration).

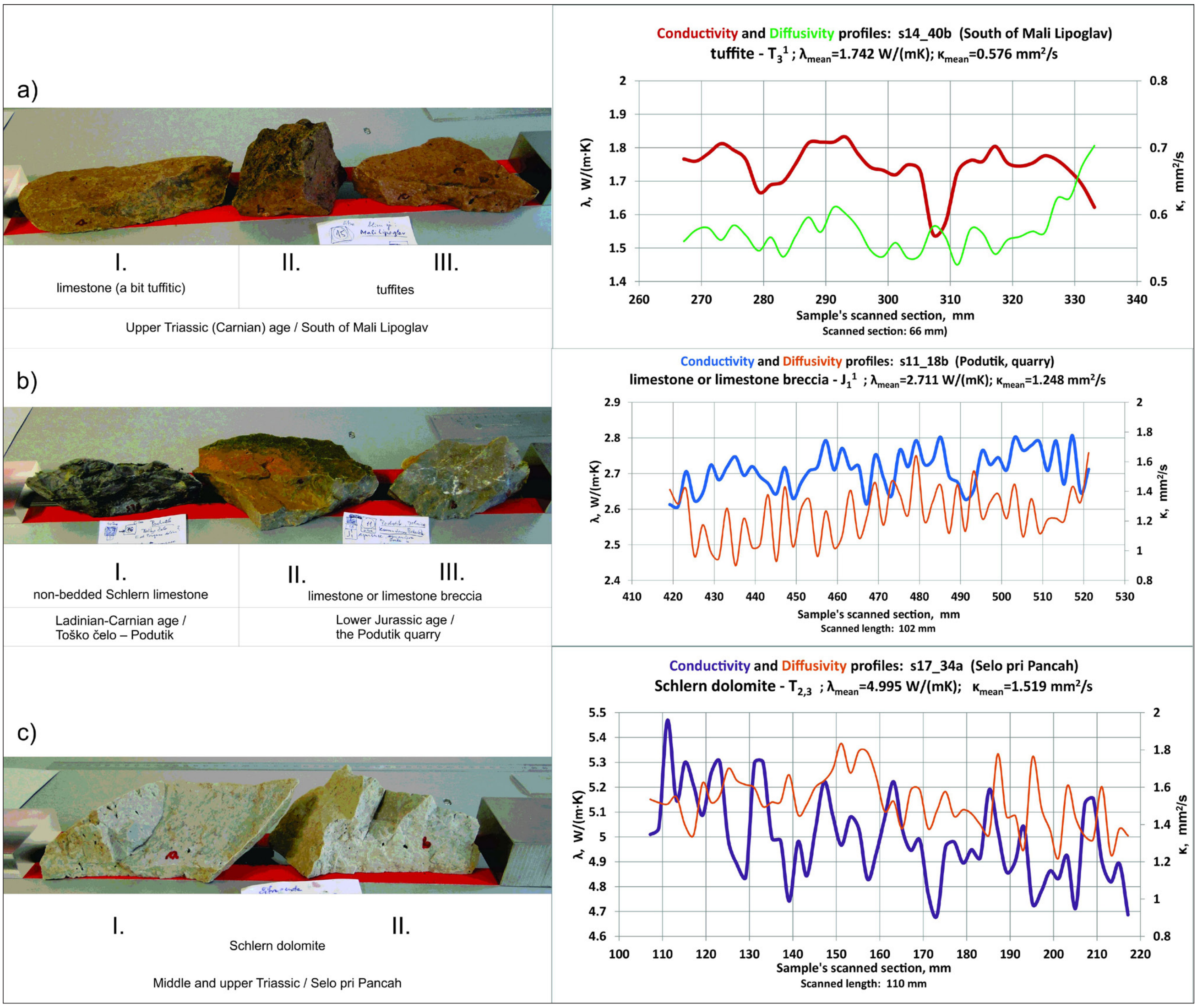

Fig. 8. Set of rock samples along the scanning line of TCS meter (left); the TC and TD profiles from the scanning of rock samples (right).

Thermal parameters

The results of TC and TD measurements show a great variety in the thermal properties of different lithological units (Table 1). The heterogeneous nature of the rock samples is noticeable, especially TC, which is a consequence of the mineral composition, rock density, their structure and texture and the pores' filling (water saturation) (Kappelmeyer & Haenel, 1974; Beck, 1988). It must be stressed that despite the efforts to simulate the natural conditions as much as possible, no rock sample could be completely water saturated, due to the lack of appropriate pressure devices. On the other hand, particularly compact solid rock samples are less susceptible to water saturation, therefore their rock status (Table 1) has been assigned as slightly or partly saturated or just wet during the TC and TD scanning. Some examples are presented herein in regard to the rock samples with typical low (Fig. 8a), average (Fig. 8b) or high (Fig. 8c) values of TC.

Table 1. The mean TC and TD values of the 47 rock samples (86 rock pieces altogether), measured with the TCS method.

Locality	Type of Rock	Rock state: saturated, slightly sat., wet or dry	Chrono-stratigraphic unit	Thermal Conductivity	Thermal Diffusivity
				λ, W/(m·K)	**κ**, mm²/s
Rašica hill, NW slope	red calcareous sandstone grading into siltstone	slightly sat	K1,2	**3,13**	**1,25**
Rašica hill, NW slope	red to pink limestone		K1,2	**3,24**	**1,26**
Rašica hill, NW slope	conglomerate (Cenomanian)	saturated	K1,2	**3,11**	**1,24**
Podutik, quarry Podutik	limestone & limestone breccia	slightly sat	J1/1	**2,79**	**1,23**
Rašica hill, NW slope, more to west	Dachstein limestone (thick bedded) grading into dolomite	wet	T3/2+3	**2,98**	**1,21**
Podutik, Dolnice, along road to Kamna Gorica	Dachstein limestone grading into dolomite (thick bedded)	saturated	T3/2+3	**3,66**	**1,40**
Podutik, Bike park	Main dolomite (thick bedded)	slightly sat	T3/2+3	**5,18**	**2,10**
N of Repče, near quarry along road	Main dolomite (thick bedded)	dry	T3/2+3	**4,21**	**1,43**
ESE of Mali Vrh at Prežganje, S of Veliko Trebeljevo	limestone & marly limestone	slightly sat	T3/1	**2,84**	**1,17**
S of Mali Lipoglav, between M. Lipoglav and Zg.Slivnica	limestone (a bit tuffitic)	slightly sat	T3/1	**2,73**	**0,98**
S of Mali Lipoglav, between M. Lipoglav and Zg.Slivnica	tuffite	slightly sat	T3/1	**1,73**	**0,56**
S of Mali Lipoglav, between M. Lipoglav and Zg.Slivnica	limestone (tuffitic?)	slightly sat	T3/1	**2,92**	**1,05**
Podutik, Toško Čelo, E of Požgane doline	non bedded limestone	slightly sat	T2,3	**3,01**	**1,49**
Podutik, Prevalnik, Toško Čelo	marly limestone with chert	slightly sat	T3/1	**3,46**	**1,53**
between Selo at Pance and Pance	Schlern dolomite	slightly sat	T2,3	**4,79**	**1,74**
Podutik, S of Bike park	tuff (pieces & weathered matrix)	wet	T2/2	**2,72**	**1,21**
Podutik, S of Bike park	tuff	slightly sat	T2/2	**3,50**	**1,45**
Toško čelo	limestone with cherts & marly limestone	wet	T2/2	**3,14**	**1,37**
Malo Trebeljevo, beyond right bend, on open meadow	dolomitic marlstone & marly dolomite	slightly sat	T2/2	**3,19**	**1,42**
Malo Trebeljevo (N part of village), roadside S of long right bend	dolomite	wet	T2/2	**4,44**	**1,25**
W of Podutik, SE of Toško Čelo	dolomite	slightly sat	T2/1	**4,44**	**1,83**
Toško Čelo, S of restaurant „Pri Bitencu“	oolite limestone (marlstone?)	slightly sat	T1	**2,39**	**0,82**
road to Toško Čelo	dolomite	partly sat	T1	**3,74**	**1,83**
road to top of hill on Toško Čelo	oolite limestone	dry	T1	**2,92**	**1,03**
road to top of hill on Toško Čelo	sandstone & siltstone	slightly sat	T1	**2,81**	**1,02**
road to top of hill on Toško Čelo	dolomitic marlstone & marly dolomite	slightly sat	T1	**3,48**	**1,37**
along road Repče - Pleše	marlstone, marly limestone	slightly sat	T1	**1,64**	**1,02**
along road Repče - Pleše	limestone	wet	T1	**2,80**	**1,01**
along road Repče - Pleše	dolomite	wet	T1	**4,05**	**1,50**
Rašica hill, SW slope, along road to Srednje Gameljne	red sandstone & shale	slightly sat	P2/2	**3,14**	**1,76**
W of Podutik, Stražni vrh, N slope	siltstone (aleurolith)	slightly sat	P2/2	**2,19**	**0,80**
W of Podutik, Stražni vrh, N slope	tuffite (light brown)	slightly sat	T2	**3,60**	**1,88**
Rašica hill, SW slope, along road to Srednje Gameljne	quartz sandstone	slightly sat	P2/2	**3,18**	**1,44**
SE of Šentpavel	quartz-dolomitic sandstone (Podmolnik beds)	slightly sat	P2	**3,24**	**1,38**
SE of Šentpavel	mudstone (Podmolnik beds)	slightly sat	P2	**2,38**	**0,90**
SE of Šentpavel, along road to south	red siltstone (Podmolnik beds)	slightly sat	P2	**2,40**	**0,72**
SE of Šentpavel, along road to south	red quartz sandstone (Podmolnik beds)	slightly sat	P2	**3,63**	**0,96**
Brezje at Podlipoglav	shale (Podmolnik beds)	slightly sat	P2	**1,86**	**0,84**
NW of Češnjica, SE of Sostro	shale	wet	C3	**1,44**	**1,09**
Javor above Besnica, NW of Javor	sandstone	partly sat	C3	**2,55**	**0,99**
NE of Malo Trebeljevo	quartz conglomerate	saturated	C3	**4,84**	**3,62**
NE of Veliki Lipoglav, W of Selo at Pance	quartz conglomerate	slightly sat	C3	**4,51**	**2,32**
along road Javor-Zagradišče, WNW of Radioamateurs' Mt. hut	quartz conglomerate	saturated	C3	**4,01**	**2,19**
Ljubljana Castle, W part of circular path	shale, partly siltstone (aleurolith) (=mudstone)	wet	C3	**2,49**	**0,93**
Ljubljana Castle, SE part of circular path at bridge	shale	wet	C3	**2,10**	**0,76**
Ljubljana Castle, SE part of circular path at bridge	shale	wet	C3	**1,70**	**0,61**
Ljubljana Castle, at NE corner of castle vineyard	siltstone (claystone?)	wet	C3	**1,68**	**0,80**
for TD: *T.D. of sample out of calibration range; Error in T.D. correction of sample. It could be mostly due to water saturated sample, even if only slightly sat.					

The results of thermal conductivity measurements (Table 1; Fig. 8) show that the rocks with high TC are especially dolomites and quartz conglomerates (3.6 to 5.4 $Wm^{-1}K^{-1}$). Those with average to high TC are marly dolomites, Dachstein limestones grading into dolomite, quartz sandstones, quartz-dolomitic sandstones, conglomerates, limestones with cherts, red limestones, tuffites and some sandstones (2.8 to 4.2 $Wm^{-1}K^{-1}$). Rocks with average TC parameter are limestones, marly limestones, (carbonate) sandstones, tuffs, most siltstones and mudstones (2.3 to 3.6 $Wm^{-1}K^{-1}$), while those showing low TC values are notably shales and some tuffites, and less remarkably some marlstones and siltstones or claystones (1.4 to 2.5 $Wm^{-1}K^{-1}$).

Table 2. The mean values of TC, thermal resistivity, volumetric heat capacity and TD from the measurements of the loose sediments.

Locality	Type of Soil or Rock	Sample Soil (Rock) state: saturated (wet), slightly wet or dry	Chrono-stratigraphic unit	Thermal Conductivity	Thermal Resistivity	Volumetric Specific Heat Capacity	Thermal Diffusivity
				λ W/(m·K)	r (rho) m·K / W	c_v MJ/(m³·K)	κ (kappa) mm²/s
Moste, Zalog, at GLS building	clay, sand, silt	partly wet	šQ2	**1,81**	0,55		
Moste, Spodnji Kašelj, S of St. Andrej church	gravel, sand - younger backfillings	mostly dry	4/ Q1; šQ2 below	**0,76**	1,32		
Center, Tabor, S of Health Center	gravel, sand, silt, soil	wet	šQ2	**1,38**	0,73	2,78	0,46
Bežigrad, Jarški prod, S of Črnuče industr. zone	sand, plant residues	dry, slightly wet	šQ2	**1,18**	0,85	1,85	0,53
Bežigrad, Jarški prod, S of Črnuče industr. zone	sand (river)	wet	šQ2	**1,41**	0,71	3,33	0,42
Bežigrad, Šmartno, ca 300 m E of football field	gravel, sand, silt	mostly dry	šQ2	**1,21**	0,82	3,22	0,38
Vič, Ljubljana Moor, Iška Loka, Ložca creek	organogenic moor sediments	wet	jQ2, bQ2	**1,01**	1,00	3,55	0,26
Vič, Ljubljana Moor, Podkraj - Strahomer	organogenic moor sediments	mostly dry	jQ2, bQ2	**0,75**	1,34		
Šentvid, Dvor-Stanežiče_sand separation	gravel, sand - younger backfillings	slightly wet	fglQ1	**1,34**	0,75		
Bežigrad, Kleče	silty clay (measured): gravel, sand, clay - younger gravel backfillings	slightly wet	4/ Q1 or fglQ1	**1,79**	0,56	2,78	0,60
Bežigrad, Torkarjeva street, new blocks of flats	gravel, sand - younger gravel backfillings	dry	4/ Q1	**0,63**	1,58		
Bežigrad, Jarše, Orehov Gaj	gravel, sand - younger backfillings	mostly dry, slightly wet	4/ Q1; šQ2 below	**1,28**	0,78	2,35	0,46

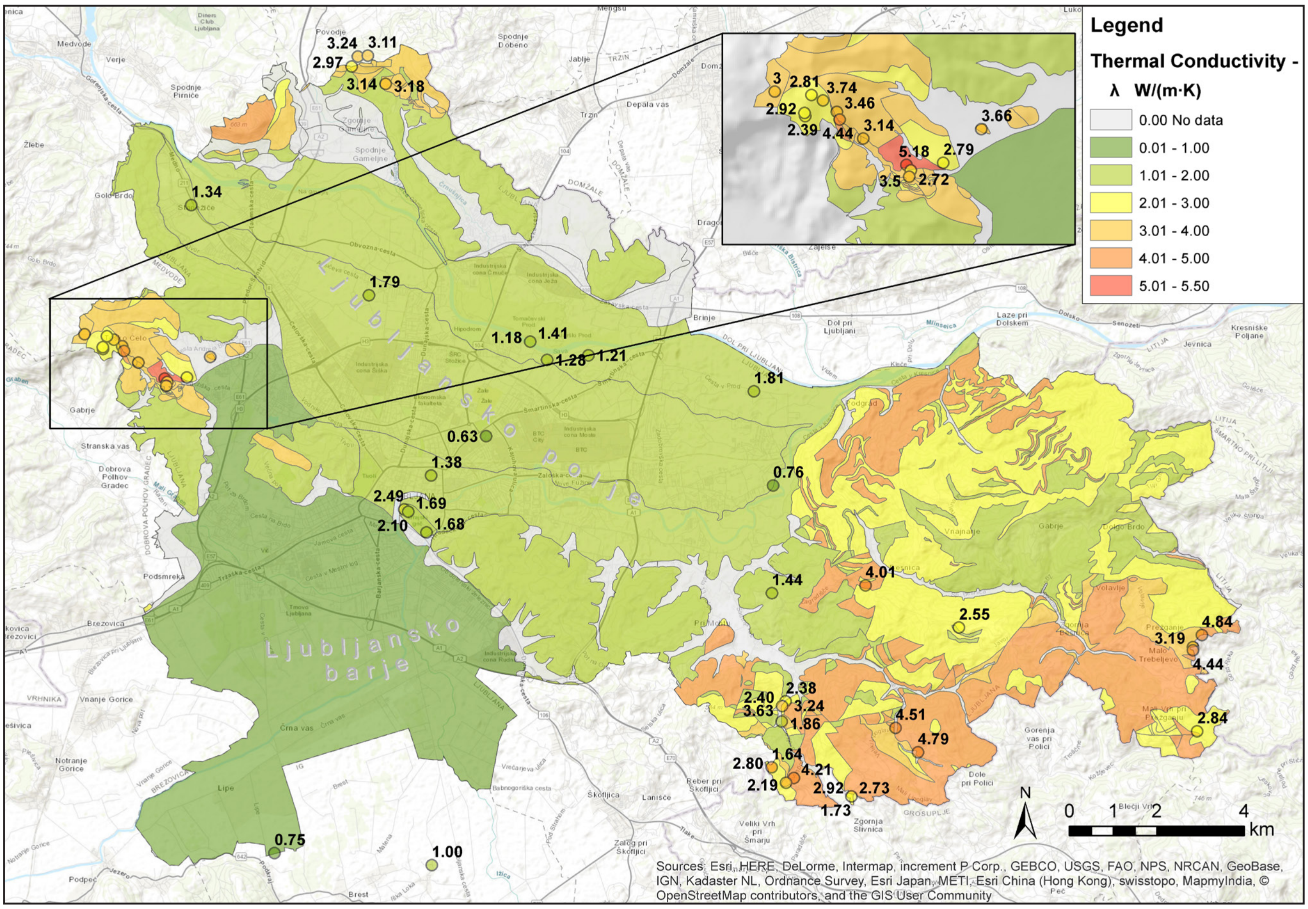

Fig. 9. The thermal conductivity map with the locations of the rock samples (circles with measured mean TC values in Table 1).

The results of the field measurements with the KD2 Pro needle probes (Table 2) show that water saturation plays a very important role. Also the manner of measurements is of great importance, as the method requires a very precise and delicate setting of the needle probes into the measured material. For 7 localities, the values of the volumetric heat capacity and thermal diffusivity are also presented. They are mostly within the expected range of these parameters. TC is obviously higher (1.2 to 1.81 $Wm^{-1}K^{-1}$) at those localities where the needle probe was inserted in a softer sediment very close to gravel pieces, and also where it was inserted in water saturated sandy clay, sand and silt. Measurements with the needle inserted in dry loose sediments gave quite low TC (0.6 to 0.8 $Wm^{-1}K^{-1}$). The spatial distribution of TC based on the harmonized geological map and measurements of TC is presented on the thermal conductivity map (Fig. 9).

Groundwater temperature

The measured groundwater temperatures (GWTs) range between 10.6 °C and 14.6 °C at the Ljubljansko polje and increase up to 15.6 °C in the deepest part of the well Pincome-6 at the Ljubljansko barje (Fig. 10; Appendix A). Measurements were performed over a period of 5 months. Despite the relatively short measurement period, some characteristics of the groundwater temperature distribution can be observed.

Measurements show relatively stable conditions and no significant changes of temperature over time. Exceptions are the measurements in the wells Delo and FLP-1/04, where fluctuations of temperature at some deeper levels are observed. These fluctuations show no trend, thus it can be assumed that they have been caused by anthropogenic influence (e.g. leaking sewage or heating systems, nearby installed heat pumps) or damaged loggers, but at the moment, the causes cannot be determined and further investigations are needed.

Stable temperature conditions indicate an absence of intensive groundwater recharge or inflow of fresh water. On the contrary, the previous GWT measurements in the well Pincome-9 (Fig. 11) located closer to the Sava River (Fig. 2), where an intensive groundwater recharge from the river has been interpreted (Janža, 2015), show annual fluctuations which follow the air or surface water temperature changes with a lag time of about 6 months.

Based on multi-level GWT measurements (Fig. 12), the observation wells can be classified into three groups. In the wells PKL-2, Pincome-1, Pincome-5, Pincome-7, and Pincome-12, there are very small changes or practically no noticeable vertical temperature gradient. In wells Pincome-11, FLP-1/04, and Delo, noticeable are temperature decreases with depth and negative

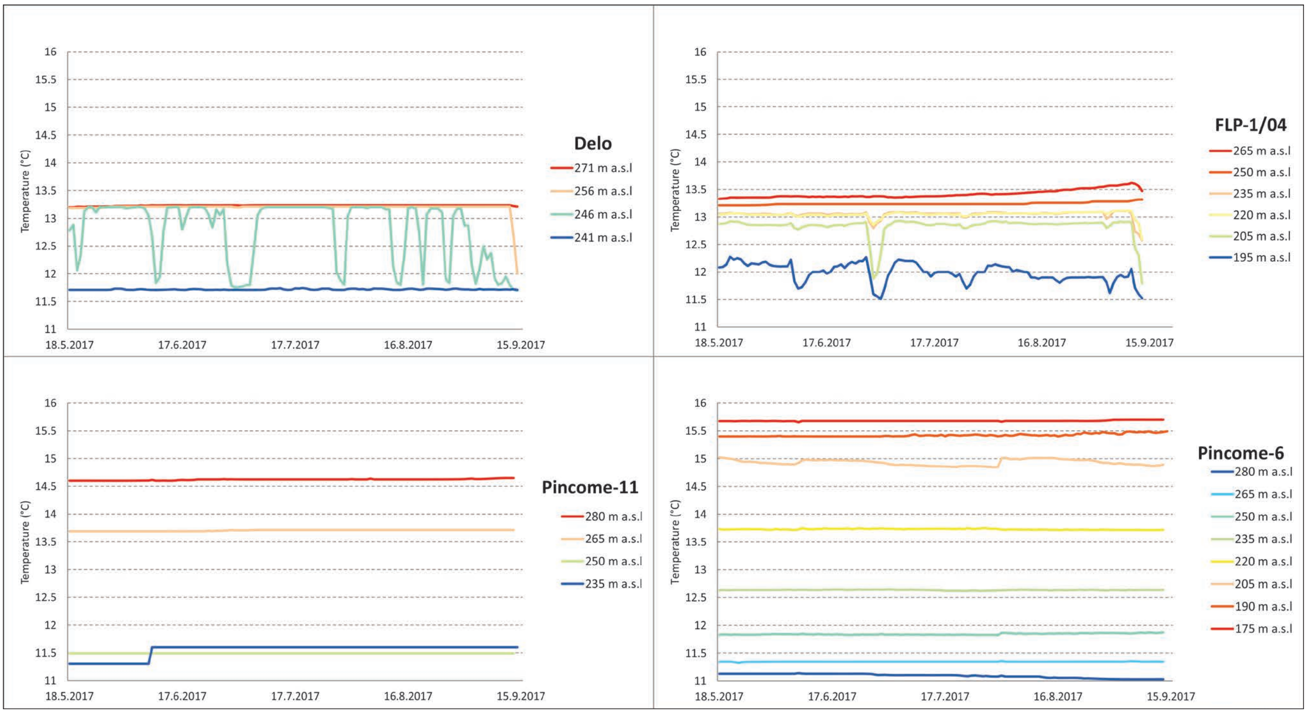

Fig. 10. Multi-level groundwater temperature time series (observation wells Delo, Pincome-11, FLP-1/04 and Pincome-6).

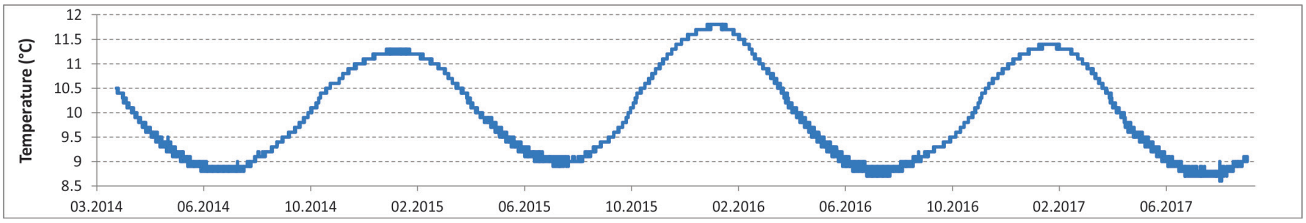

Fig. 11. Single-level groundwater temperature time series measured in observation well Pincome-9.

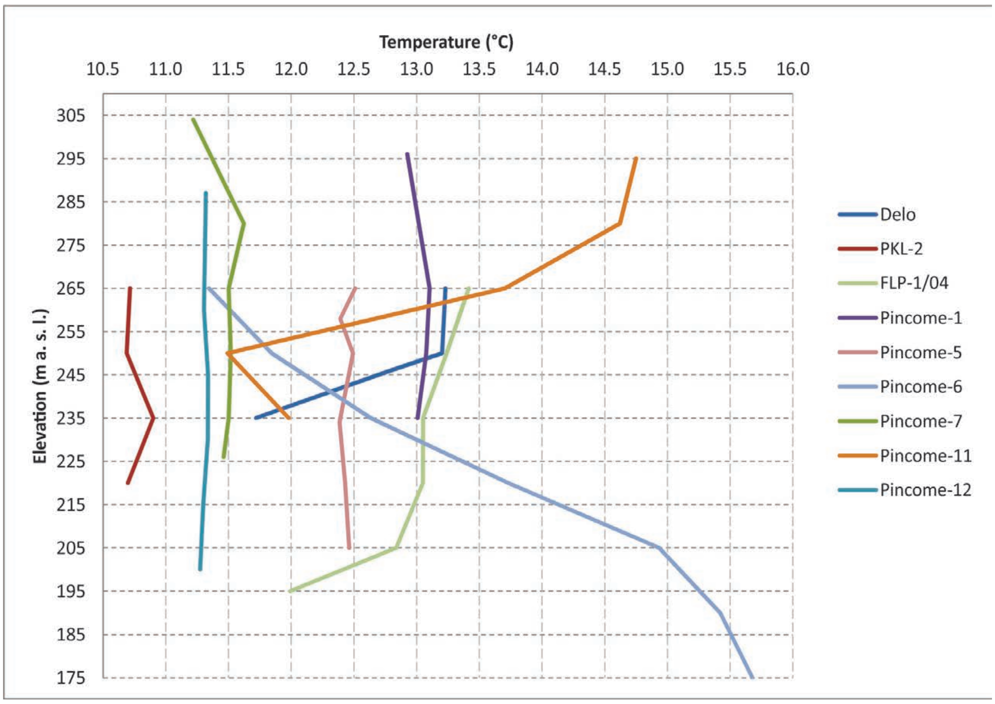

Fig. 12. Multi-level groundwater temperatures in observation wells.

gradients which slightly differ among the wells. In contrast to this, in well Pincome-6 in the Ljubljansko barje, a clear positive temperature gradient is visible and an increase of temperature with depth up to 15.6 °C, measured at 118 m depth.

The observed characteristics could be related to different factors. The first group of wells, except the well Pincome-1, is located outside or at the edge of the urban area, where the anthropogenic impact on GWT is minimal and the measured GWTs reflect undisturbed natural background conditions.

The second group of wells is located within the urban area, where increased temperatures in the upper part of the aquifer could arise from anthropogenic heat sources. Positive temperature anomalies or subsurface urban heat islands are often observed phenomena beneath cities. Measurements of groundwater temperature beneath the German cities showed subsurface urban heat islands (temperature is elevated for 1.9 to 2.4 °C), and revealed hotspots of up to + 20 °C (Menberg et al., 2013). In the city of Basel (Switzerland) an elevation of groundwater temperatures of up to 9 °C above the natural state is reported (Epting & Huggenberger, 2013).

The positive temperature gradient in well Pincome-6 probably originates from an increased heat-flow density and geothermal anomaly related to the thermal convection zone in the Triassic carbonate rocks below the Quaternary sediments (Živanović & Rajver, 2004).

Conclusions

In this paper, new research results for the assessment of the shallow geothermal potential in the area of the City of Ljubljana are presented. The distribution of ground thermal conductivity was derived with the help of a detailed geological map, representative rock sampling and measurements of the samples' thermal parameters. The results show that dolomites and quartz conglomerates have the highest thermal conductivity and, on the contrary, shales and tuffites, and some marlstones and siltstones (or claystones), have the lowest value of thermal conductivity among the geological units in the study area. This is important for the use of the shallow geothermal potential, as the higher thermal conductivity of the subsurface allows for a better heat extraction rate and higher efficiency of geothermal installations. The groundwater temperature measurements indicate relatively stable temporal conditions and a GWT range between 10.6 °C and 14.6 °C at the Ljubljansko polje and up to 15.6 °C in the deepest part of the Ljubljansko barje. Multi-level GWT measurements in observation wells show three different trends: negative, positive and no geothermal gradient in the aquifer, which in general depend on the location of the well and the related anthropogenic impact or the deeper geothermal and hydrogeological conditions.

The results obtained in this study provide a basis for the development of a 3D numerical geothermal model that will be used for the quantification of the shallow geothermal potential and for planning the efficient and sustainable use of shallow geothermal energy in the City of Ljubljana.

Acknowledgement

The authors acknowledge the project GeoPLASMA-CE co-financed by Interreg CENTRAL EUROPE Programme, and the financial support from the Slovenian Research Agency (research core funding No. P1-0020 and No. P1-0011). The authors would like to thank Nina Rman for her constructive comments.

References

Bavec, M. & Pohar, V. 2009: Kvartar (Quaternary). In: Pleničar, M., Ogorelec, B., Novak, M. (eds.): Geologija Slovenije = The Geology of Slovenia). Geološki zavod Slovenije, Ljubljana: 441-462.

Beck, A.E. 1988: Thermal properties. 4.1. Methods for determining thermal conductivity and thermal diffusivity. In: Haenel, R., Rybach, L. & Stegena, L. (eds.): Handbook of terrestrial heat-flow density determination with Guidelines and Recommendations of the International Heat Flow Commission. Kluwer academic publishers, Dordrecht, Boston, London: 87-124.

Buckley, C., Pasquali, R., Lee, M., Dooley, J. & Hunter Williams, T. 2015: »Ground source heat« & »Shallow geothermal energy«. Homeowner manual version 1.0. Department of communications, energy and natural resources, Geological Survey of Ireland: 36 p.

Buser, S. 1969: Osnovna geološka karta SFRJ 1: 100.000, List Ribnica. (Basic Geological Map of SFRY 1: 100,000. Sheet Ribnica). Zvezni geološki zavod, Beograd.

Buser, S. 2009: Geološka karta Slovenije 1 : 250.000. (Basic Geological Map of Slovenia 1 : 250,000). Geološki zavod Slovenije, Ljubljana.

Buser, S., Grad, K. & Pleničar, M. 1967: Osnovna geološka karta SFRJ 1 : 100.000, List Postojna. (Basic Geological Map of SFRY 1: 100,000. Sheet Postojna). Zvezni geološki zavod, Beograd.

COL, 2012: Energy for the City of the Future, Presentation of the Sustainable Energy Action Plan of the City of Ljubljana. City of Ljubljana, Department for Environmental Protection, Ljubljana: 73 p.

Čermák, V. 1979: Heat flow map of Europe. In: Čermák, V. & Rybach, L. (eds.): Terrestrial Heat Flow in Europe. Inter-Union Commission of Geodynamics Scientific Report No. 58. Springer-Verlag, Berlin, Heidelberg, New York: 328 p.

Decagon Devices, Inc. 2016: KD2 Pro Thermal Properties Analyzer. Operator's Manual. Decagon Devices, Inc., Pullman WA 99163: 67 p.

Epting, J. & Huggenberger, P. 2013: Unraveling the heat island effect observed in urban groundwater bodies - Definition of a potential natural state. Journal of Hydrology, 501: 193–204, doi:10.1016/j.jhydrol.2013.08.002.

Gemelli, A., Mancini A. & Longhi S. 2011: GIS-based energy-economic model of low temperature geothermal resources : A case study in the Italian Marche region. Renewable Energy, 36: 2474–2483, doi:10.1016/j.renene.2011.02.014.

Grad, K. & Ferjančič, L. 1974: Osnovna geološka karta SFRJ 1: 100.000, List Kranj = Basic Geological Map of SFRY 1: 100,000. Sheet Kranj. Zvezni geološki zavod, Beograd.

Hofmann, K., Götzl, G., Görz, I., Riedel, P., Steiner, C., Černák, R., Fricovsky, B., Janža, M., Krentz, O., Gabriel, P., Kampe, F., Franek, J., Mydłowski, A. & Hajto, M. 2017: Harmonized workflows for urban areas. Project GeoPLASMA-CE Deliverable D.T2.3.3.

Hurtig, E., Čermák, V., Haenel, R. & Zui, V. (eds.) 1992: Geothermal Atlas of Europe. - GeoForschungsZentrum Potsdam, Publ. No1, 156 p., 25 maps.

Jamšek Rupnik, P. 2013: Geomorphological evidence of active tectonics in the Ljubljana Basin = Geomorfološki dokazi za aktivno tektoniko v Ljubljanskem bazenu. PhD Thesis, University of Ljubljana, Ljubljana: 214 p.

Jamšek Rupnik, P., Benedetti, L., Preusser, F., Bavec, M. & Vrabec, M. 2013: Geomorphic evidence of recent activity along the Vodice thrustfault in the Ljubljana Basin (Slovenia) a preliminary study. Annals of geophysics 56/6: 8 p., doi:10.4401/ag-6252.

Janža, M, 2015: A decision support system for emergency response to groundwater resource pollution in an urban area (Ljubljana, Slovenia). Environmental Earth Sciences,73/7:3763–3774, doi:10.1007/s12665-014-3662-2.

Janža, M., Lapanje, A., Rajver, D., Šram, D., Gregorin, Š. & Loose A. 2017: Quantitative report on the data inventory and concepts of field measurements at the pilot area: Ljubljana. Project GeoPLASMA-CE Deliverable. D.T. 3.1.1.

Janža, M., Prestor, J., Urbanc, J. & Jamnik, B. 2005: TCE contamination plume spreading in highly productive aquifer of Ljubljansko polje. Abstr. Contrib. EGU Gen. Assem. 2005.

Kappelmeyer, O. & Haenel, R. 1974: Geothermics with special reference to application. Gebrüder Borntraeger, Berlin, Stuttgart: 238 p.

Kolar-Jurkovšek, T. & Jurkovšek, B. 1985: Nova nahajališča paleozojske flore v Posavskih gubah med Ljubljano in Litijo = New Palaeozoic macroflora from the Sava Folds area between Ljubljana and Litija (Slovenia, NW Yugoslavia). Razprave 4. razr. SAZU 26, Ljubljana: 199-218.

Kolar-Jurkovšek, T. & Jurkovšek, B. 2002: Rastlinski fosili v karbonskih plasteh na trasi avtoceste pri Bizoviku = Plant fossils in the Carboniferous beds of the motorway route at Bizovik. Geologija, 45/2, 433-438, doi:10.5474/geologija.2002.044.

Kolar-Jurkovšek, T. & Jurkovšek, B. 2007: Zgornjekarbonska flora Grajskega hriba v Ljubljani = (Late Carboniferous flora of Castle Hill in Ljubljana (Slovenia). Geologija, 50/1: 9-18, doi:10.5474/geologija.2007.001.

Kranjc, S., Mlakar, I., Božovič, M. & Matoz, T. 1989: Final report on geological investigations in the Ljubljana depression for the needs of subsurface gas storage. Borehole LK-1/88. Geological Survey Ljubljana, Ljubljana: 15 p.

Kristensen, M., Andersson, U., Sorensen, H.R. & Refsgaard, A. 2000: Water Resources Management Model for Ljubljansko Polje and Ljubljansko Barje - Model Report. DHI Water & Environment, Horsholm.

Kumar, S., Pandey, M. & Nath, V. 2015: Ground coupled heat exchangers : A review and applications. Renewable and Sustainable Energy Reviews, 47: 83-92, doi:10.1016/j.rser.2015.03.014.

Kuščer, D. 1955: Prispevek h glacialni geologiji Radovljiške Kotline = Beitrag Zur Pleistozängeologie Des Beckens Von Radovljica. Geologija, 3: 136-150.

Kuščer, D. 1991: Kvartarni savski zasipi in neotektonika = The Quaternary valley fills of the Sava River and neotectonics. Geologija, 33: 299-313, doi:10.5474/geologija.1990.007.

Lund, J. W. & Boyd, T. L. 2015: Direct utilization of geothermal energy 2015 Worldwide review. Proceedings, World Geothermal Congress 2015, Melbourne, Australia, IGA: 31 p.

Majorowicz, J. & Wybraniec, S. 2011: New terrestrial heat flow map of Europe after regional paleoclimatic correction application. International Journal of Earth Sciences, 100/4: 881-887, doi:19.1007/s00531-010-0526-1.

Menberg, K., Bayer, P. & Zosseder, K., Rumohr, S. & Blum, P. 2013: Subsurface urban heat islands in German cities. Science of the Total Environment, 442: 123–133, doi:10.1016/j.scitotenv.2012.10.043.

Mencej, Z. 1990: Prodni zasipi pod jezerskimi sedimenti Ljubljanskega barja = The gravel fill beneath the lacustrine sediments of the Ljubljansko barje. Geologija, 31/32: 517-554.

Mlakar, I. 1987: Prispevek k poznavanju geološke zgradbe Posavskih gub in njihovega južnega obrobja = A contribution to the knowledge of the geological structure of the Sava Folds and their southern border. Geologija, 28/29: 157-182.

Mlakar, I., Skaberne, D. & Drovenik, M. 1993: O geološki zgradbi in orudenju v karbonskih kameninah severno od Litije = On geological structure and mineralization in Carboniferous rocks north of Litija, Slovenia. Geologija, 35: 229-286, doi:10.5474/geologija.1992.09.

Moulin, A., Benedetti, L., Rizza, M., Jamšek Rupnik, P., Gosar, A., Bourlès, D., Keddadouche, K., Aumaître, G., Arnold, M., Guillou, V. & Ritz, J.F. 2016: The Dinaric Fault System: large-scale structure, rates of slip and Plio-Pleistocene evolution of the transpressive northeastern boundary of the Adria microplate. Tectonics, 10/35: 2258-2292, doi:10.1002/2016TC004188.

Nejat, P., Jomehzadeh, F., Mahdi, M. & Gohari, M. 2015: A global review of energy consumption, CO_2 emissions and policy in the residential sector (with an overview of the top ten CO_2 emitting countries). Renewable and

Sustainable Energy Reviews, 43: 843-862, doi:10.1016/j.rser.2014.11.066.

Novak, M. 2000: Geološka zgradba ozemlja med Podutikom in Toškim **Čelom**. BSc Thesis, University of Ljubljana. Ljubljana: 72 p.

Ouzzane, M., Eslami-nejad, P., Badache, M. & Aidoun, Z. 2015: Geothermics New correlations for the prediction of the undisturbed ground temperature. Geothermics, 53:379–384, doi:10.1016/j.geothermics.2014.08.001.

Popov, Y.A., Pribnow, D.F.C., Sass, J.H., Williams, C.F. & Burkhardt, H. 1999: Characterization of rock thermal conductivity by high-resolution optical scanning. Geothermics, 28/2: 253-276, doi:10.1016/S0375-6505(99)00007-3.

Popov, Y.A., Bayuk, I., Parshin, A., Miklashevskiy, D., Novikov, S. & Chekhonin, E. 2012: New methods and instruments for determination of reservoir thermal properties. Proceedings, 37th workshop on Geothermal Reservoir Engineering, Stanford University, Stanford, California, SGP-TR-194.

Popov, Y.A., Lippmann, E. & Rauen, A. 2017: TCS – Manual. Thermal conductivity (TC) and thermal diffusivity (TD) scanner, version 31.01.2017. TCS Lippmann and Rauen GbR, Schaufling: 53 p.

Placer, L. 1998a: Structural meaning of the Sava folds = Strukturni pomen Posavskih gub. Geologija, 41: 191-221, doi:10.5474/geologija.1998.012.

Placer, L. 1998b: Contribution to the macrotectonic subdivision of the border region between Southern Alps and External Dinarides = Prispevek k makrotektonski rajonizaciji mejnega ozemlja med Južnimi Alpami in Zunanjimi Dinaridi. Geologija, 41: 223-255, doi:10.5474/geologija.1998.013.

Placer, L. 2008: Principles of the tectonic subdivision of Slovenia = Osnove tektonske razčlenitve Slovenije. Geologija, 51/2: 205-217, doi:10.5474/geologija.2008.021.

Prelovšek, P. & Uran, B. 1984: Generalized hot wire method for thermal conductivity measurements. Journal of Physics E: Scientific Instruments, 17/8: 674-677, doi:10.1088/0022-3735/17/8/012.

Prelovšek, P., Babič, M. & Uran, B. 1982: Meritve toplotne prevodnosti kamenin z izboljšano metodo grelne žice. Geologija, 25/2: 335-339.

Premru, U. 1983: Osnovna geološka karta SFRJ 1: 100.000, List Ljubljana = Basic Geological Map of SFRY 1: 100,000. Sheet Ljubljana. Zvezni geološki zavod, Beograd.

Prestor, J., Rajver, D., Pestotnik, S. & Benček, R. 2017: Directives for drilling in shallow geothermy to the depth 300 m. Copy for trial use – 2A (In Slovene). Geološki zavod Slovenije: 80 p.

Rajver, D. & Ravnik, D. 2002: Geotermična slika Slovenije - razširjena baza podatkov in izboljšane geotermične karte. Geologija, 45/2: 519-524, doi:10.5474/geologija.2002.058.

Rajver, D., Šafanda, J. & Dědeček, P. 2006: Monitoring of air-ground temperature coupling and examples of shallow subsurface warming in Slovenia. Geologija, 49/2: 279-293.

Rajver, D., Rman, N., Lapanje, L. & Prestor, J. 2016: Geotermalni viri Slovenije. Bilanca rabe geotermalne energije v Sloveniji v letu 2015. In: Senegačnik, A. (ed.): Mineralne surovine v letu 2015: 12/1: 137-147.

Ravnik, D. 1965: Geoelektrične raziskave na Ljubljanskem barju = Geoelectric exploration of the Ljubljana moor. Geologija, 8: 80-91.

Rižnar, I., Koler, B. & Bavec, M. 2005: Identifikacija potencialno aktivnih struktur vzdolž reke Save na podlagi topografskih podatkov in podatkov nivelmanskega vlaka = Identification of potentially active structures along the Sava River using topographic, and leveling line data. Geologija, 48/1: 107-116, doi:10.5474/geologija.2005.010.

RES Directive, 2009: Directive 2009/28/EC on the promotion of the use of energy from renewable sources. European Commission.

Robertson, E.C. 1988: Thermal properties of rocks. Open-File Report 88-441, United States Department of the Interior, Geological Survey, Reston, Virginia: 106 p.

Sanner, B. 2010: Basics on geology – what engineers and drillers need to know (05a). Geotrainet Course for drillers and designers, Peine, Germany. Geo-Education for a sustainable geothermal heating and cooling market.

Šercelj, A. 1965: Paleobotanične raziskave in zgodovina Ljubljanskega barja = Paleobotanical examinations and the development of Ljubljana moor. Geologija, 8: 5-27.

Šercelj, A. 1966: Pelodne analize pleistocenskih in holocenskih sedimentov Ljubljanskega barja = Pollenanalytische Untersuchungen der pleistozänen und holozänen Ablagerungen von Ljubljansko barje. Razprave IV. razr. SAZU, 9: 431-471.

Strgar, A., Rajver, D. & Gosar, A. 2017: Investigations of the air-ground temperature coupling at location of the Malence borehole near Kostanjevica, SE Slovenia. Geologija, 60/1: 129-143, doi.org/10.5474/geologija.2017.010.

Vidic, N. J. 1998: Soil-age relationships and correlations: comparison of chronosequences in the Ljubljana Basin, Slovenia and USA. Catena, 34: 113-129.

Vidic, N. J. & Lobnik, F. 1997: Rates of soil development of the chronosequence in the Ljubljana Basin, Slovenia. Geoderma, 76: 35-64.

Žlebnik, L. 1971: Pleistocen Kranjskega, Sorškega in Ljubljanskega polja = Pleistocene Deposits of the Kranj, Sora and Ljubljana Fields. Geologija, 14: 5-50.

Žlebnik, L. 1993: Geološke posebnosti pleistocenskih zasipov na Gorenjskem = Geological peculiarities of the Pleistocene gravel and conglomerate deposits in the Upper Carniola, NW Slovenia. Geologija, 36: 207-210, doi:10.5474/geologija.1994.010.

Živanović, M. & Rajver, D. 2004: Nizkotemperaturni geotermalni potencial Ljubljanske kotline. Raziskovalna naloga za Ministrstvo za gospodarstvo in GEOT d.o.o., Gradbeni inštitut ZRMK, Ljubljana: 8 p. and 9 maps.

Internet sources:

Internet 1: http://www.interreg-central.eu/Content.Node/GeoPLASMA-CE.html (20. 10. 2017)

Internet 2: http://www.alpine-space.eu/projects/greta/en/home (20. 10. 2017)

Internet 3: http://www.eltratec.com/default.asp?lang=si&str=57&id=30 (20. 10. 2017)

Internet 4: http://www.onsetcomp.com/products/data-loggers/u22-001 (20. 10. 2017)

Appendix A. Supplementary material

Data on observation wells and measurements of temprerature (T), electric conductivity (EC) and level of groundwater table (GWL).

Observation well	Ground elevation (m a.s.l.)	GWL (m a.s.l.)	Depth of screening intervals (m)	Number of levels of T, EC, GWL measurements	Number of levels of T measurements	Depth intervals of measurement levels (m)
Ž.P.Šentvid	316	292	no data	1	0	26
Iskra stegne	310	279	no data	1	0	35
Pincome-7	309	279	27-36;42-54;60-81	1	6	2-83
PKL 2-2	308	279	55-84	1	3	43-88
Pincome-1	301	279	24-36; 40-51; 57-69	1	4	5-74
Pincome-11	300	283	54-80	1	4	5-65
Lj-Delo	299	277	no data	1	3	28-58
FlP-1/04	297	276	24-45;57-75; 87-105	1	5	32-102
Pincome-5	294	274	24-48; 54-63;72-90	1	5	5-90
Aero	294	285	no data	0	1	14
Pincome-6	293	284	89-116	1	7	13-118
Pincome-12	292	276	34-55; 58-84	1	5	5-88
PH-4	289	274	11-21	1	0	19
Ag2-04	287	273	8-20	1	0	20
PH-2	287	273	9-20	1	0	18
P-1/94	285	273	15-18	0	1	20
Pincome-10	306	280	25-39; 45-76	1	0	30

Appendix B. Supplementary material

Appendix A. Groundwater temperature time series (observation wells PKL-2, Pincome-7, Pincome-1, Pincome-12; P-1/94, Pincome-5 and AERO)

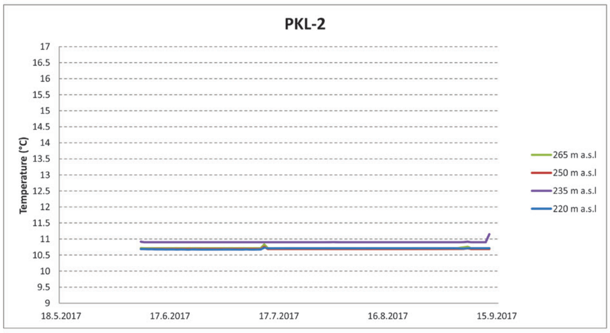

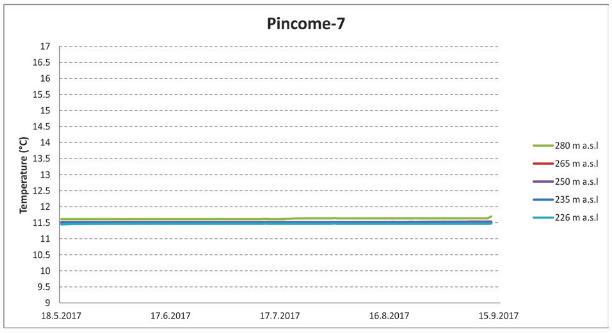

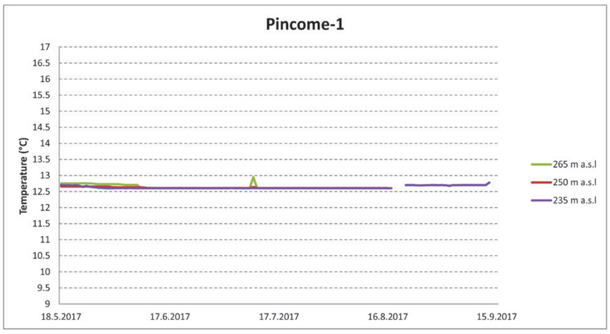

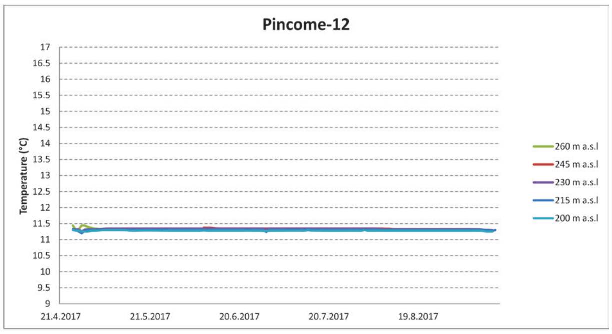

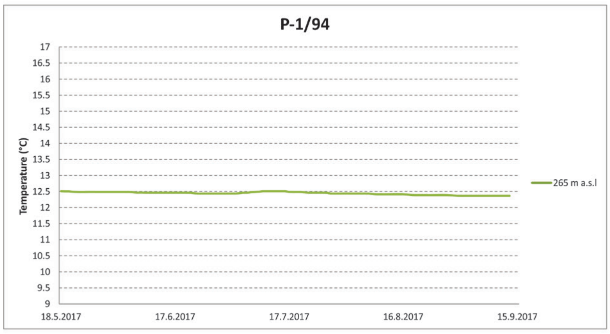

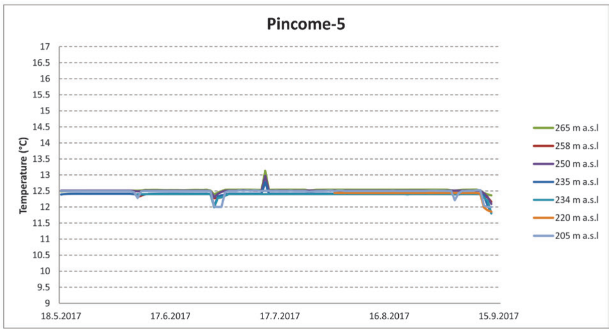

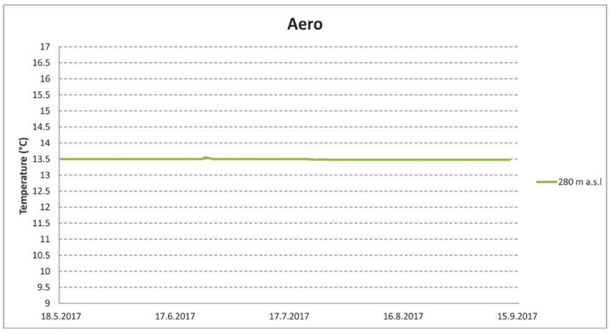

GEOLOGIJA 60/2, 328-333, Ljubljana 2017

Poročila

4. svetovni forum o zemeljskih plazovih v Ljubljani, 30. 5.–2. 6. 2017

Timotej VERBOVŠEK[1], Mateja JEMEC AUFLIČ[2] & Matjaž MIKOŠ[3]

[1]Univerza v Ljubljani, Naravoslovnotehniška fakulteta, Privoz 11, 1000 Ljubljana
[2]Geološki zavod Slovenije, Dimičeva ulica 14, 1000 Ljubljana
[3]Univerza v Ljubljani, Fakulteta za gradbeništvo in geodezijo, Jamova cesta 2, 1000 Ljubljana

V Ljubljani je letos potekal četrti Svetovni forum o zemeljskih plazovih (4th World Landslide Forum, WLF4, https://www.wlf4.org/). Forum z naslovom »Dvig kulture sobivanja z zemeljskimi plazovi« je bil organiziran v kongresnem centru Cankarjevega doma med 30. 5. in 2. 6. 2017. Izvedenih je bilo tudi več spremljajočih dogodkov, okrogla miza in razne delavnice, zaradi česar se je dogodek razločeval od siceršnjih kongresnih prireditev.

Organizatorji so bili Univerza v Ljubljani (Fakulteta za gradbeništvo in geodezijo ter Naravoslovnotehniška fakulteta) in Geološki zavod Slovenije, pod okriljem mednarodnega konzorcija za zemeljske plazove (International Consortium on Landslides, ICL, http://iplhq.org/category/home-icl/) ter Mednarodnega programa za zemeljske plazove (International Programme on Landslides, IPL). Vse tri omenjene slovenske organizacije so včlanjene v konzorcij ICL, ki vključuje preko 60 organizacij z vsega sveta (http://icl.iplhq.org/). Pretekli trije forumi so potekali v letih 2008 v Tokiu, 2011 v Rimu in 2014 v Pekingu. Letošnji dogodek je bil izveden pod častnim pokroviteljstvom predsednika Republike Slovenije Boruta Pahorja.

Foruma se je udeležilo več kot 600 raziskovalcev in strokovnjakov s področja raziskovanja in varstva pred zemeljskimi plazovi; predvsem geologije in geotehnike oziroma gradbeništva, pa tudi predstavnikov organizacij UNESCO, FAO, UNISDR, IUGG, IUGS, FAO ipd. Znanstveni odbor je štel preko 100 članov, organizacijski odbor pa več deset znanstvenikov in strokovnjakov s področja raziskovanja zemeljskih plazov.

Prijavljenih je bilo več kot 600 povzetkov in nato recenziranih skoraj 400 polnih prispevkov. Slednji so bili objavljeni v šestih knjigah založbe Springer z naslovom *Advancing Culture of Living with Landslides (Izboljševanje kulture življenja z zemeljskimi plazovi)*. Vsaka knjiga obsega eno izmed petih obravnavanih tematik, pri čemer je bila ena knjiga izdana kot dvojna številka. Obseg tiskanih prispevkov s foruma je preko 3600 strani. Teme, predstavljene v knjigah, so:

1. Sendajsko partnerstvo 2015–2025 (ta knji ga zajema dejavnosti ICL in je v elektron ski obliki prosto dostopna na spletu),
2. Napredek pri raziskovanju zemeljskih plazov,
3. Napredek pri tehnologijah sanacije ze meljskih plazov,
4. Raznolikost oblik zemeljskega plazenja in
5. Zemeljski plazovi v različnih okoljih.

V sklopu foruma so imeli uvodna predavanja štirje priznani strokovnjaki:

- Claudio Margottini (Italija): o ogroženosti naravnih in kulturnih zaščitenih območij zaradi zemeljskih plazov,
- Jordi Corominas (Španija): o padanju kamenja in fragmentaciji,
- Vit Vilímek (Češka): o poplavah iz ledeniških jezer ter
- Irasema Alcántara-Ayala (Mehika): o plazovih in družbi.

V času foruma so udeleženci sprejeli »Ljubljansko izjavo«, s katero se podpisniki obvezujejo prizadevati si za zmanjševanje tveganj in nesreč zaradi zemeljskih plazov. Izjava se navezuje na uresničevanje Sendajskega okvira za zmanjševanje tveganja nesreč 2015–2030 (Sendai Framework for Disaster Risk Reduction), ki so ga leta 2015 sprejele članice Združenih narodov.

Forumu naj bi sledile tri strokovne ekskurzije, prva po Sloveniji ter bližnjih predelih Avstrije in Italije, druga po severnem delu Italije in tretja na Hrvaško ter v Bosno in Hercegovino. Zaradi premajhnega števila prijav na drugi in tretji ekskurziji je bila organizirana le prva tridnevna s skoraj 30 tujimi udeleženci, ki je potekala v Vipavski dolini (plazovi na Rebrnicah, Slano blato, Stogovce, Selo), v dolini Soče (drobirska tokova

Strug in Stože), v Kanalski dolini v Italiji (drobirski tokovi), Ziljski dolini v Avstriji (podor na Dobraču) ter v Zgornjesavski dolini (plaz Potoška planina). Prvi dan ekskurzije se je udeležencem pridružilo tudi blizu 30 slovenskih in tujih študentov mednarodne poletne šole Univerze v Ljubljani na tematiko naravnih tveganj.

V okviru foruma je potekalo tudi več spremljajočih dogodkov in tekmovanj, podeljene so bile naslednje nagrade:

- Varnesova nagrada za strokovno odličnost na področju raziskovanja zemeljskih plazov (za leto 2015 jo je prejel Oldrich Hungr, za leto 2016 Jordi Corominas in za leto 2017 Badaoui Rouhban),
- naziv svetovnega centra odličnosti na področju zmanjševanja tveganja pred zemeljskimi plazovi je prejelo 20 ustanov, tudi dve v Sloveniji,
- nagrada za najboljše fotografije v treh kategorijah (Zemeljski plazovi iz zraka, Vpliv zemeljskih plazov na infrastrukturo in Zemeljski plazovi in družba),
- najboljši IPL projekt,
- najboljši poročevalec o zemeljskih plazovih v bazi ICL v zadnjih treh letih,
- najboljši članek v reviji *Landslides*.

Organizatorji ugotavljamo, da je dogodek uspel, saj so bili udeleženci zadovoljni tako s forumom kot z ekskurzijo. Vsem soorganizatorjem in sponzorjem, predvsem pa vsem prisotnim, se iskreno zahvaljujemo. Ponosni smo tudi, da se je Ljubljana uvrstila v družbo uglednih svetovnih prestolnic, kjer so potekali prejšnji svetovni forumi o zemeljskih plazovih. Zainteresirane vabimo na naslednji svetovni forum o zemeljskih plazovih, ki bo organiziran novembra 2020 v Kjotu na Japonskem (http://wlf5.iplhq.org/).

Sl. 1. Uvodno predavanje prof. Claudia Margottinija o ogroženosti naravnih in kulturnih zaščitenih območij zaradi zemeljskih plazov.

3. regionalni simpozij o zemeljskih plazovih v Jadransko balkanski regiji, Ljubljana 11.-13.10. 2017

Mateja JEMEC AUFLIČ[1], Timotej VERBOVŠEK[2] & Matjaž MIKOŠ[3]

[1]Geološki zavod Slovenije, Dimičeva ulica14, 1000 Ljubljana
[2]Univerza v Ljubljani, Naravoslovnotehniška fakulteta, Privoz 11, 1000 Ljubljana
[3]Univerza v Ljubljani, Fakulteta za gradbeništvo in geodezijo, Jamova cesta 2, 1000 Ljubljana

Geološki zavod Slovenije, Fakulteta za gradbeništvo in geodezijo ter Naravoslovnotehniška fakulteta Univerze v Ljubljani so organizirali 3. regionalni simpozij o zemeljskih plazovih v Jadransko balkansko regiji (3rd ReSyLAB), ki je potekal od 11. do 13. oktobra 2017 v Ljubljani.

Regionalni simpozij o zemeljskih plazovih v Jadransko-balkanski regiji (ReSyLAB) je pomemben dogodek, ki je organiziran vsaki dve leti. Prvi simpozij je bil leta 2013 v Zagrebu, drugi 2015 v Beogradu, tretji pa je bil letos v Ljubljani. Simpozij je potekal v okviru Mednarodnega konzorcija za zemeljske plazove (International Consortium on Landslides – ICL), ki je bil po predhodnih aktivnostih različnih strokovnjakov s področja varstva pred plazovi, kot mednarodna nevladna in neprofitna raziskovalna organizacija ustanovljen 2002 v Kjotu, v sodelovanju med Unescom in Univerzo v Kjotu. V okviru ICL je bilo leta 2012 ustanovljeno Jadransko-balkansko združenje (Adriatic-Balkan Network, ABN), katerega cilj je povezovanje znanosti o zemeljskih plazovih na regionalni in lokalni ravni. Usklajevanje mreže je prevzela hrvaška skupina za zemeljske plazove (Gradbena fakulteta Univerze na Reki in Rudarsko-geološka fakulteta Univerze v Zagrebu), članice mreže pa so še zagrebški Mestni urad za upravljanje v nujnih primerih, Albanski geološki zavod iz Tirane, Rudarsko-geološka fakulteta Univerze v Beogradu in trije aktivni člani ICL iz Slovenije: UL FGG (Matjaž Mikoš), UL NTF (Timotej Verbovšek) in GeoZS (Mateja Jemec Auflič).

Simpozija se je udeležilo 70 znanstvenikov, inženirjev in raziskovalcev iz 9 držav (Avstrija, Bosna in Hercegovina, Hrvaška, Češka, Italija, Makedonija, Srbija, Slovenija in Španija), ki so aktivni na področju raziskovanja zemeljskih plazov in izvajanja ukrepov za sanacijo zemeljskih plazov v Jadransko balkanski regiji in tudi drugod po svetu (sl. 1). Simpozij je bil vsebinsko razdeljen na 5 različnih sekcij, poleg tega pa je obsegal tudi različne pomembne dogodke, kot je razstava izbranih fotografij o zemeljskih plazovih iz WLF4 in dve tehnični študijski ekskurziji, ki sta potekali zadnji dan simpozija: (a) plazovi v Vipavski dolini (sl. 2) in (b) plaz Potoška planina (sl. 3). V knjigi povzetkov je objavljenih 41 povzetkov (Jemec Auflič, 2017), od katerih se jih je 28 predstavilo v petih sekcijah. Zbornik recenziranih prispevkov bo predvidoma izšel spomladi 2018.

Sl. 1. Prisotni udeleženci na slavnostni otvoritvi 3. ReSyLAB na Univerzi v Ljubljani.

V okviru simpozija je potekala tudi okrogla miza z naslovom: **Spodbujanje sodelovanja med znanostjo in končnimi uporabniki,** na kateri so udeleženci razpravljali o prioritetah raziskovanja na področju zemeljskih plazov, ki bodo imele neposredno uporabno vrednost za oblikovalce politik in končne uporabnike, predvsem za lokalne skupnosti, ki se nahajajo na območjih, kjer so tveganja za zemeljske plazove večja. Na okrogli mizi so sodelovali: Miloš Bavec (GeoZS), Mateja Jemec Auflič (GeoZS), Timotej Verbovšek (UL NTF), Branko Dervodel (URSZR), Ervin Vivoda (Ministrstvo za okolje in prostor), Igor Benko (Poveljnik civilne zaščite občine Ajdovščina), Ljiljana Herga (Direkcija Republike Slovenije za infrastrukturo), Snježana Mihalić Arbanas (Rudarsko-geološka fakulteta Univerze v Zagrebu), Željko Arbanas (Gradbena fakulteta Univerze na Reki), Veronica Tofani (Univerza v Firencah) in Hamid Begić (Zvezni urad za geologijo Bosne in Hercegovine). Okroglo mizo je vodil Matjaž Mikoš (UL FGG).

Obravnavali so teme, kako pogosto se pojavljajo plazovi in kateri so dejavniki, ki vplivajo na njihovo sprožitev, katere znanstvene raziskave se uporabljajo pri zmanjševanju tveganja pred pojavi plazov in predvsem, kako so lahko te raziska-

Sl. 2. Viadukt Podboršt, točka na študijski ekskurziji »Plazovi v Vipavski dolini«.

Sl. 3. Plaz Potoška planina.

ve in metodologije v pomoč končnim uporabnikom kot so na primer lokalne skupnosti, civilna zaščita in Direkcija RS za ceste. Okrogla miza je izpostavila tudi vprašanje prenosa metodologij za določanje ogroženih območij in načina razvrščanja v razrede ogroženosti ter kart v merilu 1: 25.000, ki jih je izdelal Geološki zavod Slovenije, v prostorske akte in pravni red na področju gradnje objektov in infrastrukture. V Sloveniji je torej stroka pripravila podlage za spremembo zakonodaje, ki bi omejila gradnjo na območjih, kjer obstaja velika verjetnost pojavljanja zemeljskih plazov, potrebna je le še volja oblikovalcev politik, da jih vnesejo v pravni red, je bil eden izmed zaključkov okrogle mize.

Podrobne informacije o simpoziju se nahajajo na spletni strani simpozija: http://www.geo-zs.si/ReSyLAB2017/

Zemeljski plazovi predstavljajo grožnjo prebivalcem in okolju v gorskih in hribovitih predelih po vsej Evropi in tudi Slovenija pri tem ni izjema. V zadnjih letih je bil tako na evropski kot tudi na slovenski ravni storjen velik napredek na področju usklajevanja pristopov za ocenjevanje tveganja pred pojavi zemeljskih plazov in tudi pri razvoju modelov za oceno verjetnosti pojavljanja zemeljskih plazov. Kot ugotavljajo udeleženci regionalnega simpozija o zemeljskih plazovih, pa bi bilo na tem področju potrebno še tesnejše sodelovanje med znanstveno in raziskovalno stroko, oblikovalci politik na nacionalni ravni ter lokalnimi skupnostmi. Prav tako je pomembno informiranje in ozaveščanje prebivalcev na območjih, kjer obstajajo večja tveganja za pojave zemeljskih plazov.

Zahvala

Organizacijski odbor 3. regionalnega simpozija o zemeljskih plazovih v Jadransko balkanski regiji se zahvaljuje vsem sponzorjem, za finančno pomoč pri organizaciji simpozija (Geoinvest d.o.o, TRUMER Schutzbauten GmbH, EHO projekt d.o.o, Geobrugg AG, Geoportal d.o.o, Geotech, Tempos d.o.o, Modri planet d.o.o, Slovensko Geološko Društvo). Posebna zahvala gre tudi članom mednarodnega znanstvenega odbora, lokalnemu organizacijskemu odboru in vsem tistim posameznikom, ki so izrazili svojo podporo pri organizaciji simpozija.

Literatura

Jemec Auflič, M. 2017: 3rd Regional Symposium on Landslides in the Adriatic - Balkan Region, Ljubljana - ReSyLAB, 11-13 October 2017, Ljubljana, Slovenia. Symposium programme. Book of abstracts. Ljubljana: Geological Survey of Slovenia: 64 str., ilustr. http://www.geozs.si/ReSyLAB2017/docs/3rd%20ReSyLAB_Abstracts.pdf

Poročilo o mednarodnem konodontnem simpoziju ICOS IV in 50-letnica Panderjevega društva

Tea KOLAR-JURKOVŠEK

Geološki zavod Slovenije, Dimičeva ul. 14, SI-1000, Ljubljana; e-mail: tea.kolar-jurkovsek@geo-zs.si

Konec junija je v španski Valenciji potekala mednarodna konferenca konodontologov (The 4th International Conodont Symposium **ICOS IV 2017**), ki jo je organiziral Oddelek za botaniko in geologijo Univerze v Valenciji. Gre za redno srečanje raziskovalcev konodontov, nenavadne izumrle vretenčarske skupine, ki spominjajo na jegulje. Od njih so se v plasteh zgornjega kambrija do zgornjega triasa ohranili le zobem podobni mikrofosili, ki jih imenujemo konodontni elementi. Skupina še danes ni povsem raziskana, saj konodonti nimajo danes živečih sorodnikov.

Štiridnevni program je vključeval uvodna predavanja o konodontni skeletni anatomiji in kompleksnosti konodontnega aparata skozi časovna obdobja s celovitim pregledom dogajanj ob izumrtju skupine.

V programu konference z naslovom “Progress on Conodont investigation” (Napredek pri raziskavah konodontov) so se zvrstili prispevki, ki zajemajo široko paleto tem po geoloških obdobjih in regijah, uporabnost konodontov kot biostratigrafsko orodje in številna poročila konodontnih raziskav dopolnjena z geokemijo, paleobiologijo, paleogeografijo in sekvenčno stratigrafijo. Program konference je obsegal naslednje tematske sekcije: Vzpon konodontov pred in med veliko ordovicijsko diverzifikacijo, GECkO (Globalni dogodki konodontne evolucije), Napredek v raziskavi srednjedevonskih konodontov, Devonski dogodki, okolje in čas, Triasna konodontna biostratigrafija, izotopi in geokemija ter Napredek v paleobiologiji konodontov. Mejnik v raziskovanju skupine predstavlja uvedba novih tehnik, kot je računalniška tomografija visoke ločljivosti, ki je odprla nove možnosti v paleobioloških študijah, ne samo pri rekonstrukciji konodontnih aparatov, temveč tudi razkritju funkcije in razvoja teh skeletnih elementov, kar uspešno raziskujemo tudi na slovenskem fosilnem materialu.

V poslovnem delu sta bila še sestanka dveh mednarodnih stratigrafskih podkomisij in sicer za silur in devon (ISSS in ISDS).

Konferenca v Valenciji (ICOS IV) je bila namenjena tudi praznovanju pol stoletnice delovanja društva konodontologov, Panderjevo društvo (The Pander Society). To je neformalna mednarodna organizacija paleontologov in stratigrafov s skupnim interesom proučevanja konodontov. Ustanovljeno je bilo leta 1967 z namenom promocije konodontologije kot pomembne veje paleontologije. Društvo nosi ime po začetniku konodontologije Heinzu Christianu Panderju (1794-1865), ki je prvi prepoznal in proučeval konodonte. Pander je bil latvijsko-nemški biolog, rojen v Rigi. Njegova radovednost in predanost naravoslovju sta ga privedla do številnih pomembnih odkritij v embriologiji in po mnenju mnogih je ustanovitelj te veje biologije. Opravil je pomembne študije na področju paleontologije in ob tem odkril konodontne elemente, ki jih je prvič opisal in ilustriral v članku leta 1856.

Člani Panderjevega društva objavljajo letno glasilo in imajo redna srečanja. Vodi ga predsednik, trenutno prof. Xulong Lai z Univerze v Wuhanu na Kitajskem.

Slovesnost ob 50. obletnici Panderjevega društva je bila zaključena s podelitvijo Panderjevih medalj za življenjske dosežke na področju konodontologije. Nagrade so prejeli Michael Orchard za izjemen prispevek k biostratigrafiji triasa, Viktor Maslov in Olga Artyushkova za izpopolnitev uporabne metode pridobivanja konodontov iz rožencev, Peter Carls za prispevek pri uvedbi devonske stratigrafije na Iberskem polotoku in njene korelacije. Na predlog avtorice tega zapisa je bila podana nominacija za Wang Cheng- yuana, ki je eden izmed pionirjev študija konodontov na Kitajskem, kjer je raziskoval združbe številnih geoloških obdobij. Prepoznavanje in uvedba dvojne konodontne conacije v permsko-triasnem intervalu je osnova vseh primerjalnih študij teh plasti po svetu in predstavlja pomemben temelj tovrstnih raziskav našega prostora, ki trenutno potekajo v sklopu mednarodnega projekta IGCP 630 »Permian-Triassic climatic and environmental extremes and biotic response«, pri katerem sodelujemo tudi slovenski raziskovalci.

Fotografija: utrinek s slavnostne podelitve Panderjeve medalje (z leve): Xulong Lai (Chief Panderer), Wang Cheng-yuan (dobitnik ene izmed Panderjevih medalj), Tea Kolar-Jurkovšek, Chris Barnes. Foto: Laura Wang.

GEOLOGIJA *60/2*, 334-336, Ljubljana 2017

V spomin dr. Ani Hinterlechner Ravnik

V noči z 11. na 12. junij 2017 je ugasnilo življenje naše dolgoletne sodelavke dr. Ane Hinterlechner Ravnik, raziskovalke, ki je postavila temelje sodobnega raziskovanja metamorfnih kamnin v Sloveniji.

Dr. Ana Hinterlechner Ravnik se je rodila 3. aprila 1928 v Ljubljani očetu Karlu in materi Nežiki. Že v ranem otroštvu in mladosti je bila tesno povezana z naravoslovjem. Njen oče, prof. dr. Karel Hinterlechner, je bil namreč zelo priznan strokovnjak na področju geoloških raziskav in leta 1919 eden od glavnih ustanoviteljev ljubljanske univerze. V letih 1927 do 1928 je bil tudi njen rektor (Brenčič, 2014). Družina Hinterlechner je izgubila očeta zelo zgodaj, oktobra 1932, ko je bilo Ančki, kot smo jo klicali vsi na Geološkem zavodu, komaj dobra štiri leta. Vendar pa to še ni bil najtežji del njenega življenja. Materialno, predvsem pa psihično najhujši udarec je družina doživela po drugi svetovni vojni, ko je bila zaradi priimka, kot nemška izgnana v Avstrijo, na Koroško (Brenčič, 2014). Samo redki so karkoli vedeli o tej boleči temi, ki jo je zaznamovala za vse življenje.

Z današnje razdalje se nam zdi skoraj samoumevno, da se je po končani srednji šoli vpisala na takratno prirodoslovno-matematično smer študija na Filozofski fakulteti v Ljubljani. Uspešno ga je zaključila leta 1954 z mineraloško temo z naslovom *Ludlamit iz rudnika Stari trg pri Kosovski Mitrovici*. Raziskala je redek fosfatni mineral ludlamit s kemično formulo $(Fe^{++},Mg,Mn)_3(PO_4)_2 \cdot 4(H_2O)$. Še istega leta se je zaposlila na takratnem Geološkem zavodu Ljubljana, predhodniku sedanjega Geološkega zavoda Slovenije.

Tako kot večina geologov v tistem času, je bila dr. Ana Hinterlechner Ravnik intenzivno vpeta v doslej najbolj obsežen geološki program, izdelavo osnovne geološke karte SFRJ za slovensko ozemlje v merilu 1:100.000. Spoprijela se je s proučevanjem kamnin Vzhodnega Alpinika pri nas. Lahko bi rekli, da je sledila očetovim stopinjam, ki je v začetku prav tako raziskoval metamorfne kamnine, vendar ga je kasneje pot zanesla drugam. To zelo zapleteno področje je zahtevalo tako raziskovalno žilico in širino, kot tudi veliko specialističnih znanj, predvsem pa disciplino in veliko časa. Prav v tem pa je bila Ana močna. Želja po znanju jo je vodila na podiplomski študij na Fakulteto za naravoslovje in tehnologijo v Ljubljani. Zaključila ga je leta 1982 z doktoratom znanosti z naslovom *Pohorske metamorfne kamenine*. Za táko nalogo niso bile dovolj samo terenske in mikroskopske študije, ampak je sistematično določila geokemično sestavo kamnin. Analize ja Ana naredila v Nancyju v sodelovanju z dr. Bernardom Moineom in rezultate skupaj z njim objavila leta 1977. Na tej osnovi je določila naravo izvornih kamnin in stopnjo njihove metamorfoze, kar je omogočilo izpeljavo paleogeografskih zaključkov. S tem je orala ledino in postavila temelje sodobnemu proučevanju metamorfnih kamnin v Sloveniji. Za svoje raziskovalne dosežke je prejela nagrado Kidričevega sklada.

Na osnovi odkritij obravnavanih v disertaciji, se je dr. Ana Hinterlechner Ravnik pri nadaljnjem raziskovanju osredotočila predvsem na visoko metamorfni facies kamnin vzhodnega Pohorja, posebno na procese, ki so privedli do njihovega nastanka. To so bile ultabazične kamnine okolice Slovenske Bistrice, spremenjene v eklogite, in granatovi peridotiti. Njena zanimiva odkritja so spodbudila mlajše kolege k raziskavam s sodobnimi metodami, s katerimi so določili celo ultravisokotlačne pogoje metamorfoze v času krede, o katerih pričajo vključki nekaj tisočink milimetra velikih zrn diamanta v granatih.

Področje delovanja dr. Ane Hinterlechner Ravnik je bilo seveda veliko širše. Na Koroškem je raziskovala kontaktno metamorfne kamnine okolice Raven na Koroškem, na Pohorju pa tudi magmatske kamnine. V okviru enega najobsežnejših projektov v Sloveniji pod naslovom *Mezozoik Slovenije* se je spoprijela s petrografijo vseh vrst spremenjenih kamnin slovenskega ozemlja, prav tako pa tudi vulkanskih kamnin, saj je bila v tistem času na Geološkem zavodu edina, ki je imela za to ustrezno predznanje. Njeno delo obsega zelene skrilavce Kranjske rebri, magmatske kamnine v Slovenskem bazenu in tudi razne vrste tufov. Prva je raziskala peridotitne nodule v bazaltnem tufu pri Gradu na Goričkem. Na področju praktične geologije se je, z enako vnemo kot s temeljnimi raziskavami, spoprijela s proučevanjem mineralnih surovin. Na to temo je v letih 1984/85 potekal poseben projekt *Raziskave kovinskih mineralnih surovin* v katerem je sodelovala tudi Ana. Nekovinske mineralne surovine je preiskovala predvsem za potrebe tako imenovanega rudnika kaolina Črna pri Kamniku, kjer so kopali illitno glino.

Resnično poznavanje problematike metamorfnih kamnin in na splošno geologije kot vede je bilo podlaga, na kateri je dr. Ana Hinterlechner Ravnik objavila številne znanstvene članke. Med njimi jih je kar 19 objavila v slovenski znanstveni reviji Geologija. Njena dela so velik prispevek k poznavanju in razumevanju te zapletene skupine kamnin pri nas in tudi k razvoju terminologije s področja metamorfne petrologije v slovenskem jeziku. Pripravila je tudi 12 izvrstnih poljudnoznanstvenih člankov za revijo Proteus, enega v soavtorstvu z dr. Ernestom Faningerjem. Posebej velja omeniti prispevke o Zemlji, ki so izšli v treh delih v

soavtorstvu s soprogom prof. dr. Danilom Ravnikom med leti 1986 in 1987. Predstavila je tudi vse glavne različke metamorfnih kamnin Pohorja: filit, blestnik, gnajs, amfibolit, eklogit, granatov peridotit in marmor. V soavtorstvu je obravnavala najdbe nekaterih redkih mineralov na Pohorju.
Dr. Ana Hinterlechner Ravnik je bila nepogrešljiva raziskovalka na Geološkem zavodu od začetka svoje kariere pa do upokojitve leta 1989. V svoji stroki je ostala aktivna še po tem. Takoj po upokojitvi se je za krajši čas spoprijela s pedagoškim delom. Študentom je predavala o metamorfnih kamninah in zanje pripravila skripta *Petrologija in petrografija metamorfnih kamenin*, ki temeljijo na teoretičnem znanju in bogatih lastnih izkušnjah. Vendar to ni bil njen prvi učbenik. Že leta 1972 je sodelovala pri pripravi skript *Mineraloško petrološko izrazoslovje*, po katerem marsikdo poseže še danes. Za revijo *Biologija v šoli*, je 1993 predstavila geologijo Pohorja in njegove metamorfne kamnine. Še ne tako davno, med leti 2008 in 2010, pa je na temo metamorfnih kamnin sodelovala pri pisanju zelo obsežne in strokovno zahtevne monografije *Geologija Slovenije*.
Dr. Ana Hinterlechner Ravnik je v letih 1971/72 sodelovala pri izdelavi geološke karte merila 1:50.000 v severni Afriki in pri raziskavah mineralnih surovin v Etiopiji. Skupaj s soprogom Danilom sta pri delu in na različnih potovanjih zbrala zelo lepe in zanimive primerke kamnin in mineralov. Zbirka, ki sta jo podarila Prirodoslovnemu muzeju Slovenije in znanstveno raziskovalna dela dr. Ane Hinterlechner-Ravnik, bodo ostala trajen spomin na véliko slovensko raziskovalko v geoznanosti.

Mirka Trajanova

Literatura

Brenčič, M., 2014. Karel Hinterlechner – utemeljitelj slovenske geološke šole. Proteus, 77/2: 55-63.

Dr. Ana Hinterlechner Ravnik - pomembnejša tiskana bibliografija

Hinterlechner, A. 1959: Ladinske kamenine in hidrotermalne spremembe črnega glinastega skrilavca v okolici Črne pri Kamniku. Geologija, 5: 129-151.

Hinterlechner, A. 1959: Spilitizirani diabazi v vzhodni Sloveniji. Geologija, 5: 152-163.

Hinterlechner-Ravnik, A. 1961: Paragonit v dolomitnem marmorju iz kraja Cvetkovo Gjubrište, Makedonija. Geologija, 7: 233-236.

Hinterlechner-Ravnik, A. 1965: Magmatske kamenine v grödenskih skladih v Sloveniji. Geologija, 8: 190-224.

Hinterlechner-Ravnik, A. 1966: Ignimbritni tufi pri Podljubelju. Geologija, 9, 391-402.

Hinterlechner Ravnik, A. 1971: Pohorske metamorfne kamenine. Geologija, 14, 187-226.

Hinterlechner-Ravnik, A. 1973: Pohorske metamorfne kamenine II. Geologija, 16, 245-264.

Hinterlechner-Ravnik, A. 1974: Pohorske metamorfne kamenine. Geologija, 17, 505-507.

Hinterlechner-Ravnik, A. 1978: Kontaktnometamorfne kamenine v okolici Črne pri Mežici. Geologija, 21/1, 77-80.

Hinterlechner-Ravnik, A. 1978: Zeleni skrilavci Kranjske rebri. Geologija, 21/2: 245-254.

Hinterlechner-Ravnik, A. 1980: Projekt mezozoik: Geokemične značilnosti keratofirsko-spilitne asociacije: spremembe triadnih vulkanskih kamnin na območju Vojnika in južno od Prebolda: 4. faza. RSS, Ljubljana.

Hinterlechner-Ravnik, A. 1981: Pohorske metamorfne kamenine. Doktorska disertacija. NTF Ljubljana.

Hinterlechner-Ravnik, A. 1982: Pohorski eklogit. Geologija, 25/2: 251-288.

Hinterlechner-Ravnik, A. 1984: Regionalna metamorfoza pelitov in karbonatno-silikatnih skrilavcev na območju severno od Raven na Koroškem. Geologija, 27: 171-199.

Hinterlechner-Ravnik, A. 1988: Granatov peridotit na Pohorju. Geologija, 30: 149-181.

Hinterlechner Ravnik, A. 1990: Ultramafični vključki v granitu Črne na Koroškem v Sloveniji. Geologija 31/32: 403-414.

Hinterlechner-Ravnik, A. 1990: Petrologija in petrografija metamorfnih kamenin. Geološki zavod Ljubljana, Ljubljana: 169 p.

Hinterlechner-Ravnik, A. 1993: Geologija Pohorja in njegove metamorfne kamenine. Biologija v šoli, 2/2: 4-13.

Hinterlechner-Ravnik, A. 1995: O geologiji Pohorja. Proteus, 57/9-10: 334-339.

Hinterlechner-Ravnik, A. 1997: Kalcijev ankilit s cerijem iz kamnoloma čizlakita na Pohorju. Proteus, 59/5: 233.

Hinterlechner-Ravnik, A. 2001: Metamorfne kamnine: marmor. Proteus, 63/9-10: 469-472.

Hinterlechner-Ravnik, A. 2002: Metamorfne kamnine Pohorja: filiti, blestniki in gnajsi. Proteus, 64/6: 264-271.

Hinterlechner-Ravnik, A. 2004: Metamorfne kamnine Pohorja: amfibolit, eklogit in granatov peridotit (1. del). Proteus, 66/6: 250-256.

Hinterlechner-Ravnik, A. 2004: Metamorfne kamnine Pohorja: amfibolit, eklogit in granatov peridotit (2. del). Proteus, 66/7: 311-318.

Hinterlechner-Ravnik, A. 2005: Žad. Proteus, 68/4: 69-171.

Hinterlechner-Ravnik, A. 2006: Ahat. Proteus, 69/2: 72-80.

Faninger, E. & Hinterlechner-Ravnik, A. 1993/1994: Najdba akvamarina na Pohorju ter splošno o beriliju in njegovih mineralih. Proteus, 56/3: 99-101.

Hinterlechner-Ravnik, A. & Mišič, M. 1985/86: Peridotitne nodule v bazaltnem tufu pri Gradu v Prekmurju. Geologija, 28/29: 205-218.

Hinterlechner-Ravnik, A. & Moine, B. 1977: Geochemical Characteristics of the Metamorphic Rocks of the Pohorje Mountains. Geologija, 20: 107-140.

Hinterlechner-Ravnik, A. & Pleničar, M. 1967: Smrekovški andezit in njegov tuf. Geologija, 10: 219-237.

Hinterlechner-Ravnik, A. & Ravnik, D. 1987: Zgradba Zemlje, njena dinamika in kamenine plašča na Slovenskem. Proteus 49/7: 266-270.

Hinterlechner-Ravnik, A. & Ravnik, D. 1986: Zgradba Zemlje, njena dinamika in kamenine plašča na Slovenskem : 1. Zgradba Zemlje. Proteus, 49/1: 34-40.

Hinterlechner-Ravnik, A. & Ravnik, D. 1986: Zgradba Zemlje, njena dinamika in kamenine plašča na Slovenskem : 2. Tektonika plošč. Proteus, 49/3: 106-111.

Hinterlechner-Ravnik, A. & Trajanova, M. 2009: Metamorfne kamnine = Metamorphic rocks. V: Pleničar, M. (ur.), et al. Geologija Slovenije = The geology of Slovenia. Ljubljana: Geološki zavod Slovenije: 69-90.

Buser, S., Hinterlechner-Ravnik, A. & Ramovš, A. (avtor, ur.) 1979: Strokovno srečanje na terenu, posvečeno paleozoiku Slovenije = Field meeting on the Paleozoic in Slovenia, NW Yugoslavia: 14. - 16. 6. 1979. Ljubljana: Jugoslovanski komite za IGPC Projekt št. 5 in 106 (Yugoslav Committee for IGCP Project No. 5 and 106; pp 41.

Grafenauer, S., Duhovnik, J. & Hinterlechner-Ravnik, A. 1972: Mineraloško petrološko izrazoslovje. Ljubljana: Fakulteta za naravoslovje in tehnologijo, pp 275.

Harrer, A., Hinterlechner-Ravnik, A. & Niedermayr, G. 1992: Über einen Neufund vom Aquamarin aus dem aufgelassenen Steinbruch nördlich von Slovenska Bistrica im östlichen Pohorje, Slowenien. Geologija, 35, 225-227.

Niedermayr, G., Hinterlechner-Ravnik, A. & Faninger, E. 1992: Alpine Kluftmineralisationen im Pohorje in Slowenien = Mineralizirane alpske razpoke na Pohorju. Geologija, 35: 207-223.

Orehek, S. & Hinterlechner-Ravnik A., 1972: Rapport geologique detaille des cartes geologiques au 1/50.000; Gites mineraux et substances utiles - examen petrographique, polarographique et chimique, sections polies. Arhiv GeoZS.

Podgoršek, V., Golob, F., Rečnik, A. & Hinterlechner-Ravnik, A. 2007: Minerali medplastnih in alpskih razpok v metamorfnih kamninah v Koritnem nad Oplotnico. V: Rečnik, A. (ur.): Nahajališča mineralov v Sloveniji. Ljubljana: Institut Jožef Stefan, Odsek za nanostrukturne materiale, 284-295.

Pleničar, M., Hinterlechner-Ravnik, A. & Faninger, E. 1991: Some Tectonic Elements and Tectonic Events on the SW Margin of the Pannonian Basin. V: Karamata, S. (ed.): Geodynamic Evolution of the Pannonian Basin: proceedings of the International symposium held from October 18 to 20, 1990, (Academic Conferences, Department of Natural and Mathematical Sciences, 62/4). Beograd: Serbian Academy of Sciences and Arts, 161-170.

Podgoršek, V., Golob, F., Rečnik, A., Dolenec, T. & Hinterlechner-Ravnik, A. 2007: Minerali pegmatitnih žil in alpskih razpok pri Cezlaku na Pohorju. V: Rečnik, A. (ur.): Nahajališča mineralov v Sloveniji. Ljubljana: Institut Jožef Stefan, Odsek za nanostrukturne materiale, 273-283.

Rečnik, A., Mazaj, M., Hinterlechner-Ravnik, A. & Niedermayr, G. 2008: Dobrova, die klassische Lokalität des Dravit. Mineralien-Welt, 19/1: 48-54.

Žorž, Z., Golob, F., Rečnik, A. & Hinterlechner-Ravnik, A. 2007: Mineralizirane alpske razpoke na Kobanskem in na severnem Pohorju. V: Rečnik, A. (ur.): Nahajališča mineralov v Sloveniji. Ljubljana: Institut Jožef Stefan, Odsek za nanostrukturne materiale, 269-272.

GEOLOGIJA *60/2*, 337-339, Ljubljana 2017

Aleksandri Orehek v slovo

Dne 8. junija 2017 nas je zapustila naša draga sodelavka in prijateljica Aleksandra Orehek, ena od prvih sedimentologinj v Sloveniji. Premagala jo je zahrbtna bolezen.

Klicali smo jo Saša, vsi po vrsti – njeni sošolci, vrstniki, in tudi mi, mnogo mlajši kolegi, katerim je že kar na začetku dovolila, da smo jo tikali. Bila je gospa iz ljubljanske meščanske družine, kljub temu pa vsem svojim sovrstnikom, kasnejšim kolegom in prijateljem tovarišica v pravem pomenu besede.

Aleksandra Orehek se je rodila 30. junija 1929 v Ljubljani, materi Alojziji in očetu Jožefu, kot dvojčica s sestro Meto in nekoliko starejšima bratom Petrom in sestro Asto. Osnovno šolo je končala leta 1941, gimnazijo pa po vojni, v času, ki je v njej pustil trajne posledice.

Leta 1950 se je vpisala na Fakulteto za naravoslovje in tehnologijo na takratno Ljubljansko montanistiko. Študij je končala lata 1957 z odmevno diplomsko nalogo z naslovom *Geološke razmere na severovzhodnem pobočju Gorjancev in ozemlju kostanjeviškega zaliva na Krškem polju*. Naslednje leto, 1958 se je zaposlila na takratnem Geološkem zavodu Ljubljana, ki se je po letu 1991 preimenoval najprej v Inštitut za geologijo, geotehniko in geofiziko in pozneje v Geološki zavod Slovenije. Že z diplomsko nalogo je začela svoje dolgoletno delovanje na področju sedimentne geologije in petrologije ter nadaljevala svojo bogato kariero vse do upokojitve leta 1992.

Saša se je odločila za študij geologije zato, ker je živela z naravo in imela iskreno rada svojo domovino. Tako je bila vzgojena že v svoji rani mladosti. Čeprav zavedna in ponosna Slovenka, je spoštovala vse druge narode, narodnosti in kulture, s katerimi se je srečevala. Vedno je s spoštovanjem govorila o ljudeh, ki jih je srečala v času službovanja v Alžiriji, kjer je sodelovala pri raziskavah za izdelavo geološke karte merila 1:50.000. Številna prijateljstva je stkala med kolegi iz nekdanje skupne države. Prepešačila je velik del domovine. Rada je imela svoj poklic in sodelavce. Sprva kot kartirajoča geologinja in nato dolga leta kot ena vodilnih sedimentologinj pri nas, je bila vključena v vse najpomembnejše projekte svojega časa. To so bile predvsem raziskave za izdelavo Osnovne geološke karte Jugoslavije v merilu 1:100.000 za liste ter karte slovenskega ozemlja ter za zelo odmeven in eden redkih povezovalnih programov Mezozoik Slovenije. Njena posebna strast so bile parageneze težkih mineralov v sedimentih in sedimentnih kamninah. Raziskovala jih je za raznovrstne študije, predvsem metalogenetske in hidrogeološke, kot tudi v povezavi z energetskimi surovinami, najpogosteje za premoge ter nafto in plin v vzhodni Sloveniji ter za ovrednotenje nahajališč nekovinskih mineralnih surovin. Med slednjimi velja omeniti steklarske peske iz Moravč. S sodelavci je objavila več del o sedimentoloških, mikrofacialnih in geokemičnih značilnostih jurskih in krednih plasti na območju Dinaridov ter o flišu v jugozahodni Sloveniji. V arhivu Geološkega zavoda Slovenije se nahajajo njena poročila o raziskavah, tudi tista s kartiranja v Alžiriji. Sodelovala je pri pripravi tiskanih vodičev za ekskurzije po Sloveniji, katerih so se udeležili mnogi priznani domači in tuji geologi.

Ob rednem delu se je bila vedno pripravljena posvetiti tudi izobraževanju mladega kadra. Bila je mentorica in svetovalka številnim mladim kolegom, katere je uvajala v svet petrologije sedimentnih kamnin Slovenije.

Saša je bila do konca ponosna in aktivna članica Združenja borcev narodnoosvobodilne borbe (NOB) ter kritična do spreobračanja zgodovine. Svoje mnenje o dogodkih iz zgodovine je vedno povedala jasno in glasno, ne glede na odziv okolice. Ni je bilo strah ne nasprotovanja, ne zasmehovanja. Trdno je stala za svojim mišljenjem in obnašanjem, kar smo znali ceniti vsi njeni prijatelji in znanci. Z veseljem je pomagala pri organizaciji raznovrstnih geoloških srečanj. Pristno in neprisiljeno je združevala svojo strokovnost in osebno dostopnost ter bila ravno zaradi tega vedno priljubljena in cenjena med kolegi. V delo je vnašala svežino in vedrino. S svojo neposrednostjo nas je pogosto nasmejala, nemalokrat na svoj račun. Prenekatero anekdoto je povedala o svoji poklicni poti, simpatijah, družini in predmetih, ki jih je izgubila na terenu ter jih na nenavaden način vedno znova spet našla. Večkrat je ponovila, kako so se šalili z imeni treh sester: »A-sta Saša in Meta doma?« Pred nekaj leti je izgubila sestro Asto, lani ji je umrla še sestra dvojčica, Meta, ki ji je bila po mamini smrti glavna opora.

Saša nas je velikokrat zbrala skupaj za razne priložnosti, nas pogostila in napolnila z optimizmom. Junija nas je poklicala zadnjikrat – za spomin na svetle trenutke – za slovo. Odšla je k svoji dragi družini.

Vedno se je bomo spominjali po njenih delih, predvsem pa z mislijo nanjo kot poštenega, neposrednega človeka širokega duha in odprtega srca.

Mirica in Miloš
(Mirka Trajanova in Miloš Markič)

Aleksandra Orehek - pomembnejša tiskana bibliografija

Benić, J., Drobne, K., Knez, M., Ogorelec, B., Orehek, A., Pavlovec, R., Pavšič, J., Pleničar, M. & Drobne, K. (ur.) 1991: Introduction to the Paleogene SW Slovenia and Istria: field-trip guidebook. Paleontološki inštitut I. Rakovca ZRC SAZU, IX, 90. Ljubljana.

Koch, R., Ogorelec, B. & Orehek, A. 1989: Microfacies and diagenesis of Lower and Middle Cretaceous carbonate rocks of NW-Yugoslavia (Slovenia, Trnovo area) = Mikrofazies und Diagenese unter- und mittelkretazischer Karbonatgesteine von NW-Jugoslawien (Slowenien, Trnovo). Facies, 21: 135-170.

Orehek, A. (ur.) 1984. Vodič strokovne ekskurzije. 6. Sedimentološki plenum Jugoslavije, Bovec, 12.-14.9.1984, 45 p.

Orehek, A. & Ogorelec, B. 1978: Sedimentološke značilnosti jurskih in krednih karbonatnih kamenin na Trnovskem gozdu. V: Babić, L. & Jelaska, V. (ur.): Sažeci predavanja. Hrvatsko geološko društvo, Zagreb: 11.

Orehek, A. & Ogorelec, B. 1980: Mineraloške in sedimentološke raziskave, Sedimentološke raziskave fliša v jugozahodni Sloveniji: Geološki vjesnik, 185-192.

Orehek, A. & Ogorelec, B. 1981: Korelacija mikrofacijalnih i geohemijskih osobina jurskih i krednih stena južne karbonatne platforme Slovenije = Correlation of microfacial and geochemical characteristics of Jurassic and Cretaceous rocks of the southern carbonate platform in Slovenia. Glasnik Republičkog zavoda za zaštitu prirode i Prirodnjačkog muzeja u Titogradu, 14: 161-181.

Ogorelec, B., Orehek, A. & Budkovič, T. 1999: Lithostratigraphy of the Slovenian part of the Karavanke road tunnel. Abhandlungen der Geologischen Bundesanstalt, 56/2: 99-112.

Orehek, A., Mišič, M. & Buser, S. 1986: Petrološke značilnosti spodnjekrednega fliša v okolici Bohinja. V: Sažeci predavanja = Abstracts, Skup sedimentologa Jugoslavije, Brioni 2-5.06. 1986. S.l.: Hrvatsko geološko društvo, 108-109.

Orehek, A., Mišič, M. & Pavšič, J. 1980: Mineraloške in sedimentološke raziskave, Sedimentološke raziskave fliša v jugozahodni Sloveniji: 3. faza. Geološki zavod: RSS, Ljubljana: 31 p.

Ogorelec, B. & Orehek, A. 1983: Microfacial characteristics of Mesozoic carbonate rocks of Slovenia, Yugoslavia. V: Jelaska, Vladimir, Tišljar, J & Glovacki, J. Ž. (ur.): Abstracts. Split: 122-124.

Ogorelec, B., Buser, S. & Orehek, A. 1987: Jurassic beds in the northern part of the Dinaric carbonate platform (Trnovski gozd, SW Slovenia). V: Colizza, E. (ur.): Communications: abstracts. Poster session: abstracts. Trieste: Università degli studi, Istituto di geologia e paleontologia, 46.

Orehek, A., Mišič, M. & Buser, S. 1986: Petrološke značilnosti spodnjekrednega fliša v okolici Bohinja. V: Sažeci predavanja = Abstracts, V: Skup sedimentologa Jugoslavije, Brioni 2-5.06. 1986. S.l.: Hrvatsko geološko društvo, 108-109.

Ogorelec, B., Orehek, A., Buser, S. & Pleničar, M. 1987: Komen beds - Skopo at Dutovlje (Upper Cretaceous). V: Colizza, E. (ur.): Excursions - 5th and 6th June 1987, E. Friuli, Karst of Gorizia and of W. Slovenia: guidebook. Trieste: Università degli studi, Istituto di geologia e paleontologia, 61-66.

Ogorelec, B., Orehek, A., Dozet, S. & Gregorič, V. 1991: Microfacies and sedimentology of Schythian beds in Slovenia. V: Abstracts. Institute of Geology, Zagreb: 67.

Šikić, D., Pleničar, M., Šparica, M., Grad, K., Rijavec, J., Buser, S., Blašković, I., Prelogović, E., Dozet, S., Drobne, F., Mioč, P., Orehek, A., Pavlovec, R., Šribar, L., Turnšek, D. & Magaš, N. 1972: Osnovna geološka karta SFRJ. L 33-89, Ilirska Bistrica. Zvezni geološki zavod, Beograd.

Šolar, S.V., Lapajne, V., Orehek, A., Zakrajšek, S. & Žuža, T. 1994: Geološke raziskave kremenovih peskov v okolici Moravč: lokalnost Zabritof - zahodni del. Inštitut za geologijo, geotehniko in geofiziko, Ljubljana.

Šolar, S. V., Petrica, R., Jerše, Z., Strgar, I., Lapajne, V., Ogorelec, B., Urbanc, J., Skaberne, D., Aničić, B., Kralj, P., Bidovec, M., Sova, D., Rokavec, D., Drobne, F., Stojanovič, B., Orehek, A., Šajn, R., Šribar, L. & Trebušak, I. 1994: Nekovinske mineralne surovine: končno poročilo o delu. Inštitut za geologijo, geotehniko in geofiziko, Ljubljana.

Soavtorica Osnovne geološke karte SFRJ merila 1:100.000 listov L 33-77, Postojna; L 33-78, Ribnica; L 33-88, Trst; L 33-54, Ravne na Koroškem.

Dr. Mihi Mišiču v slovo

Povsem nepričakovano nas je 7. julija 2017 zapustil sodelavec in prijatelj dr. Miha Mišič, strokovnjak na področju raziskovanja glin z rentgensko difrakcijo . Nismo mogli verjeti, da se je z nepolnimi oseminšestdesetimi leti poslovil od nas.

Miha se je rodil 20. avgusta 1949 v Zagrebu materi Darinki in očetu Mihi. Imel je dve leti mlajšo sestro Meto. Oče je bil vojaški uslužbenec, najmlajši polkovnik v JLA v tistem času. Narava njegove službe je zahtevala, da se je družina preselila v Beograd, kjer je Miha končal osnovno šolo. Ko je bil star 16 let, so se vrnili v Ljubljano. Oče je zapustil vojsko in po končanem študiju nastopil civilno službo. Miha je obiskoval Gimnazijo Poljane. Profesorica Brelih je prepoznala njegovo nadarjenost za naravoslovje, kar mu je omogočilo, da so ga kot maturanta poslali na mednarodni tabor na Lofote. Domov se je vrnil s polnim nahrbtnikom različnih kamnin. Še poln vtisov s potovanja, se je odločil za študij geologije. V času študija je bil navdušen jamar. S svojimi prijatelji je bil v odpravi, ki se je za nekaj dni spustila 700 m globoko v Pološko jamo. Po duši je bil Notranjec in ljubitelj prelepe narave, sanjač, ki je v mislih potoval po vesolju, galaksijah. Še posebno v zadnjih letih ga je zanimala znanstvena fantastika.

Miha se je zaposlil na Geološkem zavodu po diplomi, aprila leta 1976. Že v času študija je pokazal posebno zanimanje za instrumentalne preiskave v mineralogiji, čemur je sledila diplomska naloga z naslovom *Optične, termične in rentgenske preiskave bentonita iz okolice Zaloške gorice pri Celju*. Izdelal jo je pod mentorstvom prof. dr. Valerije Osterc, mentorice, ki ga je spodbujala ves čas študija in mu tudi pozneje vedno stala ob strani. Ob delu je svoje znanje nadgrajeval s študijem na tretji stopnji na Fakulteti za naravoslovje in tehnologijo in ga leta 1992 zaključil z magistrsko nalogo *Glineni minerali z zmesno strukturo tipa illit / montmorillonit*. Zanimanje za minerale glin je v njem raslo postopoma, saj je spoznaval njihov pomen za študij vseh vrst kamnin. Predvsem ga je pritegnila njihova široka paleta industrijske uporabe, na osnovi njihovih lastnosti pa predvsem nevarnost, ki jo lahko pomenijo pri posegih v prostor. Tako je podiplomski študij zaokrožil novembra leta 1998 s široko zastavljeno doktorsko temo posvečeno glinam z naslovom *Rentgenske raziskave glinenih mineralov v paleozojskih in mezozojskih karbonatnih formacijah Slovenije*.

Lahko bi rekli, da so mu bili minerali glin druga ljubezen, takoj za njegovo družino, ki jo je vedno omenjal z veliko ljubeznijo in ponosom. Minerale glin je sledil v flišnih kamninah zahodne Slovenije, pri procesih odkopavanja in predelave glin, predvsem v rudniku Črna pri Kamniku, pri raziskavah za cestogradnjo, v jamskih sedimentih, v usedlinah koprskega zaliva in naših jezer itd. *Čeprav s*am ni rad pisal, ga je zvestoba do mineralov glin in drugih mineralov z listasto strukturo tako zasvojila, da je, poleg svoje doktorske naloge, izdal kar tri monografije: *Filosilikati I; Atlas izračunanih difraktogramov, Sljude. 1. del, A-L* in *Atlas izračunanih difraktogramov, Sljude, lojevec, pirofilit*. V sodelovanju s številnimi kolegi je svoja dognanja predstavil v 38 znanstvenih objavah ter na okrog 30. mednarodnih in domačih znanstvenih konferencah.

Zadnja leta službe je Miha postajal utrujen. Z upokojitvijo je končno spet svobodno zadihal in si povrnil nekdanjo vedrino. Vendar za kratko, veliko prekratko! Komaj se je sprostil in umiril od vsakodnevnih obveznosti in se veselil uspehov svojih otrok ter prve vnukinje, že je posegla vmes neusmiljena usoda. Zapustil nas je še poln osebnih in družinskih načrtov.

Mihova dela bodo ostala zapisana v zgodovini Geološkega zavoda, posebno pa bo med vsemi, ki smo ga poznali, odmevala zanj značilna šaljivost in vedrina, ki ju je nemalokrat delil z nami.

Mirka Trajanova

Dr. Miha Mišič - pomembnejša tiskana bibliografija

Jarc, S., Goričan, Š., Skaberne, D., Verbič, T., Mišič, M. & Zupančič, N. 2013: K-feldspar rich shales from Jurassic bedded cherts in southeastern Slovenia. Swiss journal of geosciences, 106/3: 491-504, doi: 10.1007/s00015-013-0147-3.

Rejšek, K., Mišič, M. & Eichler, F. 2012: Sustainable forestry and iron compounds in karstic soils: qualitative and semi-quantitative results focused on the occurrence of Fe-compounds on mineral particles. Journal of forest science, 58/9: 410-424.

Šušteršič, F., Rejšek, K., Mišič, M., Eichler, F. 2009: The role of loamy sediment (terra rossa) in the context of steady state karst surface lowering. Geomorphology: an international journal of pure and applied geomorphology, 106/ 1-2: 35-45.

Dolinar, B., Mišič, M., Trauner, L. 2007: Correlation between surface area and Atterberg Limits of fine-grained soils. Clays and clay minerals, 55/5: 519-523.

Ogorelec, B., Buser, S., Mišič, M. 2006: Manganovi gomolji v jurskem apnencu Južnih Alp Slovenije = Manganese nodules in Jurassic limestone of the Southern Alps in Slovenia. Geologija, 49/1: 69-84.

Ogorelec, B., Bole, B., Leonidakis, J., Čermelj, B., Mišič, M., Faganeli, J. 2006: Recent sediment of Lake Bled (NW Slovenia): sedimentological and geochemical properties. Water, air & soil pollution, Focus, 6/ 5-6: 505-513.

Dozet, S. & Mišič, M. 2005: Ilova Gora and Čušperk bauxite deposits. Annales : anali za istrske in mediteranske študije, Series historia naturalis, 15/2: 283-290.

Trauner, L., Dolinar, B. & Mišič, M. 2005: Relationship between the undrained shear strength, water content, and mineralogical properties of fine-grained soils. International journal of geomechanics, 5/4: 350-355, doi:10.1061/(ASCE)1532-3641(2005)5:4(350).

Dolinar, B. & Mišič, M. 2005: Interaction between mineral composition, water content and mechanical properties of saturated cohesive soils. RMZ - Materials and geoenvironment: periodical for mining, metallurgy and geology, 52/2: 419-428.

Horvat, A. & Mišič, M. 2004: Mineralogy and sedimentology of diatomaceous sediments of Slovenia. RMZ - Materials and geoenvironment: periodical for mining, metallurgy and geology, 51/4: 2145-2161.

Kralj, P. & Mišič, M. 2003: Chemical composition of Kiscellian silty sediment (sivica) from the Trobni Dolarea, Eastern Slovenia = Kemična sestava sivice s Trobnega Dola, vzhodna Slovenija. Geologija, 46/1: 113-116.

Plaskan, M., Zupančič, N. & Mišič, M. 2003: REE v zgornjih delih tal, nastalih na granodioritu = REE in the upper soil developed on granodiorite. RMZ - Materials and geoenvironment: periodical for mining, metallurgy and geology, 50/2: 485-502.

Aničić, B., Ogorelec, B., Kralj, P.& Mišič, M. 2002: Litološke značilnosti terciarnih plasti na Kozjanskem = Lithology of Tertiary beds in Kozjansko, Eastern Slovenia. Geologija, 45/1: 213-246.

Mišič, M. & Kralj, P. 2002: Mineral composition of Kiscellian sediments from the Trobni Dol area, Eastern Slovenia = Mineralna sestava kiscellijskih sedimentov in sedimentnih kamnin s področja Trobnega Dola. RMZ - Materials and geoenvironment: periodical for mining, metallurgy and geology, 49/4: 471-485.

Zupančič, N. & Mišič, M. 2001: Mineraloške in geokemične značilnosti rimske žlindre iz arheoloških najdišč Bohova in Spodnje Hoče = Mineralogical and geochemical characteristics of Roman slag from archaeological sites Bohova and Spodnje Hoče. RMZ - Materials and geoenvironment: periodical for mining, metallurgy and geology, 48/3: 447-457.

Vreča, P., Dolenec, T., Šparica, M. & Mišič, M. 1999: Geokemične raziskave zdravilnega mulja iz zaliva Makirina (srednji Jadran). RMZ - Materials and geoenvironment: periodical for mining, metallurgy and geology, 46/3: 641-650.

Pezdič, J., Šušteršič, F., Mišič, M. 1998: On the role of clay-carbonate reactions in speleo-inception : a contribution on the understanding of the earliest stage of karst channel formation = O vlogi reakcij med glinenimi minerali in karbonati pri začetju: prispevek k razumevanju najzgodnejše stopnje nastanka kraških kanalov. Acta carsologica, 27/1: 187-200.

Ogorelec, B., Faganeli, J., Mišič, M. & Čermelj, B. 1997: Reconstruction of paleoenvironment in the Bay of Koper: (Gulf of Trieste, northern Adriatic). Annales: anali za istrske in mediteranske študije, Series historia naturalis, 7/11: 187-200.

Dozet, S. & Mišič, M. 1997: On Malm bauxites and adjacent carbonate rocks in Suha krajina (Central Slovenia). Rudarsko-metalurški zbornik: revija za geologijo, rudarstvo in metalurgijo, 44/ 3-4: 201-222.

Šušteršič, F. & Mišič, M. 1996: Some minerals from Najdena jama = Nekaj mineralov iz

Najdene jame. Acta carsologica, 25: 291-305.

Dozet, S., Mišič, M., Žuža, T. 1996: Malm bauxite occurrences in Logatec, Nanos and Kočevje area. Rudarsko-metalurški zbornik: revija za geologijo, rudarstvo in metalurgijo, 43, 1/2, 23-35.

Faganeli, J., Pezdič, J., Ogorelec, B., Mišič, M., Najdek, M. 1994: The origin of sedimentary organic matter in the Adriatic. Continental Shelf Research, 14/4, 365-384.

Dozet, S., Mišič, M. & Žuža, T. 1993: New data on the stratigraphic position, mineralogy and chemistry of Nanos bauxite deposits and adjacent carbonate rocks, Slovenia. Geologia Croatica: a journal of the Institute of Geology Zagreb and Croatian Geological Society, 46/2: 233-241.

Ogorelec, B., Mišič, M. & Faganeli, J. 1991: Marine geology of the Gulf of Trieste (northern Adriatic) : sedimentological aspects. Marine geology, 99: 79-92.

Placer, L., Ogorelec, B., Čar, J. & Mišič, M. 1989: Nekaj novih podatkov o Ravenski jami na Cerkljanskem = Some new facts about Ravenska jama in Cerkno region. Acta carsologica, 18: 129-138.

Štern, J., Brezigar, A., Mišič, M. & Štukovnik, J. 1987: Nekovinske mineralne surovine na ozemlju Šaleške kotline = Nichtmetallische Mineralrohstoffe im Gebiet des Šalek-Beckens. Geologija, 30: 315-331.

Ogorelec, B., Mišič, M., Faganeli, J., Stegnar, P., Vrišer, B. & Vukovič, A. 1987: Recentni sediment Koprskega zaliva = The recent sediment of the Bay of Koper (Northern Adriatic). Geologija, 30: 87-121.

Faganeli, J., Dolenec, T., Pezdič, J., Ogorelec, B. & Mišič, M. 1987: Nutrients in sediment pore water of the Gulf of Trieste (Northern Adriatic). Bollettino di oceanologia teorica ed applicata, 5/2: 95-108.

Faganeli, J., Ogorelec, B., Mišič, M., Dolenec, T. & Pezdič, J. 1987: Organic geochemistry of two 40-m sediment cores from the Gulf of Trieste (Northern Adriatic). Estuarine, coastal and shelf science, 25: 157-167.

Hinterlechner-Ravnik, A. & Mišič, M. 1985/86: Peridotitne nodule v bazaltnem tufu pri Gradu v Prekmurju = Peridotite nodules in alkali basaltic tuff in the Grad area of Prekmurje. Geologija, 28/29: 205-218.

Dolenec, T., Pezdič, J., Ogorelec, B. & Mišič, M. 1984: Izotopska sestava kisika in ogljika v recentnem sedimentu iz Blejskega jezera in v pleistocenski jezerski kredi Julijskih Alp = The isotopic composition of oxygen and carbon of the recent sediment from the Bled Lake and of the Pleistocene lacustrine chalk from the Julian Alps. Geologija, 27: 161-170.

Ogorelec, B., Jurkovšek, B., Šribar, L., Jelen, B., Stojanovič, B., Mišič, M. 1984: Karnijske plasti v Tamarju in pri Logu pod Mangartom = Carnian beds at Tamar and Log pod Mangartom. Geologija, 27, 107-158.

Faganeli, J., Mišič, M., Ogorelec, B., Dolenec, T. & Pezdič, J. 1985: Organic matter in two 41-m boreholes from the Gulf of Trieste (Northern Adriatic). Rapports et Proces Verbaux des Réunions - Commission Internationale pour l'Exploration Scientifique de la Mer Méditerranée, 29/2: 139-142.

Faganeli, J., Fanuko, N., Lenarčič, M., Malej, A., Mišič, M., Ogorelec, B., Vrišer, B., Vukovič, A. & Župan, J. 1984: Zasledovanje vpliva začasnega izpusta komunalnih odplak mesta Koper na morje v Koprskem zalivu. Slovensko morje in zaledje: zbornik za humanistične, družboslovne in naravoslovne raziskave, 7/6-7: 179-198.

Ogorelec, B., Mišič, M., Faganeli, J., Šercelj, A., Cimerman, F., Dolenec, T. & Pezdič, J. 1984: Kvartarni sediment vrtine V-3 v Koprskem zalivu = Quaternary sediment from the borehole V-3 in the bay of Koper. Slovensko morje in zaledje: zbornik za humanistične, družboslovne in naravoslovne raziskave, 7/6-7: 165-186.

Ogorelec, B., Mišič, M., Cimerman, F. & Faganeli, J. 1983: Sédiments quaternaires du forage effectué dans la Baie de Koper, Adriatique du nord, Yugoslavie. Rapports et Proces Verbaux des Réunions - Commission Internationale pour l'Exploration Scientifique de la Mer Méditerranée, 28/4: 251-253.

Ogorelec, B., Mišič, M., Šercelj, A., Cimerman, F., Faganeli, J. & Stegnar, P. 1981: Sediment sečoveljske soline = Sediment of the salt marsh of Sečovlje. Geologija, 24: 179-216.

Faganeli, J., Fanuko-Kovačič, N., Lenarčič, M., Malej, A., Mišič, M., Ogorelec, B., Vrišer, B., Vukovič, A. & Župan, J. 1981: Zasledovanje vpliva začasnega izpusta komunalnih odplak mesta Koper na morje v Koprskem zalivu. Slovensko morje in zaledje: zbornik za humanistične, družboslovne in naravoslovne raziskave, 4-5: 177-198.

Ogorelec, B., Mišič, M. & Faganeli, J. 2000: Sečoveljske soline - geološki laboratorij v naravi. Annales: anali za istrske in mediteranske študije, Series historia naturalis, 10/21: 243-252.

Navodila avtorjem

GEOLOGIJA objavlja znanstvene in strokovne članke s področja geologije in sorodnih ved. Revija od leta 2000 izhaja dvakrat letno. Članke recenzirajo domači in tuji strokovnjaki z obravnavanega področja. Ob oddaji člankov avtorji predlagajo **tri recenzente**, vendar pa si uredništvo pridržuje pravico do izbire recenzentov po lastni presoji. Avtorji morajo članek popraviti v skladu z recenzentskimi pripombami ali utemeljiti zakaj se z njimi ne strinjajo.

Avtorstvo: Za izvirnost podatkov, predvsem pa mnenj, idej, sklepov in citirano literaturo so odgovorni avtorji. Z objavo v GEOLOGIJI se tudi obvežejo, da ne bodo drugje objavili prispevka z isto vsebino.

Jezik: Članki naj bodo napisani v angleškem, izjemoma v slovenskem jeziku, vsi pa morajo imeti slovenski in angleški izvleček. Za prevod poskrbijo avtorji prispevkov sami.

Vrste prispevkov:

Izvirni znanstveni članek
Izvirni znanstveni članek je prva objava originalnih raziskovalnih rezultatov v takšni obliki, da se raziskava lahko ponovi, ugotovitve pa preverijo. Praviloma je organiziran po shemi IMRAD (**I**ntroduction, **M**ethods, **R**esults, **A**nd **D**iscussion).

Pregledni znanstveni članek
Pregledni znanstveni članek je pregled najnovejših del o določenem predmetnem področju, del posameznega raziskovalca ali skupine raziskovalcev z namenom povzemati, analizirati, evalvirati ali sintetizirati informacije, ki so že bile publicirane. Prinaša nove sinteze, ki vključujejo tudi rezultate lastnega raziskovanja avtorja.

Strokovni članek
Strokovni članek je predstavitev že znanega, s poudarkom na uporabnosti rezultatov izvirnih raziskav in širjenju znanja.

Diskusija in polemika
Prispevek, v katerem avtor ocenjuje ali dokazuje pravilnost nekega dela, objavljenega v Geologiji, ali z avtorjem strokovno polemizira.

Recenzija, prikaz knjige
Prispevek, v katerem avtor predstavlja vsebino nove knjige.

Oblika prispevka: Besedilo pripravite v urejevalniku Microsoft Word. Prispevki naj praviloma ne bodo daljši od 20 strani formata A4, v kar so všteti tudi slike, tabele in table. Le v izjemnih primerih je možno, ob predhodnem dogovoru z uredništvom, tiskati tudi daljše prispevke.

Članek oddajte uredništvu vključno z vsemi slikami, tabelami in tablami v elektronski obliki po naslednjem sistemu:
- *Naslov članka (do 12 besed)*
- *Avtorji (ime in priimek, naslov, e-mail naslov)*
- *Ključne besede (do 7 besed)*
- *Izvleček (do 300 besed)*
- *Besedilo*
- *Literatura*
- *Podnaslovi k slikam in tabelam*
- *Tabele, Slike, Table*

Citiranje: V literaturi naj avtorji prispevkov praviloma upoštevajo le tiskane vire. Poročila in rokopise naj navajajo le v izjemnih primerih, z navedbo kje so shranjeni. V seznamu literature naj bodo navedena samo v članku omenjena dela. Citirana dela, ki imajo DOI identifikator, morajo imeti ta identifikator izpisan na koncu citata. Za citiranje revije uporabljamo standardno okrajšavo naslova revije. Med besedilom prispevka citirajte samo avtorjev priimek, v oklepaju pa navajajte letnico izida navedenega dela in po potrebi tudi stran. Če navajate delo dveh avtorjev, izpišite med tekstom prispevka oba priimka (npr. Pleničar & Buser, 1967), pri treh ali več avtorjih pa napišite samo prvo ime in dodajte et al. z letnico (npr. Mlakar et al., 1992). Citiranje virov z medmrežja v primeru, kjer avtor ni poznan, zapišemo (Internet 1). V seznamu literaturo navajajte po abecednem redu avtorjev.

Imena fosilov (rod in vrsta) naj bodo napisana poševno, imena višjih taksonomskih enot (družina, razred, itn.) pa normalno. Imena avtorjev taksonov naj bodo prav tako napisana normalno, npr. *Clypeaster pyramidalis* Michelin, *Galeanella tollmanni* (Kristan), Echinoidea.

Primeri citiranja članka:

Mali, N., Urbanc, J. & Leis, A. 2007: Tracing of water movement through the unsaturated zone of a coarse gravel aquifer by means of dye and deuterated water. Environ. geol., 51/8: 1401–1412, doi:10.1007/s00254-006-0437-4.

Pleničar, M. 1993: *Apricardia pachiniana* Sirna from lower part of Liburnian beds at Divača (Triest-Komen Plateau). Geologija, 35: 65–68.

Primer citirane knjige:

Flügel, E. 2004: Mikrofacies of Carbonate Rocks. Springer Verlag, Berlin: 976 p.

Jurkovšek, B., Toman, M., Ogorelec, B., Šribar, L., Drobne, K., Poljak, M. & Šribar, Lj. 1996: Formacijska geološka karta južnega dela Tržaško-komenske planote – Kredne in paleogenske kamnine 1: 50.000 = Geological map of the southern part of the Trieste-Komen plateau – Cretaceous and Paleogene carbonate rocks. Geološki zavod Slovenije, Ljubljana: 143 p., incl. Pls. 23, 1 geol. map.

Primer citiranja poglavja iz knjige:

Turnšek, D. & Drobne, K. 1998: Paleocene corals from the northern Adriatic platform. In: Hottinger, L. & Drobne, K. (eds.): Paleogene Shallow Benthos of the Tethys. Dela SAZU, IV. Razreda, 34/2: 129-154, incl. 10 Pls.

Primer citiranja virov z medmrežja:

Če sta znana avtor in naslov citirane enote zapišemo:

Čarman, M. 2009: Priporočila lastnikom objektov, zgrajenih na nestabilnih območjih. Internet: http://www.geo-zs.si/UserFiles/1/File/Nasveti_lastnikom_objektov_na_nestabilnih_tleh.pdf (17. 1. 2010)

Če avtor ni poznan zapišemo tako:
Internet: http://www.geo-zs.si/ (22. 10. 2009)

Če se navaja več enot z medmrežja, jim dodamo še številko
Internet 1: http://www.geo-zs.si/ (15. 11. 2000)
Internet 2: http://www.geo-zs.si/ (10. 12. 2009)

Slike, tabele in table: Slike (ilustracije in fotografije), tabele in table morajo biti zaporedno oštevilčene in označene kot sl. 1, sl. 2 itn., oddane v formatu TIFF, JPG ali EPS z ločljivostjo 300 dpi. Le izjemoma je možno objaviti tudi barvne slike, vendar samo po predhodnem dogovoru z uredništvom. Obvezno je treba upoštevati zrcalo revije **172 x 235 mm**. Večjih formatov od omenjenega zrcala GEOLOGIJE ne tiskamo na zgib, je pa možno, da večje oziroma daljše slike natisnemo na dveh straneh (skupaj na levi in desni strani) z vmesnim »rezom«. V besedilu prispevka morate omeniti vsako sliko po številčnem vrstnem redu. Dovoljenja za objavo slikovnega gradiva iz drugih revij publikacij in knjig, si pridobijo avtorji sami. Table pripravite v formatu zrcala naše revije.

Če je članek napisan v slovenskem jeziku mora imeti celotno besedilo, ki je na slikah in tabelah tudi v angleškem jeziku. Podnaslovi naj bodo čim krajši.

Korekture: Te opravijo avtorji člankov, ki pa lahko popravijo samo tiskarske napake. Krajši dodatki ali spremembe pri korekturah so možne samo na avtorjeve stroške.

Prispevki so prosto dostopni na spletnem mestu: http://www.geologija-revija.si/

Oddajanje prispevkov:

Avtorje prosimo, da prispevke pošljejo na naslov uredništva:
GEOLOGIJA
Geološki zavod Slovenije
Dimičeva ulica 14, 1000 Ljubljana
bernarda.bole@geo-zs.si ali urednik@geologija-revija.si

Uredništvo Geologije

Instructions for authors

Scope of the journal: GEOLOGIJA publishes scientific papers which contribute to understanding of the geology of Slovenia or to general understanding of all fields of geology. Some shorter contributions on technical or conceptual issues are also welcome. Occasionally, a collection of symposia papers is also published.
All submitted manuscripts are peer-reviewed by at least two specialists. When submitting their paper, authors should recommend at least **three reviewers**. Note that the editorial office retains the sole right to decide whether or not the suggested reviewers are used. Authors should correct their papers according to the instructions given by the reviewers. Should you disagree with any part of the reviews, please explain why. Revised manuscript will be reconsidered for publication.

Author's declaration: Submission of a paper for publication in Geologija implies that the work described has not been published previously, that it is not under consideration for publication elsewhere and that, if accepted, it will not be published elsewhere.

Language: Papers should be written in English or Slovene, and should have both English and Slovene abstracts.

Types of papers:

Original scientific paper
In an original scientific paper, original research results are published for the first time and in such a form that the research can be repeated and the results checked. It should be organised according to the IMRAD scheme (**I**ntroduction, **M**ethods, **R**esults, **A**nd **D**iscussion).

Review scientific paper
In a review scientific paper the newest published works on specific research field or works of a single researcher or a group of researchers are presented in order to summarise, analyse, evaluate or synthesise previously published information. However, it should contain new information and/or new interpretations.

Professional paper
Technical papers give information on research results that have already been published and emphasise their applicability.

Discussion paper
A discussion gives an evaluation of another paper, or parts of it, published in GEOLOGIJA or discusses its ideas.

Book review
This is a contribution that presents a content of a new book in the field of geology.

Style guide:
Submitted manuscripts should not exceed 20 pages of A4 format (12 pt typeface, 1 line-spacing, left justification) including figures, tables and plates. Only exceptionally and in agreement with the editorial board longer contributions can also be accepted.
Manuscripts submitted to the editorial office should include figures, tables and plates in electronic format organized according to the following scheme:
- *Title (maximum 12 words)*
- *Authors (full name and family name, postal address and e-mail address)*
- *Key words (maximum 7 words)*
- *Abstract (maximum 300 words)*
- *Text*
- *References*
- *Figure and Table Captions*
- *Tables, Figures, Plates*

References: References should be cited in the text as follows: (Flügel, 2004) for a single author, (Pleničar & Buser, 1967) for two authors and (Mlakar et al., 1992) for multiple authors. Pages and figures should be cited as follows: (Pleničar, 1993, p. 67) and (Pleničar, 1993, fig. 1). Anonymous internet resources should be cited as (Internet 1). Only published references should be cited. Manuscripts should be cited only in some special cases in which it also has to be stated where they are kept. Cited reference list should include only publications that are mentioned in the paper. Authors should be listed alphabetically. Journal titles should be given in standard abbreviated form. A doi identifier, if there is any, should be placed at the end as shown in the first case.
Taxonomic names should be in italics, while names of the authors of taxonomic names should be in normal, such as *Clypeaster pyramidalis* Michelin, *Galeanella tollmanni* (Kristan), Echinoidea.

Articles should be listed as follows:
Mali, N., Urbanc, J. & Leis, A. 2007: Tracing of water movement through the unsaturated zone of a coarse gravel aquifer by means of dye and deuterated water. Environ. geol., 51/8: 1401–1412, doi:10.1007/s00254-006-0437-4.
Pleničar, M. 1993: *Apricardia pachiniana* Sirna from lower part of Liburnian beds at Divača (Triest-Komen Plateau). Geologija, 35: 65–68.

Books should be listed as follows:
Flügel, E. 2004: Mikrofacies of Carbonate Rocks. Springer Verlag, Berlin: 976 p.
Jurkovšek, B., Toman, M., Ogorelec, B., Šribar, L., Drobne, K., Poljak, M. & Šribar, Lj. 1996: Formacijska geološka karta južnega dela Tržaško-komenske planote – Kredne in paleogenske kamnine 1: 50.000 = Geological map of the southern part of the Trieste-Komen plateau – Cretaceous and Paleogene carbonate rocks. Geološki zavod Slovenije, Ljubljana: 143 p., incl. Pls. 23, 1 geol. map.

Book chapters should be listed as follows:
Turnšek, D. & Drobne, K. 1998: Paleocene corals from the northern Adriatic platform. In: Hottinger, L. & Drobne, K. (eds.): Paleogene Shallow Benthos of the Tethys. Dela SAZU, IV. Razreda, 34/2: 129-154, incl. 10 Pls.

Internet resources should be listed as follows:
Known author and title:
Čarman, M. 2009: Priporočila lastnikom objektov, zgrajenih na nestabilnih območjih. Internet: http://www.geo-zs.si/UserFiles/1/File/Nasveti_lastnikom_objektov_na_nestabilnih_tleh.pdf (17. 1. 2010)
Unknown authors and title:
Internet: http://www.geo-zs.si/ (22.10.2009)

When more than one unit from the internet are cited they should be numbered:
Internet 1: http://www.geo-zs.si/ (15.11. 2000)
Internet 2: http://www.geo-zs.si/ (10.12. 2009)

Figures, tables and plates: Figures (illustrations and photographs), tables and plates should be numbered consequently and marked as Fig. 1, Fig. 2 etc., and saved as TIFF, JPG or EPS files and submitted at 300 dpi. Colour pictures will be published only on the basis of previous agreement with the editorial office. The maximum size of full-page illustrations and tables is **172 x 235 mm**. Larger formats can only be printed as a double-sided illustration (left and right) with a cut in the middle. All figures should be referred to in the text and should normally be numbered in the sequence in which they are cited. The approval for using illustrations previously published in other journals or books should be obtained by each author.
When a paper is written in Slovene it has to have the entire text which accompanies illustrations and tables written both in Slovene and English. Figure and table captions should be kept as short as possible.

Proofs: One set of page proofs (as pdf files) will be sent by e-mail to the corresponding author. Corrections are made by the authors. They should correct only typographical errors. Short additions and changes are possible but should be paid by the authors.

Geologija is an open access journal, all pdfs can be downloaded from the website: http://www.geologija-revija.si/en/

Submission: Authors should submit their papers to the address of the editorial office:

GEOLOGIJA
Geological Survey of Slovenia
Dimičeva ulica 14, 1000 Ljubljana, Slovenia
bernarda.bole@geo-zs.si or urednik@geologija-revija.si

The Editorial Office

GEOLOGIJA

št.: 60/2, 2017

www.geologija-revija.si

GeoZS
Geološki zavod Slovenije

ISSN 0016-7789

9 770016 778002